Universidad del País Vasco Euskal Herriko Unibertsitatea

ZTF-FCT
Zientzia eta Teknologia Fakultatea
Facultad de Ciencia y Tecnología

Department of Immunology, Microbiology and Parasitology

PhD THESIS

Study of *Aspergillus fumigatus* pathogenicity and identification of putative virulence genes

Mónica Sueiro Olivares

Supervisor:

Aitor Rementeria Ruiz

Leioa, 2016

This project was carried out thanks to the Pre-doctoral Research Grants and the Grant for stays in centers different from those of the Pre-doctoral Training Program (EGONLABUR) supported by the Government of the Basque Country. Furthermore, it was partly funded by the UPV/EHU (GIU12/44, UFI11/25 and GIU15/36) and the Ministry of Economy and Competitiveness (MICINN CSD2009-00006).

Results obtained along the four years of research have been presented in national and international conferences, being part of the study published in an international journal.

Research Publications

Sueiro-Olivares M., Fernandez-Molina, J.V., Abad-Diaz-de-Cerio, A., Gorospe, E., Pascual, E., Guruceaga, X., Ramirez-Garcia, A., Garaizar, J., Hernando, F.L., Margareto, J., Rementeria, A. 2015. *Aspergillus fumigatus* transcriptome response to a higher temperature during the earliest steps of germination monitored using a new customized expression microarray. *Microbiology*. 161(Pt 3):490-502.

Proceedings

Sueiro-Olivares M, Fernández-Molina JV, Abad-Diaz-de-Cerio A, Guruceaga X, Gorospe E, Pascual E, Ramírez-García A, Garaizar J, Hernando FL, Margareto J, Rementeria A. 2015. Diseño de un nuevo microarray de genoma completo de *A. fumigatus*: análisis transcriptómico de la germinación. *Rev Iberoam Micol*. 32(2):134-145.

Poster Presentations

Sueiro-Olivares M, Fernandez-Molina JV, Abad-Diaz-de-Cerio A, Guruceaga X, Ramirez-Garcia A, Garaizar J, Hernando F, Margareto J, Rementeria A. *Aspergillus fumigatus* transcriptome reveals the reduction of metal metabolism and the increase of gliotoxin production during a disseminated murine infection. Poster presentation at 7th Advances Against Aspergiollosis, 3th-5th March 2016, Manchester, United Kingdom.

Sueiro-Olivares M, Fernandez-Molina JV, Abad-Diaz-de-Cerio A, Guruceaga X, Ramirez-Garcia A, Garaizar J, Hernando F, Margareto J, Rementeria A. *Aspergillus fumigatus* transcriptome during a disseminated murine infection reveals the metabolic adjustments once the infection has established. Poster presentation at Trends in Medical Mycology, 9th-12th October 2015, Lisbon, Portugal.

Sueiro-Olivares, M., Fernandez-Molina, J.V., Abad-Diaz-de-Cerio, A., Guruceaga, X., Ramirez-Garcia, A., Garaizar, J., Hernando, F. L., Margareto, J. & Rementeria, A. Análisis del transcriptoma de *Aspergillus fumigatus* durante una infección diseminada en ratón mediante un microarray de expresión de genoma completo. Poster presentation at the XII Congreso Nacional de Micología, 18th-20th June 2014, Bilbao, Spain.

Sueiro-Olivares M, Fernández-Molina JV, Abad-Diaz-de-Cerio A, Guruceaga X, Gorospe E, Pascual E, Ramírez-García A, Garaizar J, Hernando FL, Margareto J, Rementeria A. New costumized expression microarray for *Aspergillus fumigatus*: Effect of temperature on the transcriptome during the earliest steps of germination. Poster presentation at 6th Advances Against Aspergillosis, 27th February-1st March, 2014, Madrid, Spain.

Acknowledgements

En primer lugar quiero agradecer a mi director Aitor Rementeria la confianza que depositó en mí para realizar esta Tesis Doctoral. Gracias a él he conocido el mundo de la investigación, que tan ajeno era cuando entré en el laboratorio. También quiero agradecer su ayuda para no "panicar" en los momentos menos buenos.

I would also like to extend a sincere thanks to Elaine Bignell for giving me the opportunity to spend three months in the MFIG. Not only did I learn new techniques but I also met lovely people. Regards to everyone and especially to EB Group! Hope to meet you in the future! Imposible olvidarme de Jorge, y de tu forma de transmitir ese espíritu científico (no lo pierdas nunca!!); de Sara, que me acogiste en tus planes desde el primer día haciendo que mi estancia fuera hasta divertida; y de Briony, my British friend! I'm waiting for you in Bilbao!

A mis compañeros de labo, que habéis conseguido que nunca me olvide del Fungal and Bacterial Biomics Research Group ya sea por las comidas en el Txoko de Fernando, los congresos, o las cosas que pasan día a día. También quiero agradecer al resto de compañeros del departamento por los buenos momentos y por estar siempre dispuestos a ayudar.

A Jimena, mi mentora y confidente. Mis primeros años de tesis no hubieran sido iguales sin ti. A Ana, la superviviente del grupo *Aspergillus,* y a Vero, Aitor (mini), Aitana e Iker, que erais mi desconexión entre las largas horas delante del ordenador. También a Zaloa, Claudia e Itxaso. Zalo, que si antes de empezar esta aventura ya éramos amigas estos cuatro años nos han unido mucho mas y eso que me alegro! e Itxasito, una persona que no me esperaba encontrar y de la que no me voy a olvidar. Los momentos que he pasado con vosotras simplemente no tienen precio! Gracias por vuestra paciencia y vuestro apoyo!

También agradecer el apoyo de Jan, y nuestra forma de cuadrar horarios para quedar o irnos de vacaciones al menos 4 días; de Marta, que de casi no vernos hemos pasado a tener una quedada semanal; y de Nuria, por nuestros cafés cortos de 1 hora!

Las últimas líneas se las dedico a mi familia. A mis padres, por apoyarme en los momentos más bajos y animarme a ver el vaso medio lleno (incluso cuando no quedaba ni una gota). Y por supuesto a mi hermano, que con su "ranciosidad" siempre consigue que me olvide de las cosas y sin el cual una parte de esta tesis hubiera sido interminable. Para que luego digan que un ingeniero no puede entender nada de biología y una bióloga nada de electrónica. Juntos dominaríamos el mundo, y lo sabes!

TABLE OF CONTENTS

[a]Annexes are included on the CD attached to this Thesis.

ABBREVIATIONS

µJ	Microjoules
µl	Microliter
µm	Micrometer
µM	Micromolar
ABC	ATP-binding cassette
ABPA	Allergic bronchopulmonary aspergillosis
Act1	Actin 1
ADN	Deoxyribonucleic acid
AIDS	Advanced HIV infections
AMM	*Aspergillus* Minimal Medium
AMML	*Aspergillus* Minimal Medium Liquid
ATCC	American type culture collection
ATL	Atlanta
ATP	Adenosine triphosphate
AWAFUGE	Agilent Whole *A. fumigatus* Genome Expression 44K microarray
BLAST	Basic Local Alignment Search Tool
BLASTN	Nucleotide BLAST
bp	Base pair
CA	California
CADRE	Central *Aspergillus* Data REpository
CDF	Cation diffusion facilitator
cDNA	Complementary DNA, synthesized from mRNA
CEEA	Animal Experimentation Ethics Committee (previously CEBA, Ethics Committee for Animal Welfare)
CFU	Colony forming units
cm	Centimeter
CNA	Chronic necrotising aspergillosis
COPD	Chronic obstructive pulmonary disease
Ct	Threshold cycle
Cy3	Cyanine
DDBJ	DNA DataBank of Japan
DNAse	Deoxyribonuclease
dNTP	Nucleoside triphosphate
E	Efficiency
EBI	European Bioinformatics Institute
ECM	Extracellular matrix
EDTA	Ethylenediaminetetraacetic acid
EMBL	European Molecular Biology Laboratory
F	Primer fordward
FAD	Flavin adenine dinucleotide

FBS	Fetal bovine serum
FL	Florida
FunCat	Munich Information Center for Protein Sequence Functional Catalogue
g	g-force
g	Gram
GAG	Galactosaminogalactan
GpdA	Glyceraldehyde 3-phosphate dehydrogenase
GTP	Guanosine-5'-triphosphate
HCl	Hydrochloric acid
HIV	Human immunodeficiency virus
HSP	Heat shock protein
IA	Invasive aspergillosis
ICBN	International Code of Botanical Nomenclature
IFC	Integrated fluidic circuit
Ig	Inmunoglobulin
IPA	Invasive pulmonary aspergillosis
kb	Kilobase
kDa	Kilodalton
kg	Kilogram
KNN	K-Nearest Neighbour
KOH	Potassium hydroxide
l	Liter
LB	Luria Bertani
log	Logarithm
M	Molar
MA	Massachusetts
MEA	Malt Extract Agar
MFS	Major facilitator superfamily
mg	Miligram
$MgCl_2$	Magnesium chloride
min	Minute
MIPS	Munich Information Center for Protein Sequence
ml	Mililiter
mM	Milimolar
MnSOD	Manganase superoxide dismutase
mRNA	Messenger RNA
NADPH	Nicotinamide adenine dinucleotide phosphate
NaN	Not a Number
NCBI	National Center for Biotechnology Information
nm	Nanometer
nt	Nucleotide

NTC	No-Template Control
PCR	Polymerase chain reaction
PDA	Potate Dextrose Agar
PDB	Protein DataBase
qPCR	Real Time PCR
R	Primer reverse
R^2	Coefficient of determination
RIA	Reductive iron assimilation
RIN	RNA integrity number
RMA	Robust Multi-Array Average
RNAse A	Ribonuclease A
ROI	Reactive Oxygen Intermediates
ROS	Reactive oxigen species
rpm	Revolutions per minute
RT-qPCR	Reverse Transcription PCR
s	Seconds
S.O.C.	Super Optimal Broth with catabolite repression
SDS	Sodium dodecyl sulfate
SGIKer	Service of Advanced Research Facilities
SMM	Stabilized Minimal Medium
SS-T	Saline/Tween Solution
TBE	Tris-Borate-EDTA
TE	Tris-EDTA
TEER	Trans-epithelial electric resistance
TIGR	The Institute for Genome Research
Tm	Melting temperature
TX	Texas
U	Units
UK	United Kingdom
UPV-EHU	University of the Basque Country
US	United States
USA	United States of America
UV	Ultraviolet
V	Volt
w/v	Weight/Volume
Ω	OMS
ºC	Degree Celsius

1. INTRODUCTION

1.1. *Aspergillus* genus

Aspergillus genus is classified within the division Ascomycota, class Eurotiomycetes, order Eurotiales, family Trichocomaceae. It was firstly described in 1729 by the Italian biologist Pier Antonio Micheli, who marked the starting point of the Micology as a science in his work "Nova Plantarum Genera". However, these fungi did not start to be considered as agents of decay and animal and human diseases until the middle of 19th century (Raper & Fennel, 1965).

The name *Aspergillus* comes from the morphological resemblance of conidiophores to the "aspergillum", religious object used to scatter holy water. This genus is formed by mitosporic, filamentous fungi whose main characteristic is the production of specialized hyphae called conidiophores. These structures have three different parts: vesicle, stipe and foot cell (Abarca, 2000) (Fig. 1.1). Conidiophores emerge from the vegetative mycelium, as erect, aseptate, thick-walled and specialized hyphae that expand apically to form a vesicle. On this vesicle, numerous conidiogenous cells or phialides, flask-shaped elements whose interior successively produces conidia in interconnected chains, emerge synchronically. These conidia are strongly hydrophobic, and generally, hyaline or pale, but in mass, they may be of different colors that are reproduced in the colonies. In some species, between the vesicle and phialides, metulae can be found. In these cases, conidiogenous cells are called biseriate. In absence of metulae, conidiogenous cells are considered uniseriate.

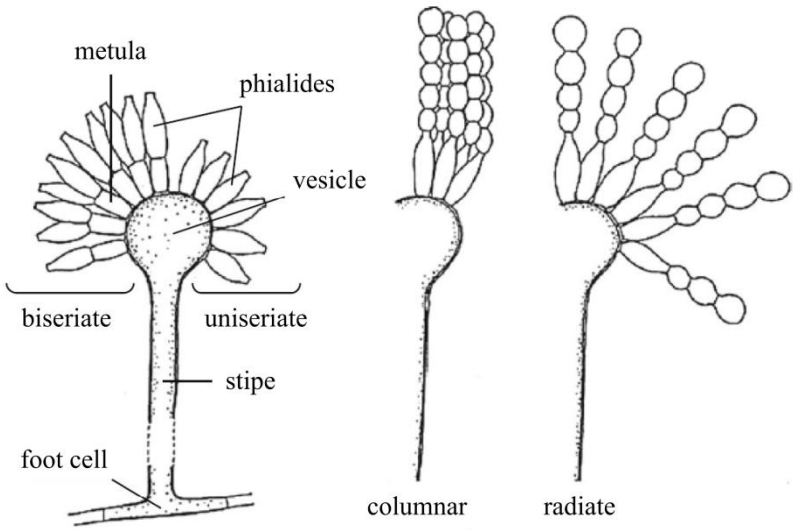

Fig. 1.1. Diagram of terminology used for the identification of *Aspergillus* species (extracted from Guarro *et al*., 2010).

So far the genus *Aspergillus* contains around 339 species (Samson *et al*., 2014). At first, it was classified in subgenus and groups according to its macro- and microscopic morphological characters (Raper & Fennel, 1965). However, at first this classification did not have any nomenclatural status so Gams *et al.* (1985) introduced names of subgenera and sections according to the International Code of Botanical Nomenclature (ICBN). Afterwards, the classification of this genus was subjected to constant modifications. Peterson (2008) classified the species in 5 subgenera and 16 sections, although years later, its division in 8 subgenera and 18 sections was suggested (Samson &Varga 2012). Two years ago, Houbraken *et al.* (2014) and Hubka *et al.* (2014) proposed 4 subgenera (*Aspergillus*, *Circumdati*, *Fumigati* and *Nidulantes*) and 20 sections, but the classification is still being reviewed owing to phylogenetic analyses based on molecular characteristics.

The type of reproduction in filamentous fungi is a determinant factor in their classification. Traditionally, *Aspergillus* genus was included within Deuteromycota or "imperfect fungi" due to the unkwon sexual form or teleomorph (Carlile *et al*., 2001). Nevertheless, nowadays, the teleomorph phases of different species are already known, allowing their classification within the division Ascomycota. These findings have had implications when it comes to denominating fungi, as species with sexual reproduction have two different names, one referring to its anamorph form and the other to the teleomorph form. One example can be found in *A. nidulans* (anamorph) and *Emericella nidulans* (teleomorph). This "dual nomenclature" was established by the ICBN in 1910 in order to solve the problem of those fungi with pleomorphic cycles (anamorph and teleomorph phases) (Samson & Varga, 2009), but, even so, misunderstandings remained. Therefore, under the initiative "One fungus = One name", the necessity to establish one single name to each fungal species started to emerge (Taylor, 2011) and in the symposium "One fungus = Which name" celebrated in Amsterdam (The Netherlands) in April 2011, the anamoprh name was suggested to denominate all *Aspergillus* genus species (Hawksworth *et al*., 2011). In fact, a website was developed (www.aspergilluspenicillium.org) so that the nomenclature proposed to any species included within *Aspergillus* and *Penicillium* genus can be consulted.

Some of the *Aspergillus* species have been used in the production of certain substances such as amino acids, organic acids, enzymes and secondary metabolites. However, due to their capacity to generate diseases both in human and in animals their study and

knowledge in the last years have increased considerably. Amongst all the species included within *Aspergillus* genus, 33 have been associated with human infectious diseases or aspergillosis. The most common etiological agent is *A. fumigatus*, followed by A. *flavus*, *A. niger*, *A. terreus* and other species with lower incidence (Guarro, 2003; Hope *et al*., 2005a; Nicolle *et al*., 2011; Alastruey-Izquierdo *et al*., 2013).

1.2. *Aspergillus fumigatus*

Aspergillus fumigatus is a haploid, anamorphic fungus with a quick filamentous growth that produces grayish turquoise or dark turquoise to dark green or dull green colonies. It produces abundant ellipsoid conidia, 2 to 3 µm in diameter, from uniseriate, columnar conidial heads. The vesicle, 10-26 µm in diameter, is pyriform or subclavate and the foot cell has a diameter of 6-10 µm (Latgé *et al*., 1999; Samson *et al*., 2007) (Fig. 1.2).

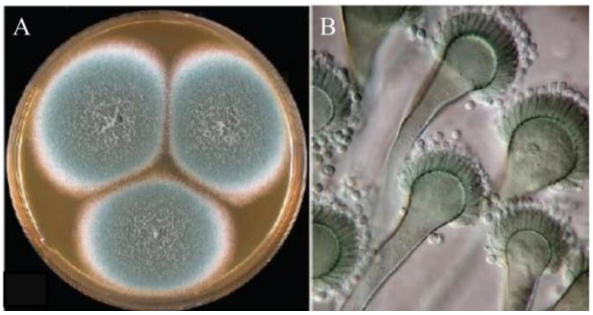

Fig. 1.2. *Aspergillus fumigatus* (extracted from Samson *et al*., 2007). A) Colonies grown on Malt Extract Agar (MEA), incubated at 25ºC for 7 days. B) Uniseriate, columnar conidiophores (x40).

Several years ago, the perfect form or teleomorph phase of *A. fumigatus* was described with the name of *Neosartorya fumigata* (O'Gorman *et al*., 2009). According to these authors, teleomorph form is heterotalic, presenting superficial, globose cleistothecia (150-480 µm in diameter) surrounded by mycelium. Cleistothecia are yellowish white at first, and then, turn light yellow to grayish yellow and have irregularly sub-globose, eight-spored, evanescent asci. Ascospores turn yellowish white to greenish white, and they are one-celled, broadly lenticular, rarely spherical, with two equatorial crests (0.3-1.0 µm wide), convex surface and a reticulate ornamentation. Nevertheless, this description has not been corroborated yet and it should be highlighted that 6 months were needed to describe it.

1.2.1. *Aspergillus fumigatus* conidia

Aspergillus fumigatus is a saprophytic filamentous fungus typically found in soil and decaying vegetation, where it plays an important role in the recycling of carbon and nitrogen (Tekaia & Latgé, 2005). Even though this species is not the most prevalent fungal species in the world, it is one of the most ubiquitous of those with airbone conidia. It sporulates abundantly, and each conidial head produces thousands of conidia, which, through disturbances of the environment and strong air currents, are released into the atmosphere (Latgé, 1999). These conidia are extremely well-suited for air dispersal thanks to their small size (2-3 µm) and hydrophobicity, which allow them to remain airbone for long periods. Moreover, they are thermotolerant and contain melanin and related pigments in their cell walls providing UV protection (O´Gorman, 2011, Krijgsheld *et al*., 2013).

Conidial concentration indoors and outdoors is estimated to be 1-100 conidia/m^3 so that, people can inhale more than 100 spores daily (Kwon-Chung & Sugui, 2013). Due to this ubiquity, *A. fumigatus* may get in touch with hosts through respiratory or digestive system, skin, eyes or ears, being their inhalation the main route of access. Moreover, the small size of conidia allows this fungus to easily bypass the defense mechanisms of the nasal cavity and upper respiratory tract to reach the lung alveoli. In immunocompetent individuals, this inhalation, rarely have any adverse effect, since the conidia are eliminated efficiently by innate immune mechanisms. Only in hypersensitive immunocompetent people conidia inhalation can cause allergic responses such as allergic bronchopulmonary aspergillosis (ABPA), asthma or allergic sinusitis, being chronic diseases rarely developed. However, it is in immunocompromised patients where conidia might overcome immune defenses, resulting in their establishment in the lung (Latgé, 1999). Once there, conidia germinate and subsequently start to colonize or even invade the surrounding tissue (Dagenais & Keller, 2009), causing serious diseases (Osherov, 2007) with the invasive aspergillosis (IA) as the most severe form.

1.2.2. *Aspergillus fumigatus* conidial germination

A crucial event in the infectious process of this pathogen is conidial germination, given that at this stage conidia have to adapt to the host environment, overcome the immune system and germinate. The first step in conidial germination consists of breaking the spore dormancy, which is achieved with the exposure to water, air and/or inorganic salts, amino acids and fermentable sugars (Osherov & May, 2001; Thanh *et al*., 2005). Afterwards, the isotropic growth, also known as swelling, takes place. During this phase, the diameter of conidia increases two fold or more owing to the water uptake and, in turn, the micro-viscosity of the cytoplasm decreases (van Leeuwen *et al.* 2010). This second phase occurs at the same time that several metabolic activities, such as respiration or DNA, RNA and protein synthesis (Mirkes, 1974; Osherov & May, 2001), and when molecules are directed to the cell cortex to enable the addition of new plasma membrane and cell wall (Momany, 2002). The third stage of germination consists of the establishment of cell polarity, germ tube formation and the maintenance of polarized growth (Barhoom & Sharon, 2004; Harris & Momany, 2004). During this stage, the morphogenetic machinery is redirected to the site of polarization. This machinery includes the cytoskeleton, the vesicle trafficking system, landmark proteins, signaling pathways and endocytic partners like Rho GTPase modules, polarisome and Arp2/3 complexes (d'Enfert, 1997; Momany, 2002; Harris & Momany, 2004; Harris, 2006). Furthermore, the lipid composition of the plasma membrane changes by the appearance of sterol-rich domain (Van Leeuwen *et al*., 2008). At larger stages, the growth speed of the germ tube increases and the functional organization of the hyphal tip area acquires its full potential (Taheri-Talesh *et al*., 2008; Köhli *et al*., 2008). Finally, a fungal mycelium is established by branching and inter-hyphal fusion (Glass *et al*., 2004).

Despite the knowledge about the different stages of *Aspergillus* spp. germination, little is known about the molecular aspects of the processes that take place during this period. Osherov & May (2001) tried to explain this lack of information basing on the multiple sensors and pathways that activate during the germination, because even though they work in combination, each one seems to be sensitive to a particular environmental stimulus. They also discussed about the difficulty in differentiating early signaling events and essential endogenous and metabolic activities that occur at the very beginning of this process. Therefore, shedding light of the germination from a molecular point of view is a pending task. Given that this phase is crucial in the

establishment of the fungus in the host and the subsequent development of the infection, understanding its molecular aspects might lead to the development of new therapeutic alternatives which could prevent the infection since its beginning.

1.2.3. *Aspergillu fumigatus* biofilm

Once *A. fumigatus* conidia have adhered and germinated, hyphae begin to intertwine forming a monolayer whose structural complexity increases with time. Moreover, this mycelium is surrounded by an extracellular hydrophobic matrix that acts as a cohesive linkage. This extracellular matrix (ECM) is composed of galactomannan, α-1,3-glucans, galactosaminogalactan, monosaccharides and polyols, melanin and proteins, including major antigens and hydrophobins (Beauvais *et al*., 2007).

Although convincing studies of *A. fumigatus* biofilm development *in vivo* have not been performed, the presence of ECM is clinically recognized as the primary evidence of biofilm formation. Indeed, the ability of *A. fumigatus* to form different types of biofilms in aspergilloma and invasive pulmonary aspergillosis with varied ECM composition has also been reported (Loussert *et al*., 2010; Müller *et al*., 2011), as well as the presence of numerous *A. fumigatus* hyphae in the form of dense intertwined mycelial balls or grains, similar to the biofilms formed by *Candida* species *in vivo* (Kaur & Singh, 2014).

1.3. Aspergillosis

Aspergillosis are opportunistic infections caused by *Aspergillus* spp., being *A. fumigatus* the most common etiologic agent, followed by *A. flavus, A. niger*, *A. terreus* and other species which are associated with much lower incidence (Nicolle *et al*., 2011). A population-based survey developed in Spain of filamentous fungus and their antifungal resistance (Alastruey-Izquierdo *et al*., 2013) reflected a prevalence of 1.6/1,000,000 inhabitants, *Aspergillus* being the most frequent genus isolated in 86.3% of the cases. Amongst aspergillosis, *A. fumigatus* was the most prevalent species (56.11%), followed by *A. flavus* (9.71%), *A. terreus* (9.35%), *A. tubingensis* (7.91%), *A. niger* (7.55%), *A. nidulans* (2.88%) and others with lower incidence.

Aspergillosis range from allergies to IA, standing out because of their seriousness, ABPA, aspergilloma and several forms of IA such as invasive pulmonary aspergillosis (IPA) or chronic necrotizing aspergillosis (CNA) (Fig. 1.3). These infections are mainly

acquired by inhalation, being lungs the primary focus and in less proportion paranasal sinus.

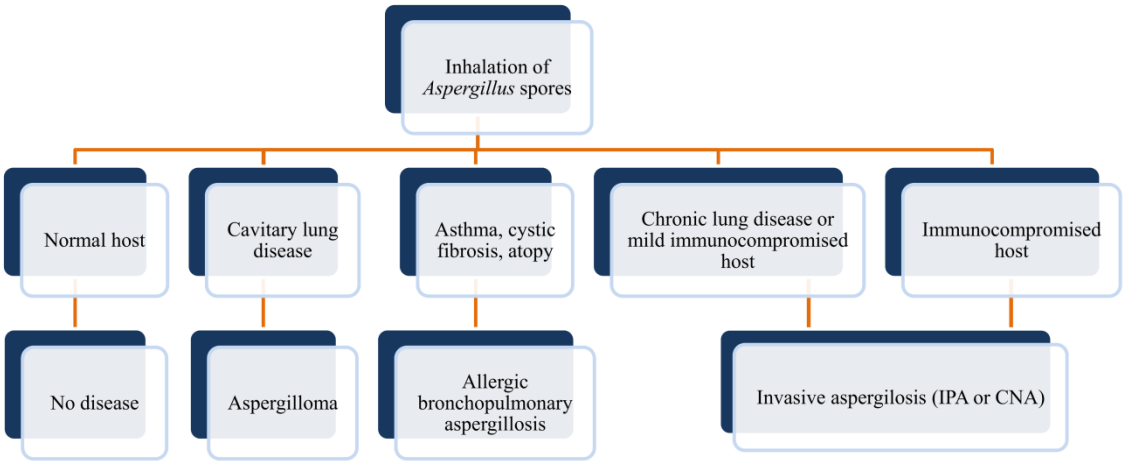

Fig. 1.3. The spectrum of pulmonary aspergillosis (modified from Kousha *et al*., 2011).

Allergic bronchopulmonary aspergillosis is a hypersensitivity pulmonary disease due to an environmental exposure to *A. fumigatus* allergens. The fungus grows saprophytically colonizing bronchial tube and causing a persistent inflammatory response by immunoglobulin E (IgE) which leads to bronchial obstruction. This disease is related to patients with asthma or cystis fibrosis (Zmeili & Soubani, 2007).

Aspergilloma is the *Aspergillus* colonization in preexistent lung cavities owing to tuberculosis, sarcoidosis, bullous emphysema, bronchiectasis, and other causes. This disease can be classified in simple or complex aspergilloma based on radiographic criteria. The simple form differs from the complex because of the absence of constitutional symptoms, para-cystic lung opacities, cyst expansion, or progressive pleural thickening (Greene, 2005; Kousha *et al*., 2011).

Invasive aspergillosis is a nosocomial serious disease which affects primarily immunocompromised patients with mortality rates that depend on the underlying disease and affected organs, reaching 85-100% in liver and pancreas transplant recipients or after hematopoietic progenitor cell transplantation. The first IA description in humans was in 1951, and since then, it has become the main cause of fungal infection produced by filamentous fungus, and the second invasive fungal infection after *Candida* infections (Latgé, 1999; Alastruey-Izquierdo *et al*., 2012). Moreover, as a result of HIV epidemic, the development of chemotherapeutic treatments, the increase of organ transplantations and the utilization of pharmaceutical immunosuppressors, the number

of immunocompromised patients have risen considerably, and with it IA cases (Lumbreras & Gavaldà, 2003; Maschmeyer *et al*., 2007).

As mentioned above, IA is developed in immunocompromised individuals. It is usually acquire by the inhalation of conidia, causing a lung disease and, less frequently, sinus and inner ear infection (del Palacio *et al*., 2003). Its clinical manifestation is variable, nonspecific and late, being essential to suspect it on risk situations. Due to nonspecific signs and symptoms, the immunosuppression degree and the underlying disease its clinical diagnosis is hard and late (Denning, 1998). In addition, this disease has mortality rates over 50%, and can even reach 95% in certain situations, which might be attributed to the weakness of immune response of the patient, the virulence of the fungus itself, the late diagnosis and the lack of effective antifungal therapies (Abad *et al*., 2010).

Invasive aspergillosis can also affect other organs. Invasive sinusitis, which is not diagnosed in many cases owing to the lack of a detailed examination, is one of them. The fungus invades the mucosa, dispersing the infection to adjacent structures. Generally, maxillary sinus is affected, followed by ethmoid, sphenoid and frontal sinus (Drakos *et al*., 1993). Disseminated IA appeared when endovascular or bloodstream infection is implicit in the pathogenesis. This concept should be distinguished from local spread or extension across tissue planes (sinus aspergillosis with direct extension to the meninges and brain for instance), multifocal disease within one organ, and situations in which there is more than one site of infection within the same organ system (Hope *et al*., 2005b).

The main risk factors associated with the development of IA are hematopoietic stem cell transplantation, solid organ transplantation, lengthy treatments with high dose of corticosteroids, hematologic neoplasms, citotoxic therapy, advanced HIV infections (AIDS) and cronic granulomatous diseases (Gerson *et al*., 1984; Soubani & Chandrasekar, 2002; Segal & Walsh, 2006; Fortún *et al*., 2012). In neutropenic patient, it is estimated that the risk for the development of IA increases 1% each day during the first three weeks and, since then, 4% each day (Gerson *et al*., 1984). Apart from the described diseases, diabetes, lengthy antimicrobial treatments, several viral infections, an increase in *Aspergillus* conidia in the environment, extensive surgery, severe burns,

stay in intensive care units, renal insufficiency and hemodialysis are others risk factors that could be mentioned (Table 1.1).

Table 1.1. Incidence and mortality rate of IA among distinct patient populations (Maschmeyer *et al*., 2007).

Disease	Incidence (%)	Mortality (%)
Acute leukemia	5-24	30-40
Allogeneic hematopoietic stem cell transplantation	10	60
Solid organ transplantation	11-14	50-60
Other causes of immunosuppression (burns, AIDS, alemtuzumab therapy, intensive care unit)	4-7	70-85

1.4. Animal infections

One of the major advancements on the study of *A. fumigatus* pathogenesis, its virulence and the therapy against IA has been *in vivo* studies. These studies have allowed scientists to obtain information about biological and medical issues that would have not been completely responded by *in vitro* assays. Moreover, these studies enable to understand what happens during a real infection and extrapolate their results to human cases.

The use of animal models has been critical to shed light on *A. fumigatus* pathogenesis. Nevertheless, the significance and validity when results are extrapolated to human cases depends on the animal model chosen (Hau, 2008). Despite the high number of animals models developed with birds, guinea pigs, rabbits and rats, murine models have set as the predominant choice for researchers. The reasons for this choice are based on the availability of genetically defined strains of mice, immunological reagents, ease of handling and cost (Clemons & Stevens, 2005). These models have been performed to study the virulence of isolated strains of *A. fumigatus* as well as to test their antifungal susceptibility (McDonagh *et al*., 2008, Gehrke *et al*., 2010, Park *et al*., 2012, Salas *et al*., 2013, Seyedmousavi *et al*., 2013, Amarsaikhan *et al*., 2014, Jiang *et al*., 2014).

Murine infections can be established by intranasal, intravenous or intra-abdominal routes. Unlike the two first, intra-abdominal infections are barely carried out, being one of its prerequisites that *A. fumigatus* conidia have to be germinated before the administration (Schmidt, 2002). Intravenous infection is a method easily standardized because the fungal inoculum is directly injected into the blood stream, resulting in a good correlation between infection dose and mortality rates (Paulussen *et al*., 2014). Moreover, in many cases, five animals per test group are sufficient to assess significant

differences, which go along with the aim of decreasing the number of individuals used in each assay. This infection is valuable for the development of new antifungal or vaccination strategies. On the other hand, despite its high similarity to human infections, intranasal infection has difficult reproducibility and standardization, limiting its choice to study the pathogenicity or virulence of *A. fumigatus* strains. Furthermore, unlike intravenous infection, this type of infection requires a larger number of individuals to obtain reproducible data, which is not in accordance with using the fewest number of animals per assay (Schmidt, 2002).

It should be highlighted that murine infections are not only performed with healthy individuals. Thanks to the availability of immunological agents, such as cyclophosphamide or corticosteroids, models with immunocompromised animals have been performed in order to simulate the immune status of IA patients or study the pathogenesis of *Aspergillus* genus relative to the immune status. Cyclophosphamide is an agent that interferes in the replication of DNA and one of the most widely used, as its administration generates neutropenic animals. Corticosteroids, however, have effect on alveolar macrophages, first barrier pathogens have to deal with to develop the infections. Thus, depending on the immune status required, one of these immunological agents, or a combination of both of them if a total immunosuppression is desired, can be used.

1.5. *Aspergillus fumigatus* virulence factors

The survival and growth in a wide range of environmental conditions, the effective dispersal in the air, the physical characteristics that allow conidia to reach the distal airways and the swift adaptability to the host environment are some of the characteristics that make this fungus be the most prevalent etiologic agent in IA (Kwon-Chung & Sugui, 2013). In fact, the importance of its infection are reflected on the large number of reviews published regarding its biology and pathology and on the huge effort made to identify virulence factors (Latgé, 1999; Brakhage & Langfelder, 2002; Askew, 2008; Banerjee & Kurup, 2003; del Palacio *et al*., 2003; Rementeria *et al*., 2005; Tekaia & Latgé, 2005; Hohl & Feldmesser, 2007; Osherov, 2007; Krappmann, 2008; Dagenais & Keller, 2009; Abad *et al*., 2010; Kwon-Chung & Sugui, 2013). A great deal of genes that has been associated with virulence has been studied through strains in which they were suppressed or deleted, comparing their pathogenicity to the wild type.

Nevertheless, most of the studies have not succeeded in proving that the deletion of one or two genes has a drastic effect on the pathogenicity, indicating that *A. fumigatus* virulence might be controlled by several genes. Furthermore, so far, some studies have demonstrated that the pathogenesis of this fungus is multifactorial, owing to the combination between its biological characteristics and the immune system of the patient (Beauvais & Latgé, 2001; Tekaia & Latgé, 2005; Osherov, 2007; Abad *et al*. 2010).

It should be pointed out that the participation of specific virulence factors of *A. fumigatus* in IA is not clear enough. Nowadays, the idea that adaptive capabilities of the fungus growing as a saprophyte in the nature can contribute to its development as human pathogen seems to be gaining in importance. This implies a dual use of its adaptive stress capabilities: survival and growth in nature and adaptation and growth in the host (Hartmann *et al.* 2011). In this way, it seems plausible to assume that most of the virulence factors that allow the fungus to develop the infection can be considered as adaptive mechanisms to environmental stress. Some polygenic factors that influence on conidial size, germination rate, and conidial resistance to removal mechanisms of the host favor the development of the infection. Moreover, once conidia have germinated, pathogenesis can be influenced by factors that have an effect on the growth rate of hyphae, the resistance to host removal mechanisms, tissue invasion and dissemination, and secondary metabolite production.

1.5.1. Thermotolerance of *A. fumigatus*

This fungal species is a thermophilic fungus capable of growing at temperatures higher than 50ºC and surviving at more than 75ºC (Beffa *et al*., 1998; Ryckeboer *et al*., 2003). Thus, it is plausible to think that proteins involved in temperature adaptation could contribute to the virulence of this fungus (Bhabhra & Askew, 2005). So far, some genes have been associated with the thermotolerance of this pathogen, such us *thtA*, *afpmt1*, *kre2/afmnt1*, *cgrA* and *hsp1/aspf12* (Abad *et al*., 2010). Nonetheless, only the protein Hsp1/Asp F 12 seems to be involved in the pathogenesis since it is one of the most immunodominant antigens in IA (Kumar *et al*., 1993). Nierman *et al*. (2005) studied the expression changes between the *A. fumigatus* growth at 30 and 37ºC and 30 and 48ºC, detecting genes up-regulated at 37ºC. However, to day, a direct relation among these genes and *A. fumigatus* pathogenesis has not been demonstrated, concluding that host temperature is not enough to activate genes related to virulence.

1.5.2. Cell wall of *A. fumigatus*

The cell wall of *A. fumigatus* is mainly formed by polysaccharides, proteins, lipids, melanin and other pigments (Gastebois *et al*., 2009). It provides cellular structure, mediates adherence to different surfaces, acts as a molecular sieve allowing selective passage of molecules into and out of the cell, and generates extracellular matrices that forms the basis for the development of a biofilm (Lee & Sheppard, 2016). Furthermore, it is a dynamic structure whose composition varies according to the modifications that occur in the environment. Thus, *A. fumigatus* capacity to maintain cell wall integrity, its functionality and its composition changes in order to adapt to the environment have been other characteristics related to its virulence.

Conidia has a double-layered cell wall, containing the outer layer mainly melanin, a pigment synthesized during conidiation, and hydrophobins, which forms a water-repelent monolayer. The inner layer contains α-(1,3)-glucan (14%), β-(1,3)-glucan (13%), galactomannan (13%), and chitin/chitosan (0.5%), which are covalently associated forming a tightened network of macromolecules. In hyphae, the cell wall also contains two layers. However, unlike conidia, these two layers are composed by polysaccharides. The inner layer contains β-(1,3)-glucan (30%), chitin/chitosan (17%), galactomannan (5%), galactosaminogalactan (GAG) (4%), and β-(1,3;1,4)-glucans (3%), while the outer layer contains α-(1,3)-glucan (42%), GAG (2.3%) and galactomannan (1.4%) (Lee & Sheppard, 2016). It should be highlighted that fungal surface components are not restricted to hyphae and conidia. The mycelium of *A. fumigatus* is surrounded by an extracellular matrix that contains melanin, hydrophobins, glucan, galactomannan and GAG.

1.5.3. Evasion of immune response

Several genes and molecules related to surface structures of *A. fumigatus* activate and interact with the immune system of the host (Osherov, 2007). Amongst them, hydrophobic proteins might be pointed out. These proteins help in conidial dispersion and attachment to solid surfaces (Latgé 1999; Linder *et al*., 2005) and in the adhesion to respiratory epithelium (Thau *et al*., 1994), but they also might be related to the resistance to host cells (Paris *et al*., 2003a). Six genes that encode these proteins have been found in *A. fumigatus*, *rodA* and *rodB* being the most studied. Nevertheless, none

of their deletions have originated an avirulent strain or a strain with an attenuated virulence (Shibuya, 1999; Paris *et al*., 2003a).

Another surface component associate with *A. fumigatus* virulence is melanin, a pigment located on conidia which protects against UV radiation and elevated temperatures, allowing the maintenance of genomic integrity. It also decreases phagocytosis and intracellular traffic to acidic compartments, increases the resistance to reactive oxygen species (ROS) and protects against microbial lytic enzymes and defensins (Jahn *et al*., 2002; Brakhage & Liebmann, 2005; Heinekamp *et al*., 2013). Genes involved in the biosynthesis of this pigment are organized in a gene cluster and they are the following: conidial pigment polyketide synthase *pksP/alb1*, conidial pigment biosynthesis protein *ayg1*, conidial pigment biosynthesis 1,3,6,8-tetrahydroxynaphthalene reductase *arp2*, conidial pigment biosynthesis scytalone dehydratase *arp1*, conidial pigment biosynthesis oxidase *abr1/brown1* and conidial pigment biosynthesis oxidase *abr2* (Tsai *et al*., 1999). This metabolic pathway starts with acetyl-CoA and malonyl-CoA that are converted by Pks/Alb1 and Ayg1 into 1,3,6,8 tetrahydroxynaphtalene (THN). Afterwards, and by successive steps of reduction by Arp2 and dehydration by Arp1 and Abr1, this metabolite is converted to 1,8-dihydroxynaphthalene (DHN), finally polymerized to DHN-melanin by Abr2 (Fig. 1.4).

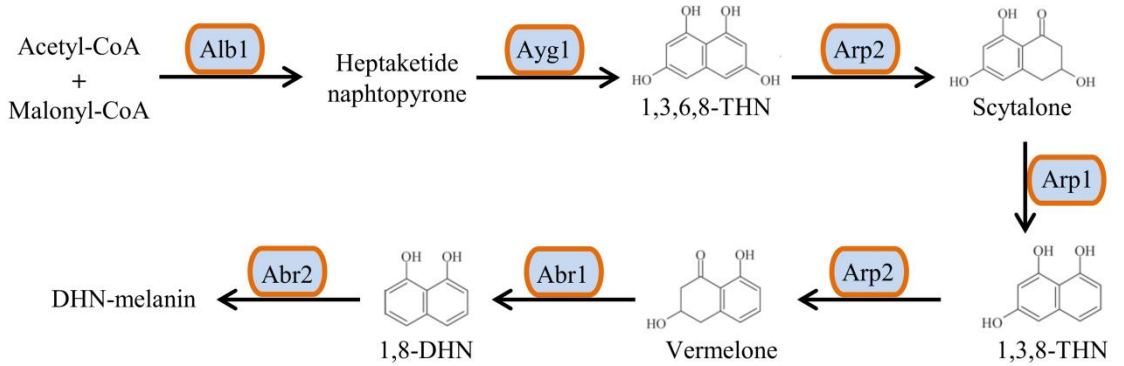

Fig. 1.4. Biosynthetic pathway of melanin in *A. fumigatus* (extracted from Pihet *et al*., 2009). This route initiates with acetyl-CoA and malonyl-CoA which are converted into 1,3,6,8 tetrahydroxynaphtalene (THN) by Pks/Alb1 and Ayg1 enzymes. Then, a series of reduction and dehydration by Arp2, Arp1 and Abr1 enzymes are carried out, synthesizing 1,8-dihydroxynaphthalene (DHN). This metabolite is finally polymerized to DHN-melanin by the enzyme Abr2.

ROS resistance development is another characteristic of this pathogen to evade the immune response. This fungus is provided with 5 genes coding for catalases (*catA*, *catB*/*cat1*, *catC*, *catE* and *cat2*). One of them, encoded by *catA* gene, is found in conidia, and those encoded by *cat1/catB* and *cat2* in hyphae (Paris *et al*., 2003b; Calera *et al*., 1997). It has also been detected 4 genes that code for superoxide dismutases, which eliminate superoxide radicals (Holdom *et al*., 2000; Flückiger *et al*., 2002; Lambou *et al*., 2010). However, their redundancy for ROS detoxification complicates their verification as virulence factors.

1.5.4. Toxins

Up to 10 proteins, some located in conidia and others in hyphae, have been described as toxins produced by *A. fumigatus* that directly attack the host. Associated with conidia, a 14 kDa diffusible substance, unidentified yet, has been described. This toxin affects reversibly macrophages inhibiting ROS release, phagocytosis and cytokines expression (Mitchell *et al*., 1997; Bertout *et al*., 2002). Other toxins located in conidia are fumigaclavines A and C (Coyle *et al*., 2007), alkaloid metabolites that inhibit DNA synthesis, T-cell proliferation and adhesion to extracellular matrix, as well as TNFα production (Zhao *et al*., 2004); and aurasperon C which provokes dysfunctions in the nervous system (Mitchell *et al*., 1997).

Aspergillus fumigatus hyphae produce toxins such as helvolic acid, fumigacine or fumagillin. Fumigacine belongs to a small family of steroidal antibiotics known as fusidanes. At high concentrations, it might affect the oxidative burst of macrophages (Mitchell *et al*., 1997), the metabolism of low density lipoproteins (Shinohara *et al*., 1993), and *in vivo* it induces ciliostasis and rupture of epithelial cells (Amitani *et al*., 1995). On the other hand, fumagillin is an antitumor antibiotic that inhibits angiogenesis and *in vitro* directly inhibits endothelial cell proliferation and cilial movement in respiratory epithelium (Bünger *et al*., 2004). Both toxins, fumigacine and fumagillin, are produced by secondary metabolisms, but their concentrations *in vivo* are still unclear (Rementeria *et al*., 2005).

Another toxin *A. fumigatus* is able to produce is the ribotoxin, protein that have a highly specific activity against the sarcin/ricin domain universally preserved in 28S ribosomal RNA, inhibiting protein biosynthesis (Kao & Davies, 1995; 1999). This toxin is also

known as restrictocin or Asp F 1 and it is related to allergic process, as it is one of the immunodominant antigens of allergic aspergillosis (Arruda *et al*., 1990). This fungus also produces a hemolysin encoded by the *aspHS* gene, which has hemolytic activity on rabbit and sheep erythrocytes, cytotoxic effects on macrophages and endothelial cells *in vitro* (Kumagai *et al*., 1999), and can be detected during infection *in vivo* (Yokota *et al*., 1977). Fumitremorgin A and fumitremorgin B production has also been described (Yamazaki *et al*., 1980; Liu *et al*., 1996). These proteins are neurotropic toxins that cause tremors, seizures, and abnormal behavior in mice, depending on the dosage. Other toxins such as aflatoxin B1 and G1 or verruculogen have been detected in culture filtrates of *A. fumigatus*, but their presence during the infection has not been yet demonstrated (Pepeljnjak *et al*., 2004).

Nevertheless, if there is any toxin that stands out among those produced by *A. fumigatus*, this is gliotoxin. This toxin belongs to the family of epipolythiodioxopiperazines, and it seems to be produced by a group of genes that are activated when secondary metabolism begins (Reeves *et al*., 2004). It has various immunosuppresor effects, among which macrophage phagocytosis, mitogen-activated T cell proliferation, mast cell activation, cytotoxic T-cell response, and monocyte apoptosis are included (Müllbacher & Eichner, 1984; Eichner *et al*., 1986; Yamada *et al*., 2000; Stanzani *et al*., 2005). It also inhibits the NADPH of neutrophils, suppresses ROS production and impairs neutrophil phagocytic capacity, reduces the ciliary movement of epithelial cells and leads to epithelial cells damage (Amitani *et al*., 1995; Watanabe *et al*., 2004; Tsunawaki *et al*., 2004; Orciuolo, 2007). Its presence has been detected in lung and serum of mice suffering from aspergilosis and even in patients with IA, whose gliotoxin levels were 166-785 ng/ml in 80% of them (Richard *et al*., 1996; Lewis *et al*., 2005). Even though its production is not as frequent as in other species of the genus *Aspergillus*, more than 95% of the *A. fumigatus* isolates produce this toxin, regardless of their environmental or clinical origin (Kupfahl *et al*., 2008).

Thirteen genes are included within gliotoxin cluster. These genes encode enzymes involved in the production of this toxin, although the function of two of them (*gliH* and *gliM*) is still unknown (Dolan *et al*., 2015). The transcription factor gliZ is the main regulator of this cluster. Its deletion interrupts the expression of biosynthetic genes and, in turn, gliotoxin production (Bok *et al*., 2006). However, several studies have demonstrated that *gliZ* is not the only regulator of this pathway, as other regulators,

such as the global regulator of secondary metabolism *laeA*, the C_2H_2 transcription factors *gipA* or the *mtfA* transcription factor, also influence on the expression of some gliotoxin related genes (Sugui *et al*., 2007a; Schoberle *et al*., 2014; Smith *et al*., 2014). GliP is a nonribosomal peptide synthase that catalyzes the first step of gliotoxin biosynthesis using phenylalanine and serine as substrates (Cramer *et al*., 2006; Kupfahl *et al*., 2006; Sugui *et al*., 2007b; Spikes *et al*., 2008) (Fig. 1.5). Another gene that must be highlighted is *gliT* since, in addition to its participation in gliotoxin synthesis, it confers self-resistance to *A. fumigatus* against gliotoxin (Schrettl *et al*., 2010; Scharf *et al*., 2010). Finally, this toxin is secreted into extracellular medium through the MFS gliotoxin efflux transporter GliA, which also contributes in self-protection (Wang *et al*., 2014).

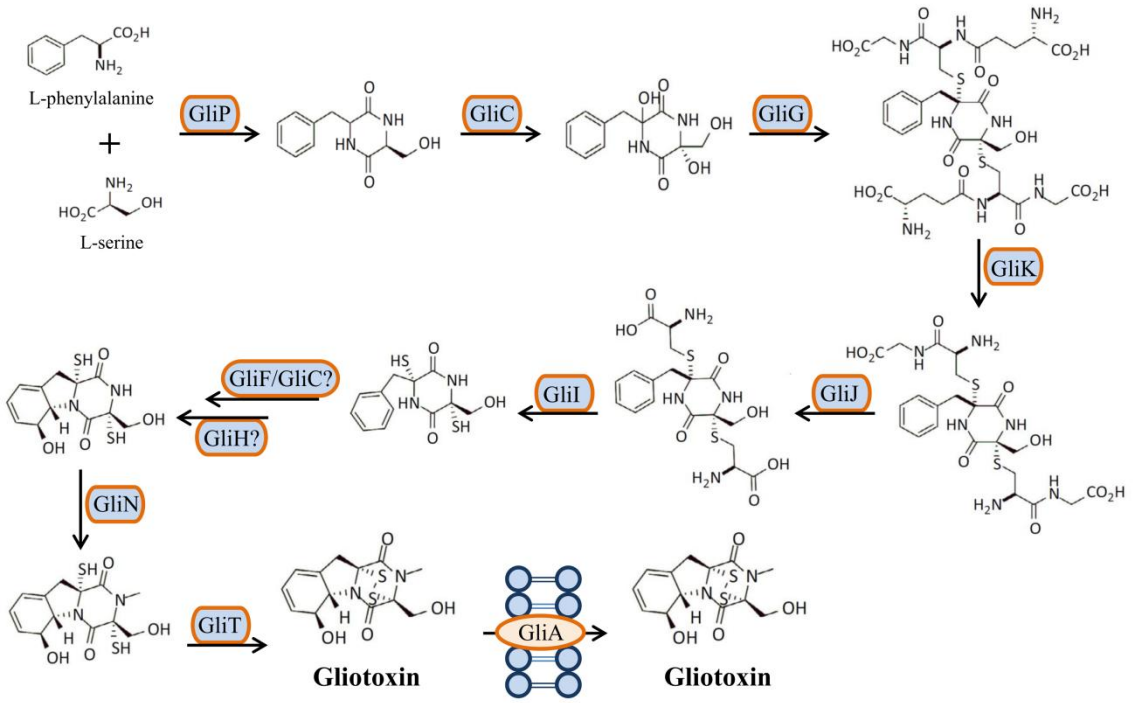

Fig. 1.5. Gliotoxin biosynthesis pathway (modified from Dolan *et al*., 2015). The biosynthesis of this toxins initiates with phenylalanine and serine. This compounds act as substrates to the nonribosomal peptide synthase GliP protein, originating the first intermediate of the pathway. Afterwards, this compound is modified by the following enzymes: cytochrome P450 oxidoreductase GliC , glutathione S-transferase GliG, gliotoxin biosynthesis protein GliK, membrane dipeptidase GliJ, aminotransferase GliI, cytochrome P450 oxidoreductase GliF, toxin biosynthesis protein GliH, methyltransferase GliN and thioredoxin reductase GliT. The secretion of this toxin is carried out through the MFS gliotoxin efflux transporter GliA. Question marks indicate a putative implication that has not been yet demonstrated.

1.5.5. Nutrient uptake

1.5.5.1. Degrading enzymes

Aspergillus fumigatus genome encodes a large number of degrading enzymes, which might explain the ubiquitous growth of this fungus (de Vries & Visser, 2001). This fungus secretes extracellular enzymes, many of them proteases, which degrade and recycle organic matter. However, during an infection, these proteins might break down the structural barriers of the host releasing nutrients into de medium. Several reviews have focused on these kinds of enzymes and on their implication in the pathogenesis of this fungus (Rementeria *et al*., 2005; Hohl & Feldmesser, 2007; Osherov, 2007; Krappmann, 2008; Abad *et al*., 2010). Some proteases can degrade collagen and elastin, main components of the lung matrix. Indeed, previous studies have demonstrated the relation between the elastase activity of *A. fumigatus* strains and their invasive capability, concluding that this kind of activity facilitates the fungus adaptation to the host (Kolattukudy *et al*., 1993; Blanco *et al*., 2002; García *et al*., 2006). Nevertheless, other authors found no statistical correlation between the existence of elastase or acid proteinase activity and the development of invasive disease. Amongst them, serin alkaline protease (Alp, also known as allergen Asp F 13), which degrades elastin, collagen, fibrinogen and casein (Reichard *et al*., 1990; Kolattukudy *et al*., 1993); serine protease Alp2, associated with cell wall; or the extracellular metalloprotease Mep, known as allergen Asp F 5, which degrades collagen and elastine, can be mentioned (Markaryan *et al*., 1994; Sirakova *et al*., 1994). Kauffman *et al*., (2000) demonstrated that secreted proteases induce proinflammatory cytokine release in infected macrophages and epithelial cells, alerting immune system. Nevertheless, their deletion has not shown a clear implication in virulence (Monod *et al*., 2002), probably as a result of the large number of secreted proteases and the functional redundancy amongst them (Robson *et al*., 2005).

Phospholipases are another group of degrading enzymes that *A. fumigatus* produces. These enzymes break the ester bond of phosphoglycerides and may destabilize the host cell membranes causing cell lysis. Phospholipases B, encoded by *plb1*, *plb2* and *plb3* genes, has phospholipase, lisophospholipase and lysophospholipase transacylase activity (Shen *et al*., 2004). Although their implication in the virulence of some especies, such as *Candida albicans* or *Cryptococcus neoformans*, has been described

(Ibrahim *et al*., 1995; Cox *et al*., 2001), their role in *A. fumigatus* pathogenesis is still questioned, since their production in clinical strains is lower than in environmental ones. However, phospholipase C, which was not detected in other species, has higher levels of production in clinical strains (Birch *et al*., 2004).

1.5.5.2. Nitrogen uptake

Nutrient uptake and the ability to incorporate them in limiting environments, such as those found in the host are other important aspects in *A. fumigatus* virulence. One metabolism that has been related to pathogenesis is nitrogen metabolism, as the limitation of this element provokes an important stress during the first steps of the *A. fumigatus* infection (McDonagh *et al*., 2008).

Regarding the utilization of this nutrient only the nitrate assimilation route has been widely studied. This pathway is carried out by 3 components: a nitrate-specific transporter (CrnA) and two enzymes which catalyze the reduction of nitrate via nitrite to ammonium (NiaD and NiiA) (Pateman& Cove, 1967; Johnstone *et al*., 1990), all of them located in a gene cluster. The expression of these genes is regulated by the transcriptional factors AreA and NirA (Kudla *et al*., 1990; Burger *et al*., 1991) (Fig. 1.6) and it is strictly repressed in presence of ammonium and highly induced in presence of nitrate. The total reduction of nitrate produces ammonium, compound finally incorporated in the amino acids glutamate and glutamine. No defined mutant strains for one of the genes located in the nitrate assimilation cluster have been yet tested for their virulence capacities, but the role of the regulator gene *areA* in pulmonary aspergillosis has been scrutinized. The deletion of this transcription factor suggested that the nitrogen sources that are accessible to the fungus during growth in the lung of the host are unlikely to be ammonium or glutamine and that the *areA* gene product contributes to fungal growth in the murine lung (Hensel *et al*., 1998; Krappmann & Braus, 2005).

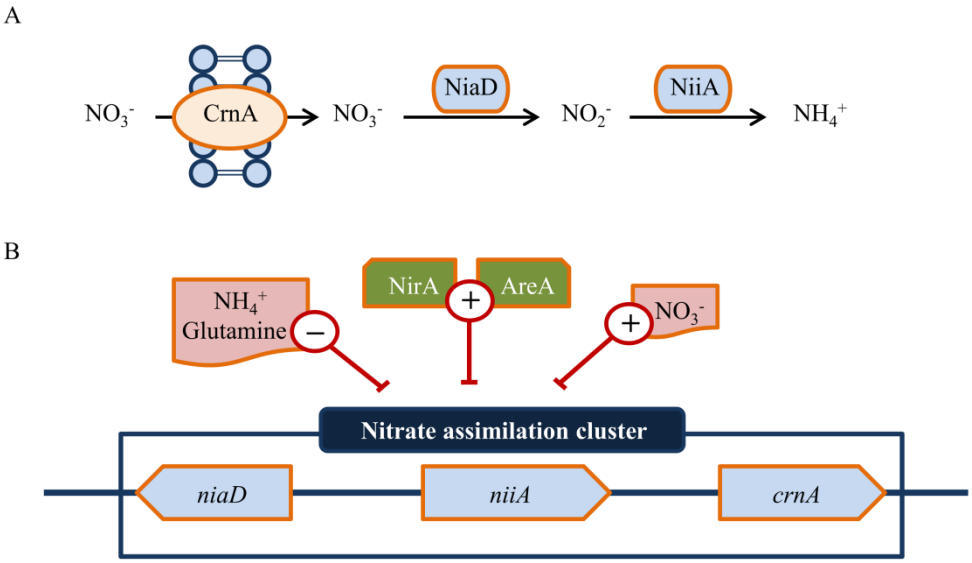

Fig. 1.6. Uptake and utilization of nitrogen (extracted from Krappman & Braus, 2005). A) Extracellular nitrate uptake through the transporter CrnA followed by its reduction to nitrite by the nitrate reductase (NiaD), and its following reduction to ammonium by nitrite reductase (NiiA). B) Genetic organization and regulation of nitrate assimilation cluster. The activation of the cluster requires the presence of nitrate and the absence of ammonium or glutamine metabolites. The transcription factors AreA and NirA induce the expression of the genes involved in nitrate assimilation.

This opportunist pathogen can use a wide range of nitrogen sources, such as ammonium, nitrate, amino acids, or complex substrates (collagen or elastin for instance) (Krappman & Braus, 2005). Therefore, even though glutamate and glutamine are the main nitrogen sources to the fungus, nitrate, purines and other amino acids are considered secondary sources (Marzluf, 1993). Moreover, the implication of other genes involved in nitrogen sensing has also been reported. One example can be found on the gene *rhbA*. This gene codes for a Ras-related protein whose expression is increased in nitrogen-limiting conditions and its deletion results in attenuation in virulence (Panepinto *et al*., 2002; 2003).

Amino acids constitute another important nitrogen source. Even though during the infectious process not all of them are available, Ibrahim-Granet *et al*. (2008) suggested that these compounds act as nitrogen sources during the invasive growth of *A. fumigatus*. Furthermore, the fungal biosynthesis of these elements has received a great interest as fungi, unlike mammals, are able to synthesize *de novo* the 20 amino acids (Krappmann & Braus, 2005). The transcription factor CpcA activates the expression of those genes that encode components of amino acids biosynthetic pathways under stress conditions or under their starvation (Rhodes & Brakhage, 2006) and its deletion has been associated with *A. fumigatus* pathogenesis (Krappmann *et al*., 2004). The role in mammalian pathogenicity of several amino acid biosynthetic genes has already been

tested. However, the uptake of exogenous amino acids and the different niche-specific nutritional requirements raise doubt about the potential of these pathways as targets for antifungal treatments (Amich & Bignell, 2016).

1.5.5.3. Zinc acquisition

Zinc is a critical nutrient in the regulation of gene expression. Roughly 44% of the transcription factors are zinc-dependent and 50% of eukaryotic proteins are zinc-binding proteins (Hood & Skaar, 2012). The amount of labile zinc in host tissues is very low, since the majority of them are bound to proteins (Iyengar & Woittiez, 1988). Moreover, its availability could be decreased along the infectious process because of its chelation by the calprotectin or metallothionein produced by the immune system (Corbin *et al*., 2008; Subramanian Vignesh *et al*., 2013). Furthermore, if zinc concentration exceeds the maximum tolerated by the fungus, it might became a toxic compound as it can react with -SH prosthetic groups of proteins (Amich & Calera, 2014). When it comes to its role in pathogens, its implication in superoxide dismutase activity might be mentioned, protecting fungal cells from oxidative stress (Lamarre *et al*., 2001; Hwang *et al*., 2003).

Proteins that participate in zinc homeostasis in zinc-limiting conditions and that allow the fungus to overcome its starvation belong to ZIP family of eukaryotic zinc transporters. On the other hand, transporters involve in protecting fungal cells from zinc toxicity belong to the cation diffusion facilitator (CDF) family of zinc transporters. Their function consists of transporting zinc and/or other metal ions from extracellular medium or lumen of intracellular organelles to cytoplasm (Gaither & Eide, 2001). Analyzing the *A. fumigatus* genome, 8 genes that encode ZIP transporters (ZrfA-H), being *zrfA*, *zrfB* and *zrfC* the most studied, and 8 that code for CDF transporters (*mscA*, *zrgA*, *zrcA*, *zrcB*, *zrcC*, *mmtA*, *mtpA* and *mtpB*) have been found. It has also been reported cysteine-rich transporters and proteins which could be involved in zinc homeostasis, its export and detoxification (Sinclair & Krämer, 2012; Porcheron *et al*., 2013; Shafeeq *et al*., 2013), as well as 3 proteins related to the COG0523 family of putative metal chaperones that could participate in zinc homeostasis (Haas *et al*., 2009). Thus, *A. fumigatus* is well equipped to face the starvation and even the excess of this metal.

The homeostasis of this metal is regulated by the transcription factor ZafA (Moreno *et al*., 2007). In acid zinc-limiting conditions, this regulator induces the expression of the transporters *zrfA* and *zrfB* (Vicentefranqueira *et al*., 2005). However, when the pathogen is in alkaline zinc-limiting medium, condition typically found in lung tissues, ZafA induces the expression of the transporter *zrfC* (Amich *et al*., 2010). Therefore, the transporters ZrfA and ZrfB are responsible for taking this metal in acid conditions (Vicentefranqueira *et al*., 2005, Amich *et al*., 2014), whereas ZrfC does so in alkaline conditions (Amich *et al*., 2010; 2014). It should be pointed out that the expression of this last transporter has been also regulated by the transcription factor PacC (Amich *et al*., 2010), which regulates gene expression in response to pH changes in the medium (Peñalva *et al*., 2008). Moreover, this gene is located next to the gene that encodes the allergen Asp F 2, whose expression is regulated by *zafA* and *pacC* in the same way as *zrfC* (Amich *et al*., 2010), indicating a possible implication of Asp F 2 in zinc homeostasis. Finally, it should be mentioned that zinc homeostasis regulation as well as its acquisition seems to be useful in antifungal therapies since the deletions of *zafA* and *zrfC* genes demonstrated their implication in *A. fumigatus* virulence (Moreno *et al*., 2007; Amich *et al*., 2014).

1.5.5.4. Iron acquisition

Iron is an indispensable cofactor in a large number of cellular process including respiration, tricarboxylic acid cycle, amino acid metabolims, nitrogen fixation, and DNA and sterol biosynthesis. However, an increase in its concentration can lead to ROS (Halliwell & Gutteridge, 1984). Moreover, iron proteins act as sensors and regulators of gene expression in different pathways (Philpott *et al*., 2012).

Micromolecular levels of free iron are essential in fungal growth, but in the host iron-binding proteins restrict the amount of ionic iron available in body fluids to 10^{-18} M (Bullen, 1981). Among these proteins, transferring, lactoferrin, ferritin or hemoglobin stand out (Haas, 2014). This way, to take iron, *A. fumigatus* has developed three systems: low-affinity iron uptake, reductive iron assimilation (RIA) and siderophore-mediated iron uptake (Haas *et al*., 2008). This last strategy has demonstrated to be highly related to the virulence of this pathogen. *A. fumigatus* produces 4 different siderophores. Two of them, fusarine C (FsC) and triacetylfusarine C (TAFC), are extracellular and used in iron uptake. On the other hand, ferricrocine (FC) and

hydroxyferricrocin (HFC) are intracellular and responsible for iron distribution and storage in hyphae and conidia, respectively (Schrettl *et al*., 2007).

Siderophore biosynthesis pathway starts with two different compounds, L-arginine and mevalonate. The first one is converted to L-ornithine by the arginase AgaA when L-ornithine is exported from the mitochondrion to the cytosol via the transporter AmcA. On the other hand, mevalonate is synthesized by the hydroxymethylglutaryl-CoA (HMG-CoA) reductase Hmg1 using the HMG-CoA as substrate (Hass, 2004). Once synthesized, both precursors are modified by the activity and implication of the following enzymes: L-ornithine N5-oxygenase SidA, siderophore biosynthesis protein SidL, nonribosomal siderophore peptide synthase SidC, long-chain-fatty-acid-CoA ligase SidI, enoyl-CoA hydratase/isomerase family protein SidH, siderophore biosynthesis acetylase AceI (SidF), 4'-phosphopantetheinyl transferase PptA, nonribosomal peptide synthase SidD and GNAT family acetyltransferase SidG (Fig. 1.7).

The cellular adaptation to iron starving conditions requires the up-regulation of high affinity iron uptake, its consumption and its storage. Nevertheless, the adaptation to its excess requires the opposite processes (Schrettl *et al*., 2008). The main iron regulators at transcriptional levels in *A. fumigatus* are the transcription factors SreA and HapX (Schrettl *et al*., 2008, Schrettl *et al*., 2010). When iron concentrations are high enough, SreA represses high affinity iron uptake systems in order to prevent its toxicity. In iron starvation conditions it is HapX that represses iron consumption pathways, such as respiration and other iron-dependent process, and activates iron uptake through siderophores. It should be pointed out that Gsaller *et al*. (2014) demonstrated that this transcription factor is also essential in iron resistance as it activates the vacuolar iron storage in non-limiting conditions, activation that is repressed in starving situations. In addition to these regulators, other transcription factors involved in iron homeostasis (SrbA, AcuM, PrtT, HacA/Irea, MpkA) and which act in combination with SreA and HapX or independently have also been described (Moore, 2013).

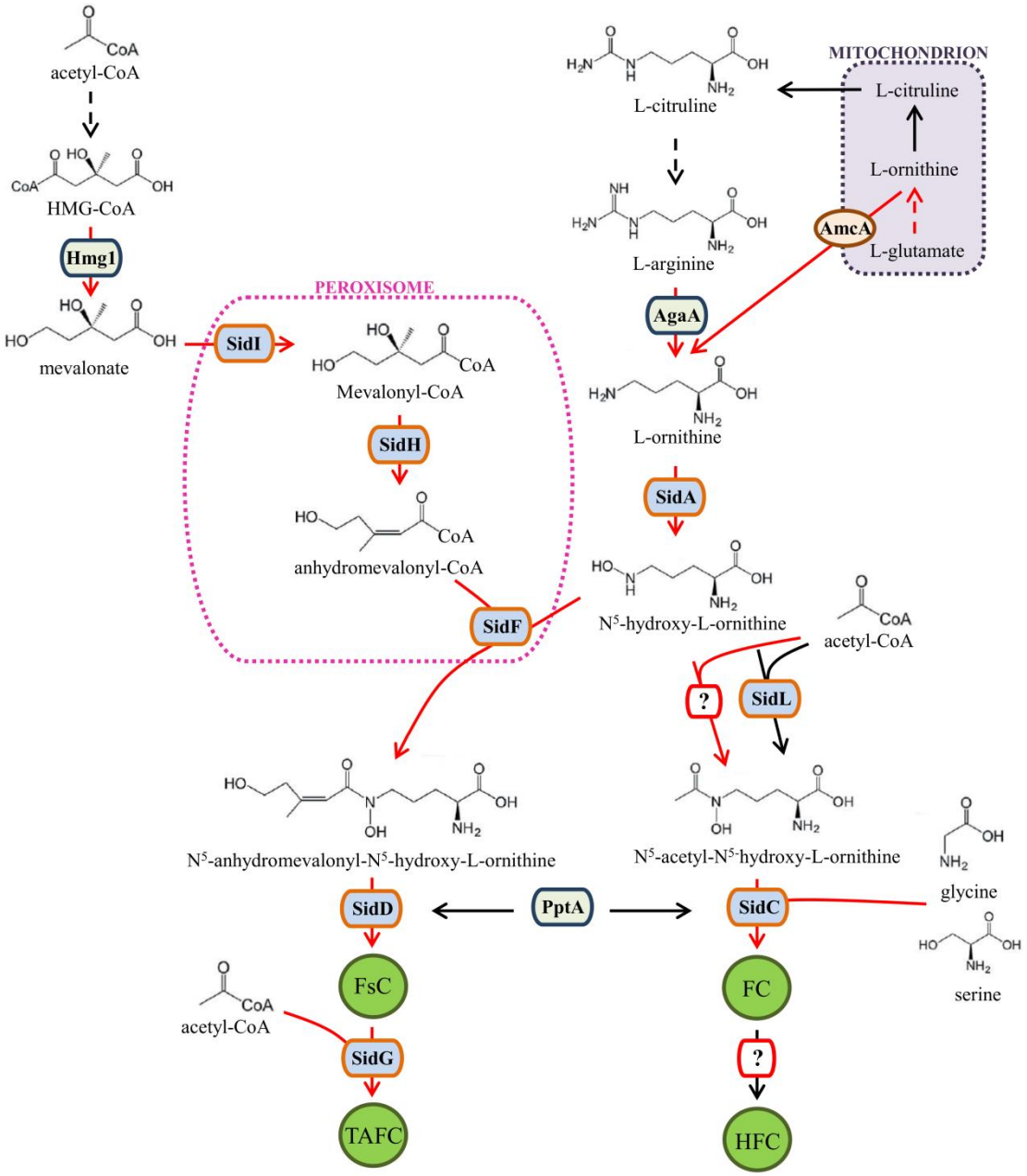

Fig. 1.7. *Aspergillus fumigatus* siderophore biosynthesis pathway (extracted from Haas, 2014). Fusarine C (FsC), triacetylfusarine C (TAFC), ferricrocine (FC) and hydroxyferricrocin (HFC) appear in green circles. Enzymes and putative enzymes involved in this pathway are represented in blue boxes with orange borders and white-greenish boxes with blue borders, respectively. Question marks symbolize unknown enzymes that must catalyze the reactions. Red arrows indicate those routes up-regulated in iron-limiting conditions, and discontinuous arrows indicate reactions in which more than one enzyme is involved. Mitochondrion and peroxisome are represented in purple and pink, respectively.

The deletion of genes involved in the biosynthesis of extracellular siderophores (Δ*sidI*, Δ*sidH*, Δ*sidF* and Δ*sidD*) showed a reduction in growth, conidation, and oxidative stress resistance during iron starvation but not under non-limiting conditions, as iron uptake is compensated by other systems, such as RIA (Schrettl *et al.*, 2007). On the other hand, with the deletion of genes related to the synthesis of intracellular siderophores (Δ*sidC* and Δ*sidL*), conidation, conidial size, and oxidative stress resistance are decreased,

sexual development blocked, and even germination delayed under iron starvation conditions (Eisendle *et al*., 2006, Oide *et al*., 2007, Schrettl *et al*., 2007, Blatzer *et al*., 2011, Wallner *et al*., 2009). With regard to their implication in virulence, both extra- and intracellular siderophores are essential in *A. fumigatus* pathogenesis given that the deletion of *sidA*, first enzyme that catalyzes siderophore biosynthesis pathway, generates an avirulent strain in murine models of aspergillosis (Schrettl *et al*., 2004, Hissen *et al*., 2005). However, the deletion of genes involved in either extracellular (Δ*sidI*, Δ*sidH*, Δ*sidF* and Δ*sidD*) or intracellular (Δ*sidC*) siderophores causes a partial attenuation of virulence (Schrettl *et al*., 2007, Yasmin *et al*., 2012). Moreover, during an infection and after murine alveolar macrophage phagocytosis, siderophores are also important for intracellular growth and fungal survival (Schrettl *et al*., 2010). Indeed, *sidA* was one of the most up-regulated genes after the phagocytosis of *A. fumigatus* by epithelial cells (Oosthuizen *et al*., 2011). Thus, siderophore biosynthesis pathway represents a promising target for therapeutic intervention.

RIA is carried out by plasma membrane-localized ferrireductases which are associated with a ferroxidase and the iron permease Ftr. Nevertheless, even though this system has not been directly related to *A. fumigatus* virulence, there are some evidence that suggest it might play a role during the infection: The partial attenuation of virulence detected with extracellular siderophores deletion; the inability of mutants lacking both *sidA* and *Ftr* to growth without high iron conditions or supplementation with siderophores (Schrettl *et al*., 2004); and the induction of siderophore system and RIA during iron starvation observed in a transcriptomic study (McDonagh *et al*., 2008)

1.5.6. Allergens

Aspergillus fumigatus produces a large number of allergenic molecules that react with IgE in patients with asthma or ABPA (Knutsen *et al*., 2004). So far, 22 allergens produced by this fungus have been described and have names in the range Asp F 1-Asp F 34 (Table 1.2). Amongst them, there are several enzymes that are secreted into extracellular medium and associated with host invasion (Asp F 5, Asp F 10, Asp F 15 and Asp F 18). Allergen such as Asp F 8, Asp F 12, Asp F 22 and Asp F 23 appear not to be neither secreted nor cell wall-associated proteins (Osherov, 2007). Nonetheless, these molecules might be cytosolic proteins that following the damage caused by immune system would be secreted into extracellular medium or proteins located in cell

surface with unknown function (López-Ribot *et al*., 2004). It should be highlighted that some allergens show cross-reactivity with various conserved proteins, including some human proteins. Asp F 6 (manganese superoxide dismutase, MnSOD), Asp F 8 (60S acidic ribosomal protein P2), Asp F 11 and Asp F 27 (cyclophilins), and Asp F 28 and Asp F 29 (thioredoxins) can cause autoimmunity problems in patients due to this cross-reactivity (Abad *et al*., 2010).

Table 1.2. *A. fumigatus* allergens (extracted from Abad *et al*., 2010; Low *et al*., 2011).

Allergen	Gene product description[a]	Locus ID[b]	Activity related to pathogenesis[c]
Asp F 1	Major allergen and cytotoxin Asp F 1	AFUA_5G02330	Protein biosynthesis inhibition Cytotoxin Apoptosis
Asp F 2	Major allergen Asp F 2	AFUA_4G09580	Adhesion
Asp F 3	Allergen Asp F 3, peroxysomal protein	AFUA_6G02280	
Asp F 4	Allergen Asp F 4, glucosidase	AFUA_2G03830	
Asp F 5	Elastinolytic metalloproteinase Mep	AFUA_8G07080	Tissue destruction/invasion
Asp F 6	Mn superoxide dismutase MnSOD	AFUA_1G14550	ROS protection Autoimmunity
Asp F 7	Allergen Asp F 7, glucosidase	AFUA_4G06670	
Asp F 8	60S acidic ribosomal protein P2/allergen Asp F 8	AFUA_2G10100	Autoimmunity
Asp F 9	Extracellular cell wall glucanase Crf1/allergen Asp F 9	AFUA_1G16190	
Asp F 10	Aspartic endopeptidase Pep1/aspergillopepsin F	AFUA_5G13300	Tissue destruction/invasion
Asp F 11	Peptidyl-prolyl cis-trans isomerase	AFUA_2G03720	Autoimmunity
Asp F 12	Molecular chaperone and allergen Mod-E/Hsp90/Hsp1	AFUA_5G04170	Chaperone activity and protein transport in growth at 37ºC Stress response during inflammation Autoimmunity
Asp F 13	Allergenic cerato-platanin Asp F 13	AFUA_2G12630	
Asp F 15	Alkaline serine protease Alp1	AFUA_4G11800	Tissue destruction/invasion
Asp F 17	Cell wall serine-threonine-rich galactomannoprotein Mp1	AFUA_4G03240	Adhesion
Asp F 18	Autophagic serine protease Alp2	AFUA_5G09210	Tissue destruction/invasion
Asp F 22	Enolase/allergen Asp F 22	AFUA_6G06770	
Asp F 23	60S ribosomal protein L3	AFUA_2G11850	
Asp F 27	Peptidyl-prolyl cis-trans isomerase/cyclophilin, putative	AFUA_3G07430	Autoimmunity
Asp F 28	Thioredoxin	AFUA_6G10300	Autoimmunity
Asp F 29	Thioredoxin TrxA	AFUA_5G11320	Autoimmunity
Asp F 34	Cell wall protein PhiA	AFUA_3G03060	

Note: Every allergen provokes type I hypersensitivity reaction.
[a]Gene product description.
[b]GenBank accession number.
[c]Allergenic activity that has been related to *A. fumigatus* pathogenesis.

Among the allergens produced by this fungus, some of them have structural, toxic or enzymatic functions, but others, apart from acting as allergens, have also been described as virulence factors (Asp F 1, Asp F 2 and Asp F 6, for instance) (Abad *et al*., 2010).

Asp F 1 not only has allergenic and ribonuclease activity, but it also has cytotoxic and apoptotic activity, being even involved in protein biosynthesis inhibition (Arruda *et al*., 1990, Smith *et al*., 1993; Priyadarsiny *et al*., 2003). Asp F 2 seems to be associated with adhesion (Banerjee *et al*., 2003; Amich *et al*., 2010) and epithelial damage of host, which leads to an inflammatory reaction in mucosal surface or in the center of colonization (Crameri, 1999). Furthermore, as mentioned above, this allergen appears to be involved in zinc homeostasis (Amich *et al*., 2010). Finally, Asp F 6 is a MnSOD that confers protection to *A. fumigatus* against ROS and that might cause certain degree of autoimmunity to the host (Crameri, 1998; Crameri *et al*., 2010, Lambou *et al*., 2010). Nevertheless, it should be pointed out that even though the presence of allergens on conidia, their release after the destruction of spores by pulmonary phagocytes, or their production during fungal growth have been described, their behavior in IA is still unclear (Abad *et al*., 2010).

1.5.7. Transcription factors

Transcription factors bind to particular DNA sequences in gene regulatory regions and control their transcription with a positive or an inhibiting effect on transcription (Latchman, 1993). *A. fumigatus* possesses around 500 transcription factors and so far only a little part of them has been studied. Nevertheless, taking into consideration that a single transcription factor frequently controls the expression of more than one gene, the study of these genes is becoming an alternative approach to study the virulence of this pathogen.

Main pathways related to the virulence of this fungus are regulated by one or more transcription factors and the implication of some of them in virulence has been already studied. In some cases, the deletion of a transcription factor did not really show a clear implication in virulence, even though the genes it regulates appear to be involved in pathogenesis. Amongst these transcription factors, *areA*, which is implicated in nitrogen metabolism (Hensel *et al*., 1998); *afyapI*, the major regulator for defense against ROS (Lessing *et al*., 2007); *prtT*, which controls the expression of multiple secreted proteases (Sharon *et al*., 2009); or *mpkA*, involved in cell wall integrity, oxidative stress response, gliotoxin production and iron adaptation (Jain *et al*., 2011) might be mentioned. However, in other cases, the deletion did cause attenuation of virulence. Examples can be found in *cpcA*, involved in amino acid biosynthesis (Krappmann *et al*., 2004); *gliZ*,

which regulates gliotoxin production (Bok *et al*., 2006); *zafA*, implicated in zinc homeostasis (Moreno *et al*., 2007); *srbA*, required for cell polarity, hypoxia adaptation and azole drug resistance (Willger *et al*., 2008); *ace2*, realted to pigment production and conidiation (Ejzykowicz *et al*., 2009); *hapX*, related to iron homeostasis (Schrettl *et al*., 2010) or *somA*, required for adhesion and development (Lin *et al*., 2015).

1.6. Study of *A. fumigatus* virulence

1.6.1. *Aspergillus fumigatus* knockout strains

The disruption of a gene of interest by homologous recombination has been the main strategy to study the virulence of *A. fumigatus*. This technique consists of replacing a specific gene with a marker, such as a resistance gene, by homologous recombination. To do so, a deletion cassette has to be constructed adding to the marker gene the 5' and 3' flanking regions of the gen of interest. The construction of this cassette can be made through different cloning techniques or through a PCR and the subsequent fusion of PCR products (Fig. 1.8).

Aspergillus fumigatus transformation is carried out following the generation of protoplasts, germinated conidia whose cell wall has been removed by lytic enzymes, which facilitates the uptake of exogenous DNA. This way, once protoplasts have been obtained, the deletion cassette is co-incubated with the pathogen so that it penetrates into fungal cells and homologous recombination takes place. Given that the gene of interest is generally replaced by an antibiotic resistance gene, every colony that is able to growth in the medium with the antibiotic chosen would correspond to a knockout strain. However, the deletion has to be confirmed by PCR and Sourthen Blot.

The development of *A. fumigatus* knockout strains has allowed studying the role of selected genes during the germination or fungal growth by comparing their germination and growth rate to the wild type (Jadoun *et al*., 2004; Liebmann *et al*., 2004; Schrettl *et al*., 2004; Coyle *et al*., 2007; Schrettl *et al*., 2010; Oliver *et al*., 2012). Nevertheless, to assess the virulence of a knockout, every study ends up with an animal infection in which the survival rate of animals is compared to those obtained with the wild type (Liebmann *et al*., 2004; Schrettl *et al*., 2004; Hissen *et al*., 2005; da Silva Ferreira *et al*., 2006; Bok *et al*., 2006; Moreno *et al*., 2007; Spikes *et al*., 2008; Schrettl *et al*., 2010; Oliver *et al*., 2012; Beauvais *et al*., 2013; Muszkieta *et al*., 2014; Amich *et al*., 2016).

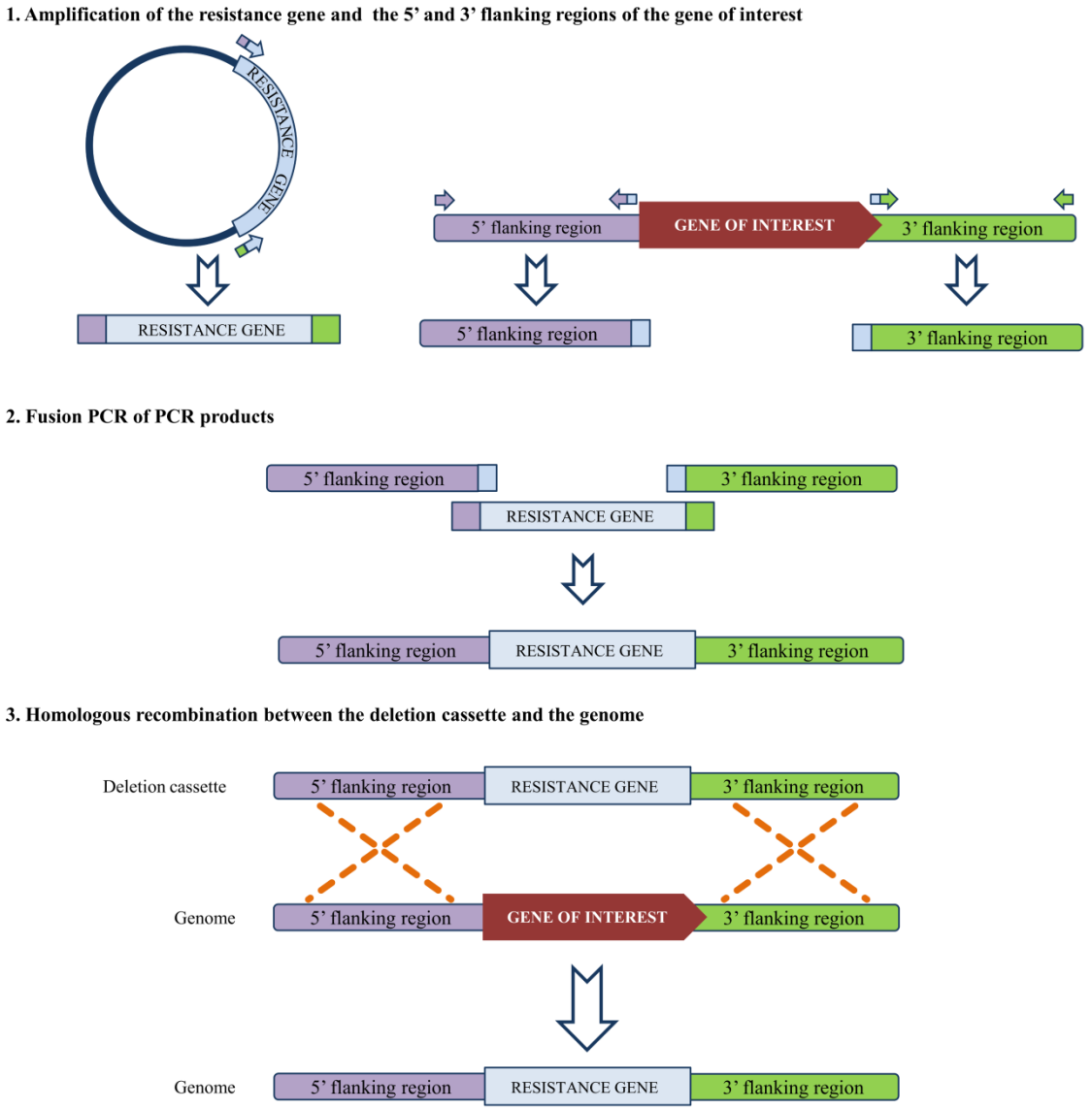

Fig. 1.8. Schematic representation of gene replacement by homologous recombination. This method consists of three different steps. Step 1: Amplification of the resistance gene and the 5' and 3' flanking regions of the gene of interest. Step 2: Fusion PCR of the PCR products obtained in Step 1. The final product of this step is the deletion cassette. Step 3: Homologous recombination between the deletion cassette and the genome. The gene of interest is replaced by the resistance gene.

Even though the implication of several genes in the virulence of this pathogen has been demonstrated by these kinds of studies, none of the deletions have proved to be significant enough in the pathogenicity of this fungus, supporting the theory that *A. fumigatus* virulence is polygenic. Therefore, the generation of knockout strains is a strategy that shows certain degree of limitation in the study of *A. fumigatus* pathogenesis. To obtain more accurate results the number of deletions should be increased, process that would raise the price and take more time.

1.6.2. Transcriptomic studies

The whole genome sequencing of *A. fumigatus* has led to the post-genomic era whose main aim is to understand how the fungus behaves based on nucleotide sequences. Even though mRNA (messenger RNA) is not the final product of a gene, transcription is the first step in gene regulation, and the information obtained from its transcriptomic levels is indispensable to shed light on the regulation of cell pathways and processes. Furthermore, establishing mRNA levels is not a very expensive technique and it might be performed in a more accurate way than proteomic studies. Despite the fact that the correlation between mRNA and protein has not to be direct, the absence of a transcript implies that its protein is not synthesized or that it is but at very low levels. Therefore, using mRNA, proteome might be quantitatively estimated (Brazma & Vilo, 2000). Basing on this technique some issues have started elucidating, such as the main role of genes, cell processes in which they are involved, or how their expression levels change according to the cell type, during an infection o regarding therapeutic treatments.

Research on *A. fumigatus* expression may help to understand the pathogenesis of this fungus, as well as on the genes involved in it. These studies might be carried out by reverse transcription polymerase chain reaction (RT-PCR) or microarrays, which allow analyzing the expression of the whole fungal genome (Breakspear & Momany 2007).

1.6.2.1. Reverse transcription polymerase chain reaction (RT-qPCR)

Real time PCR (qPCR) is a modification of conventional PCR that has revolutionized biological research. It was firstly used in 1992 by Higuchi *et al*. (1992, 1993) and since then its use has substantially increased. It has been used in genotyping (Alker *et al*., 2004; Cheng *et al*., 2004; Gibson, 2006), quantification of viral load in patients (Ward *et al*., 2004), and determination of gene copy number in cancer cells (Bièche *et al*., 1998; Königshoff *et al*., 2003; Kindich *et al*., 2005). Unlike other methods, such as northern blot or RNase protection assay, which are time consuming and sometimes prove difficult to reliably generate accurate measurements of gene expression levels, qPCR offers several advantages: it can be performed with a small amount of sample, gives the opportunity to analyze more than one gene at once, and has the ability to reproduce rapid and accurate data (Fraga *et al*., 2008).

When the Real Time PCR is combined with a reverse transcription reaction (RT-qPCR) it is able to determine the amount of mRNA of a sample by relative quantification. This is the field in which this technique has had a major impact. The quantification of expression levels allow identifying the cellular type or the tissue in which a gene is expressed, revealing expression levels relative to certain conditions, and detecting expression changes due to a specific stimulus. The quantification of the product is performed by adding fluorophores that bind to the amplicon. Thus, the more product is synthesized, the more fluorescence is detected. In RT-qPCR two fluorochromes are commonly used. One of them, widely used because of its reduced price, is SYBR Green or Eva Green, which binds nonspecifically to double-stranded DNA. The other alternative, more expensive but recommended when specificity problems appears, is TaqMan or hydrolysis probes. In this case, the quantification of the cDNA (complementary DNA, synthesized from mRNA) of interest is specific even when unspecific amplifications are present in the sample owing to primer dimmers or genomic DNA.

In RT-qPCR, the gene expression of each sample is determined by relative quantification, which is based on the expression levels of a target gene *versus* one or more housekeeping genes (reference genes with no variation in their expression). This is known as normalization of gene expression or normalization relative to the amount of total RNA that are found in the samples. Thus, if the level of housekeeping genes varies, it is due to the amount of total RNA used in cDNA synthesis and not to expression changes. 18S rRNA, glyceraldehyde 3-phosphate dehydrogenase or beta-actin are housekeeping genes commonly used. However, there is no gene whose expression does not change regardless of the conditions so, for each experiment, this election must be thoughtfully assessed.

Depending on the efficiency and comparison among the target and housekeeping genes, there are two quantification methods. One of them is ΔΔCt method. By this method, Cts (threshold cycle) from the gene of interest are firstly compared to those obtained with housekeeping genes in each sample and afterwards, Cts of each condition studied are compared to those obtained in the control condition. On the other hand, another method is based on a standard curve designed with known amounts of cDNA. This curve allow extrapolating the amount of a gene found in a sample using its Ct as reference. With the

amount determinate, the relation between target and housekeeping genes are established and then, the relation amongst different conditions calculated.

1.6.2.2. Expression microarrays

Understanding the complex genetic processes that underlie the interaction of *A. fumigatus* and the host would provide scientists with an important knowledge about IA and the subsequent improvement in diagnostic, treatment and prevention. The ability to monitor gene expression at transcriptomic level has been possible thank to the design of expression microarrays, as they allow analyzing thousands of gene transcripts simultaneously in a single experiment.

Microarray technology is based on the Southern or Northern hybridization, capacity of DNA to hybridize with other DNA or RNA that has a complementary nucleotide sequence. The main advantage microarrays present over conventional hybridization technologies (dot-blot) is the amount of genes that can be analyze at once. A microarray consists of a large number of DNA molecules attached to a solid surface, such as a glass slide. These molecules can be oligonucleotides, cDNA or PCR products. Nucleic acids attached to the slides are called "probes" and their number is variable (10,000 - 244,000 spots/cm^2). Moreover, the flexibility found on the microarray manufacturing process gives the opportunity to design customized microarrays and to attach DNA fragments of interest. For instance, once identified a virulence factor of a fungus, this technique might be used to design customized systems that allow panfungal identification.

Nucleic acid samples are labeled by different methods, such as enzymatic or fluorescent methods, and incubated with the microarray. During this process, the labeled sample hybridizes to complementary sequences attached to the slide. DNA or RNA samples are usually labeled with a fluorescent dye so, the fluorescence emitted allows the identification and quantification of the nucleic acids present in the sample. Finally, the quantitative ratio between the two samples (interest condition *versus* control condition) gives information about the up- or down-regulation of the gene expression. In addition, this technique offers the possibility to hybridize two samples simultaneously if each one is labeled with a different dye (competitive hybridization). However, this strategy has some drawbacks given that the incorporation of fluorophores is not uniform for all assays.

The main advantage of this technology is found in its small size and high sensitivity, allowing the detection of differences that might be almost undetectable with other molecular methods. Furthermore, the simultaneous analysis of a large number of genes, the use of an initial sample with low volume and the possibility to compare results of different samples are other reasons that explain its success (van Hal *et al*., 2000).

The quantity of data generated from microarray experiments can be enormous but it is only useful if it can be interpreted. The fact that a gene is up-regulated under a particular condition is not an answer in itself but only the first step in understanding how it behaves (Bryant *et al*., 2004). Therefore, microarrays offer the potential to revolutionize the research in several biological fields and the management of many diseases, being determinant to develop diagnostic, treatment and prevention strategies.

The genome of *A. fumigatus* Af-293 was sequenced in 2005 (Nierman *et al*., 2005), and since then expression microarrays have been developed to analyze the transcriptome of this fungus. The first one was developed by The Institute for Genome Research (TIGR) and commercialized by J. Craig Venter Institute, in whose last version 10,003 probes of *A. fumigatus* Af-293 were attached. Several articles have been published studying the transcriptome of this pathogen under different conditions, such as its exposure to high temperatures (Nierman *et al*., 2005) or amphotericin B and voriconazole (da Silva Ferreira *et al*., 2006); during the germination and hyphal development (Sugui *et al*., 2008); and even during the infection of human cells (Oosthuizen *et al*., 2011; Morton *et al*., 2011; Perkhofer *et al*., 2015). All these studies have allowed shedding light on the function and behavior of some genes and understanding how the fungus behaves in the presence of antifungals or in the host environment. Nevertheless, the pathogenicity mechanism is not clear enough, restricting the development of diagnostic or treatment targets.

2. OBJECTIVE

Due to the multifactorial and polygenic virulence of *A. fumigatus*, transcriptomic analysis seems to be one of the best strategies to understand its pathogenesis. Therefore, the aim of this project consists of developing an expression microarray covering the entire genome of *A. fumigatus* and analyzing its transcriptome during the germination and throughout a disseminated infection in order to select specific genes that might be involved in *A. fumigatus* virulence.

To achieve this aim the objectives are:

1. To design a whole genome expression microarray of *A. fumigatus* to perform transcriptomic studies in different conditions.

2. To analyze the *A. fumigatus* transcriptome response to a higher temperature during the earliest steps of germination.

3. To analyze the *A. fumigatus* transcriptome throughout a disseminated infection.

4. To select genes and generate knockout strains to study their implication in the virulence of this pathogen.

3. MATERIALS & METHODS

3. 1. Microorganisms and culture conditions

3.1.1. Solutions and culture media

3.1.1.1. Saline/Tween Solution (SS-T)

NaCl	9 g
Tween 20	200 µl
Distilled water	1 l

It was sterilized by autoclaving at 121ºC for 15 minutes.

3.1.1.2. Saline Solution 0.9%

NaCl	9 g
Distilled water	1 l

It was sterilized by autoclaving at 121ºC for 15 minutes.

3.1.1.3. 20X Salt Solution

$NaN0_3$	120 g
KCl	10.4 g
$MgSO_4.7H_2O$	10.4 g
KH_2PO_4	30.4g
Distilled water	1 l

It was sterilized by autoclaving at 121ºC for 15 minutes.

3.1.1.4. Trace Elements Solution

$ZnSO_4.7H_2O$	2.2 g
H_3BO_3	1.1 g
$MnCl_2.4H_2O$	0.5 g
$FeSO_4.7H_2O$	0.5 g
$CoCl_2.6H_2O$	0.16 g
$CuSO_4.5H_2O$	0.16 g
$(NH_4)_6Mo_7O_{24}.4H_2O$	0.11 g
EDTA	5 g
Distilled water	80 ml

pH was adjusted to 6.5 with KOH pellets and the volume increased up to 100 ml with distilled water. It was sterilized by autoclaving at 121ºC for 15 minutes.

3.1.1.5. Sabouraud Glucose Agar (SGA) (Cultimed, Barcelona, Spain. Ref. 413802)

D(+)-Glucose	40 g
Mixture of peptic digest animal tissue and pancreatic digest of casein	10 g
Agar	15 g
Distilled water	1 l

It was sterilized by autoclaving at 121ºC for 15 minutes.

3.1.1.6. Sabouraud Glucose Agar with Chloramphenicol (Cultimed. Ref. 413842)

D(+)-Glucose	40 g
Chloramphenicol	0.05 g
Mixture of peptic digest animal tissue and pancreatic digest of casein	10 g
Agar	15 g
Distilled water	1 l

It was sterilized by autoclaving at 121ºC for 15 minutes.

3.1.1.7. Potato Dextrose Agar (PDA) (Pronadisa, Madrid, Spain. Ref. 1022.00)

Dextrose	20 g
Infusion from potato	4 g
Agar	15 g
Distilled water	1 l

It was sterilized by autoclaving at 121ºC for 15 minutes.

3.1.1.8. *Aspergillus* Minimal Medium Agar (AMM)

20X Salt solution	50 ml
Trace Elements Solution	1 ml
D(+)-Glucose	10 g
Agar	15 g
Distilled water	1 l

It was sterilized by autoclaving at 121ºC for 15 minutes.

3.1.1.9. Stabilized Minimal Medium 1.5% (SMM)

20X Salt solution	50 ml
Trace Elements Solution	1 ml
D(+)-Glucose	10 g
Yeast extract	1 g
Sorbitol	218.6 g
Agar	15 g
Distilled water	1 l

It was sterilized by autoclaving at 121ºC for 15 minutes.

3.1.1.10. Luria Bertani (LB) Agar (Scharlau, Barcelona, Spain. Ref. 01-385)

Casein peptone	10 g
Yeast extract	5 g
Sodium chloride	10 g
Agar	15 g
Distilled water	1 l

It was sterilized by autoclaving at 121ºC for 15 minutes.

3.1.1.11. Glucose Sabouraud Broth (GSB) (Panreac Química, Ref. 413804)

D(+)-Glucose	20 g
Mixture of peptic digest animal tissue and pancreatic digest of casein	10 g
Distilled water	1 l

It was sterilized by autoclaving at 121ºC for 15 minutes.

3.1.1.12. *Aspergillus* Minimal Medium Liquid (AMML)

20X Salt solution	50 ml
Trace Elements Solution	1 ml
D(+)-Glucose	10 g
Yeast extract	5 g
Distilled water	1 l

It was sterilized by autoclaving at 121ºC for 15 minutes.

3.1.1.13. Luria Bertani (LB) Broth

Tryptone	10 g
Yeast extract	5 g
Sodium chloride	5 g
Distilled water	1 l

It was sterilized by autoclaving at 121ºC for 15 minutes.

3.1.1.14. RPMI-1640 medium with L-glutamine and without $NaHCO_3$ (Sigma Aldrich, Madrid, Spain. Ref. R6504-10L)

10.4 g were dissolved in 1 l of distilled water and pH was adjusted to 7.2. The medium was sterilized by filtration using 0.22 μm pore size filters.

3.1.1.15. DMEM medium (Sigma Aldrich. Ref. D5796)

DMEM medium was supplemented with 10% fetal bovine serum (FBS) (Sigma Aldrich. Ref. F2442) and 1% Penicillin-Streptomycin (Sigma Aldrich. Ref. P4333).

3.1.1.16. DMEM/F12 medium (Invitrogen. Carlsbad, CA, USA. Ref. 31331093)

DMEM/F12 medium was supplemented with 10% fetal bovine serum (FBS) and 1% Penicillin-Streptomycin.

3.1.2. Strains and culture conditions

The fungal species used in transcriptomic studies was *Aspergillus fumigatus* Af-293 and the strain used to obtain *A. fumigatus* mutant isolates *A. fumigatus* Δ*akuB*^{ku80}, kindly gifted by Dr. Gustavo H. Goldman (da Silva Ferreira *et al*., 2006). In both cases, *A. fumigatus* was grown in test tubes containing inclined PDA medium at 28ºC for 7 days. Cultures were maintained on the same medium at 4ºC for short term storage.

E. coli strains were grown in LB broth at 37ºC with shaking at 120 rpm for 16 hours. In each case, media was supplemented with suitable antibiotics. These bacteria were used to maintain the hygromycin gene and the deletion cassettes for *A. fumigatus* mutant strains. *E. coli* DH5α contained the plasmid pA-Hyg-OSCAR (Addgene plasmid. Cambridge, MA, USA. Ref. 29640) (Paz *et al*., 2011), which was used to amplify the hygromycin resistance gene. One Shot® TOP10 Chemically Competent *E. coli* (Thermo Fisher Scientific, MA, USA. Ref. K2040-01) was used to clone each deletion cassette inserted into the pCR™ 2.1 vector.

3.1.2.1. Harvest of *A. fumigatus* conidia and mycelia

Once *A. fumigatus* strains were grown according to section 3.1.2, 3 ml of SS-T was added to each test tube and conidia were resuspended by vortexing, transferring the solution into a sterile 50 ml Falcon tube. This step was repeated twice and afterwards, spore solution was centrifuged at 2,500 g for 5 minutes. The supernatant was removed and spore pellet was washed twice with SS-T. The final pellet was resuspended in 10 ml of SS-T and the concentration of conidia was determined using a hemocytometer. The viability was evaluated in terms of the percentage of conidia that were able to grow on SGA considering colony forming units per ml (CFU/ml) after incubating at 37ºC for 24 hours, assessed by recounting the conidia with the hemocytometer. The viability was calculated by the following formula:

$$\text{Viability (\%)} = \frac{\text{CFU/ml}}{\text{conidia/ml}} \text{ x } 100$$

To obtain the germinated conidia used in transcriptomic studies, a concentration of 10^7 conidia/ml were grown in 50 ml of RPMI 1640 medium and incubated at 37 for 6.5 hours or 24ºC for 18 hours, both with shaking at 120 rpm. Following the incubations, cultures were centrifuged at 2,500 g for 5 minutes and washed twice with SS-T. The final pellet of these samples was weighed, placed in 10 µl/mg of RNAlater (Qiagen, Valencia, CA, USA) and stored at -20°C until RNA extraction.

The harvest of *A. fumigatus* mycelium was achieved after the incubation of $1x10^5$ conidia/ml in GSB at 28ºC with shaking at 120 rpm for 24-48 hours. The culture was then centrifuged at 2,500 g for 5 minutes and supernatant removed. The pellet was washed twice with saline solution 0.9% and the final pellet was weighed and stored in aliquots (100 mg) at -80ºC until DNA extraction.

3.1.3. Germination rate

The germination rate was determined on the basis of 3 independent assays. *A. fumigatus* conidia at a concentration of 10^7 conidia/ml were grown in 50 ml of RPMI 1640 medium and incubated at 24 or 37°C, both with shaking at 120 rpm. Once inoculated, aliquots of 500 µl of each sample were fixed every hour with 50 µl of fixing solution (10% formaldehyde/10% SDS). Germination rate of each time was determined and those times whose germination rate was between 15-30% were chosen to carry out the transcriptomic analysis with the expression microarray or by RT-qPCR. Moreover, the pH of the medium was measured at starting and harvesting time to assess whether the medium retained the same characteristics in all samples.

To study the effect of the growth and nutrient consumption because of the temporal differences found in 15-30% germination rate samples at 37 and 24ºC (6.5 and 18 hours, respectively), a germination study with the addition of fresh medium was performed. To do so, 10^7 conidia/ml were grown in 50 ml of RPMI 1640 medium and incubated at 24°C with shaking at 120 rpm for 16 hours. After that, cultures were centrifuged at 2,500 g for 5 minutes and supernatant was removed. The pellet was resuspended in fresh medium, preheated at 24 or 37ºC, and incubated again at 24ºC and 37ºC, respectively. Aliquots of 500 µl of each sample were fixed every hour as mentioned above, determining the germination rate of each time. Finally, 3 independent samples

from each temperature with 15-30% and 40-60% germination rates were used in RT-qPCR assays.

3.1.4. Colony growth

The characteristic of the colony of each strain used in this project was evaluated by radial growth spotting 2 µl of 10^5 conidia/ml suspensions on AMM, PDA and SGA plates and incubating them at 28ºC for 7 days. To give an insight into what would happen during an infection porcine lung and kidney agar were used. Five grams of fresh tissue were snap-frozen in liquid nitrogen and pulverized using a pre-cooled mortar. The resulting power was put into a 50 ml reaction tube, filled up with an equal amount of sterile saline and briefly incubated in a 50°C warm water bath, followed by the addition of an equal amount of 50°C warm, liquid water agar (1.5% agar in water). To suppress bacterial growth, media were supplemented with 50 µg/ml tetracycline (Sigma Aldrich. Ref. 87128-25G). The suspension was finally vortexed for 10 seconds and poured onto solidified water agar. Plates were incubated at 37°C for 3 days (Amich *et al*., 2013). In all cases the diameter of knockout strains was statistically compared to the wild type. These essays were performed with 3 independent samples and 3 technical replicates for each strain and medium.

3.1.5. Utilization of different carbon sources

To assess if the genes deleted were involved in the utilization of carbon sources conidial suspensions from 10^6 to 10^2 conidia of each strain in a final volume of 5 µl were spotted on AMM plates without glucose and supplemented with 0.5% ethanol, 50 mM acetate, 1% glycerol or 1% glucose. Plates were incubated at 37ºC for 2 days. Afterwards, the diameter of knockout strains was compared to the wild type. These essays were performed with 3 independent samples and 3 technical replicates.

3.1.6. Stress sensitivity assays

The stress sensitivity assays were performed spotting conidial suspensions from 10^6 to 10^2 conidia/ml of each strain in a final volume of 5 µl onto AMM plates that contained a specific concentration of the appropriate stress treatment. Osmotic stress was applied using NaCl (0.5 and 1 M) or D-sorbitol (0.5, 1 and 2 M); oxidative stress using H_2O_2 (0.1 mM, 0.5 mM, 2 mM, 10 mM, 30 mM); and cell wall stress using Calcofluor White

(25, 50 and 100 ug/ml) or Congo Red (Panreac Quimica, Barcelona, Spain. Ref. 25611.1605) (25 o 50 ug/ml). In all cases plates were incubated at 37°C for 2 days and the diameter of knockout strains was compared to the wild type. All essays were performed with 3 independent samples and 3 technical replicates.

3.2. Animal infection

3.2.1. Animals

Ten female BALB/c mice with a weight of 16-20 g were used for infection models in 3 independent assays. All animals were maintained in the General Animal Unit Service of the University of the Basque Country (UPV/EHU), with water and food *ad libitum*, handled in biological safety cabinets, and kept in sterilized cages with negative-pressure ventilation and filters. Animal experimental procedures were approved by the Animal Experimentation Ethics Committee (CEEA) of the UPV/EHU (reference number CEBA/36-P03-01/2010/REMENTERIA RUIZ and CEBA/36-P03-03/2010/REMENTERIA RUIZ).

3.2.2. Immunosuppression

The immunosuppression was carried out by intraperitoneal injections using cyclophosphamide (Sigma Aldrich, Madrid, Spain. Ref. C3250000) dissolved in saline solution and sterilized by filtration. Doses of 150 mg/kg and 100 mg/kg on days -4 and -1 prior to the infection, respectively, were used.

3.2.3. Infection with *Aspergillus fumigatus* Af-293

Aspergillus fumigatus Af-293 was the strain used in the *in vivo* infection model and conidia were harvested according to the section 3.1.2.1. Three independent assays were performed. In each experiment, 8 immunocompromised animals were intravenously infected with 10^5 conidia in 200 µl of saline solution whereas 2 were used as controls. The physical condition of the mice was monitored daily by trained personnel. Over the first four days of infection, two infected animals with the worst health status were euthanized by cervical dislocation per day, while the controls were euthanized on the fifth day. Dead animal were used for counting colony forming units (CFUs), histology and RNA isolation, organs being processed as indicated in the section 3.2.4.

3.2.4. Processing of infected animal organs

Animals were aseptically dissected extracting the following organs: spleen, lung, kidneys, liver, heart and brain. The organs from one animal were used for histology and for counting CFUs. Those destined to count CFU, were introduced into a sterile bag (Deltalab, Barcelona, Spain. Ref 200326) and weighed. Afterwards, 4 ml of saline solution were added and the organs were grinded using a rod as a rolling pin. Finally, 100 µl of the sample and of the 1:10 diluted sample were inoculated onto SGA with chloramphenicol plates, all of them in duplicate. Plates were incubated at 37ºC and CFUs were counted after 24 and 48 hours.

Organs from the second animal were used for RNA isolation. In this case, it was introduced in a sterile bag and weighed, adding 10 µl/mg of RNAlater. Samples were kept at -20°C until RNA isolation.

3.3. Calcofluor White staining

Samples fixed in germination studies were stained with 0.04 mg/ml Calcofluor White (Becton Dickinson and Company, Madrid, Spain. Ref. 261195), pipetting until all lumps disappeared. Each sample was wrapped in aluminum foil to prevent the loss of fluorescence and incubated for 30 minutes in agitation. Stained conidia were centrifuged at 14,500 g for 30 seconds, washing the pellet twice with PBS and resuspended the final pellet in 500 µl PBS when the second centrifugation finished. Finally, 15-20 µl of the stained sample were placed on a glass slide and observed using a fluorescence microscope (450-490 nm filter).

To visualize infected organs, equal parts of Calcofluor White solution and organs grinded in sterile bags were placed on a glass slide. After homogenizing the sample, a coverslip was placed and the sample was observed by the fluorescence microscope (450-490 nm filter).

3.4. Histology of infected tissues

Kidneys collected from mice were fixed with 10% neutrally buffered formalin (Sigma. Ref. HT501128-4L) for 24 hours with a volume of 10 times the size of the sample. Afterwards, dehydration and paraffin embedding were performed using the tissue

processor Leica TP 1020® (Leica Biosystems, Barcelona, Spain). For dehydration samples were processed with 60, 70 and 80% ethanol for 1 hour in each case, 96% ethanol for 2 hours, and repetitive steps of absolute ethanol for 1 hour. Then, ethanol was removed by treating the samples with xylene for 1 hour, and finally they were embedded in paraffin at 57-59ºC.

Once embedded, paraffin blocks were made with liquid paraffin at 57ºC for better tissue penetration and maximum hardening. Paraffin blocks were transferred to a cold plate for solidification and subsequently, samples were sectioned, using the microtome Leica RM2255 (Leica Biosystems), at the desired thickness (approximately 2-3 μm). Sections were transferred to a 37ºC water bath, being picked up with a glass slide. Finally, slides were incubated at 57ºC to melt the wax and to bond the samples to the glass. Hematoxylin and eosin; periodic acid-Schiff; and Grocott's methenamine silver stains were used to visualize the fungal infection.

3.5. Manipulation of nucleic acids

All working surfaces and those in contact with samples, such as agate mortar and pippettes, were treated before and after each nucleic acid isolation with Termi-DNA-tor solution (Biotools B&M Labs S.A., Madrid, Spain. Ref. 22.001) in order to ensure the complete elimination of residual DNA and RNA. Furthermore, in all cases barrier tips that were ARN-, DNA-, RNase-, DNase- and pyrogens-free were used.

3.5.1. RNA isolation

RNA isolations were carried out using the RNeasy® Plant Mini Kit from Qiagen (Valencia, CA, USA. Ref. 74904).

3.5.1.1. Sample preparation

RNA isolation of germinated conidia was performed as follows. Samples of 75-100 mg (wet weight) were ground using an agate mortar in the presence of liquid nitrogen. This process was repeated twice.

To isolate the RNA of infected organs, frozen pieces of animal tissues of 50-100 mg (wet weight), obtained according to the section 3.2.4, were thawed, placed in sterile bags with 2 ml of sterile distilled water, and homogenized using a rod as a rolling pin.

Disintegrated material was recovered, transferred into a microcentrifuge tube, and centrifuged at 13,000 g for 3 min. The supernatant was discarded and the pellet was ground 3 times using an agate mortar in the presence of liquid nitrogen, as mentioned above.

3.5.1.2. Materials

- Kit RNeasy® Plant Mini Kit: It provides the following materials:
  - RLT Buffer: Lysis buffer. It contains guanidine thiocyanate.
  - RW1 Buffer: Washing buffer. It contains ethanol.
  - RPE Buffer: Washing buffer. 44 ml of ethanol (96-100%) (v/v) must be added.
  - RNase-free water
  - QIAshredder spin column
  - RNeasy spin column
  - 2 ml collection tubes
  - 1.5 ml collection tubes
- β-mercaptoethanol
- Ethanol 96% (v/v)
- DNase- and RNase-free microcentrifuge tubes

3.5.1.3. RNA isolation method

Grinded material obtained in the section 3.5.1.1 was resuspended with 450 µl of RLT Buffer containing 4.5 µl of β-mercaptoethanol. The sample was transferred to a QIAshredder spin column placed in a 2 ml collection tube, and centrifuged at 14,500 g for 2 minutes. The flow-through was transferred to a DNase- and RNase-free microcentrifuge tube and 200 µl of ethanol (96-100%) were added, mixing by pipetting. Sample was transferred to an RNeasy Mini spin column, which was centrifuged at 8,000 g for 15 seconds, discarding the flow-through. Then, 700 µl of RW1 Buffer and 500 µl of RPE Buffer were added in consecutive steps, centrifuging at 8,000 g for 15 seconds and discarding the flow-through in each step. Subsequently, 500 µl of RPE Buffer were added and the sample was centrifuged at 8,000 g for 2 minutes. Following the last centrifugation, the column was transferred to a 1.5 ml collection tube and 50 µl of RNase-free water, pre-heated at 60ºC, were directly added to the spin column

membrane. Finally, the sample was centrifuged at 8,000 g for 1 minute to elute the RNA.

3.5.1.4. DNase treatment

The RNA eluted was treated with the DNase I amplification grade (Sigma Aldrich, Ref. AMPD1). To each 50 µl RNA sample 6.25 µl of 10X Reaction Buffer (200 mM Tris-HCl (pH 8.3) and 20 mM $MgCl_2$) and 6.25 µl of DNAse I (1 U/µl in 50% of glycerol, 10 mM Tris-HCl (pH 7.5), 10 mM $CaCl_2$ and 10 mM $MgCl_2$) were added. The final solution was mixed by inversion and incubated at room temperature for 15 minutes. Afterwards, 6.25 µl of 50 mM EDTA Solution were added and the sample was incubated at 70ºC for 10 minutes to denature the DNA. Finally, the RNA sample was stored at -80ºC until its use.

3.5.1.5. Determination of RNA concentration and integrity

RNA concentration and purity were measured with a NanoPhotometer (Implen, Schatzbogen, Germany), discarding those samples with A260/A280 or A260/A230 ratios lower than 1.8. Furthermore, RNA integrity was assessed using a 2100 Bioanalyzer (Agilent Technologies, Santa Clara, CA, USA) by the Service of Advanced Research Facilities (SGIker) at the UPV/EHU. The 2100 Bioanalyzer generated a RNA integrity number (RIN) which indicated the suitability of RNA samples for gene expression analysis. Only those samples with a RIN number > 5 were used in the different studies.

3.5.2. DNA isolation

DNA isolation was carried out following a modified protocol described by Liu *et al*. (2000).

3.5.2.1. Sample preparation

Samples of 50-100 mg (wet weight) of fungal mycelium, grinded 3 times using an agate mortar in the presence of liquid nitrogen, were used for DNA extraction.

3.5.2.2. Materials

- Lysis Buffer (pH 8): 400 mM Tris-HCl, 60 mM EDTA, 150 mM NaCl and 1% (w/v) SDS (Lui *et al*., 2000)
- Potassium acetate mixture (pH 8): 6 ml of 5M of potassium acetate, 1.15 ml of glacial acetic acid and 2.85 ml of distilled water (Lui *et al*., 2000)
- RNase A (Fermentas, St. Leon-Rot, Germany. Ref. EN0531)
- Isopropanol 99.8% (v/v)
- Ethanol 70% (v/v)
- PCR-grade water (Bioline, London, UK. Ref. BIO-37080)
- Microcentrifuge tubes

Every reagent was sterilized by filtration using 0.22 µm pore size filters and treated with UV light for 30 minutes.

3.5.2.3. DNA isolation method

The processed samples obtained (section 3.5.2.1) were recovered after the addition of 500 µl of Lysis Buffer and transferred to a microcentrifuge tube. Afterwards, 40 µg/ml RNase (final concentration) treatment was carried out, incubating the sample at room temperature for 10 minutes. Then, 150 µl of potassium acetate mixture were added. After mixing the sample it was centrifuged at 8,000 g for 5 minutes to precipitate proteins, being the supernatant transferred to a clean tube and centrifuged again as previously. Supernatant was recovered again and 600 µl of cold isopropanol were added, homogenizing by inversion. The sample was centrifuged at 14,500 g for 15 minutes and supernatant was discarded. Subsequently, 300 µl of cold ethanol were added, centrifuging the sample at 14,500 g for 10 minutes and discarding the supernatant. To remove any residual ethanol the sample was incubated at room temperature for 10-15 minutes. Finally, the DNA pellet was resuspended in 50 µl of PCR-grade water by soft pipetting to prevent DNA damage, and stored at -80ºC until use.

For each set of 4 samples processed, positive and negative controls were used to check the DNA isolation method. Positive controls consisted of DNA extracted from *A. fumigatus* Af-293 mycelium, while negative controls were carried out using water instead of a biological sample.

3.5.2.4. Determination of DNA concentration and purity

DNA concentration and purity was determined by absorbance at 230, 260 and 280 nm using the NanoPhotometer. Only those samples with A260/A280 or A260/A230 ratios higher than 1.8 were used.

3.6. Expression microarray

3.6.1. Expression microarray design

The Agilent Whole *A. fumigatus* Genome Expression 44K (AWAFUGE) microarray v.1 was designed using the eArray system (Custom Microarray Design, Agilent Technologies: http://earray.chem.agilent.com/erray/) and it includes 28,890 probes to monitor the expression of the 9,630 *A. fumigatus* genes. For each gene three 60-bp probes were included. In addition, 62 quality control genes were incorporated, also with 3 targets per gene and each one repeated 5 times on the microarray, to correct the variations caused by biological and technical factors. Of these control genes, 52 were chosen from the 9,630 genes of *A. fumigatus*, 5 from *Mus musculus* genome and the other 5 from *Homo sapiens* genome (Table 3.1). Lastly, the eArray system automatically included positive and negative controls, resulting in a final microarray of 45,220 probes. The format adopted was 4 microarrays per glass slide (4x44K), being the slide made of glass and the type of union with samples covalent. The AWAFUGE microarray (v.1) designed was submitted to the ArrayExpress database at the European Bioinformatics Institute (EBI, http://www.ebi.ac.uk/arrayexpress/) under accession number A-MEXP-2352.

3.6.2. Hybridization of samples with the expression microarray

The hybridizations of the samples with the microarray were carried out by Tecnalia Research & Innovation (Biscay, Spain). Three independent RNA samples obtained from each condition studied were used. Total RNA (1 μg) from each sample was amplified and labeled with Cy3-fluorescent dye using an Amino Allyl MessageAmp^{TM} II aRNA Amplification Kit (Ambion, Austin, TX, USA. Ref. AM1753) and hybridized to individual arrays (one sample per array) in accordance with the manufacturer's recommendations (Agilent Technologies). After washing, microarray slides were scanned using a Gene Pix 4100A scanner (Axon Instruments, Union City, CA, USA)

and image analysis was performed using the associated software, GenePiX Pro 6.0 (Molecular Devices, Sunnyvale, CA, USA). Transcriptome profiles were obtained according to the sections 3.11.1 and 3.11.2.

Table 3.1. Quality control genes included in the expression microarray.

Gene product description	Locus ID[a]	Gene product description	Locus ID[a]
Aspergillus fumigatus			
40S ribosomal protein S8e	AFUA_1G04320	Aquaporin	AFUA_4G03390
60S ribosomal protein L15	AFUA_1G04660	60S ribosomal protein L13	AFUA_4G04460
60S ribosomal protein P0	AFUA_1G05080	Mannose-1-phosphate guanylyltransferase	AFUA_4G11510
40S ribosomal protein S12	AFUA_1G05500	50S ribosomal protein L2	AFUA_4G12170
Aconitate hydratase, mitochondrial	AFUA_1G06810	Glutamine synthetase	AFUA_4G13120
Glycerol-3-phosphate dehydrogenase, mitochondrial	AFUA_1G08810	Isocitrate lyase acud	AFUA_4G13510
50S ribosomal subunit protein L15	AFUA_1G11940	Histone H2A	AFUA_5G01950
60S ribosomal protein L3	AFUA_1G12730	NADH-ubiquinone oxidoreductase	AFUA_5G02080
Histone H4.1 (hhfa)	AFUA_1G13780	Aminopeptidase	AFUA_5G04330
Histone H3	AFUA_1G13790	Transaldolase	AFUA_5G09230
40S ribosomal protein s10a	AFUA_2G02150	Cysteinyl-trna synthetase	AFUA_5G09610
Acetyl-coa carboxylase	AFUA_2G08670	Cytochrome c oxidase subunit V	AFUA_5G10560
60S ribosomal protein L10	AFUA_2G09210	Cofilin	AFUA_5G10570
Glucose-6-phosphate isomerase	AFUA_2G09790	37S ribosomal protein S12	AFUA_5G10750
50S ribosomal protein L13	AFUA_2G10510	37S ribosomal protein S5	AFUA_5G11540
Mannitol-1-phosphate dehydrogenase	AFUA_2G10660	Triosephosphate isomerase	AFUA_5G13450
Vesicular-fusion protein sec17	AFUA_2G12870	Fumarate hydratase, putative	AFUA_6G02470
Arginyl-trna synthetase	AFUA_2G14030	Malate synthase acue	AFUA_6G03540
60S ribosomal protein l37a	AFUA_2G16880	Phosphoserine aminotransferase	AFUA_6G04970
Histone H2B	AFUA_3G05350	Malate dehydrogenase, NAD-dependent	AFUA_6G05210
Histone H2A	AFUA_3G05360	Integral membrane protein	AFUA_6G07470
Histone H1	AFUA_3G06070	Phosphoenolpyruvate carboxykinase acuf	AFUA_6G07720
40S ribosomal protein S9	AFUA_3G06970	Phosphoenolpyruvate carboxykinase acuF	AFUA_6G07720
40S ribosomal protein s7e	AFUA_3G10730	40S ribosomal protein s10b	AFUA_6G12660
Arginase	AFUA_3G11430	Integral membrane protein	AFUA_6G12730
		ATP synthase subunit alpha	AFUA_8G05320
Mus musculus		***Homo sapiens***	
6-phosphofructo-2-kinase/fructose-2,6-biphosphatase 4	NM_173019.5	Actin, beta	NM_001101.3
Actin, beta	NM_007393.3	Glyceraldehyde-3-phosphate dehydrogenase	NM_002046.3
Beta-2 microglobulin	NM_009735.3	Phosphoglycerate kinase 1	NM_000291.3
60S ribosomal protein l13a	NM_009438.4	Ubiquitin-40S ribosomal protein s27a	NM_002954.5
60S ribosomal protein L5	NM_016980.2	60S ribosomal protein L19	NM_000981.3

[a]GenBank accession number.

3.7. Validation of microarray data

3.7.1. Selection of genes

Genes that showed the highest up-regulation as well as those that had been related to virulence were chosen to validate the results obtained with the microarray. Selected

genes to validate the transcriptomic study about the effect of temperature on *A. fumigatus* germination are shown in Table 3.2 and those selected to validate the results obtained during a disseminated infection in Table 3.3. Furthermore, in each experiment, 4 housekeeping genes were included to normalize the results.

3.7.2. Primer design

Specific primer pairs were designed using Primer3 software v.0.4.0. (http://bioinfo.ut.ee/primer3-0.4.0/) (Table 3.2 & 3.3). For their design the following conditions were taken into account: amplicon of desired size; Tm and %GC around 58-62ºC and 30-80%, respectively; no more than 4 consecutive guanines; and no more than 2 guanines or cytosines in the last 5 bases at the 3' end.

The specificity of each primer pair was assessed using The Basic Local Alignment Search Tool (BLAST, http://blast.ncbi.nlm.nih.gov/Blast.cgi). Primers had to exclusively amplify the gene of interest in *A. fumigatus* Af-293. Finally, the formation of hairpin loops and homo and heterodimers of the primers designed was determined by the OligoAnalyzer tool developed by Integrated DNA Technologies (https://eu.idtdna.com/calc/analyzer).

Table 3.2. Genes selected and primers designed to validate the expression data obtained during the germination of *A. fumigatus*.

Target[a]	Name[b]	Sequence (5´→3´)	Tm[c]	%GC[d]	Amplicon (pb)[e]
Most up-regulated at 37ºC					
L-amino acid oxidase Laoa	F-LaoA	ttcaagacagttgccagtgc	60.03	50.00	148
	R-LaoA	attcacgccaatcgaggtag	60.10	50.00	
Extracellular proline-rich protein	F-Extracel	tccatccacagtcacggtaa	59.96	50.00	120
	R-Extracel	ccagtgccagtaccaggatt	59.99	55.00	
NACHT domain protein	F-NACHT	ataggcgacgtggttgtagg	60.02	55.00	127
	R-NACHT	cacttctgcctgcgttcata	60.01	50.00	
Dimethylallyl tryptophan synthase Sird-like	F-SirD	atttgtttccccatcatcca	59.99	40.00	121
	R-SirD	gtgctgtacacccggagatt	60.00	55.00	
CobW domain protein	F-CobW	gtcattgagagcacgggaat	60.08	50.00	108
	R-CobW	ctcatccaccagcatctcct	60.22	55.00	
Nitrite reductase Niia	F-NiiA	tcctcgctacaggctcagat	60.12	55.00	113
	R-NiiA	agcgaactcgatgagacgtt	60.02	50.00	
Thioredoxin	F-Thiored	ttgatgtcgatgagcaggag	59.94	50.00	103
	R-Thiored	cccacagcttcaccaatctt	60.11	50.00	
Ribonuclease H1	F-H1	cttaaagaacggccaagacg	59.88	50.00	129
	R-H1	gctcgtaactcggctacctg	60.04	60.00	
RTA1 domain protein	F-RTA1	caacctgcgtctttgctaca	60.05	50.00	111
	R-RTA1	acacgtaaccgcaatcatca	60.00	45.00	
C4-dicarboxylate transporter/malic acid transport protein, putative	F-C4	ggactggctcttctgattgc	59.96	55.00	134
	R-C4	tgcaaaacgaatctcagcac	60.00	45.00	

Table 3.2. *(continued)*

Target[a]	Name[b]	Sequence (5´→3´)	Tm[c]	%GC[d]	Amplicon (pb)[e]
Most up-regulated at 24ºC					
Catalase	F-Catal R-Catal	ccatccagatgtgtggtgag cgaatggatcaaatcccaac	59.95 60.13	55.00 45.00	150
Pyruvate dehydrogenase E1 component alpha subunit	F-E1 R-E1	aatcatgaggtggcagaagc cacggtacgtcctcggtact	60.23 60.05	50.00 60.00	117
NAD dependent epimerase/dehydratase family protein	F-NAD R-NAD	cggttgcaaagccaactact tctggaaggactccgtatcg	60.30 60.21	50.00 55.00	143
FAD binding monooxygenase	F-FADmon R-FADmon	acggaacagcattcatcctc ctgcagcgtctttgactgag	60.08 59.92	50.00 55.00	123
ATP/GTP-binding protein	F-ATP/GTP R-ATP/GTP	gtggactaccccaaggaaca cggaatgcgaaagagaagtc	59.82 59.96	55.00 50.00	128
Nmra-like family protein	F-NmrA R-NmrA	tttgctatgctgtgctctgg ccacctctcgaaatccttca	60.16 60.19	50.00 50.00	131
Glycosyltransferase	F-Glyco R-Glyco	cactgcaaccgtcaaagcta gtgtcgtggcctgatatcct	60.05 59.96	50.00 55.00	124
Zn^{2+} dependent hydrolase	F-Zn2 R-Zn2	tttggagaccgattcctttg tgcccaagttgagaatagca	60.04 59.42	45.00 45.00	140
Replication factor C subunit	F-FactorC R-FactorC	gtgcatgacgtccagatacg tttgtgcagtgtggtccatt	60.14 60.01	55.00 45.00	139
Conidiation-specific protein Con-10	F-Con10 R-Con10	atctctctggcggaccacta aacacccctggctctacctc	59.83 60.51	55.00 60.00	145
Related to virulence					
C6 finger domain protein GliZ	F-GliZ R-GliZ	gggcatgtctttgaacccta accagcgtactccgaaactg	59.93 60.31	50.00 55.00	137
Nonribosomal peptide synthase GliP	F-GliP R-GliP	tcgtgaccttgctcattctg gtcaatgtcgcccaagagat	59.98 60.08	50.00 50.00	115
Nonribosomal peptide synthase SidD	F-SidD R-SidD	accaggatgctacgaacacc tccaccaagagcgaagaagt	60.00 59.99	55.00 50.00	134
Siderophore transcription factor SreA	F-SreA R-SreA	cctgcctacaacaaccgagt attctttcccgcatcgtttt	60.17 60.80	55.00 40.00	126
Nitrate reductase NiaD	F-NiaD R-NiaD	gacgccctgctagtgagaag cactcggaaccaaggattgt	60.16 59.97	60.00 50.00	102
Major allergen and cytotoxin Asp F 1	F-AspF1 R-AspF1	ccacagccgtgtctgttcta cgcttgtcttcccatttgtt	59.90 60.11	55.00 45.00	109
Major allergen Asp F 2	F-AspF2 R-AspF2	tctgtgatcgcagctacacc acagcaggcacatggtacag	60.02 59.78	55.00 55.00	133
Mn superoxide dismutase MnSOD	F-MnSOD R-MnSOD	cctacgtcaatggcctgaat tccagaagagggaatggttg	59.96 60.04	50.00 50.00	138
Housekeeping genes					
Actin 1 (Act1)	F-Act1 R-Act1	tcatcatgcgcgacagctta cgtgctcgatggggtatctg	63.95 63.86	50.00 60.00	179
Glyceraldehyde 3-phosphate dehydrogenase GpdA	F-GdpA R-GpdA	ctccctccaacaaggactgg agcttgccgttgagagaagg	61.99 61.98	60.00 55.00	115
Translation elongation factor EF-1 alpha subunit	F-TEF1 R-TEF1	cttcaacggtgacaacatgc cctcgatgagggtcttacca	60.16 60.07	50.00 55.00	107
1,3-beta-glucan synthase catalytic subunit FksP	F-FksP R-FksP	ctcctgtaccgggttgaaaa caatcttgaacttgcgacga	59.96 59.99	50.00 45.00	106

[a]Gene product description of the genes chosen to validate microarray data.
[b]Name of each primer. F: Forward, R: Reverse.
[c]Melting temperature of each primer, according to Primer3.
[d]Percentage of guanine and cytosine content of each primer, according to Primer3.
[e]Size of cDNA amplification product.

Table 3.3. Genes selected and primers designed to validate the expression data obtained during a disseminated infection.

Target[a]	Name[b]	Sequence (5´→3´)	Tm[c]	%GC[d]	Amplicon (pb)[e]
Gliotoxin biosynthesis[f]					
C6 finger domain protein GliZ	F-2GliZ R-2GliZ	tccagcggtagcgagaatac gaaaggtcggaatcggagat	60.37 60.41	55.00 50.00	86
Nonribosomal peptide synthase GliP	F-2GliP R-2GliP	aaccgcaaggttgactatcg gattccgtccgcaatagaag	60.13 59.67	50.00 50.00	126
MFS gliotoxin efflux transporter GliA	F-GliA R-GliA	tcttcctcatctcgctcgac gaaagaaggcggacccatac	60.64 60.83	55.00 55.00	108
Iron metabolism[f]					
Nonribosomal peptide synthase SidD	F-SidD R-SidD	accaggatgctacgaacacc tccaccaagagcgaagaagt	60.00 59.99	55.00 50.00	134
Siderophore transcription factor SreA	F-SreA R-SreA	cctgcctacaacaaccgagt attctttcccgcatcgtttt	60.17 60.80	55.00 40.00	126
bZIP transcription factor HapX	F-HapX R-HapX	ggatgctgcggaggtaaag cgaagatcccgacgatgtat	60.75 59.92	57.90 50.00	108
Mycelial catalase Cat1	F-Cat1 R-Cat1	cgaagatttcattttccgtca tcgccatatgaagtgaagactc	60.06 59.34	38.10 45.50	114
Nitrogen metabolism[f]					
Nitrate reductase NiaD	F-2NiaD R-2NiaD	aatcagatcacagccccaat ccttttgatttccgcactgt	59.37 60.11	45.00 45.00	80
Nitrite reductase NiiA	F-2NiiA R-2NiiA	cgtgctatctgatggcttga cgaagttgcgtttgtggtaa	59.97 59.77	50.00 45.00	80
Nitrate transporter CrnA	F-CrnA R-CrnA	atggtatgcgtttccacctc tttgcgacttgttgctgtgt	59.82 60.49	50.00 45.00	75
MAP kinases[f]					
MAP kinase kinase Mkk2	F-Mkk2 R-Mkk2	agcactccagatccctcgt agaagtccgttgacgctgtt	59.81 59.91	57.9 50.00	95
MAP kinase MpkA	F-MpkA R-MpkA	tgatctacagggtcggaagg ctcgccagtatgaacattcg	60.07 59.30	55.00 50.00	136
MAP kinase SakA	F-SakA R-SakA	tgtcaagtccctaccgaagc ctagaagatcgaccgcctca	60.25 60.50	55.00 55.00	83
Allergens[f]					
Major allergen and cytotoxin Asp F 1	F-2AspF1 R-2AspF1	agtcaagccaaagccgaaag agccgttagtgaaccagtgc	61.78 60.32	50.00 55.00	91
Major allergen Asp F 2	F-2AspF2 R-2AspF2	ttgcagtatttcgcccttga gtgactctcgccagcacat	61.65 60.00	45.00 57.90	75
Mn superoxide dismutase MnSOD	F-2MnSOD R-2MnSOD	attaccacaacccacgacca cgaggctttgtcgttcaagt	61.08 60.43	50.00 50.00	108
Aldehyde dehydrogenases[f]					
Aldehyde dehydrogenase AldH12	F-AldH12 R-AldH12	gccgctgtacctgttaacct gcagaaacgctagtgatctcg	59.27 60.17	55.00 52.40	93
Alpha-amylase	F-Amyl R-Amyl	ggacggggtgctgaattac gctgctcatactgccacttg	60.33 59.62	57.90 55.00	76
Conidial hydrophobin Hyp1/RodA	F-RodA R-RodA	agcggttccctcattggac caggatagaaccaagggcaat	61.45 60.33	61.10 47.60	53
Conidial biosynthesis[f]					
Conidial pigment polyketide synthase PksP/Alb1	F-Alb1 R-Alb1	cgatcaaggtcactggtcct gtcggcgaagttgagactgt	60.11 60.45	55.00 55.00	143
Conidial pigment biosynthesis 1,3,6,8-tetrahydroxynaphthalene reductase Arp2	F-Arp2 R-Arp2	ggaggacttcaacgaggtgt ggatgtggtcgtaggcgtag	59.15 60.54	55.00 60.00	77
Conidial pigment biosynthesis scytalone dehydratase Arp1	F-Arp1 R-Arp1	agacagctatgacgccaagg aggcatgtcatcccactttc	60.42 59.93	55.00 50.00	106

Table 3.3. (*continued)*

Target[a]	Name[b]	Sequence (5´→3´)	Tm[c]	%GC[d]	Amplicon (pb)[e]
Conidial pigment biosynthesis oxidase Abr1/brown 1	F-Abr1	catcaatgggcagacatacg	59.95	50.00	120
	R-Abr1	tggacgacgaagggatttac	59.93	50.00	
Conidial pigment biosynthesis oxidase Arb2	F-Arb2	ccgaggaattgacccagat	59.87	52.60	59
	R-Arb2	caacgagctgttgaggatagc	60.03	52.40	
Phospholipases[f]					
Phosphatidylglycerol specific phospholipase C	F-PhosC	gaccctcctactcgtcacctt	59.61	57.10	100
	R-PhosC	ggtctcggtgtaggtcttgc	59.73	60.00	
Lysophospholipase Plb2	F-Plb2	accacgaactcaacccacag	61.02	55.00	65
	R-Plb2	cccgaaagataagtcgctga	60.34	50.00	
Extracelullar proteins[f]					
Extracellular alpha-1,3-glucanase/mutanase	F-Glucamuta	tggtgagtcccactacatcg	59.55	55.00	52
	R-Glucamuta	gaatagctcatacccgccttc	60.07	52.40	
Extracellular glycosyl hydrolase/cellulase	F-Hydrocell	aatggaaacgctgcctactc	59.34	50.00	50
	R-Hydrocell	ccagcagggttgctaatgtc	60.66	55.00	
Extracellular exo-polygalacturonase	F-Exopol	cgttttgcctccgataagaa	60.20	45.00	62
	R-exopol	ttgctaccgccagtgatgta	60.28	50.00	
Extracelular cellulose binding protein (Cip2)	F-Cip2	atccgcactgctcgtttc	59.95	55.60	111
	R-Cip2	tccccgcataattcttctga	60.54	45.00	
Proteases[f]					
Aspartic-type endopeptidase	F-endopep	acgacgaataacaggcaacc	60.00	50.00	147
	R-endopep	caatccacccagagtcaggt	59.96	55.00	
Serine protease	F-protease	agacatgccaaatccactcc	59.93	50.00	104
	R-protease	ctcagcgggttgtttatcgt	60.13	50.00	
Most up-regulated during the infection[f]					
Polyphenol monooxygenase	F-Polyph	gtcggcctttcgatacaacc	61.76	55.00	122
	R-Polyph	gaaactcctggatcgtctgc	59.81	55.00	
GABA permease	F-GABA	gcatacagcagcatcgtctc	59.58	55.00	130
	R-GABA	cataccgccctaaatcgaag	59.56	50.00	
Ctr copper transporter family protein	F-Ctr	tgtacagacgctggagttgg	59.90	55.00	81
	R-Ctr	ttaatgcgtaacccaccaga	59.04	45.00	
Most down-regulated during the infection[f]					
Cytochrome b5 reductase	F-b5reduc	aaaagatgcgactcggtttg	60.25	45.00	58
	R-b5reduc	ggaggtcggctgaataacac	59.56	55.00	
Ribonuclease H1	F-2H1	ttcaaggcaattgagcgtct	60.91	45.00	92
	R-2H1	gcgtcacgattattcctcct	59.15	50.00	
Cytochrome P450 monooxygenase	F-P450mono	tcctgcccaagctgatctat	59.80	50.00	149
	R-P450mono	ctacgcatccgacttgtacg	59.37	55.00	
Housekeeping genes[f]					
Alpha/beta hydrolase	F-alphabeta	actggtcgtgacactgttgg	59.62	55.00	102
	R-alphabeta	cgcattgtggatgctagact	58.9	50.00	
Mis12-Mtw1 family protein	F-Mis12	gctctcgaattggtttggac	59.68	50.00	75
	R-Mis12	atgtttttcgggttcggttt	60.57	40.00	
Beta galactosidase	F-betagal	atctccttcgtgctctcgac	59.56	55.00	94
	R-betagal	gcggattgtaccgaccatac	60.22	55.00	
Aspartate transaminase	F-aspart	acaccgtcgtcgttaatctg	58.65	50.00	100
	R-aspart	tcttcgttcgtcaggacctt	59.84	50.00	

[a]Gene product description of the genes chosen to validate microarray data.
[b]Name of each primer. F: Forward, R: Reverse.
[c]Melting temperature of each primer, according to Primer3.
[d]Percentage of guanine and cytosine content of each primer, according to Primer3.
[e]Size of cDNA amplification product.
[f]Group of proteins or metabolism in which the gene is involved.

3.8. Polymerase chain reaction (PCR)

PCR was performed with every primer pair designed to check its specificity using DNA of *A. fumigatus* Af-293 as template. The final concentrations of reagents in PCR reactions were the same for each gene.

3.8.1. Materials

- BioTaq polymerase (5 U/µl) (Bioline. Ref. BIO-21040)
- Triphosphate nucleotides, dNTP mix (Bioline. Ref. BIO-39028)
- PCR-grade water
- MJ Mini Gradient Thermal Cycler (Bio-Rad Laboratories, Madrid, Spain. Ref. PCT 1148)

3.8.2. Reaction mixture

PCR reactions had a final volume of 25 µl and its reaction mixture was the following:

Buffer 10X	2.5 µl
$MgCl_2$ (50 mM)	1.25 µl
dNTPs (2.5 mM)	2 µl
BioTaq polimerase (5 U/µl)	0.15 µl
Primer Forward (10 µM)	4 µl
Primer Reverse (10 µM)	4 µl
DNA (10 ng/µl)	1 µl
PCR-grade water	10.1 µl

3.8.3. Amplification program

The conventional PCR was carried out in the MJ Mini Personal Thermal Cycler and its amplification program was the following:

Step 1: Denaturalization	95ºC	10 minutes
Step 2: 32 cycles	95ºC	30 seconds
	60ºC	30 seconds
	72ºC	30 seconds/kb
Step 3: Extension	72ºC	10 minutes

Positive amplifications were those in which only one amplicon with the expected size was obtained for each primer pair. In each amplification program a negative control per gene was included in which water was added to the reaction instead of DNA.

3.9. Agarose gel electrophoresis

3.9.1. Materials

- Loading dye 5X: 65% (p/v) sacarose, 10 mM Tris-HCl (pH 7.5), 10 mM Na_2 EDTA and 0.3% (p/v) Bromophenol blue.
- Tris-Borate-EDTA (TBE) buffer 5X (National Diagnostics, Patton, ATL, USA. Ref. EC-861): 0.445 M Tris-borate (pH 8.3) and 10 mM Na_2EDTA. This buffer was diluted to the 1X with distilled water.
- Molecular Weight Markers.
  - Hyperladder 1kb range: 200-10,037 bp (Bioline. Ref. BIO-33025).
  - Hyperladder IV range: 100-1000 bp (Bioline. Ref. BIO-33029).
  - 1K DNA ladder range: 500-10,000 bp (New England biolabs. Hertfordshire, UK. Ref. N3232S)
  - O'GeneRuler Low Range DNA Ladder, Ready-to-Use range: 25-700 bp (Thermo Scientific, Waltham, MA, USA. Ref. SM1203)
- GelRed™ Nucleic Acid Stain (Biotium, Hayward, CA, USA. Ref. 41003).
- Electrophoresis equipment

3.9.2. Electrophoresis method

PCR products were visualized by agarose gel electrophoresis using 1% (w/v) agarose gel with 1X concentration of GelRed. Each well was loaded with 15 µl of DNA sample and 5 µl of loading dye 5X. Finally, samples were run at 110 V for 60 minutes and bands were visualized with a gel documentation system (u:Genius, Syngene, Cambridge, UK) using UV light.

3.10. Reverse transcription polymerase chain reaction (RT-qPCR)

All RT-qPCR experiments were carried out by the SGIKer at the UPV/EHU.

3.10.1. Synthesis of copy DNA (cDNA)

The cDNA was generated from 1 µg of total RNA using an AffinityScript Multiple Temperature cDNA Synthesis Kit (Agilent Technologies) in a total volume of 20 µl. Oligo(dt) (1 µl of 0.5 µg/µl) and random (1 µl of 0.1 µg/µl) primers were used. After an initial incubation at 65ºC for 5 minutes, retrotranscription protocol was followed by

25ºC for 10 minutes, 42ºC for 120 minutes and 70ºC for 15 minutes. The final concentration of cDNA was 50 ng/µl.

To assess the PCR efficiency, concentrate cDNA was synthesized using a global pool of RNA. To determine the possible genomic DNA contamination in every sample, a negative control was included performing a retrotranscription reaction with the same amount of RNA but without adding the retrotranscriptase.

3.10.2. qPCR using 7900HT Fast Real-Time PCR System

The qPCR experiments were performed in 96-well plates in a 7900HT Fast Real-Time PCR System (Applied Biosystems, Foster City, CA, USA). Three amplification of each condition were performed per gen selected. In order to obtain the standard curve for each gene, 5 serial dilutions (1:10 or 1:5) of the concentrate cDNA synthesized with the pool of RNA were included, also in triplicate. In addition to this, No-Template Controls (NTC) and minus-reverse transcriptase controls (samples in which no reverse-transcriptase was added) were also included to determine the presence of primer dimmers or contamination.

For the reaction, Brilliant III Ultra-Fast QPCR Master Mix (Agilent Technologies. Ref. 600880) was used, in which 300 nM of ROX, 10 ng of cDNA and 500 nM of primer pairs were added. The final volume of each reaction was 10 µl. The PCR protocol was the following:

Step 1: Denaturalization	95ºC	3 minutes
Step 2: 40 cycles	95ºC	5 seconds
	60ºC	20 seconds
Step 3: Dissociation curve	60ºC	3 seconds
	60ºC-95ºC	

3.10.3. Expression analysis with BioMark HD Nanofluidic qPCR System

This analysis was also carried out using BioMark HD Nanofluidic qPCR System technology (Fluidigm, San Francisco, CA, USA) combined with GE 48.48 Dynamic Arrays IFC (Fluidigm).

3.10.3.1. Preamplification of cDNA

The cDNA synthetized according to the section 3.10.1 was preamplified using the QIAGEN Multiplex PCR Kit (Qiagen. Ref. 206143) and 50 nM of the forward and reverse primers in a final volume of 5 µl. The amplification conditions were the following:

Step 1: Denaturalization	95ºC	15 seconds
Step 2: 14 cycles	95ºC	15 seconds
	60ºC	4 minutes

3.10.3.2. Treatment with Exonuclease I

The preamplified cDNA was treated with Exonuclease I (New England Biolabs. Ref. M0293S) to remove the primers that were not incorporated. To each sample, 0.2 µl of Exonuclease I Reaction Buffer (pH 9.5, 67 mM glycine-KOH, 6.7 mM $MgCl_2$, 10 mM 2-mercaptoethanol), 0.2 µl of Exonuclease I (20 U/µl) and 1.4 µl of PCR-grade water were added. The protocol to carry out the digestion was 37ºC for 30 minutes, followed by 80ºC for 15 minutes to inactivate the Exonuclease I. Afterwards, preamplified cDNA was diluted to 1:10 with TE buffer (pH 8, 10 mM Tris HCl and 0.1 mM de EDTA).

3.10.3.3. Quantitative PCR (qPCR) protocol

Gene expression analysis of the preamplified amplicons was performed with 48.48 Dynamic Array integrated fluidic circuit (IFC) (Fluidigm). The amplification of each gene and condition was carried out in triplicate. The standard curve of each gene with 5 serial dilutions (1:10 or 1:5) of the concentrate cDNA synthesized with the pool of RNA were included, also in triplicate. In addition to this, NTCs and minus-reverse transcriptase controls were also included in these assays to determine the presence of primer dimmers or DNA contamination.

The protocol followed was the Fast Gene Expression Analysis Using EvaGreen on the BioMark or BioMark HD System, Advanced Development Protocol (Fluidigm. Ref. PN 100-3488). To each reaction, the Master Mix SsoFast™ Evagreen® Supermix with Low Rox (Bio-Rad Laboratories. Ref. PN 172-5211) was used, in which 2.7 µl of preamplified cDNA and 500 nM of primer pairs were added. The PCR amplification conditions were the following:

Step 1	70ºC 60ºC	40 minutes 30 seconds	Ramp 5.5ºC/s Ramp 5.5ºC/s
Step 2: Denaturalization	95ºC	1 minutes	Ramp 5.5ºC/s
Step 3: 35 cycles	96ºC 60ºC	5 seconds 20 seconds	Ramp 5.5ºC/s Ramp 5.5ºC/s
Step 4: Dissociation curve	60ºC 60ºC-95ºC	3 seconds	Ramp 1ºC/s Ramp 1ºC/3 s

3.11. Data analysis

3.11.1. Normalization and statistical analysis of microarray data

Gene expression data obtained after microarray hybridizations were normalized using two programs. The normalization procedure of the data obtained from the germination study was carried out using the GeneSpring GX software v.12 (Agilent Technologies) and specific recommendations for one-color hybridizations. Basically, after subtracting the background intensity and $\log_2$ data transformation, a global normalization (75th percentile shift normalization) was performed followed by a baseline transformation to the median of all samples.

Gene expression data obtained during the disseminated infection and germination were analyzed using the Babelomics server (http://www.babelomics.org) (Medina *et al*., 2010). Raw data were normalized applying the RMA (Robust Multi-Array Average) algorithm for background correction, and the quantile normalization. The intensity of each gene was estimated by the median polish technique. Finally, the minimum percentage of existing values was established at 50-70% and missing values were imputed by K-Nearest Neighbour (KNN) imputation (k-value = 15). In both analyses, a gene was considered to be positively expressed if all the specific probes designed for it were hybridized in all samples analyzed.

To identify genes differentially expressed in *A. fumigatus* germination at 24 and 37ºC, levels of expression were compared using the Student´s t-test with the GeneSpring GX software v.12. When the disseminated infection was compared to the germination at 37ºC, statistical comparisons were performed using the Limma package of Bioconductor, available in Babelomics server. On the other hand, to compare the expression of the 4 days of infection analyzed, ANOVA test was applied, which performs a classical analysis of variance to test for mean differences between array

groups. In all cases, multiple testing with Benjamini-Hochberg correction was applied in order to control for the occurrence of false positives. A gene was considered to be differentially expressed if $p < 0.05$. When two conditions were compared, results were expressed as $\log_2$ fold-change, representing the $\log_2$ of the condition of interest *minus* the $\log_2$ of the control condition. Therefore, a negative fold-change meant an up-regulation in the control condition and a positive value an up-regulation in the condition of interest. These results were graphically represented with volcano plots.

With the aim of getting to know those genes whose expression increased throughout *A. fumigatus* infection a hierarchical cluster analysis was carried out. This study was performed with those genes that showed differential expression between each day of infection and the germination at 37ºC. The analysis was performed using GeneSpring GX software v.12. The metric and linkage applied were Euclidean distance and Wards's linkage rule, respectively.

3.11.2. Functional classification and chromosomal location of differentially expressed genes

Differentially expressed genes were classified into functional groups according to the Munich Information Center for Protein Sequence Functional Catalogue (FunCat; http://pedant.helmholtz-muenchen.de). Those genes that encoded hypothetical or unclassified proteins were classified in two non-functional groups. Moreover, using FungiFun 2.2.8 (Priebe *et al*., 2011, Priebe *et al*., 2014) (https://elbe.hki-jena.de/fungifun/fungifun.php) the enrichment p-value of each FunCat category was performed to get to know those significant functional groups up-regulated in each condition. Fisher´s test and Benjamini-Hochberg adjustment method were applied. A category was considered significant if $p < 0.05$.

Those genes that showed different expressions in each comparison were located into *A. fumigatus* chromosomes to assess whether they followed any particular distribution pattern. This study was carried out with the transcriptomic comparison between the germination at 24 and 37ºC and with the comparison of each day post-infection relative to the germination at 37ºC. Heat maps obtained with the MultiExperiment Viewer 4.9.0. software (MeV, Saeed *et al*., 2003) were used to visualize the distribution of genes. The expression was shown using two colors. Those genes up-regulated in the control condition appeared in green and those up-regulated during the condition of interest in

red. Finally, the ratio of up-regulated genes found in the condition of interest *versus* the up-regulated ones in the control condition was determined. This ratio was calculated for each chromosome to determine whether any of them stood out.

3.11.3. Analyses of RT-qPCR results and correlation with microarray data

The analysis of RT-qPCR results obtained with the 7900HT Fast Real-Time PCR System was carried out using the SDS 2.4 software (Applied Biosystems). However, when the BioMark HD Nanofluidic qPCR System was performed, the results were analyzed with Real-Time PCR Analysis Software v.3.1.3 (Fluidigm). In both cases, the softwares determined the Ct values for each reaction after setting the threshold manually. Afterwards, correction and normalization processes, and gene expression and its significance were determined using GenEx v.5.4 (MultiD Analyses, Gothenburg, Sweden).

PCR efficiency of each gene was assessed based on the slope of the standard curve obtained with the serial dilutions applying the following formula:

$$\text{Efficiency (E)} = [10(-1/\text{slope})] - 1$$

Once the efficiency was determinate, the average of the replicates was calculated and the possible genomic DNA contamination subtracted. The analysis of expression stability of housekeeping genes was performed applying the NormFinder algorithm, whose results were confirmed by the GeNorm algorithm. The normalization was carried out with the best combination to decrease or remove every systematic and technical variation introduced in the different steps of RT-qPCR, and to compensate the different amount of sample added to each reaction. After normalization, relative quantification of each sample was determined using the following formula:

$$2^{-(\text{CtNorm} - \text{CtAver})}$$

Being CtNorm the normalized Ct value of each gene in each sample, and CtAver the average Ct value obtained for each gene in all the samples analyzed.

Finally, relative quantifications were transformed to $\log_2$ and analyzed statistically in order to assess the significant differences amongst the groups. When two conditions were compared, Student's t-test was applied and results were expressed as $\log_2$ fold-

change, subtracting to the condition of interest the expression obtained in the control condition. The $\log_2$ fold change thresholds were set over 1 and under -1, meaning an increase of the expression in more than twice in the condition of interest and an increase in more than twice in the control one, respectively. When more than two conditions were compared ANOVA test was applied. In all cases a gene was considered to be differentially expressed if $p < 0.05$.

Gene expression obtained by RT-qPCR assays were compared to microarray data using Pearson's correlation. The correlation was graphically represented and the validation was confirmed in those cases in which the correlation value was higher than 0.8.

3.12. Accession numbers of microarray data

The *A. fumigatus* gene expression data obtained after the hybridization with the microarray were submitted to the ArrayExpress database. Transcriptomic data of *A. fumigatus* germination were deposited under accession number E-MTAB-1910 and those obtained along a disseminated infection under accession number E-MTAB-3674.

3.13. Construction of knockout strains

3.13.1. Design of primers

To generate knockout strains, the hygromycin resistance gene present in the plasmid pA-Hyg-OSCAR as well as the 5' and 3' flanking regions of the gene of interest, whose sequences were obtained in the Central *Aspergillus* Data REpository (C*A*DRE; http://www.cadre-genomes.org.uk; Mabey Gilsenan *et al*., 2012), were amplified. Primers for each amplification were designed according to the section 3.7.2. However, as the aim was to fuse the 3 PCR products, complementary sequences were added to hygromycin primers and to the reverse and forwards primers of 5' and 3' flanking regions, respectively (Table 3.4). For the amplification of the deletion cassette another primer pair was designed with a high Tm, to prevent unspecific amplifications. This primer pair was also used to amplify the fragment for reconstituted strains using the *A. fumigatus* Δaku^{KU80}as template. Finally, to confirm the deletion and/or insertion, primers within the gen of interest were also designed.

Table 3.4. Primer designed for knockout and reconstituted strains.

Target	Name[a]	Sequence (5'→3')[b]	Tm[c]	%GC[d]	Amplicon (pb)[e]
Δ*abr1/brown1* knockout strain					
5' flanking region	5'Abr-F 5'Abr1-R	gtacatcgactacgggagcc **tccactagttctagagcggcc**gggctgagtccatcgagata	59.6 60.2	60.00 55.00	1,102
Hygromycin gene	Hyg-F Hyg-R	**tatctcgatggactcagccc**ggccgctctagaactagtgga **tgatggctcatacatgtagatga**gtagaattcctgcagcccaac	60.9 61.0	57.14 52.38	1,454
3' flanking region	3'Abr1-F 3'Abr1-R	**gttgggctgcaggaattctac**tcatctacatgtatgagccatcaa atccccatttacatccgcacc	59.5 65.6	37.50 52.38	1,190
Deletion cassette	CassAbr1-F CassAbr1-R	cactggacacaaaccatctgc ccatttacatccgcaccccag	65.6 66.6	52.38 57.14	3,552
abr1/brown1 gene	abr1-F abr1-R	cagcacaccatgttccattc gtcacccccctgtagtcgtgt	59.9 59.9	50 60	2082
Knockout strain for the trancription factor AFUA_1G02860					
5' flanking region	5'FT-F 5'TF-R	ccgaaggtggtaaaaaccaa **tccactagttctagagcggcc**tgtcacgggtcacaggataa	59.8 59.9	45 50	1,237
Hygromycin gene	HygTF-F HygTF-R	**ttatcctgtgacccgtgaca**ggccgctctagaactagtgga **atgtatgccctttctgtccg**gtagaattcctgcagcccaac	60.9 61.0	57.14 52.38	1,454
3' flanking region	3'TF-F 3'TF-R	**gttgggctgcaggaattctac**cggacagaaagggcatacat gagatgagggaacgtcttcg	59.9 59.8	50 55	1,273
Deletion cassette	CassTF-F CassTF-R	ctggatcgaccaggcaaagg cggactttccccgtaagctg	65.2 64.1	60 60	3,860
Transcription factor	TF-F TF-R	tgatgtccccgagacctatc gctaaataccctcccgcagt	59.5 60.5	55 55	688

[a]Name of each primer. F: Forward, R: Reverse.
[b]Sequence of each primer. In chimeric primers, complementary sequences of the primers to which they have to fuse are shown in bold.
[c]Melting temperature of each primer, according to Primer3.
[d]Percentage of guanine and cytosine content of each primer, according to Primer3.
[e]Size of cDNA amplification product.

3.13.2. Construction of the deletion cassette

3.13.2.1. Materials

- Q5 High-Fidelity DNA polymerase (New England Biolabs. Ref. M0491G).
- Triphosphate nucleotides, dNTP mix
- BioTaq Polymerase
- Triphosphate nucleotides, dNTP mix
- PCR-grade water
- MJ Mini Gradient Thermal Cycler
- High Pure PCR Product Purification Kit (Roche, Ref. 11732668001). It provides the following materials:
  - Binding Buffer (pH 6.6). It contains guanidine-thiocyanate.
  - Washing Buffer (pH 7.5). It contains ethanol.

- Elution Buffer (pH 8.5)
- High Pure Filter Tubes
- 2 ml Collection tubes

- PCR-grade water
- Microcentrifuge tubes

3.13.2.2. Amplification of the regions needed for the construction of the deletion cassette

The amplifications were carried out using the primer pairs designed to amplify the hygromycin gene and 5' and 3' flanking regions of each gene of interest (Table 3.4). To amplify the flanking regions and the resistance gene *A. fumigatus* Δ*akuB*^{ku80} DNA and the plasmid pA-Hyg-OSCAR were used as template, respectively. PCR reactions had a final volume of 50 µl and its reaction mixture was the following:

5X Q5 Reaction Buffer	10 µl
dNTPs (10 mM)	1 µl
Q5 High-Fidelity DNA polymerase	0.5 µl
Primer Forward (10 µM)	2.5 µl
Primer Reverse (10 µM)	2.5 µl
DNA (10 ng/µl)	1 µl
PCR-grade water	32.5 µl

The conventional PCR was carried out in the MJ Mini Personal Thermal Cycler and its amplification program was the following:

Step 1: Denaturalization	95ºC	10 minutes
Step 2: 33 cycles	95ºC	30 seconds
	60ºC	30 seconds
	72ºC	45 seconds/kb
Step 3: Extension	72ºC	10 minutes

Positive amplifications were those in which only one amplicon with the expected size was obtained for each primer pair. In each amplification program a negative control per gene was included in which water was added to the reaction instead of DNA. PCR products were visualized by agarose gel electrophoresis (section 3.9), purified according to the section 3.13.2.4 and stored at -20ºC until use.

3.13.2.3. Fusion PCR of amplified products

Fusion PCR consisted of 2 consecutive rounds of PCR. In the first one, PCR products obtained in the section 3.13.2.2 were included in the same PCR reaction. Given that they already had complementary sequences, primers were not necessary because the 5' and 3' flanking regions of each gene of interest acted as primers for the hygromycin gene. As a result, the fusion of the 3 fragments was achieved.

PCR reactions had a final volume of 50 µl and its reaction mixture was the following:

5X Q5 Reaction Buffer	10 µl
Q5 High-Fidelity DNA polymerase	0.5 µl
dNTPs (10 mM)	1 µl
5'flanking region (20 ng/µl)	1 µl
3' flanking region (20 ng/µl)	1 µl
Hygromycin gene (20 ng/µl)	1 µl
PCR-grade water	35.5 µl

The conventional PCR was carried out in the MJ Mini Personal Thermal Cycler and its amplification program was the following:

Step 1: Denaturalization	98ºC	3 minutes
Step 2: 32 cycles	98ºC	10 seconds
	55ºC	30 seconds
	72ºC	30 seconds/kb
Step 3: Extension	72ºC	2 minutes

The second round of the fusion PCR consisted of amplifying the deletion cassette. Primer pairs designed with a high Tm (CassAbr1 or CassTF, depending on the gene of interest) (Table 3.4) were included using the product of the first round as DNA template. In this case, BioTaq Polymerase was used as it produces poly(A) 3′ ends, required for the following insertion of the fragment into the cloning vector.

PCR reactions had a final volume of 50 µl and its reaction mixture was the following:

Buffer 10x	5 µl
$MgCl_2$ (50 mM)	2.5 µl
dNTPs (2.5 mM)	4 µl
BioTaq polimerase (5 U/µl)	0.5 µl
Primer Forward (10 µM)	2.5 µl
Primer Reverse (10 µM)	2.5 µl
Fused product	1 µl
PCR-grade water	32 µl

The conventional PCR was carried out in the MJ Mini Personal Thermal Cycler and its amplification program was the following:

Step 1: Denaturalization	95ºC	10 minutes
Step 2: 32 cycles	95ºC	30 seconds
	66ºC	30 seconds
	72ºC	30 seconds/kb
Step 3: Extension	72ºC	10 minutes

Positive amplifications were those in which only one amplicon with the expected size was obtained. A negative control was also included in which water was added to the reaction instead of DNA. PCR product was visualized by agarose gel electrophoresis (section 3.9), purified according to the section 3.13.2.4 and stored at -20ºC until use.

3.13.2.4. Purification of PCR products

PCR-grade water was added to each PCR reaction up to 100 µl and the reaction was transferred to a new microcentrifuge tube. Subsequently, 500 µl of Binding Buffer were added, being afterwards transferred to a High Pure Filter Tube and centrifuged at 14,500 g for 1 minute. The flow-through was discarded and 500 and 200 µl of Washing Buffer were added and centrifuged at 14,500 g for 15 seconds in consecutive steps, discarding the flow-through in each step. Following the last centrifugation, the column was transferred to a microcentrifuge tube and 50 µl of Elution Buffer were directly added to the column membrane. Finally, the sample was centrifuged at 14,500 g for 1 minute and purified PCR products were visualized by agarose gel electrophoresis. The concentration and purity of the amplicon were determined by absorbance at 230, 260 and 280 nm using the NanoPhotometer and samples were stored at -80ºC until use.

3.13.3. Ligation of the deletion cassette and transformation of *E. coli*

3.13.3.1. Materials

- TA Cloning® Kit with pCR™ 2.1 Vector and One Shot® TOP10 Chemically Competent *E. coli* (Thermo Fisher Scientific, Ref. K2040-01). It provides the following materials:
  - pCR™ 2.1 Vector, linearized (25 ng/µl)
  - ExpressLink™ T4 DNA ligase (5 U/µl)
  - One Shot® TOP10 Chemically Competent *E. coli*

- 5X T4 DNA Ligase Reaction Buffer
- Super Optimal Broth with catabolite repression (S.O.C.) medium
- Sterile water

- LB Agar plates with kanamycin (50 mg/ml) (Sigma Aldrich. Ref. K1377-5G)
- X-Gal (Life Technologies. Ref. R0404)

3.13.3.2. Method

Following the fusion PCR and the purification of the final amplicon, its concentration was measured with the NanoPhotometer and the volume required for the ligation was determined with the following formula:

$$\frac{(\text{pb PCR product})(50 \text{ ng pCR 2.1 vector})}{3{,}929 \text{ pb of pCR 2.1 vector}} = \text{X ng of PCR product}$$

The ligation was carried out with an incubation at room temperature for 15 minutes after mixing 2 µl of 5X T4 DNA Ligase Reaction Buffer, 2 µl of pCR™ 2.1 vector (25 ng/µl), the volume of PCR product determined, 1 µl of DNA ligase (5 units) and sterile water up to 10 µl. Afterwards, it was centrifuged and 2 µl were transferred to a vial of One Shot® TOP10 Chemically Competent *E. coli*, mixing gently by pipetting. The vial was incubated on ice for 30 minutes, followed by a heat shock at 42ºC for 30 second, and then transferred into ice immediately. Subsequently, 150 µl of S.O.C. medium were added and vials were shaken horizontally at 37ºC with shaking at 225 rpm for 1 hour. Finally, 100 µl were poured onto LB Agar plates with kanamycin (50 µg/ml) and 40 µl X-Gal (1.6 mg/ml) spread over the surface. Plates were incubated at 37ºC for 16 hours shifting them to 4°C for 2-3 hours to allow proper color development. Those colonies with the vector incorporated appeared in white whereas those without the vector in blue.

3.13.4. Plasmid purification

The purification of the plasmid was carried out with the GenElute™ Plasmid Miniprep (Sigma Aldrich. Ref. PLN70-1KT).

3.13.4.1. Materials

- GenElute™ Plasmid Miniprep (Sigma Aldrich. Ref. PLN70-1KT). It provides the following materials:
  - Resuspension Solution

- RNase A Solution
- Lysis Solution
- Neutralization/Binding Solution
- Column Preparation Solution
- Optional Wash Solution
- Wash Solution Concentrate. It contains ethanol (95-100%)
- Elution Solution (pH 8): 10 mM Tris-HCl, 1 mM EDTA
- GenElute Miniprep Binding Column
- 2 ml Collection tubes

- LB broth with kanamycin (50 µg/ml)

3.13.4.2. Method

One colony of *E. coli* was grown in 5 ml of LB Broth with the appropriate antibiotic -ampicillin (100 µg/ml) or kanamycin (50 µg/ml)- at 37ºC with shaking at 150 rpm for 16 hours. The culture was centrifuged at 4,000 g for 10 minutes, being the pellet resuspended in 200 µl of the Resuspension Solution. Then, 200 µl of Lysis Solution were added, mixing by inversion until homogeneous, and 350 µl of Neutralization/Binding Solution were added, inverting the tube 4-6 times. Sample was centrifuged at 14,500 g for 10 minutes to remove cell debris, proteins, lipids, SDS and chromosomal DNA. Supernatant was transferred to a GenElute Miniprep Binding Column, previously treated with the Column Preparation Solution, and it was centrifuged at 12,000 g for 1 minute. The flow-through was discarded and 500 µl and 750 µl of the Optional Wash Solution and Wash Solution Concentrate, respectively, were added in consecutive steps, centrifuging at 12,000 g for 15 seconds and discarding the flow-through in each step. Afterwards, the sample was centrifuged at 14,500 g for 2 minutes to remove excess ethanol. Finally, the column was transferred to a 2 ml collection tube, being 100 µl of Elution Buffer added and the sample centrifuged at 12,000 g for 1 minute. The concentration of plasmid DNA was determined using the NanoPhotometer and stored at -20ºC until use.

3.13.5. Amplification of the DNA for the transformation of *A. fumigatus* strains

To generate the knockout strains, the plasmid isolated from the One Shot® TOP10 Chemically Competent *E. coli* (section 3.13.4) was used as DNA template. The amplification of the cassette was carried out using the Deletion cassette primer pairs (CassAbr1 or CassTF, depending on the gene of interest) (Table 3.4.). On the other hand, to generate the reconstituted strains, no fusion PCR was required as the sequence in which the homologous recombination took place was amplified using the same primers as above (CassAbr1 or CassTF) and the *A. fumigatus* Δ*akuB*^{ku80} DNA as template. PCR reactions had a final volume of 100 µl and its reaction mixture was the following:

Buffer 10x	10 µl
$MgCl_2$ (50 mM)	5 µl
dNTPs (2.5 mM)	8 µl
BioTaq polimerase (5 U/µl)	1 µl
Primer Forward (10 µM)	8 µl
Primer Reverse (10 µM)	8 µl
DNA for transformation (1 µg)	X µl
PCR-grade water	Up to 100 µl

PCR was carried out in the MJ Mini Personal Thermal Cycler and its amplification program was the same as section 3.8.3. PCR products were visualized by agarose gel electrophoresis and their concentrations were determined with the NanoPhotometer.

For *A. fumigatus* transformation a concentration of 1 µg/µl in a final volume of 50 µl of the amplicon was required. When lower concentration was achieved after the PCR, a precipitation and concentration of PCR products were performed. In that case, PCR reaction was transferred to a microcentrifuge tube and 10 µl of potassium acetate mixture (section 3.5.2.2.) and 230 µl of cold isopropanol were added. After mixing the sample by inversion, it was centrifuged at 14,500 g for 15 minutes and supernatant was discarded. Then, 300 µl of cold ethanol (70%) were added and samples were centrifuged at 14,500 g for 10 minutes, discarding the supernatant and incubating at room temperature for 10-15 minutes to remove any residual ethanol. Finally, the DNA pellet was resuspended in 50 µl of PCR-grade water and the concentration was determined with the NanoPhotometer. Samples were stored at -20ºC until use.

3.14. *Aspergillus fumigatus* Protoplast Preparation

3.14.1. Materials

- Lysing enzymes from *Trichoderma harzianum* (Sigma Aldrich. Ref. L1412-5G)
- Osmotic Medium (pH 8): 1.2 M $MgSO_4$ and 10 mM Sodium Phosphate Buffer (9.09g of NaH_2PO_4 and 18.79g of $NaH_2PO_4.H_2O$ in 100 ml distilled water). It was sterilized by filtration using 0.22 μm pore size filters and stored at 4ºC.
- Protoplast Trapping Buffer (pH 7): 0.6 M Sorbitol and 0.1 M Tris-HCl. It was sterilized by autoclaving at 121ºC for 15 minutes and stored at 4ºC.
- STC Buffer (pH 7.5): 1.2 M Sorbitol, 10 mM Tris-HCl and 10 mM $CaCl_2$. It was sterilized by autoclaving at 121ºC for 15 minutes and stored at 4ºC.
- 50 ml Falcon tubes.
- Microcentrifuge tubes.

3.14.2. Method

A concentration of $1x10^7$ *A. fumigatus* conidia/ml were poured into 250 ml of AMML and incubated at 28ºC with shaking at 250 rpm for 12 hours to obtain germ tubes 2-5 times the diameter of the spores. Once achieved, the culture was leaned at 45º for 5 minutes so that germinated conidia settled down to the bottom of the flask. Afterwards, 150 ml of media were removed without disturbing the germlings and spores were transferred to 2 Falcon tubes. Samples were centrifuged at 3,000 g for 8 minutes, discarding the supernatant. The final pellet was distributed in 4 Falcon tubes containing 10 ml of Osmotic Medium and 35 mg of Lysing enzymes previously mixed. The conidia of each tube were vigorously resuspended and incubated with an inclination of 45º at 28ºC with shaking at 100 rpm for 5 hours.

After the digestion process, each sample was transferred to a new Falcon tube and 5 ml of Protoplast Trapping Buffer were added, 1 ml at a time, to create an interface between the fungal digestion culture and the trapping buffer. The tube was leaned at 45º for 10 minutes, letting the trapping buffer trickle down the sides of the glass tube. Subsequently, samples were centrifuged at 5,000 g for 15 minutes at room temperature using a centrifuge with a swinging bucket rotor. At this point, several layers were observed in the tubes, with protoplast in a thin cloudy layer (the most superficial layer).

Protoplasts from the 4 tubes were collect into a new Falcon tube, previously kept on ice. These samples were kept on ice until the end of the transformation.

Immediately after, 3X volume of the protoplasts recovered of cold STC was added to the sample, mixing by inversion, and the tube was centrifuged at 5,000 g for 15 minutes using a centrifuge with a swinging bucket rotor. The supernatant was discarded and the protoplasts resuspended in 1 ml of cold STC and transferred to a microcentrifuge tube. Sample was centrifuged at 13,000 g for 13 seconds, discarding the supernatant, and the final pellet was resuspended in 300 µl of cold STC. The number of protoplasts was determined using a hemocytometer.

3.15. *Aspergillus fumigatus* Protoplast Transformation

3.15.1. Materials

- DNA for transformation (1 µg/µl): Deletion cassette to generate the knockout strain or the original sequence to generate the reconstituted strain.
- Polyethyleneglycol (PEG) Solution (pH 7.5): 60% PEG 6000, 50 mM $CaCl_2$ and 50 mM Tris-HCl .
- STC Buffer (pH 7.5) (section 3.14.1)
- Hygromycin (Life Technologies. Ref. 10687-010)
- Top agar with or without hygromycin (200 µg/ml): 50 ml of 20X Salt Solution, 1 ml of Elements Trace Solution, 10 g of D-Glucose, 1,2 M of Sorbitol, 1 g of Yeast Extract and 7 g of Agar in 1 l of distilled water. It was sterilized by autoclaving at 121ºC for 15 minutes and stored at 4ºC.
- SMM plates with or without hygromycin (200 µg/ml)
- AMM plates with or without hygromycin (200 µg/ml)

3.15.2. Method

The transformation was carried out using 2 aliquots of protoplasts with a final concentration of $1x10^6$ protoplasts in 500 µl of cold STC buffer, obtained according to the section 3.14.2. One aliquot was used for transformation, adding 50 µl of the DNA for transformation (50 µg final concentration), whereas the other one was used as a negative control of the transformation process adding 50 µl of STC buffer. Both samples were incubated on ice for 50 minutes and then, 1.25 ml of PEG Solution were

added to each one, mixing softly by pipetting. Once homogenized, they were incubated for 20 minutes and centrifuged at 2,700 g for 1 minute. Supernatants were discarded to remove PEG Solution and the final pellets were resuspended in 1 ml of cold STC Buffer.

The sample in which transformation took place was plated onto SMM with hygromycin plates. Five ml of top agar with hygromycin, previously stored at 45ºC, were inoculated with 100 µl of the sample and poured into a plate of SMM with hygromycin. This step was repeated until the entire sample was plated. To determine if protoplast were able to grow in presence of hygromycin, 2 plates of SMM with hygromycin were inoculated with 100 µl of the negative control. This sample was also used to determine the regeneration capability of protoplast, plating 100 µl on SMM without hygromycin. Plates were incubated at 37ºC for 24-36 hours until transformants appeared. As soon as a colony grew, it was picked and grown in AMM with hygromycin at 37ºC for 3-4 days until sporulation. Finally, each colony was grown on PDA, as described in section 3.1.2, to continue with mycelium harvesting, DNA isolation, PCR, sequencing and Southern Blot assays.

When the knockout strain was transformed to generate the reconstituted strain, SMM without hygromycin plates were used so that every protoplast was able to growth. Before sporulation, each colony was poured onto AMM with hygromycin plates and plates were incubated at 37ºC for 3-4 days to identify those which had lost the resistance gene. Once identified, colonies were isolated in AMM plates without hygromycin at 37ºC for 3-4 days until sporulation and afterwards, they were grown on PDA, as described in section 3.1.2, to continue with mycelium harvesting, DNA isolation, PCR, sequencing and Southern Blot assays.

3.15.3. Confirmation of knockout and reconstituted strains by PCR and sequencing

To confirm the correct deletion a conventional PCR was performed according to the section 3.8. Two reactions were carried out with each colony, one with the primers designed for the gene of interest (abr1 or TF primers) and another one with the primers used to amplify the hygromycin resistance gene (Table 3.4). As positive controls DNA from the wild type (*A. fumigatus ΔakuB*^{ku80}) and the plasmid pA-Hyg-OSCAR were included to amplify the gene of interest and the hygromycin gene, respectively. PCR

products were visualized by agarose gel electrophoresis, as described in section 3.9. Knockout strains were those in which only a band for the hygromycin gene appeared and the reconstituted ones those in which only the gene of interest was amplified. The amplicon of those colonies that seemed to have incorporated the correct fragment in each transformation were sequenced by the SGIKER at UPV/EHU to check if any mutations were incorporated into the sequence.

3.15.4. Southern Blot

3.15.4.1. Probe design

3.15.4.1.1. Materials

- PCR DIG Probe Synthesis Kit (Roche. Ref. 11 636 090 910). It provides the following materials:
  - PCR buffer with $MgCl_2$
  - PCR DIG Labeling Mix
  - Enzyme mix
- PCR-grade water

3.15.4.1.2. Method

To determine the number of copies of the fragment inserted in each transformation of *A. fumigatus* Δ*akuB*^{ku80} or the knockout strains, two probes were designed per gene of interest. One of the probes was designed within the 5' flanking region of that in which the homologous recombination took place and the other one within the hygromycin gene. The design of each probe was carried out with a conventional PCR using the PCR DIG Probe Synthesis Kit and specific primer pairs designed according to the section 3.7.2 (Table 3.5).

Table 3.5. Primers designed to obtain the probes used in Southern Blot assays.

Name[a]	Sequence (5'→3')[b]	Tm[c]	%GC[d]	Amplicon (pb)[e]
Primers to design the *abr1/brown1* 5' flanking region probe				
Abr1SB-F	gccttttcccaccagataca	59.9	50	524
Abr1SB-R	cttgtccagcttgaccatga	59.8	50	
Primers to design the hygromycin probe				
HYGSB-F	gggagatgcaataggtcagg	59.5	55	500
HYGSB-R	gtcagatcagccccacttgt	60.1	55	
Primers to design the transcription factor 5' flanking region probe				
TFSB-F	acaatggctcgaccgtaatc	59.7	50	562
TFSB-R	gcatggcaattctccttgat	60.0	45	

[a]Name of each primer. F: Forward, R: Reverse.
[b]Sequence of each primer.
[c]Melting temperature of each primer, according to Primer3.
[d]Percentage of guanine and cytosine content of each primer, according to Primer3.
[e]Size of the amplification product.

To design the probes located at the 5' flanking regions *A. fumigatus* Δ*akuB*^{ku80} DNA was used as template whereas to design the probe within the hygromycin gene the plasmid pA-Hyg-OSCAR was included as template. The amplification was carried out with the primer pairs designed for each case (Table 3.5).

PCR reactions had a final volume of 50 µl and its reaction mixture was the following:

PCR buffer with $MgCl_2$ 10x	5 µl
PCR DIG Labelling Mix	5 µl
Primer Forward (10 µM)	5 µl
Primer Reverse (10 µM)	5 µl
Enzyme Mix	0.75 µl
DNA (10 ng/µl)	1 µl
PCR-grade water	28.25 µl

The conventional PCR was carried out in the MJ Mini Personal Thermal Cycler and its amplification program was the following:

Step 1: Denaturalization	95ºC	2 minutes
Step 2: 10 cycles	95ºC	10 seconds
	60ºC	30 seconds
	72ºC	2 minutes
Step 3: 30 cycles	95ºC	10 seconds
	60ºC	30 seconds
	72ºC	2 minutes
Step 3: Extension	72ºC	7 minutes

PCR products were visualized by agarose gel electrophoresis (section 3.9). Positive amplifications were those in which only one amplicon with the expected size was obtained for each primer pair. In each amplification program a negative control per gene was included in which water was added to the reaction instead of DNA.

3.15.4.2. DNA digestion

3.15.4.2.1. Materials

- 10X CutSmart Buffer® (pH 7.8-8) (New England Biolabs. Ref. B7204S)
- ScaI-HF® (New England Biolabs. Ref. R3122S)
- StuI (New England Biolabs. Ref. R0187S)
- MscI (New England Biolabs. Ref. R0534S)
- TBE Buffer (section 3.9.1)
- Loading dye 5X (section 3.9.1)
- SYBER® SAFE DNA Gel Stain (Thermo Fisher Scientific, Ref. S33102).

3.15.4.2.2. Method

DNA isolated from the mycelia of each strain was digested using suitable enzymes. The choice of enzymes was made using the Sequence Manipulation Suite version 2 (http://www.bioinformatics.org/sms2/rest_map.html) choosing those that cut upstream and downstream to the 5' and 3' flanking regions of the region where homologous recombination took place, and within the hygromycin gene. To analyze the number of copies of the fragments for the deletion and insertion of *abr1/brown1* gene ScaI-HF® and StuI were used whereas for the deletion and insertion of the transcription factor AFUA_1G02860 ScaI and MscI were those showing the best digestion (Table 3.6).

Table 3.6. Restriction enzymes chosen for the DNA digestion.

Restriction enzymes[a]	Strain[b]	Size[c]
Gene *abr1/brown1*		
ScaI-HF® 5' flanking region and hygromycin gene	*A. fumigatus Δabr1/brown1*	3,561 bp 2,821 bp
StuI 3' flanking region	*A. fumigatus* Δ*abr1/brown1::abr1/brown1*$^{+}$	7,132 bp
	A. fumigatus ΔakuB^{KU80}	7,132 bp
Transcription factor AFUA_1G02860		
MscI 5' and 3' flanking regions	*A. fumigatus Δtf*	2,857 bp 3,860 bp
ScaI Hygromycin gene	*A. fumigatus ΔakuB*^{KU80}	6,916 bp

[a]Restriction enzymes used for the DNA digestion and the regions in which they cut.
[b]Strains digested with the restriction enzymes. *A. fumigatus ΔAbr1/brown1* and *A. fumigatus Δtf* were obtained after the transformation of *A. fumigatus ΔakuB*^{KU80} and *A. fumigatus* Δ*abr1/brown1::abr1/brown1*$^{+}$ after the transformation of *A. fumigatus Δabr1/brown1*.
[c]Size of the fragment obtained following the digestion.

DNA digestions were carried out with 4 µl of each restriction enzyme, 1-4 µg of DNA and 13 µl of 10X CutSmart Buffer® in a total volume of 120 µl. Samples were incubated at 37ºC for 16 hours and afterwards the reactions were stopped by adding 25 µl of gel loading dye 5X. The digested DNA was resolved on 1% (w/v) agarose gel using the Owl™ EasyCast™ B3 Gel system with Built-In Recirculation (Thermo Fisher Scientific, Ref. B3). The digestions were visualized with a ChemiDoc™ MP System (Bio-Rad Laboratories. Ref. 1708280) after incubating the gel in TBE with 20 µl of SYBER® SAFE DNA Gel Stain (Thermo Fisher Scientific, Ref. S33102). Afterwards, gel was washed in water with shaking at 25 rpm for 10 minutes.

3.15.5. DNA transference

3.15.5.1. Materials

- Depurination Solution: 24.55 ml of 33-35% HCl
- Denaturation Solution: 1.5M NaCl and 0.5M NaOH
- Neutralization Solution (pH 7.5): 1.5M NaCl and 0.5M Tris-Cl
- SSC 20X: 3M NaCl and 0.3M Sodium citrate
- Stratalinker® UV Crosslinker (Agilent Technologies. Ref. 400071)
- Saran wrap (Scientific Laboratory Supplies, Nottingham, UK. Ref. FIL1040)
- Filter paper
- Scott® Pullman Hand towel (Kimberly-Clark, Kent, UK. Ref. 6644)
- Nylon membranes, positively charged (Roche. Ref. 11417250001)

3.15.5.2. Method

Agarose gel obtained in section 3.15.4.2.2 was depurinated in 250 ml of Depurination Solution at room temperature with shaking at 25 rpm for 15 minutes and washed in water for 10 minutes. Subsequently, the gel was denaturized twice with the Denaturation Solution at room temperature with shaking at 25 rpm for 15 minutes and then washed in water for 10 minutes. It was submerged twice with Neutralization Solution at room temperature with shaking at 25 rpm for 15 minutes, washed in water for 10 minutes, and equilibrated twice in SSC 20X for 10 minutes. The Southern Transfer Tower was set up (Fig. 3.1) and left overnight. Finally, the membrane was sided up on filter paper soaked in SSC 2X and pulsed at 1,200 µJ for 25-50 seconds in the UV Crosslinker.

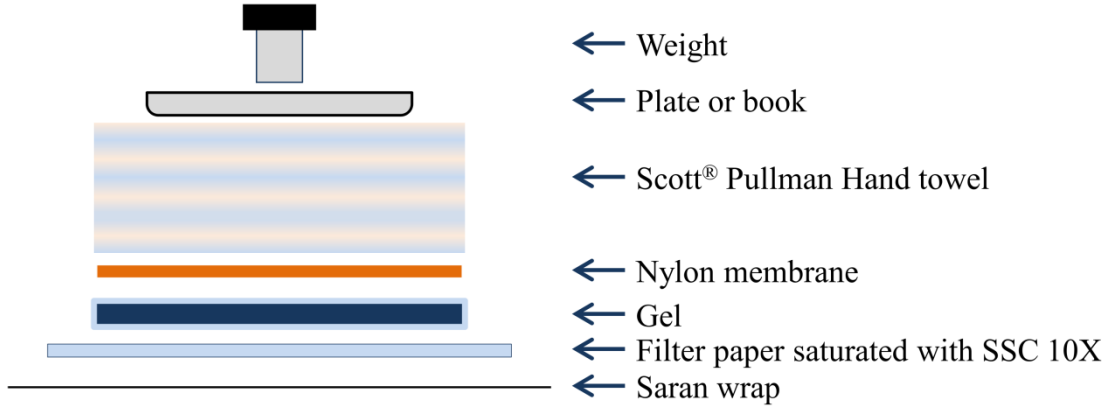

Fig. 3.1. Schematic illustration of a Southern Transfer Tower.

3.15.6. Hybridization

3.15.6.1. Materials

- DIG Easy Hyb kit (Roche. Ref. 11 603 558 001).
- Low Stringency Buffer: SSC 2X and 0.1% (w/v) SDS
- High stringency buffer: 0.5% SSC and 0.1% (w/v) SDS
- Washing Buffer (pH 7.5): 0.3% Tween 20 in Maleic Acid Buffer 10x (pH 7.5, 1M Maleic acid, 1.5 M NaCl)
- Blocking solution (pH 7.5): 3g of blocking reagent (Roche. Ref. 11096176001), 30 ml of Maleic Acid Buffer 10x and 300 ml distilled water.
- Antibody Solution: 30 ml of Blocking Solution and 3 µl of anti-digoxigenin-AP Fab fragments (Roche. Ref. 11093274910)
- Detection Buffer (pH 9.5): 0.1 M Tris-Cl and 0.5 M NaCl
- CDP-Star, ready-to-use (Roche. Ref. 12 041 677 001)
- Stripping buffer: 0.2 M NaOH and 1% (w/v) SDS
- HB-1D Hybridiser hybridization incubator (Techne, Staffordshire, UK. Ref. FHB1DE)
- Acetate sheets (Hobbycraft, Staffordshire, UK. Ref. 572870)
- ChemiDoc™ MP System (Bio-Rad Laboratories)

3.15.6.2. Method

The hybridization was carried out following the DIG Easy Hyb kit. The temperature of hybridization for each probe was calculated following this formula:

$$T_m = (49.82 + 0.41\ (GC\ \%) - 600 / \text{length in bases})$$

$$T_{opt} = Tm - (20 \text{ to } 25)$$

Hybond N membrane obtained in the section 3.15.5.2 was pre-hybridize with pre-warmed DIG Easy Hyb for 3 hours at the appropriate temperature in a HB-1D Hybridiser hybridization incubator, being then discarded and replaced by 20 ml of DIG Easy Hyb. Subsequently, 10 µl of the probe was denaturalized in 40 µl of PCR-grade water at 100ºC for 5 minutes and added to the membrane. The hybridization was left overnight at the appropriate temperature in the hybridization incubator.

Membrane was washed twice with the Low Stringency Wash Buffer with shaking at 25 rpm for 5 minutes and incubated twice at 65ºC for 15 minutes in the hybridization incubator with 20 ml of High Stringency Wash Buffer. After being washed with the Washing Buffer for 2 minutes, it was blocked in Blocking Reagent with shaking at 25 rpm for 3 hours and then incubated for 1 hour with the Antibody Solution. Membrane was washed twice with Wash Solution and with shaking at 25 rpm for 15 minutes and then equilibrated in Detection Buffer for 3 minutes at room temperature. The membrane was incubated for 5 minutes with the substrate CDP-Star between two acetate sheets and then bands were visualized with the ChemiDoc™ MP System. To reuse the membrane in further hybridizations, it was washed twice with water for 10 minutes and then, incubated twice with Stripping Solution at 37ºC in the hybridization incubator for 15 minutes. Finally, it was placed over a filter paper saturated with SSC 2X, wrapped in saran wrap and kept at 4ºC.

3.16. Cell line infections

Two different cell line infections were performed to study the virulence of *A. fumigatus* knockout and reconstituted strains relative to the wild type. The first one was a detachment assay performed with the human pulmonary carcinoma epithelial cell line A549 (American type culture collection (ATCC), Middlesex, UK. Ref. CCL-185). The second assay was a transwell infection that allowed studying the effect of each strain on epithelial integrity. In this case Calu-3 cells (ATCC. Ref. HTB-55), a well-differentiated and characterized cell line derived from human bronchial submucosal glands that forms tight polarized monolayer in culture, were used.

Cells were cultured in a 75 cm^2 cell culture flask (Corning. Ref. 430720U), containing 6 ml of the proper media (DMEM or DMEM-F12) supplemented with 10% FBS and 1% Penicillin-Streptomycin, at 37°C with 5% CO_2. Their maintenance was carried out

every 3 days discarding the culture medium and rinsing the cell layer with 5-10 ml of unsupplemented media to remove all traces of serum. Afterwards, 4 ml of Typsin-EDTA solution (Sigma Aldrich. Ref. T4299) were added, incubating the sample at 37°C for 2-5 minutes for A549 cells and 5-10 minutes for Calu-3 cells. The detachment of cells was checked using the microscope. Once detached, 6 ml of complete medium were added, being the cells aspirated by gently pipetting. They were transferred to a 50 ml falcon tube and after mixing gently, 2 ml of cells were added to a new flask containing 10 ml of complete medium.

After the trypsin/EDTA treatment, 100 µl of cell suspension were transferred into an eppendorf to which 100 µl of trypan blue (Sigma Aldrich. Ref. T8154-20ML) were added. The number of cells was assessed adding 10 µl of the mixture to a hemocytometer. The viability of the cells was determined assessing the percentage of live cells relative to total cells.

3.16.1. *Aspergillus fumigatus* conidia and culture filtrate

Infections were performed with conidia and the culture filtrate of each *A. fumigatus* strain. Conidia were harvested according to the section 3.1.2.1 and a concentration of 10^6 conidia in 1 ml of appropriate media (DMEM or DMEM/F12) was used as stock.

To obtain the culture filtrate, 10^6 conidia/ml were grown in 20 ml of DMEM supplemented at 37°C with shaking at 180 rpm for 48 hours. Afterwards, culture was firstly filtrate with miracloth (EMD Millipore, Billerica, MA, USA. Ref. 475855-1R) and then with 0.22 µm pore size filters. The purity of the culture filtrate was checked pouring 100 µl of filtrate onto two SGA plates and incubating the plates at 37°C for 24-48h.

3.16.2. Detachment assay

This infection was carried out with A549 cell line in 24 well plates (Greiner bio-one, Stonehouse, UK. Ref. 662892) containing 1 ml of DMEM supplemented with 10% FBS and 1% Penicillin-Streptomycin. A concentration of 10^5 cells/ml was seeded in each well and incubated at 37°C with 5% CO_2 until they reached confluence. Afterwards, media was replaced with fresh DMEM supplemented and cells were infected with 100 µl of *A. fumigatus* conidia (10^5 conidia) or 100 µl of culture filtrate and incubated at

37°C with 5% CO_2 for 16 hours. Negative controls, in which neither conidia nor culture filtrate were added, were also included. The assay was carried out with three independent samples and three technical replicates.

Cells were rinsed 3 times with 1 ml of pre-warmed PBS (Sigma Aldrich. Ref. D8537-500ML) and then incubated with 1 ml of 4% formaldehyde in PBS (Alfa Aesar, Heysham, UK. Ref. J60401) at room temperature for 10 minutes. Subsequently, 4% formaldehyde was removed and fixed cells were permeabilized with 0.2% Triton X-100 in PBS (Sigma Aldrich. Ref. X100-100ML) at room temperature for 2 minutes. Triton X-100 was removed and samples were rinsed 3 times with 1 ml pre-warmed PBS. Once washed, 1 ml of 300 nM DAPI stain solution (Life technologies. Ref. D1306) was added to cover the cells, incubating at room temperature for 5 minutes and protecting plates from light. The stain solution was removed and samples were rinsed 3 times with 1 ml pre-warmed PBS. Finally, 1 ml of pre-warmed PBS was added to each well.

Staining cells were observed using the Eclipse E2000-E microscopy (Nikon, Surrey, UK). Images were captured using the MetaMorph software (Molecular Devices) and analyzed using the FIJI software (http://fiji.sc/). Finally, the results obtained for each strain were graphically represented and statistically compared to the wild type using Student's t-test.

3.16.3. Cell monolayer integrity

The infection was performed using CALU-3 cells in 12-well plates (Corning, New York, USA. Ref. 353503) containing a falcon cell culture insert with 1.0 µm pore membrane (Scientific Laboratory Supplies. Nottingham, UK. Ref. 353103). A concentration of 10^6 Calu-3 cells in a total volume of 1 ml was added to a falcon cell culture insert placed into a well containing 1 ml of supplemented DMEM-F12. The plate was incubated at 37°C with 5% CO_2 for 10 days to achieve the monolayer, being the media changed every 3-4 days after measuring the trans-epithelial electric resistance (TEER) with the EVOM^2 Epithelial Volt/Ohm meter (World Precision Instruments, Sarasota, FL, USA. Ref. EVOM2). The infection was carried out when cells reached above >1000 Ω.

A concentration of 10^5 conidia in a final volume of 100 µl or 100 µl of the culture filtrate was added to each falcon cell culture insert. Negative controls, in which neither

conidia nor culture filtrate were added, and wells with 1% (w/v) SDS were also included. Plates were incubated at 37˚C with 5% CO_2 for 24 hours and afterwards the TEER was measured. The assay was carried out with three independent samples and three technical replicates.

TEER measurements obtained after 24 hours of infection were normalized according to the viability of conidia (section 3.1.2.1). The loss of integrity was determined subtracting the TERR values obtained before the infection to those normalized at the end of the experiment. Data from negative controls were also subtracted to each sample. Results were graphically represented and the Student's t-test was applied to detect statistical differences among mutant strains and the wild type.

3.17. Bioinformatic tools

Several bioinformatic tools were used in the development of this dissertation whose applications and programs are available online.

3.17.1. NCBI

The National Center for Biotechnology Information of USA (http://www.ncbi.nlm.nih.gov) provides access to biomedical and genomic information. The databases used in this dissertation were the following:

- Entrez Pubmed (http://www.pubmed.com) is a US National Library of Medicine that comprises more than 26 million citations for biomedical literature from MEDLINE, life science journals, and online books published since 1948. This website was used to gain access to full-text articles and reviews.

- Entrez Nucleotide database (http://www.ncbi.nlm.nih.gov/nuccore/) is a collection of sequences from several sources, including GenBank, RefSeq and PDB (Protein DataBase). GenBank is a genetic sequence database with all publicly available DNA sequences. It comprises the DNA DataBank of Japan (DDBJ), the European Molecular Biology Laboratory (EMBL), and GenBank at NCBI, which exchange data on a daily basis. This database was used to look for mRNA sequences of *A. fumigatus* genome as well as those quality genes from *Mus musculus* and *Homo sapiens* to design the expression microarray.

- BLAST (http://blast.ncbi.nlm.nih.gov/Blast.cgi), the Basic Local Alignment Search Tool, finds regions of local similarity between nucleotide or protein sequences. In this Thesis, nucleotide blast (BLASTN) and Primer-Blast were used to find homology between the primers designed and the genome database.

3.17.2. Primer3

Primer3 (v. 0.4.0) software (http://bioinfo.ut.ee/primer3-0.4.0/) was used to design the primer pairs of those genes selected to validate microarray data and for the development of knockout and reconstituted strains.

3.17.3. OligoAnalyzer 3.1

This website belongs to Integrated DNA Technologies (http://eu.idtdna.com/calc/analyzer) and it was used to analyze the primers designed and check whether they form hairpin loops or homo and heterodimers.

3.17.4. GeneSpring GX software v.12

GeneSpring is a software designed by Agilent Technologies that offers an interactive environment promoting investigation and enabling understanding of transcriptomics, metabolomics and proteomics data within a biological context. This software was used to normalize the transcriptomic data from the germination of *A. fumigatus* and to perform the hierarchical clustering between the disseminated infection and the germination.

3.17.5. Babelomics server

Babelomics (http://www.babelomics.org) is an integrative platform for the analysis of transcriptomics, proteomics and genomic data. This server was used to normalize and statistically analyze the transcriptomic results obtained throughout an intravenous infection and the germination of *A. fumigatus*.

3.17.6. MultiExperiment Viewer

MultiExperiment Viewer is a program designed by TIGR and it is a versatile microarray data analysis tool. It was used in this project to develop Heat Maps, graphical representations of data where values contained in a matrix are represented as colors.

3.19.7. PEDANT 3 database

PENDANT 3 (http://pedant.helmholtz-muenchen.de) is a database designed by Munich Information Center for Protein Sequence (MIPS) that provides exhaustive automatic analysis of genomic sequences by a large variety of bioinformatics tools. Amongst them, the prediction of cellular roles and functions stand out, which are made based on high stringency BLAST searches against protein sequences with manually assigned functional categories according to the Functional Catalogue (FunCat) developed by MIPS and Biomax Informatics AG. This database was used in this dissertation to determine the biological functions of differentially expressed genes.

3.17.8. FungiFun 2.2.8.

FungiFun 2.2.8 (https://elbe.hki-jena.de/fungifun/fungifun.php) is a bioinformatic tool that assigns functional annotations to fungal genes or proteins, performing, at the same time, an enrichment analysis. Thus, it allows determining which functional categories show significant p-values based on genetic or proteomic results. In this project, this tool was used to determine the enriched functional categories of the differentially expressed genes.

3.17.9. CADRE

The Central Aspergillus Data REpository (CADRE; http://www.cadre-genomes.org.uk/index.html) is a public database that gathers all genomic information about *Aspergillus* genus. In this dissertation this database was used to obtain the FASTA sequences needed to develop the deletion fragments.

3.17.10. Sequence Manipulation Suite

Sequence Manipulation Suite v.2 (http://www.bioinformatics.org/sms2/rest_map.html) is a collection of JavaScript programs for generating, formatting, and analyzing short DNA and protein sequences. This program allowed choosing the restriction enzymes to digest the DNA used in the Southern Blots.

4. RESULTS

4.1. Expression microarray design

Using the information available in the NCBI database (http://www.ncbi.nlm.nih.gov/) and the eArray system (Custom Microarray Design, Agilent Technologies: http://earray.chem.agilent.com/erray/) a whole *A. fumigatus* expression microarray was designed, which was named Agilent Whole *A. fumigatus* Genome Expression 44K (AWAFUGE) microarray v.1. This microarray included 45,220 probes. Amongst them, 28,890 belonged to *A. fumigatus*, as 9,630 genes constitute its genome and 3 probes were designed for each one. On the other hand, 62 quality control genes were also incorporated, with 3 probes for each gene and each repeated 5 times on the microarray. Furthermore, the eArray system automatically included positive and negative controls. Glass slide, a format of 4 microarrays per glass slide (4x44K), and a covalent union with the samples were chosen for microarray manufacturing (Fig. 4.1). Finally, the AWAFUGE microarray (v.1) design was submitted to the ArrayExpress database through the MIAMExpress tool under accession number A-MEXP-2352.

Fig. 4.1. Microarray designed with the gasket cover slide. The format adopted was 4 microarrays per slide (4x44K), being the slide made of glass, with a covalent union with samples. The microarray includes 45,220 probes, among which 28,890 monitor the expression of *A. fumigatus*.

4.2. Viability and germination of conidia

The viability of *A. fumigatus* Af-293 conidia used in this study was 75.82 ± 14.50%. The germination study at 37 and 24ºC showed how conidia started to germinate earlier with an increase in temperature (Fig. 4.2). After 4 hours of incubation at 37ºC the germination rates were 6.03%, reaching 100% at 10 hours. On the other hand, when the incubation was performed at 24ºC, germination was not observed until 14.5 hours of incubation, with germination rates of 3.6%, achieving 100% germination rates at 30 hours (Fig. 4.2B). To study the early expression of this fungus with the microarray designed, a germination rate of 15-30% was selected given the size of the germinated conidia (Fig. 4.2A). In cultures at 37 and 24ºC, cells reached these germination rates after 6.5 and 18 hours of incubation, respectively. No differences in pH were detected between starting (pH 7.2) and harvesting times in either of the cultures (pH 7.1 ± 0.11).

Due to the different incubation times needed to achieve 15-30% germination rates at 37 and 24ºC (6.5 and 18 hours, respectively), it could be thought that, in addition to the temperature, other factors might affect gene expression. Thus, a modified germination study was designed to check whether the differences between each incubation time showed any effect on expression due to culture medium conditions, for example. In order to reduce the different incubation times, cultures incubated at 24ºC for 16 hours with 1-4% germination rates and in which swelling had already taken place were used as starting point. At that moment, culture medium was replaced by fresh medium and cultures were incubated at 24 or 37ºC. As in continuous incubation, without the addition of fresh medium, the germination at 37ºC was faster than at 24ºC (Fig. 4.2).

For transcriptomic studies, 15-30% germination rate samples obtained from continuous incubations were used either in microarray experiments or in the validatin by RT-qPCR assays. To study the effect of the incubation times on gene expression, samples with 15-30% and 40-60% germination rates after the addition of fresh medium, which were achieved after 1.5 and 3 hours of incubation at 37ºC and 3 and 6 hours at 24ºC, were harvested and used in RT-qPCR studies.

4.3. Gene expression during the germination in response to temperature

Three independent RNA samples from the growth of *A. fumigatus* at each temperature were transcribed into cDNA and hybridized with the AWAFUGE microarray (v.1). Slides were scanned using the Gene Pix® 4100ª scanner and the data obtained was deposited in the ArrayExpress database under accession number E-MTAB-1910. Following hybridizations, normalized data were graphically represented (Fig. 4.3), showing similar expression at the two temperatures. However, statistical comparisons showed that among the 9,630 genes, 1,249 genes were differentially expressed. In figure 4.4 expression differences in $\log_2$ are represented relative to the statistical significance ($-\log_{10}$ p-value). Negative $\log_2$ fold change values meant up-regulation at 37ºC whereas positive values up-regulation at 24ºC. A value of 1 and -1 means a two-fold increase and decrease in expression, respectively. Overall, 591 genes were up-regulated at 37°C and 658 at 24°C.

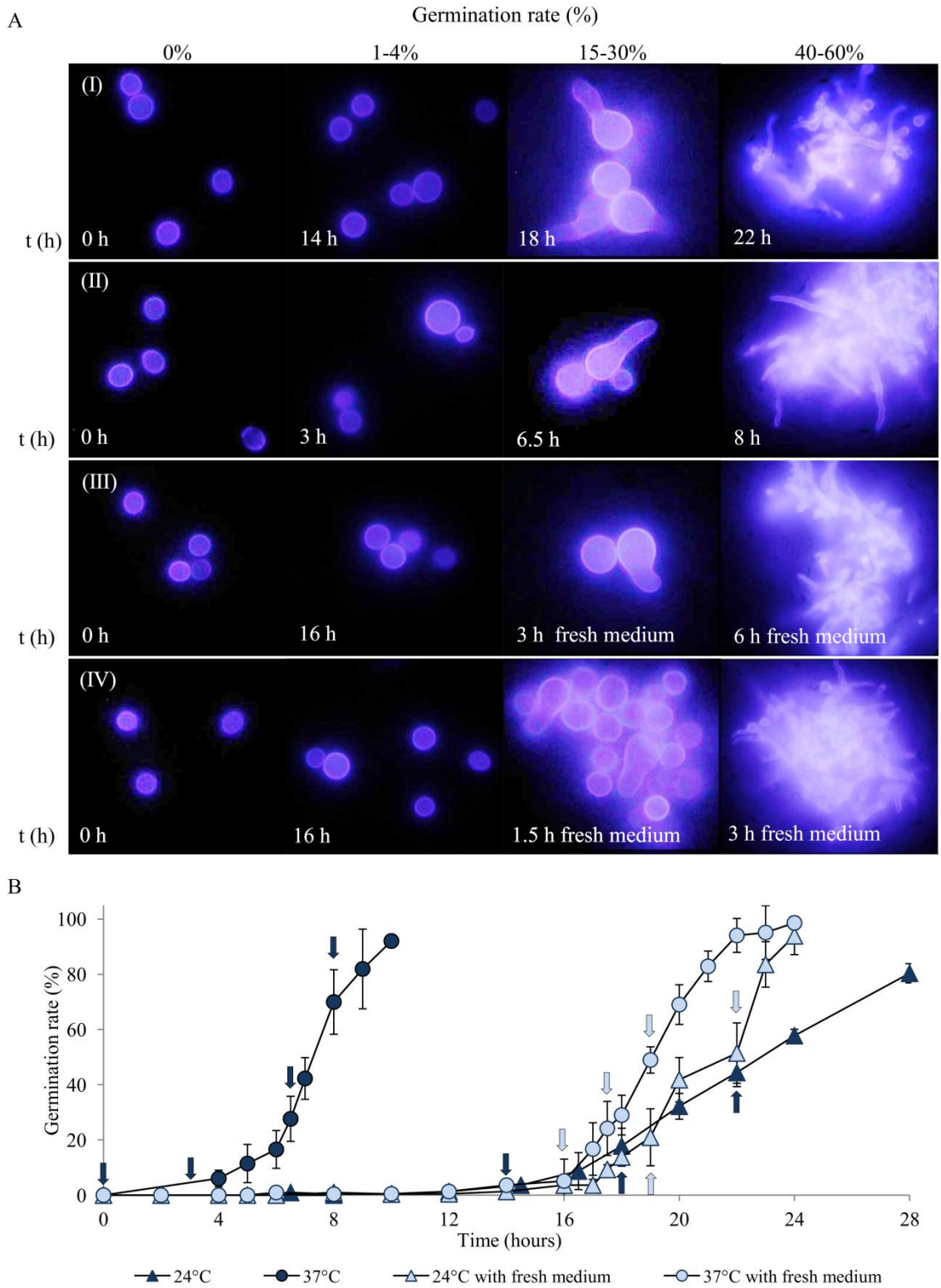

Fig. 4.2. Germination of *A. fumigatus*. A) Calcofluor white staining of *A. fumigatus* Af-293. Each picture showed the percentage of germination and the hours of incubation. B) Curves of germination rates of *A. fumigatus* Af-293. Each point represents the mean value ± standard deviation of three independent samples of each time. Dark and light blue arrows indicate the time points at which samples were obtained. Continuous incubation at 24ºC (I and dark blue triangles) and at 37ºC (II and dark blue circles). Incubation at 24ºC (III and light blue triangles) and at 37ºC (IV and light blue circles) following the addition of fresh medium after 16 hours of incubation at 24ºC.

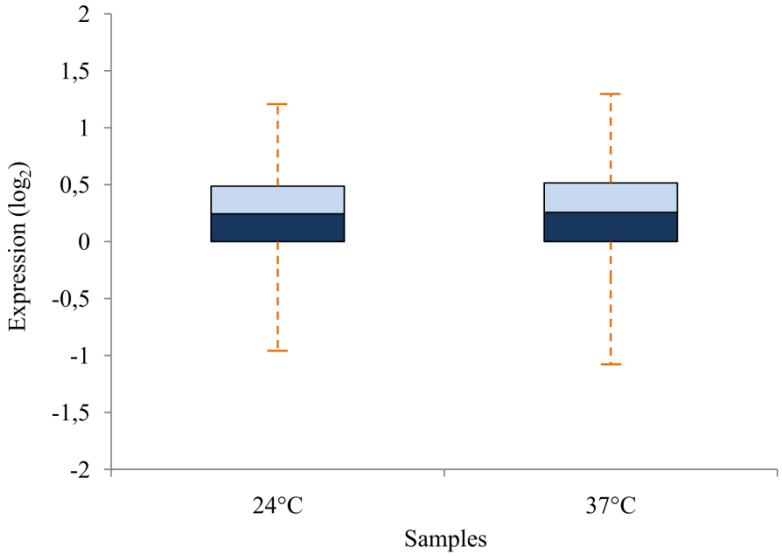

Fig. 4.3. Box plot representing the distribution of gene expression. Each sample corresponds to the mean expression of three independent samples obtained from the growth at 24 or 37ºC, respectively. The Y-axis values represent the gene expression (log_2).

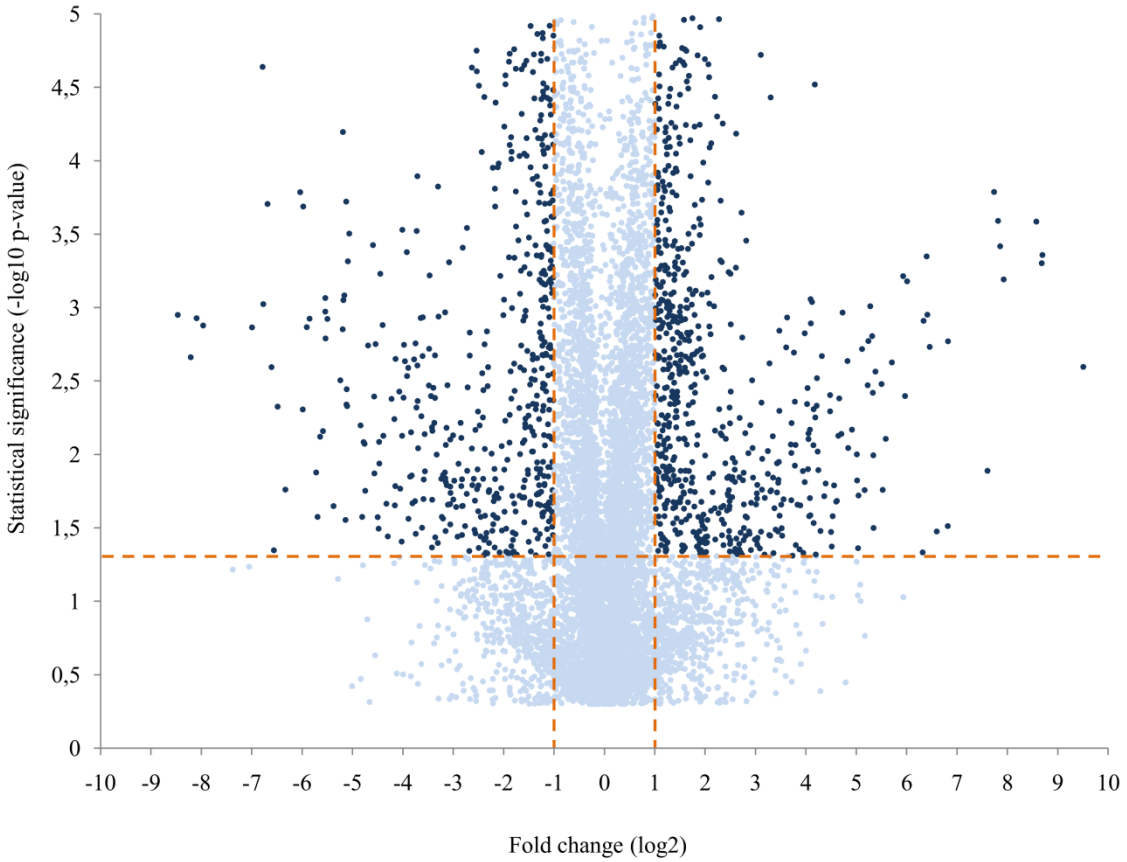

Fig. 4.4. Volcano plot of gene expression analysis. Differentially and non-differentially expressed genes are shown in dark blue or light blue, respectively. The X-axis values represent the fold change (log_2) of microarray data and the Y-axis values the statistical significance ($-log_{10}$ p-value). Spots with negative fold change values indicate up-regulation at 37ºC and spots with positive values up-regulation at 24ºC.

Those genes that coded for functional proteins were classified according to the FunCat categorization except those that encoded hypothetical or unclassified proteins, which were classified in two non-functional groups. The most common functions were metabolism, transport, transcription, and cell rescue, defense and virulence, followed by energy, interaction with the environment, and protein fate. However, more than a half of the differentially expressed genes encoded hypothetical and unclassified proteins with 385 and 326 genes, respectively (Table 4.1).

Tabla 4.1. Classification of those genes that showed significant differences in the study about the effect of temperature during the germination.

Main category[a]	Total number of genes[b]	24ºC[c]	37ºC[c]
Metabolism	313	148	165
Transport	147	73	74
Cell rescue, defense and virulence	93	37	56
Energy	68	27	41
Interaction with the environment	68	36	32
Protein fate	58	35	23
Biogenesis of cellular components	52	31	21
Cell type differentation	25	13	12
Cell cycle and DNA processing	45	37	8
Cell fate	20	14	6
Cellular comunication/signal transduction mechanism	18	13	5
Transcription	102	98	4
Regulation of metabolism and protein functions	15	12	3
Development	7	5	2
Protein synthesis	55	55	0
Hypothetical proteins	326	170	156
Unclassified proteins	385	181	204

Note: One gene can be involved in more than one biological function, which explains why the total number of genes is larger than the differentially expressed genes of *A. fumigatus*.

[a]Functional category according to the Munich Information Center for Protein Sequence Functional Catalogue (FunCat; http://pedant.helmholtz-muenchen.de). Genes that encode hypothetical or unclassified proteins were classified in two non-functional groups.

[b]Number of genes that showed significant differences and that are involved in each category.

[c]Number of genes found in each condition.

Focusing on the percentage for each condition, 24 and 37ºC, and taking into account only genes with well-known functions, metabolism, transport, cell rescue, defense and virulence, and energy groups appeared to have the largest number of up-regulated genes at 37°C. In the rest of the groups the number of up-regulated genes was higher at 24 than at 37ºC, transcription, protein synthesis, and cell cycle and DNA processing being the main groups (Table 4.1). Nevertheless, to determine in a specific way which functions were significant at each temperature, an enrichment analysis was carried out. According to it, 8 categories were significantly enriched at 37°C, being C-compound and carbohydrate metabolism, secondary metabolism, lipid, fatty acid and isoprenoid metabolism, non-vesicular cellular import, NAD/NADP binding, non-ribosomal peptide synthesis, fatty acid metabolism and degradation of leucine. At 24°C, 8 categories also

appeared to be enriched, although in this case the functional groups were rRNA processing, ribosome biogenesis, rRNA synthesis, RNA binding, rRNA modification, tRNA processing, tRNA modification and RNA degradation (Table 4.2).

Tabla 4.2. Enriched FunCat categories at 24 and 37°C.

Germination at 37°C			Germination at 24°C		
Functional category[a]	p-value[b]	Genes/Category[c]	Functional category[a]	p-value[b]	Genes/Category[c]
C-compound and carbohydrate metabolism	2.45^{-9}	97 / 858	rRNA processing	1.91^{-47}	85 / 188
Secondary metabolism	6.72^{-3}	77 / 870	Ribosome biogenesis	4.61^{-22}	58 / 182
Lipid, fatty acid and isoprenoid metabolism	6.72^{-3}	56 / 577	rRNA synthesis	4.62^{-12}	27 / 70
Non-vesicular cellular import	1.96^{-2}	24 / 190	RNA binding	3.36^{-11}	59 / 308
NAD/NADP binding	1.99^{-2}	24 / 193	rRNA modification	4.18^{-5}	9 / 17
Non-ribosomal peptide synthesis	2.06^{-2}	8 / 32	tRNA processing	4.66^{-2}	12 / 60
Fatty acid metabolism	2.43^{-2}	19 / 142	tRNA modification	4.66^{-2}	10 / 45
Degradation of leucine	3.99^{-2}	6 / 21	RNA degradation	4.66^{-2}	13 / 70

[a]Functional classification according to the Munich Information Center for Protein Sequence Functional Catalogue (FunCat; http://pedant.helmholtz-muenchen.de)
[b]Enrichment p-value of each FunCat description obtained after Fisher´s test and the Benjamini-Hochberg correction.
[c]Number of up-regulated genes found in each functional group relative to the total number of each category.

The chromosomal location of the 1,259 significantly expressed genes did not show any specific distribution. The ratio of up-regulated genes found at 24°C *versus* those found at 37°C was around 1 in each chromosome, the highest ratio being observed in chromosome I followed by chromosome VII and VII. In these three chromosomes, the number of of genes up-regulated at 24ºC was larger than at 37ºC (Fig. 4.5).

4.3.1. Genes related to *A. fumigatus* virulence and nutrient uptake

Some of the 1,259 differentially expressed genes were involved in pathways related to *A. fumigatus* virulence, such as gliotoxin biosynthesis, nutrient uptake systems and allergens. Involved in gliotoxin synthesis, up-regulation at 37ºC was observed in the genes that encoded GliP, GliJ, GliZ and a GliP-like proteins (Table 4.3). On the other hand, 17 proteases and one phospholipase, implicated in nutrient uptake, were up-regulated at 37ºC, whereas only 5 proteases and one phospholipase showed up-regulation at 24ºC (Table 4.4).

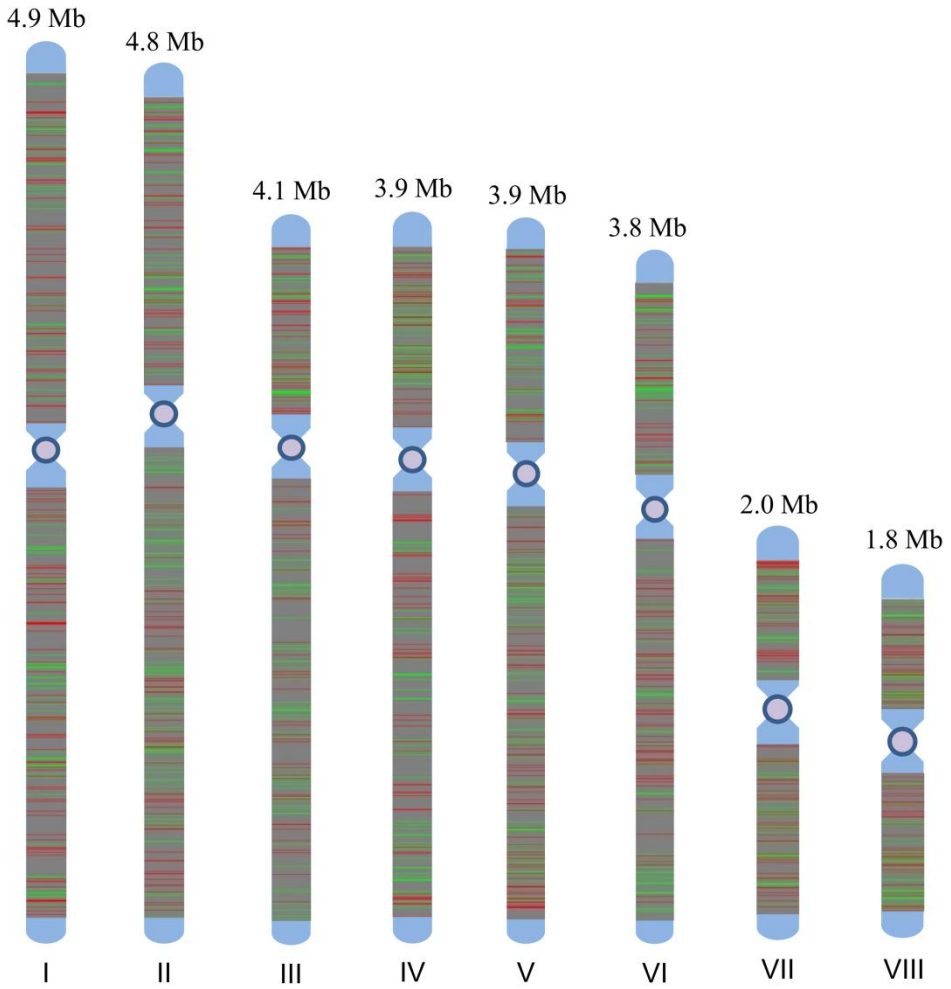

24ºC	110	95	77	81	93	80	58	64
37ºC	75	103	79	75	89	75	42	53
Ratio	**1.47**	**0.92**	**0.97**	**1.08**	**1.04**	**1.07**	**1.38**	**1.21**

Fig. 4.5. Chromosomal location of differentially expressed genes during the germination at 24 and 37ºC. Genes up-regulated at 24ºC are represented in red color and those up-regulated at 37ºC in green color. Blue ends correspond to telomeres and purple cycles to centromeres. The number of each chromosome and its size are indicated below and above each chromosome, respectively. The number of the up-regulated genes found at each temperature, as well as the ratio, is shown at the botton of each chromosome.

Table 4.3. Differentially expressed genes related to gliotoxin biosynthesis.

Gene product description[a]	Locus ID[b]	24ºC[c]	37ºC[c]	Fold change[d]
Nonribosomal peptide synthase GliP	AFUA_6G09660	-3.37	1.69	-5.06
Membrane dipeptidase GliJ	AFUA_6G09650	-4.57	-0.18	-4.39
C6 finger domain protein GliZ	AFUA_6G09630	-1.64	1.48	-3.12
Nonribosomal peptide synthase GliP-like	AFUA_3G12920	-1.17	0.19	-1.36

[a]Genes product description of the genes found on the microarray.
[b]GenBank accession number.
[c]Normalized expression data in $\log_2$ of each condition. The normalization was carried out using GeneSpring GX software. After subtracting the background intensity and $\log_2$ data transformation, a global normalization was performed followed by a baseline transformation to the median of all samples.
[d]Fold change in $\log_2$ obtained for each gene. This value represents the $\log_2$ at 24ºC minus the $\log_2$ at 37ºC. Negative fold changes mean an up-regulation at 37ºC and positive fold changes an up-regulation at 24ºC.

Table 4.4. Differentially expressed genes that code proteases or phospholipases.

Gene product description[a]	Locus ID[b]	24ºC[c]	37ºC[c]	Fold change[d]
Dimethylallyl tryptophan synthase SirD-like	AFUA_3G12930	-3.47	4.75	-8.22
NlpC/P60-like cell-wall peptidase, putative	AFUA_5G13730	-3.74	1.42	-5.16
Membrane dipeptidase GliJ	AFUA_6G09650	-4.57	-0.18	-4.39
ADAM family of metalloprotease ADM-A	AFUA_6G14420	-3.39	0.68	-4.07
Ubiquitin carboxyl-terminal hydrolase	AFUA_5G11950	-2.64	1.14	-3.78
Carboxypeptidase Y	AFUA_5G14610	-2.36	0.54	-2.90
Gamma-glutamyltranspeptidase	AFUA_4G13580	-1.02	0.97	-1.99
Carboxypeptidase S1	AFUA_5G07330	-0.71	0.81	-1.52
Carboxypeptidase S1	AFUA_1G00420	-0.81	0.66	-1.47
Carboxypeptidase S1	AFUA_5G01200	-0.69	0.69	-1.38
Tripeptidyl-peptidase (TppA), putative	AFUA_4G03490	-0.60	0.68	-1.28
Carboxypeptidase S1	AFUA_8G04120	-0.58	0.70	-1.28
Pyroglutamyl peptidase type I, putative	AFUA_6G08155	-0.48	0.74	-1.23
A-pheromone processing metallopeptidase Ste23	AFUA_5G02010	-0.48	0.57	-1.05
Peptidase family M20/M25/M40 protein	AFUA_2G12570	-0.56	0.49	-1.04
Elastinolytic metalloproteinase Mep	AFUA_8G07080	-0.72	0.45	-1.17
Aspartic endopeptidase Pep1/aspergillopepsin F	AFUA_5G13300	-1.14	0.74	-1.88
O-sialoglycoprotein endopeptidase	AFUA_6G04510	0.37	-0.68	1.05
Metallopeptidase family M24	AFUA_6G09190	0.61	-0.85	1.46
Methionine aminopeptidase, type I	AFUA_6G07330	0.73	-0.82	1.55
Dipeptidase	AFUA_6G11500	1.80	-2.22	4.02
Dipeptidyl peptidase III	AFUA_5G06940	3.67	-2.04	5.71
Lysophospholipase Plb3	AFUA_3G14680	-0.91	1.04	-1.95
Lysophospholipase Plb2	AFUA_5G01340	0.68	-4.36	5.04

[a]Genes product description of the genes found on the microarray.
[b]GenBank accession number.
[c]Normalized expression data in $\log_2$ of each condition. The normalization was carried out using GeneSpring GX software. After subtracting the background intensity and $\log_2$ data transformation, a global normalization was performed followed by a baseline transformation to the median of all samples.
[d]Fold change in $\log_2$ obtained for each gene. This value represents the $\log_2$ at 24ºC minus the $\log_2$ at 37ºC. Negative fold changes mean an up-regulation at 37ºC and positive fold changes an up-regulation at 24ºC.

Turning to the iron metabolism, there was up-regulation at 37ºC in the gene which encoded the bZIP transcription factor HapX and genes related to siderophores biosynthesis and transporters (*sidD*, *sidC*, *mirB* and *mirC*). However, metalloreductases, ferric-chelate reductases and the transcription factor *sreA* showed up-regulation at 24ºC. Zinc metabolism also stood out with 4 zinc importers (ZrfA, ZfrC, ZrfF and Smf2) up-regulated at 37ºC and 4 exporters up-regulated at 24ºC (Table 4.5).

Table 4.5. Differentially expressed genes related to iron and zinc acquisition.

Gene product description[a]	Locus ID[b]	24ºC[c]	37ºC[c]	Fold change[d]
Iron acquisition[e]				
Siderophore biosynthesis				
GNAT family acetyltransferase, putative (SidG)	AFUA_3G03650	-1.90	1.84	-3.74
Long-chain-fatty-acid-CoA ligase, putative (SidI)	AFUA_1G17190	-1.28	1.13	-2.42
Nonribosomal peptide synthase SidD	AFUA_3G03420	-1.09	0.69	-1.78
Nonribosomal siderophore peptide synthase SidC	AFUA_1G17200	-0.65	0.67	-1.31
Mitochondrial ornithine carrier protein AmcA/Ort1, putative	AFUA_8G02760	-0.53	0.48	-1.01
Homoaconitase LysF	AFUA_5G08890	0.95	-1.13	2.08
Siderophore-iron transporter genes				
MFS siderochrome iron transporter MirB	AFUA_3G03640	-2.50	2.20	-4.69
Siderochrome-iron transporter MirC	AFUA_2G05730	-0.35	0.70	-1.05
Metalloreductase Fre8	AFUA_3G02980	0.49	-0.69	1.18
Metalloreductase transmembrane component	AFUA_8G06210	0.44	-0.85	1.29
Metalloreductase	AFUA_6G02820	0.93	-0.37	1.30
Ferric-chelate reductase	AFUA_3G10820	0.33	-1.39	1.72
Ferric-chelate reductase	AFUA_5G00260	0.46	-1.66	2.12
transcription factors				
bZIP transcription factor HapX	AFUA_5G03920	-1.10	0.85	-1.95
Siderophore transcription factor SreA	AFUA_5G11260	0.58	-0.63	1.22
RIA				
FRE family ferric-chelate reductase	AFUA_1G17270	-1.10	0.87	-1.97
Zinc acquisition[e]				
Zinc importers				
ZIP Zinc transporter (ZrfC)	AFUA_4G09560	-3.21	0.80	-4.01
ZIP metal ion transporter (ZrfF)	AFUA_2G08740	-0.53	0.66	-1.19
Transporter protein Smf2	AFUA_4G10990	-0.72	0.40	-1.12
High affinity zinc ion transporter, putative (ZrfA)	AFUA_1G01550	-1.64	2.81	-4.45
Zinc exporters				
Copper resistance-associated P-type ATPase (Ccc)	AFUA_3G12740	-0.56	1.03	-1.59
MFS transporter (ZifB)	AFUA_8G04150	0.60	-0.71	1.31
DUF614 domain protein (PcrB)	AFUA_1G14190	0.82	-0.77	1.58
Cation diffusion facilitator family metal ion transporter (ZrcA)	AFUA_7G06570	0.46	-1.17	1.63
Other related				
Major allergen Asp F2	AFUA_4G09580	-2.86	0.17	-3.03

[a]Genes product description of the genes found on the microarray.
[b]GenBank accession number.
[c]Normalized expression data in $\log_2$ of each condition. The normalization was carried out using GeneSpring GX software. After subtracting the background intensity and $\log_2$ data transformation, a global normalization was performed followed by a baseline transformation to the median of all samples.
[d]Fold change in $\log_2$ obtained for each gene. This value represents the $\log_2$ at 24ºC minus the $\log_2$ at 37ºC. Negative fold changes mean an up-regulation at 37ºC and positive fold changes an up-regulation at 24ºC.
[e]Pathway in which each gene is involved.

With regard to nitrogen utilization, 3 genes involved in nitrate assimilation (*niiA*, *niaD* and AFUA_5G10420) and 10 genes related to amino acid transport and modification showed up-regulation at 37ºC. Nevertheless, 15 genes related to the utilization of this nutrient were up-regulated at 24ºC (Table 4.6).

Table 4.6. Differentially expressed genes related to nitrogen utilization.

Gene product description[a]	Locus ID[b]	24ºC[c]	37ºC[c]	Fold change[d]
Nitrate, nitriles and ammoniun[e]				
Nitrite reductase NiiA	AFUA_1G12840	-4.98	2.68	-7.66
Nitrate reductase NiaD	AFUA_1G12830	-1.33	1.68	-3.01
Citrate synthase Cit1	AFUA_6G03590	-0.80	0.91	-1.71
Nitrate reductase	AFUA_5G10420	-0.27	0.94	-1.21
Amino acids[e]				
GABA permease	AFUA_4G01230	-1.22	0.83	-2.05
Amino acid permease	AFUA_6G00412	-1.42	0.56	-1.98
Aromatic amino acid and leucine permease	AFUA_8G05860	-0.68	1.00	-1.68
GABA permease	AFUA_4G10090	-0.82	0.75	-1.58
Amino acid permease Gap1, putative	AFUA_7G04290	-0.74	0.79	-1.53
GABA permease Uga4	AFUA_4G03370	0.41	-0.59	1.00
Amino acid permease	AFUA_5G02790	0.47	-0.81	1.28
Amino acid permease	AFUA_6G11100	0.64	-0.82	1.46
Amino acid permease Dip5	AFUA_2G08800	0.91	-1.11	2.02
Neutral amino acid permease	AFUA_5G09120	0.80	-1.31	2.12
Amino acid permease	AFUA_4G03220	0.50	-1.88	2.39
Neutral amino acid permease	AFUA_1G10770	1.56	-1.45	3.01
MFS peptide transporter	AFUA_8G02550	0.58	-0.60	1.18
Amino acid transporter	AFUA_2G17480	0.79	-1.05	1.84
Ammonium transporter MeaA	AFUA_2G05880	0.92	-1.04	1.96
Small oligopeptide transporter, OPT family	AFUA_6G10050	0.76	-1.31	2.08
Amino acid transporter	AFUA_4G01570	3.21	-3.10	6.32
Acetamidase	AFUA_7G01690	-0.69	0.59	-1.28
Acetamidase/formamidase family protein	AFUA_2G03900	-1.18	0.07	-1.24
Aromatic amino acid aminotransferase	AFUA_5G02990	-0.76	0.75	-1.51
Aminotransferase	AFUA_6G00390	-0.47	0.72	-1.19
Branched-chain amino acid aminotransferase	AFUA_7G06900	1.02	-1.31	2.33
Glutamyl-tRNA(Gln) amidotransferase, subunit A	AFUA_7G06800	-4.21	2.40	-6.61
Urea, uracile and uridine[e]				
Urea amidolyase	AFUA_1G15520	2.32	-0.11	2.43
Urea hydro-lyase/cyanamide hydratase	AFUA_1G10870	0.73	-0.47	1.20

[a]Genes product description of the genes found on the microarray.
[b]GenBank accession number.
[c]Normalized expression data in $\log_2$ of each condition. The normalization was carried out using GeneSpring GX software. After subtracting the background intensity and $\log_2$ data transformation, a global normalization was performed followed by a baseline transformation to the median of all samples.
[d]Fold change in $\log_2$ obtained for each gene. This value represents the $\log_2$ at 24ºC minus the $\log_2$ at 37ºC. Negative fold changes mean an up-regulation at 37ºC and positive fold changes an up-regulation at 24ºC.
[e]Gene product description involved in the utilization of each nitrogen source.

Finally, 9 genes that encoded allergens were up-regulated at 37ºC. Amongst them, those that coded for the manganese superoxide dismutase (MnSOD) or Asp F 6, the major allergen Asp F 2 and the major allergen and cytotoxin Asp F 1 showed the highest up-regulation. In contrast, only a cell wall glucanase/allergen F 16-like protein showed up-regulation at 24ºC (Table 4.7).

Table 4.7. Differentially expressed genes that code allergens.

Gene product description[a]	Locus ID[b]	24ºC[c]	37ºC[c]	Fold change[d]
Mn superoxide dismutase MnSOD (Asp F 6)	AFUA_1G14550	-2.16	1.60	-3.76
Major allergen Asp F 2	AFUA_4G09580	-2.86	0.17	-3.03
Major allergen and cytotoxin Asp F 1	AFUA_5G02330	-1.87	0.94	-2.82
Aspartic endopeptidase Pep1/aspergillopepsin F	AFUA_5G13300	-1.14	0.74	-1.88
Allergenic cerato-platanin Asp F 13	AFUA_2G12630	-0.99	0.84	-1.83
Cell wall galactomannoprotein Mp2/allergen F 17-like	AFUA_2G05150	-0.77	0.80	-1.57
Cell wall serine-threonine-rich galactomannoprotein Mp1	AFUA_4G03240	-0.66	0.81	-1.47
Elastinolytic metalloproteinase Mep (Asp F 5)	AFUA_8G07080	-0.72	0.45	-1.17
Extracellular cellulase CelA/allergen Asp F 7-like, putative	AFUA_5G08030	-0.31	0.71	-1.03
Cell wall glucanase/allergen F 16-like	AFUA_6G03230	0.56	-0.65	1.22

[a]Genes product description of the genes found on the microarray.
[b]GenBank accession number.
[c]Normalized expression data in $\log_2$ of each condition. The normalization was carried out using GeneSpring GX software. After subtracting the background intensity and $\log_2$ data transformation, a global normalization was performed followed by a baseline transformation to the median of all samples.
[d]Fold change in $\log_2$ obtained for each gene. This value represents the $\log_2$ at 24ºC minus the $\log_2$ at 37ºC. Negative fold changes mean an up-regulation at 37ºC and positive fold changes an up-regulation at 24ºC.

4.4. Validation of microarray data obtained during the germination by RT-qPCR

Twenty genes that showed the greatest differential expression in the microarrays, 10 of them up-regulated at 37ºC and the other 10 at 24ºC, as well as 8 genes related to virulence, were selected for RT-qPCR analysis to validate the results obtained with microarray experiments. In addition, 4 housekeeping genes were also included in the study to determine the best combination of two genes for normalization of the results obtained by RT-qPCR assays. For each gene, a primer pair was designed using Primer3. Their sequences, Tm, %GC and amplicon size are indicated in Table 3.2. In figure 4.6, the result obtained for the allergen and cytotoxin Asp F 1 (AFUA_5G02330) is shown as an example.

The specificity of each primer pair was analyzed by PCR using *A. fumigatus* Af-293 DNA as template. In all cases one amplicon of the expected size was observed (Fig. 4.7). The presence of unspecific amplifications and the PCR efficiency were also analyzed for each primer pair using dissociation and standard curves. In all cases, a single amplicon appeared whereas no peaks were detected in No-template controls (NTCs). With regard to PCR efficiency, it was higher than 85% in all samples. An example is found in figure 4.8 in which the results obtained for the primers that amplified the nitrate reductase NiaD (AFUA_1G12830) are shown.

Primer3 Output

```
No mispriming library specified
Using 1-based sequence positions
OLIGO            start  len      tm      gc%   any   3' seq
LEFT PRIMER         35   20   59.90    55.00  6.00  2.00 CCACAGCCGTGTCTGTTCTA
RIGHT PRIMER       143   20   60.11    45.00  2.00  0.00 CGCTTGTCTTCCCATTTGTT
SEQUENCE SIZE: 531
INCLUDED REGION SIZE: 531

PRODUCT SIZE: 109, PAIR ANY COMPL: 3.00, PAIR 3' COMPL: 1.00

    1 ATGGTTGCAATCAAAAATCTTTTCCTGCTGGCTGCCACAGCCGTGTCTGTTCTAGCTGCT
                                        >>>>>>>>>>>>>>>>>>>>

   61 CCCTCGCCCCTCGACGCTCGTGCGACCTGGACATGCATCAACCAACAGCTGAATCCCAAG

  121 ACAAACAAATGGGAAGACAAGCGGCTTCTATACAGTCAAGCCAAAGCCGAAAGCAACTCC
         <<<<<<<<<<<<<<<<<<<

  181 CACCACGCACCTCTTTCCGACGGCAAGACCGGTAGCAGCTACCCGCACTGGTTCACTAAC

  241 GGCTACGACGGGAATGGCAAGCTCATCAAGGGTCGCACGCCCATCAAATTCGGAAAAGCC

  301 GACTGTGACCGTCCCCCGAAGCACAGCCAGAACGGCATGGGCAAGGATGACCACTACCTG

  361 CTGGAGTTCCCGACTTTTCCAGATGGCCACGACTATAAGTTTGACTCGAAGAAACCCAAG

  421 GAAGACCCGGGCCCAGCGAGGGTCATCTATACTTATCCCAACAAGGTGTTTTGCGGCATT

  481 GTGGCCCATCAGCGGGGGAATCAGGGAGACTTGAGACTGTGTTCTCATTAG
```

Fig. 4.6. Primer pair designed for the amplification of the major allergen and cytotoxin Asp F 1 (AFUA_5G02330) using Primer3. The hybridization sequences of forward (>) and reverse (<) primers are shown in red.

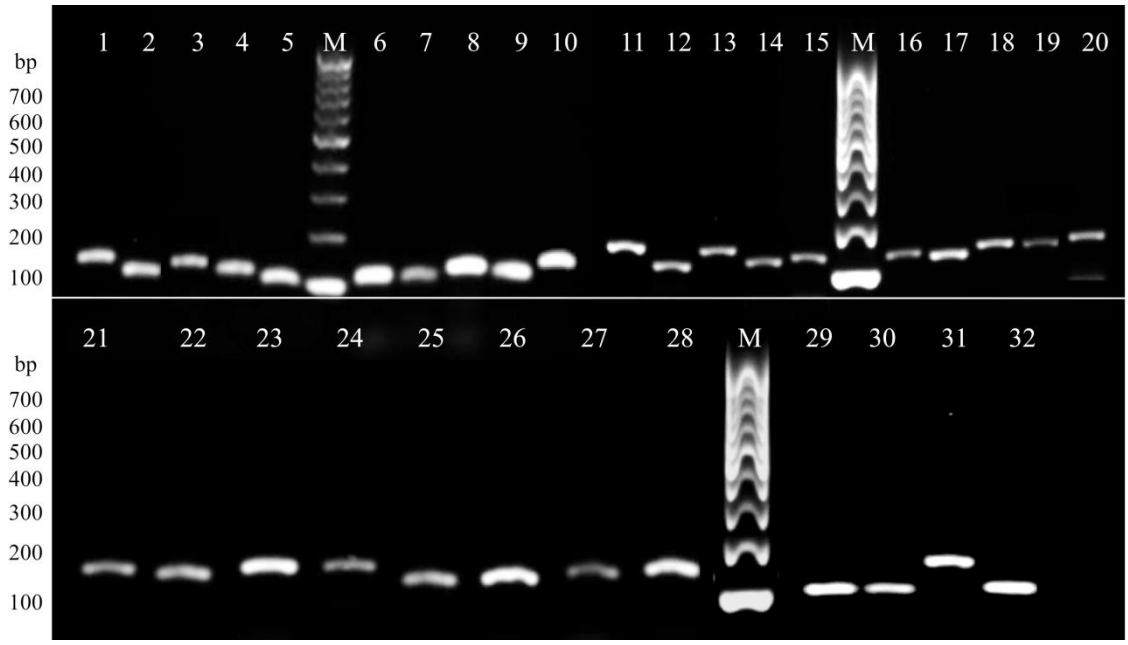

Fig. 4.7. Agarose gel electrophoresis of the PCR products obtained with each primer pair using *A. fumigatus* Af-293 DNA as template. The primer pair used in each reaction was as follows: 1. Laoa; 2. Extracel; 3. NACHT; 4. SirD; 5. CobW; 6. NiiA; 7. Thiored; 8. H1; 9. RTA1; 10. C4; 11. Catal; 12. E1; 13. NAD; 14. FADmon; 15. ATPGTP; 16. NmrA; 17. Glyco; 18. Zn2; 19. FactorC; 20. Con10; 21. GliZ; 22. GliP; 23. SidD; 24. SreA; 25. NiaD; 26. AspF1; 27. AspF2; 28. MnSOD; 29. TEF-1; 30. FksP; 31. Act1; 32. GdpA; M: Molecular weight marker. Hyperladder IV, 100-1000 bp.

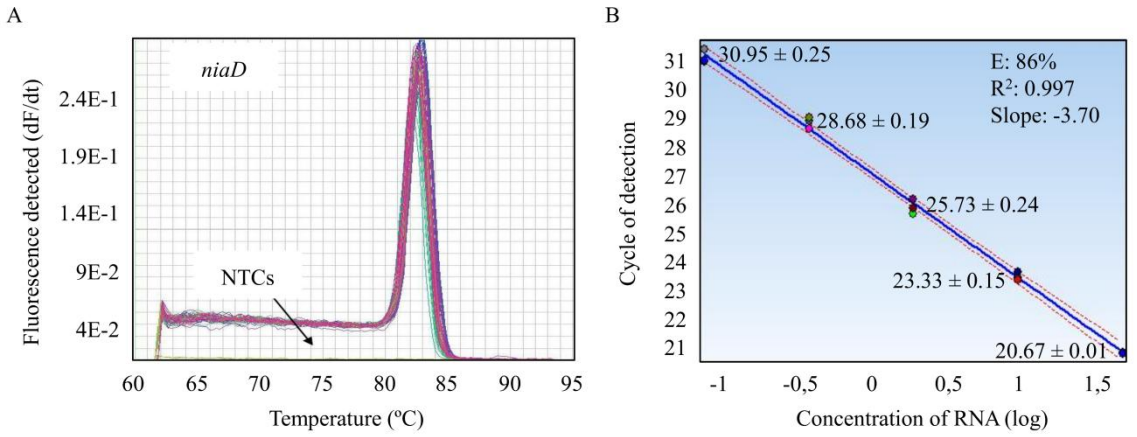

Fig 4.8. Dissociation and standard curves of the gene that encode the nitrate reductase NiaD (AFUA_1G12830). A) Dissociation curve of the PCR product. The fluorescence detected in NTCs is shown in green. B) Standard curve relating concentration of RNA (log) to cycle of detection. The efficiency (E), coefficient of determination (R^2) and slope (Slope) are shown in the upper right-hand corner of the graph. Numbers indicate the Ct value ± standard deviation of three independent samples.

Once the efficiencies were corrected and the fluorescence due to genomic DNA contamination subtracted, RT-qPCR results were normalized. The analysis with NormFinder and GenNorm algorithms showed that *act1* and *gpdA* genes were the genes with the best stability. Therefore, this combination was chosen to normalize the results obtained.

Statistical analysis applying the Student's t-test showed that in all cases significant differences appeared between the expression obtained at 37 and 24ºC. Considering the germination at 37ºC as the control condition, a negative $\log_2$ fold change was interpreted as meaning genes were up-regulated at 37ºC, whilst a positive $\log_2$ fold change was taken to indicate an up-regulation at 24ºC. As shown in figure 4.9, the direction of the expression changes was the same in microarray and RT-qPCR results. Furthermore, the Pearson's correlation coefficient between both methods was high, with a value of 0.91(Fig. 4.10).

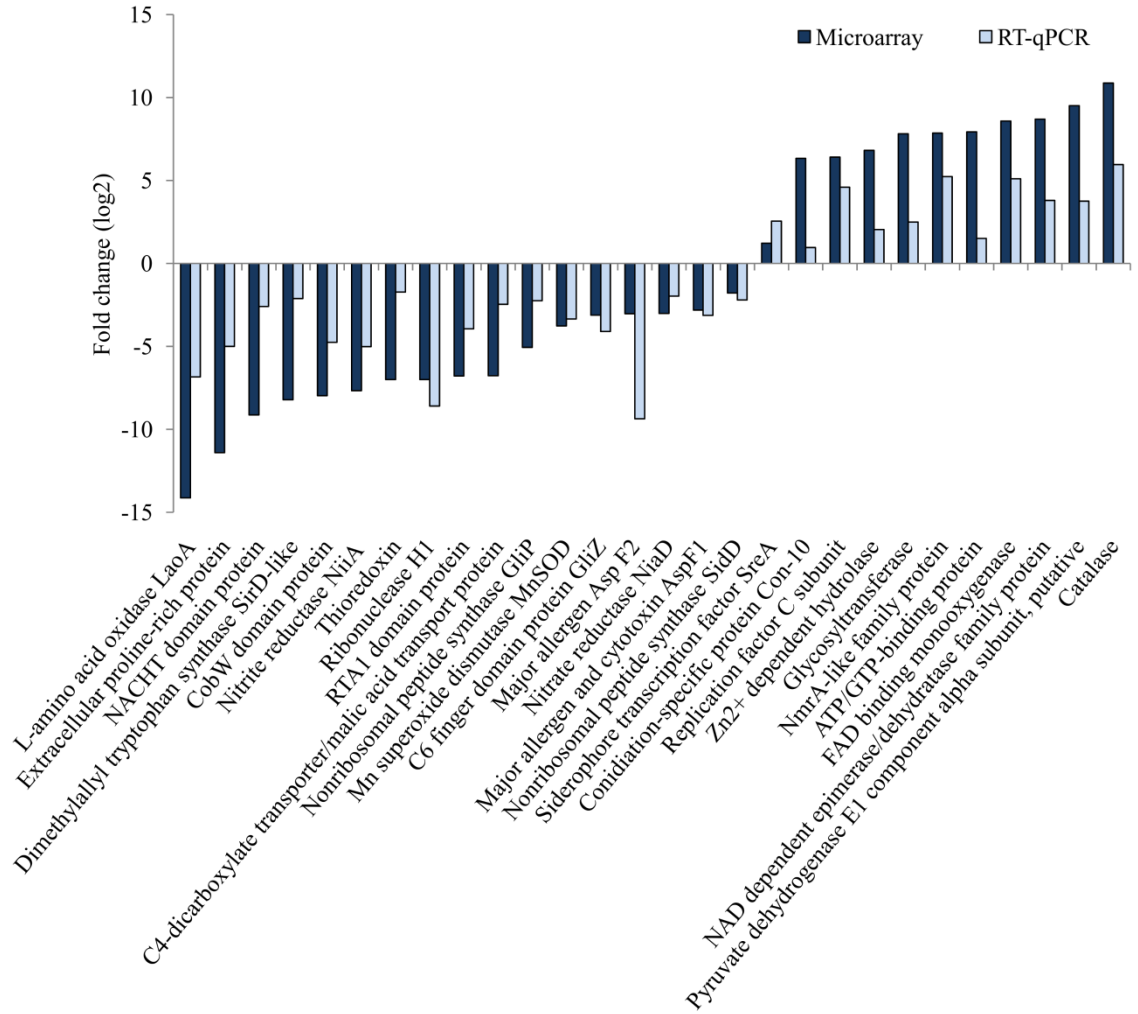

Fig. 4.9. Comparative levels of gene expression between the microarray and RT-qPCR. Each point corresponds to the mean value from three independent samples. Negative fold changes indicate up-regulation at 37ºC and positive fold changes up-regulation at 24ºC.

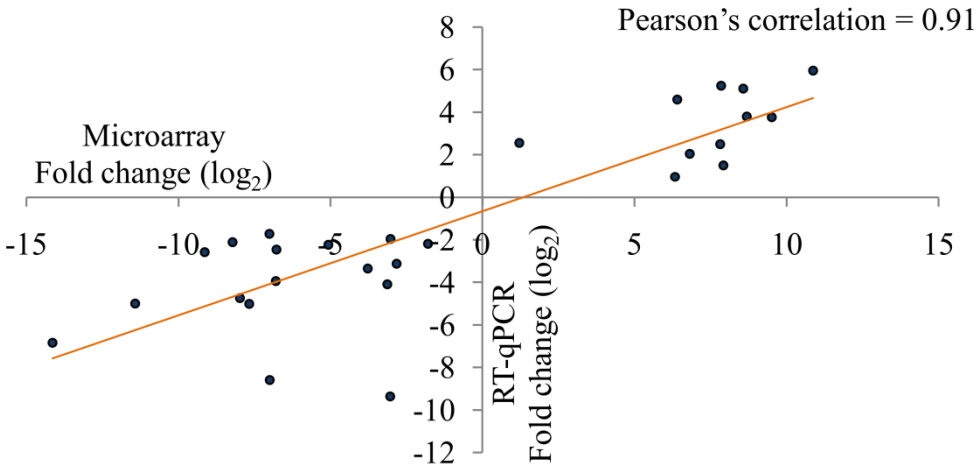

Fig. 4.10. Correlation analysis between microarray and RT-qPCR data. The X-axis values represent the fold change (log_2) of microarray data and the Y-axis values the fold change (log_2) of RT-qPCR results. Each point corresponds to the mean value from three independent samples. Negative fold changes indicate up-regulation at 37ºC and positive fold changes up-regulation at 24ºC.

4.5. Effect of the addition of fresh medium during the germination on gene expression by RT-qPCR

The expression of the genes chosen for the validation of microarray data was also analyzed after the addition of fresh medium and compared to the previous results to determine whether the temperature was the only factor affecting the expression. This analysis showed that the expression of 14 genes agreed with microarray; Pearson's correlation between these results being 0.86.

As shown in Table 4.8, only 4 genes appeared to have a different expression pattern relative to microarray analysis (those that encoded the NACHT domain protein, the ATP/GTP-binding protein, the nitrite reductase *niiA* and the nonribosomal peptide synthase *sidD*) whereas 10 genes had fold changes below the thresholds previously established. In samples with 40-60% germination rates after the addition of fresh medium, 17 genes agreed with the expression found on the microarray. Nevertheless, 5 genes showed different expression, which encoded for the Zn^{2+} dependent hydrolase, the ATP/GTP-binding protein, the FAD binding monooxygenase, the glycosyltransferase and the MnSOD.

Focusing on the genes related to virulence (Fig. 4.11), 3 out of 9 genes agreed with the microarray data in samples with 15-30% germination rates. Amongst the genes involved in gliotoxin biosynthesis only *gliZ* appeared to be up-regulated at 37ºC in all cases. In iron metabolism, there was up-regulation of the nonribosomal peptide synthase *sidD* at 24ºC in 15-30% germination rate samples, whereas in nitrogen metabolism, up-

regulation at 37ºC was only found in 40-60% germination samples. Finally, amongst the allergens analyzed, only Asp F 2 and Asp F 6 were up-regulated at 37ºC in 15-30% germination rate samples.

Table 4.8. Gene expression obtained in samples after the addition of fresh medium.

Gene product description[a]	Locus ID[b]	Fold change (log_2)[c]		
		Continuous incubation[d]	Fresh medium[e]	
		15-30%	15-30%	40-60%
Most Up-regulated at 37ºC				
Thioredoxin	AFUA_8G01090	-1.79	-14.77	-13.56
Extracellular proline-rich protein	AFUA_5G01620	-5.00	-5.77	-5.50
CobW domain protein	AFUA_8G02620	-4.75	-3.98	-1.41
RTA1 domain protein	AFUA_5G05640	-3.93	-2.46	-15.20
Ribonuclease H1	AFUA_1G10020	-8.60	-1.93	-12.38
C4-dicarboxylate transporter/malic acid transport protein, putative	AFUA_8G04630	-2.46	-0.56	-1.39
Dimethylallyl tryptophan synthase Sird-like	AFUA_3G12930	-2.11	-0.07	-1.32
L-amino acid oxidase Laoa	AFUA_7G06810	-6.84	0.84	-10.69
Nitrite reductase Niia	AFUA_1G12840	-5.01	1.18	-2.80
NACHT domain protein	AFUA_6G03160	-1.22	1.79	-3.07
Most Up-regulated at 24ºC				
Catalase	AFUA_2G00200	5.95	4.56	2.71
Nmra-like family protein	AFUA_5G10160	5.23	4.28	3.44
Replication factor C subunit	AFUA_5G14820	4.59	3.47	3.15
NAD dependent epimerase/dehydratase family protein	AFUA_8G00600	3.79	2.94	1.85
Glycosyltransferase	AFUA_8G02020	2.50	1.51	-12.54
Pyruvate dehydrogenase E1 component alpha subunit	AFUA_2G04870	3.75	1.27	0.75
Conidiation-specific protein Con-10	AFUA_5G03830	0.96	0.59	0.38
Zn^{2+} dependent hydrolase	AFUA_4G01090	1.00	-0.12	-9.88
FAD binding monooxygenase	AFUA_7G00270	5.10	-0.71	-5.19
ATP/GTP-binding protein	AFUA_3G00530	0.57	-2.11	-2.90
Related to virulence				
C6 finger domain protein GliZ	AFUA_6G09630	-4.09	-4.42	-1.60
Major allergen Asp F 2	AFUA_4G09580	-9.37	-1.60	0.01
Mn superoxide dismutase MnSOD (Asp F 6)	AFUA_1G14550	-3.35	-1.30	1.01
Nonribosomal peptide synthase GliP	AFUA_6G09660	-2.24	-0.75	0.30
Siderophore transcription factor SreA	AFUA_5G11260	2.55	-0.64	0.91
Nitrate reductase NiaD	AFUA_1G12830	-1.97	0.04	-1.26
Major allergen and cytotoxin Asp F 1	AFUA_5G02330	-3.12	0.17	0.15
Nitrite reductase Niia	AFUA_1G12840	-5.01	1.18	-2.80
Nonribosomal peptide synthase SidD	AFUA_3G03420	-2.20	2.39	-0.69

[a]Genes product description of the genes found on the microarray.
[b]GenBank accession number.
[c]Fold change in log_2 obtained for each gene and sample analyzed. This value represents the log_2 at 24ºC minus the log_2 at 37ºC. Negative fold changes values mean an up-regulation at 37°C and positive fold changes values an up-regulation at 24°C.
[d]Expression of samples with 15-30% germination rates with continuous incubation that were hybridized with the microarray and validate by RT-qPCR.
[e]Expression of samples with 15-30% and 40-60% germination rates after the addition of fresh medium.

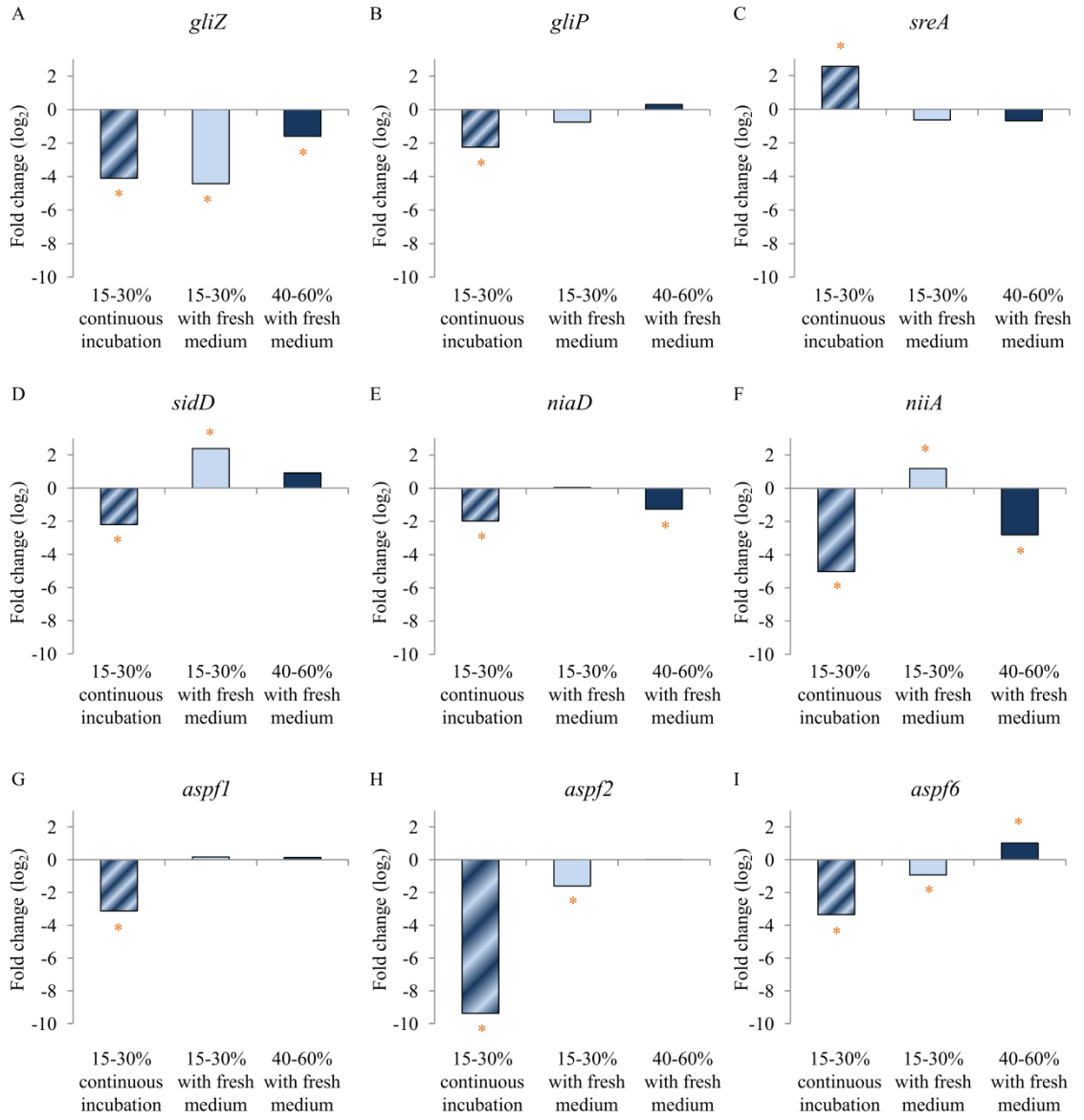

Fig. 4.11. Gene expression levels of genes related to virulence. *gliZ* (A), *gliP* (B), *sreA* (C), *sidD* (D), *niaD* (E), *niiA* (F), *aspf1* (G), *aspf2* (H), and *aspf6* (I). Negative $\log_2$ fold changes indicate up-regulation at 37ºC and positive fold up-regulation at 24ºC. The asterisk shows data above or below of the thresholds established (over 1 and under -1). Samples with continuous incubation are shown as blue striped bars, whereas samples with 15-30% and 40-60% germination rates after the addition of fresh medium are shown as light blue and dark blue bars, respectively.

4.6. Animal infection

To develop an *in vivo* model for experimental infection, female BALB/c mice previously immunocompromised by cyclophosphamide treatment were used. The infection was intravenously performed with the strain *A. fumigatus* Af-293 and with doses of 10^5, 10^6 and 10^7 conidia/animal in 200 µl of saline solution to establish the appropriate fungal dose. Survival studies are shown in figure 4.12.

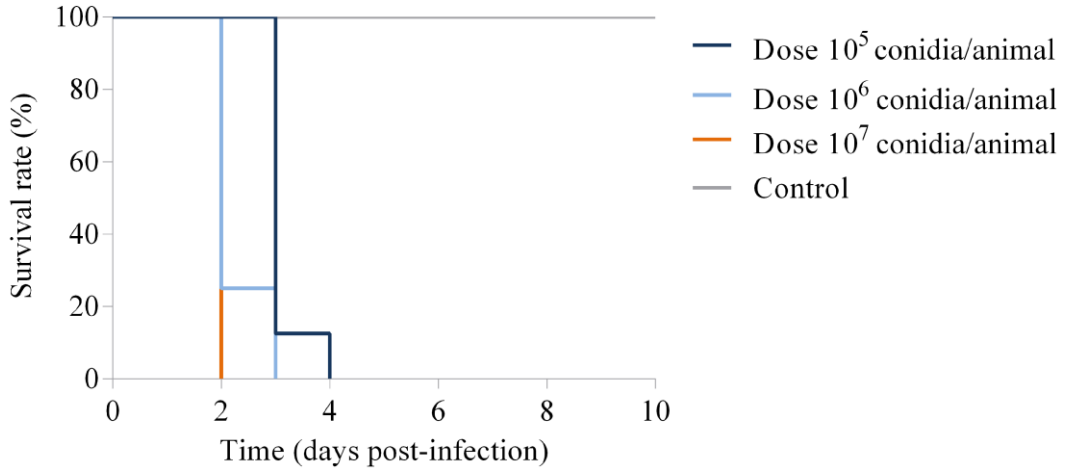

Fig. 4.12. Survival rate of mice infected with *A. fumigatus* Af-293 conidia. Immunosuppression was carried out using doses of cyclophosphamide of 150 mg/kg and 100 mg/kg on days -4 and -1 prior to the infection. Doses of conida were intravenously injected on day 0 of infection.

With 10^7 and 10^6 conidia 100% mortality rates were achieved on day 2 and 3 post-infection, respectively. Nevertheless, with 10^5 conidia, a 100% mortality rate was achieved on day 4. Therefore, this dose was chosen as the one to infect murine animals given that it allowed working with lower risk and studying the infection throughout 4 days post-infection. Three independent infections were carried out infecting 8 animals and using 2 mice as controls. Along the first four days of the infection, the spleen, lungs, kidneys, liver, heart and brain of two infected animals that had died due to the infection or by cervical dislocation were extracted. The organs from the control animals were extracted on day 5 after cervical dislocation. On each day post-infection, organs from one of the animals were used for counting CFUs and histology, whereas the organs from the second animal were used for RNA isolation.

A different fungal burden was found in each organ extracted (Fig. 4.13), the highest being detected in the spleen on day 1 and 2 of infection, in which 55.63 and 32.63 CFU/mg were found, respectively. However, the fungal burden decreased on the last two days, reaching 5.63 CFU/mg on day 4. Something similar, although at a lower

level, was observed in the liver, whose CFU/mg seemed to increase at first but decreased on day 3 and 4. In lungs, brain and heart the fungal burden was remarkably low even though a slight increase was observed during the infection. Only in the kidney a significant increase in fungal burden over time was found. In this organ, the CFU/mg rose from 1.52 on day 1 to 20.65 CFU/mg on day 4, being chosen for transcriptomic analysis.

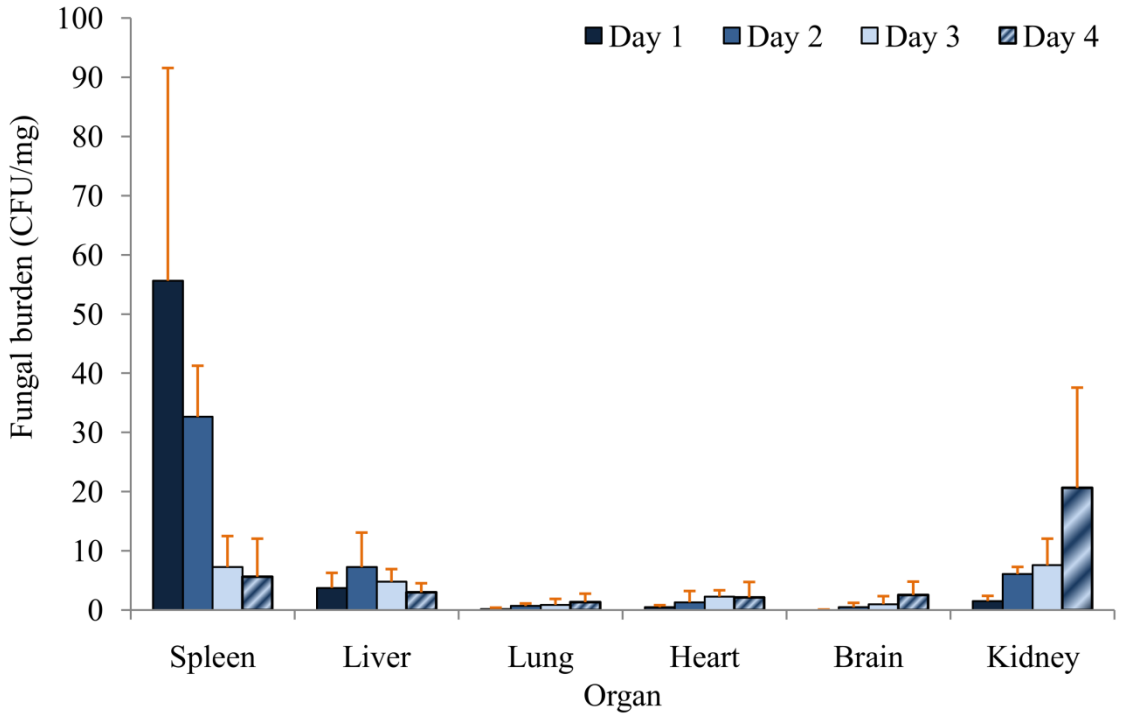

Fig. 4.13. Fungal burden of infected mouse organs during the disseminated infection. The infection doses were 10^5 conidia of *A. fumigatus* Af-293/animal in 200 µl of saline solution. Immunosuppression was carried out using doses of cyclophosphamide of 150 mg/kg and 100 mg/kg on days -4 and -1 prior to the infection. Organs were extracted during the first 4 days after infection. In each organ, the fungal burden mean and standard deviation of three independent samples are represented.

Histology studies showed that there was no inflammatory response in kidneys. Hyphae were difficult to visualize with hematoxylin and eosin stain, as well as with periodic acid-Schiff stain. However, when samples were stained with Grocott's methenamine silver stain, the presence of fungal structures was clearly observed (Fig. 4.14). On day 2 the affectation of renal parenchyma and renal pelvis was around 10-15% and on day 3 it increased to 20-25%. Necroses appeared in the renal cortex and in the renal medulla, in which septate, branching and mature hyphae were observed. However, neither conidia nor spheroids forms were detected. On the other hand, the *A. fumigatus* hyphae found in a grinded kidney after staining with Calcofluor white are shown in figure 4.14VI.

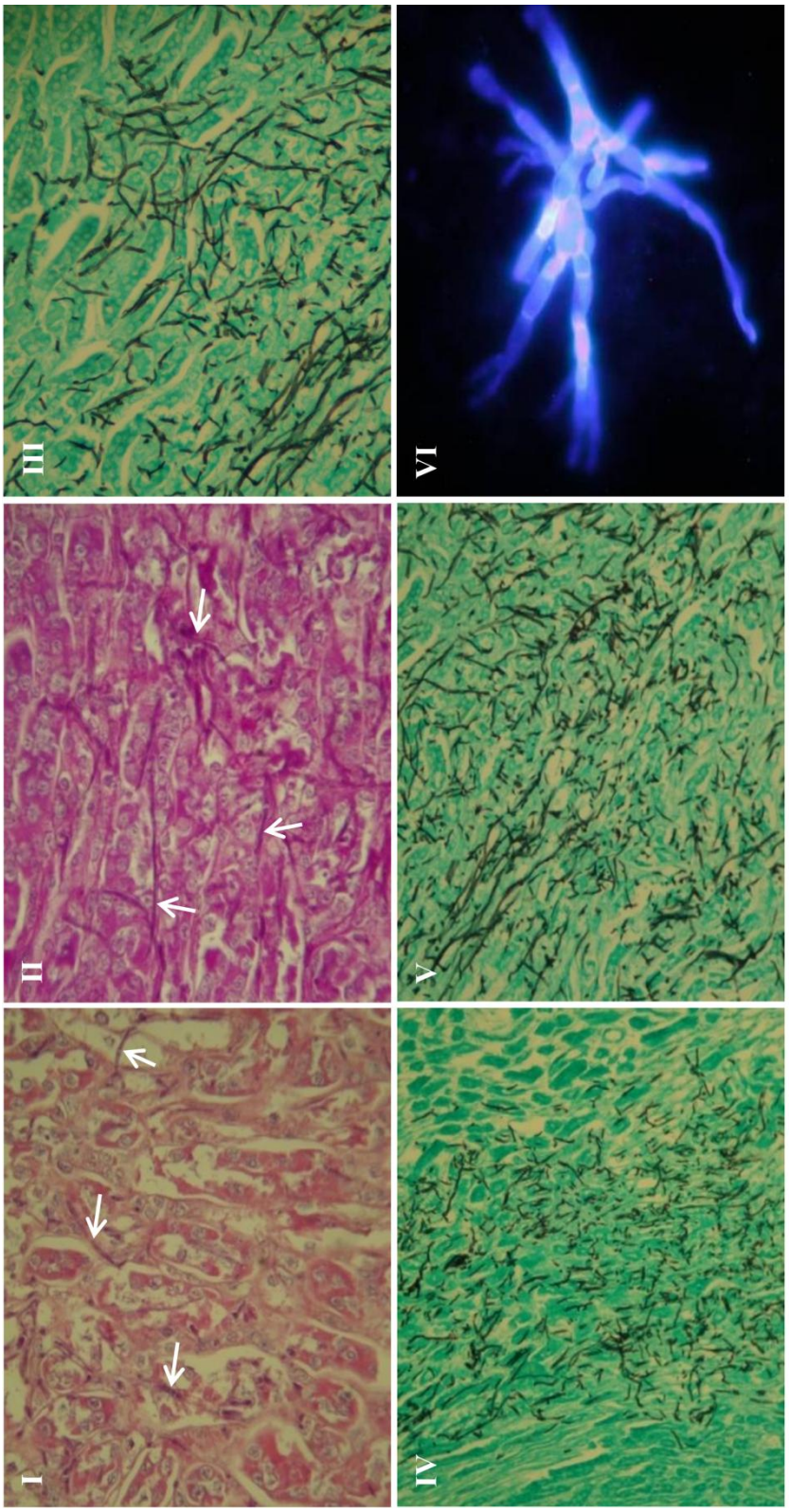

Fig. 4.14. Histology of infected kidneys. (I-III) Kidneys from day 3 post-infection (x40) stained with hematoxylin and eosin (I); periodic acid-Schiff (II); and Grocott's methenamine silver (III) stains. Arrows point at the hyphae observed in the histology. (IV-V) Histology from day 2 (IV) and 3 (V) post-infection (x20) stained with Grocott's methenamine silver stain. (VI) Calcofluor white staining of *A. fumigatus* Af-293 hyphae found in a grinded kidney on day 4 post-infection (x1000).

4.7. Transcriptomic data of *A. fumigatus* Af-293 during a disseminated infection and validation by RT-qPCR

From each independent animal infection, RNA isolated from infected kidneys on each day of infection was hybridized with the microarray. The data obtained in these transcriptomic studies were deposited in ArrayExpress through the MIAMExpress tool (accession number E-MTAB-3674).

Genes that showed the greatest differential expression in the microarrays as well as 32 genes randomly chosen amongst those related to virulence were selected for RT-qPCR analysis to validate the results obtained with the microarray experiments. Furthermore, 4 housekeeping genes, different from those used in the germination study, were included to determine the best combination of two genes for normalization of the results obtained by RT-qPCR assays. As in the previous study, for each gene a primer pair was designed using Primer3. Their sequences, Tm, %GC and amplicon size are indicated in Table 3.3. An example can be found in figure 4.15, in which the results obtain for the gene that encode the protein GliZ (AFUA_6G09630) is shown.

The specificity of each primer pair was analyzed by PCR using *A. fumigatus* Af-293 DNA as template. In all cases one amplicon of the expected size was observed (Fig. 4.16). The presence of unspecific amplifications and PCR efficiency were also analyzed for each primer pair. In all cases, a single amplicon appeared whereas no peaks were detected in NTCs. With regard to PCR efficiency, it was higher than 85% in all samples. In figure 4.17, the results obtained for the primers that amplified the aspartate transaminase (AFUA_6G02490) are shown as an example.

Primer3 Output

```
No mispriming library specified
Using 1-based sequence positions
OLIGO            start  len      tm     gc%   any    3' seq
LEFT PRIMER        294   20   60.37   55.00  4.00  2.00 TCCAGCGGTAGCGAGAATAC
RIGHT PRIMER       379   20   60.41   50.00  5.00  3.00 GAAAGGTCGGAATCGGAGAT
SEQUENCE SIZE: 630
INCLUDED REGION SIZE: 630

PRODUCT SIZE: 86, PAIR ANY COMPL: 3.00, PAIR 3' COMPL: 1.00

    1 AGCGGGAGCAGCGGGTGGCAGCGGCTGCAGAATCCGCTCGGATAGCAGGAAATCCCTCCG

   61 CCCTAGCCTCACTCCCGGCTACATCGACATGTACATCTACAGCAACAACAGCAGCAGCAG

  121 CAGCAGCAGCAACAACAACAACAACAATAGCAACAACCACAGCTCCCTCCCAGGGTCCAG

  181 CTGTGGACAGCGCGGCTGCCGCTGCCGCTGCCACCACATCAACCGTCGCGTCTCCTCGCG

  241 CGGACGACTGCCTCGGTCTGTTCGACGACGATGAGGAATCGAACCCGTTTTTCTCCAGCG
                                                          >>>>>>>

  301 GTAGCGAGAATACCGGGGGGACTTCGTTTTCCCCGGACTGGATCCCTCCTCTGCCGTCCA
      >>>>>>>>>>>>>                                             <

  361 TCTCCGATTCCGACCTTTCTTTCCCGTTATTAGAGTCCTGTTTAGGGCCGGACCATGACT
      <<<<<<<<<<<<<<<<<<<

  421 GCAACGACTCCCTTTTCTGGAGCACCACCGCCGAGCCGGACTGCCAGCCGACGAGCAAGG

  481 AGCCGCTGGATCCTCGATCCAAGCTGCTGCGCTCCTGCAAATGCCTCCAGACCCTCAGCA

  541 GCCTAACCGCTCGAGATATCCGCCGATTTGATGCCACCTTTGTCTTTGTGCGGAACTATG

  601 CGCGCGCATTTTCCGCCTTCTACCACTGTT
```

Fig. 4.15. Primer pair designed for amplification of the gene *gliZ* (AFUA_6G09630) using Primer3. The sequence corresponds to a partial sequence of its mRNA. The hybridization sequences of forward (>) and reverse (<) primers are shown in red.

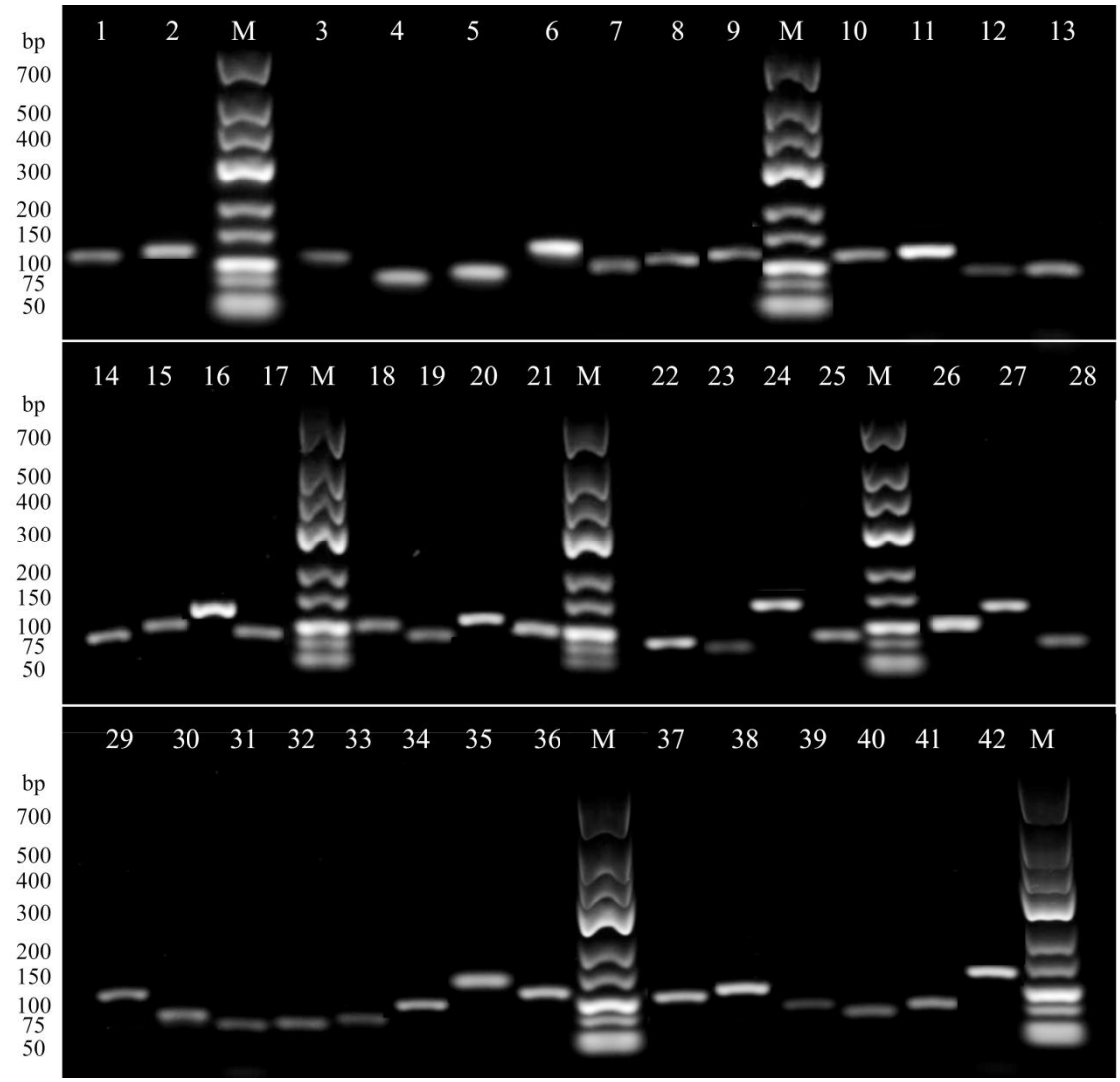

Fig. 4.16. Agarose gel electrophoresis of the PCR products obtained with each primer pair using *A. fumigatus* Af-293 DNA as template. Primer pair used in each reaction was as follows: 1. Betagal; 2. Aspart; 3. Alphabeta; 4. Mis12; 5. 2GliZ; 6. 2GliP; 7. GliA; 8. SreA; 9. SidD; 10. HapX; 11. Cat1; 12. 2NiaD; 13. 2NiiA; 14. CrnA; 15. Mkk2; 16. MpkA; 17. SakA; 18. 2AspF1; 19. 2AspF2; 20. 2MnSOD; 21. AldH12; 22. Amyl; 23. RodA; 24. Alb1; 25. Arp2; 26. Arp1; 27. Abr1; 28. Arb2; 29. PhosC; 30. Plb2; 31. Glucamuta; 32. Hydrocell; 33. Exopol; 34. Cip2; 35. Endopep; 36. Protease; 37. Polyph; 38. GABA; 39. Ctr; 40. b5reduct; 41. 2H1; 42. P450mono; M: Molecular weight marker. O'GeneRuler Low Range DNA Ladder, 25-700 bp.

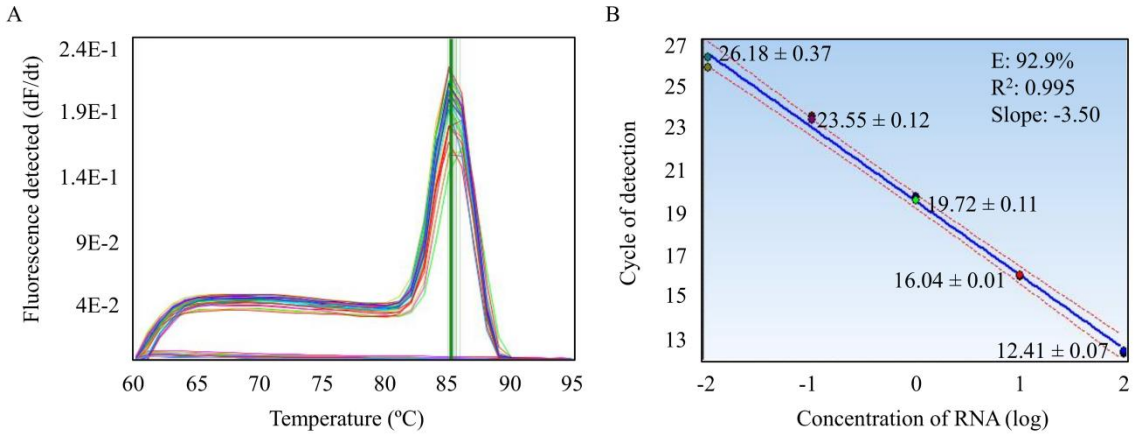

Fig. 4.17. Dissociation and standard curves of the gene that encode the aspartate transaminase (AFUA_6G02490). A) Dissociation curve of the PCR product. B) Standard curve relating concentration of RNA (log) to cycle of detection. The efficiency (E), coefficient of determination (R^2) and slope (Slope) are shown in the upper right-hand corner of the graph. Numbers indicate the Ct value ± standard deviation of three independent replicates.

Once the efficiencies were corrected and the fluorescence due to genomic DNA contamination subtracted, RT-qPCR results were normalized. The analysis with NormFinder and GenNorm algorithm showed that those genes that coded for the alpha/beta hydrolase (AFUA_2G02920) and Mis12-Mtw1 family protein (AFUA_3G13950) were the genes with the best stability. Therefore, this combination was chosen to normalize the results obtained by RT-qPCR.

On the other hand, transcriptome profile data obtained after the hybridization with the microarray were normalized using the 4 algorithms Babelomics server offers. In addition to normalizing samples from infected kidneys, transcriptomic data from *A. fumigatus* germination at 37ºC were also normalized with Babelomics server so that comparisons among *in vivo* and *in vitro* experiments could be performed. Amongst the 4 algotihms, two (Substract and Half) generated a large number of Not a Number (NaN) values, indicating that they were not suitable for our samples, whereas with Normexp and RMA algorithms, NaN values did not appeared. After analyzing the results obtained with both algorithms and their correlation with RT-qPCR data, the RMA was chosen as the one to apply given that with this algorithm the best normalization and the highest correlation with the RT-qPCR results were achieved (Table 4.9). As shown in figure 4.18, when each day post-infection was compared to the germination at 37ºC the Pearson's correlation coefficient between microarray and RT-qPCR data was higher than 0.85 in all cases, validating, in turn, the microarray results. Only 4.6% of the genes analyzed by RT-qPCR showed a different expression relative to those found with microarray data (Table 4.10).

Table 4.9. Correlation coefficient obtained between microarray data normalized with RMA or NormExp algorithm for background correction and RT-qPCR results obtained in the validation.

Comparison[b]	Pearson's correlation [a]	
	RMA and RT-qPCR[c]	NormExp and RT-qPCR[d]
Day 1 *vs* 37ºC	0.88	0.78
Day 2 *vs* 37ºC	0.86	0.84
Day 3 *vs* 37ºC	0.90	0.90
Day 4 *vs* 37ºC	0.85	0.83

[a]Correlation coefficient applied.
[b]Comparison analyzed. Each day of infection was compared to the control condition (germination at 37ºC).
[c]Correlation coefficient of each comparison between microarray data normalized with the RMA algorithm of Babelomics server and RT-qPCR results.
[d]Correlation coefficient of each comparison between microarray data normalized with NormExp algorithm of Babelomics server and RT-qPCR results.

4.8. Transcriptomic analysis of *A. fumigatus* during a disseminated infection

Following normalization (Fig. 4.19), the ANOVA test amongst the 4 days post-infection showed that there were no differentially expressed genes, which was also observed with RT-qPCR data. However, statistical comparisons of each day of infection relative to the *A. fumigatus* germination at 37ºC showed that 4,080, 377, 3,604 and 1,645 genes were significantly expressed comparing this data *versus* those obtained on days 1, 2, 3 and 4 of infection, respectively (Fig. 4.20). In all cases, a negative fold change (log_2) indicated up-regulation during the germination at 37ºC and a positive value up-regulation during the infection. When day 1 post-infection was compared to the germination, 1,675 genes were up-regulated on that day and 2,405 were up-regulated *in vitro*. In the comparison with day 2, 189 genes were up-regulated in the infected tissue, 188 being up-regulated during the germination. On day 3, 1,139 genes appeared to be up-regulated on that day while 2,465 showed up-regulation *in vitro*. Finally, 563 genes were up-regulated on day 4 post-infection and 1,082 during the germination at 37ºC.

A

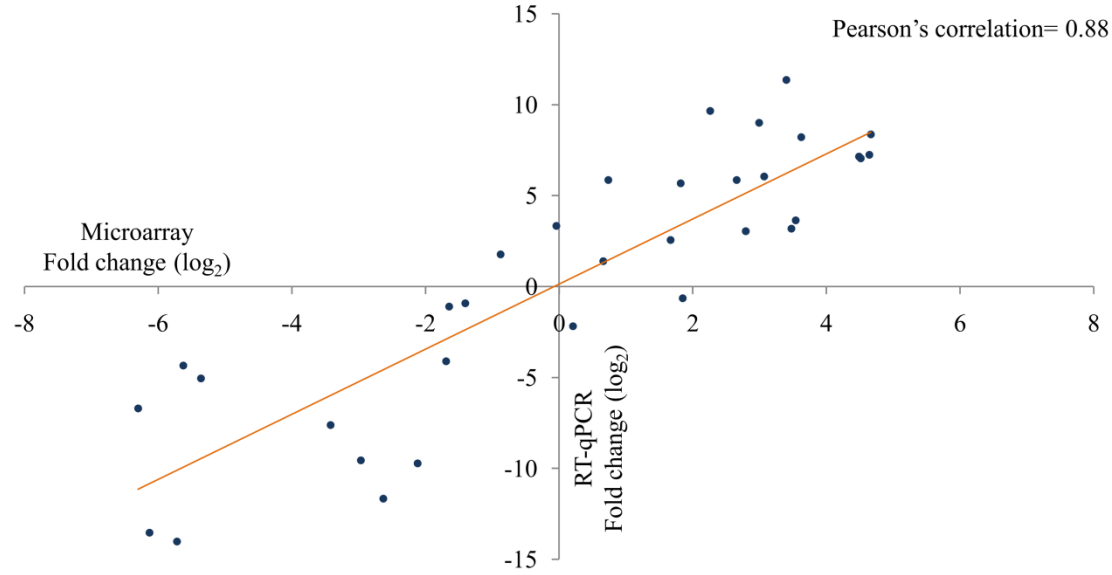
Pearson's correlation= 0.88
Microarray
Fold change (log2)
RT-qPCR
Fold change (log2)
15
10
5
0
-5
-10
-15
-8
-6
-4
-2
0
2
4
6
8

B

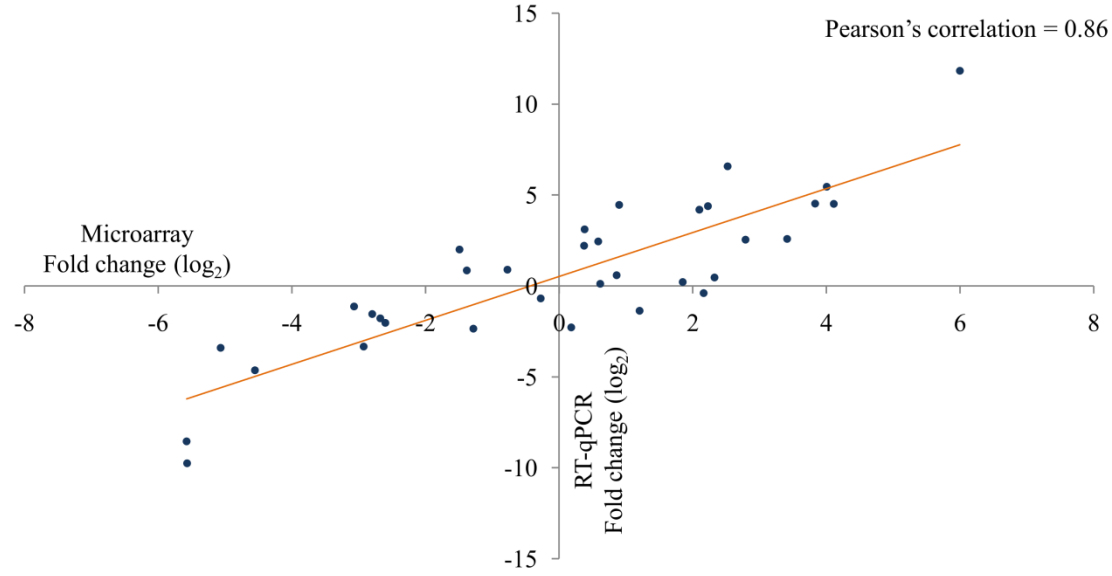
Pearson's correlation = 0.86
Microarray
Fold change (log2)
RT-qPCR
Fold change (log2)
15
10
5
0
-5
-10
-15
-8
-6
-4
-2
0
2
4
6
8

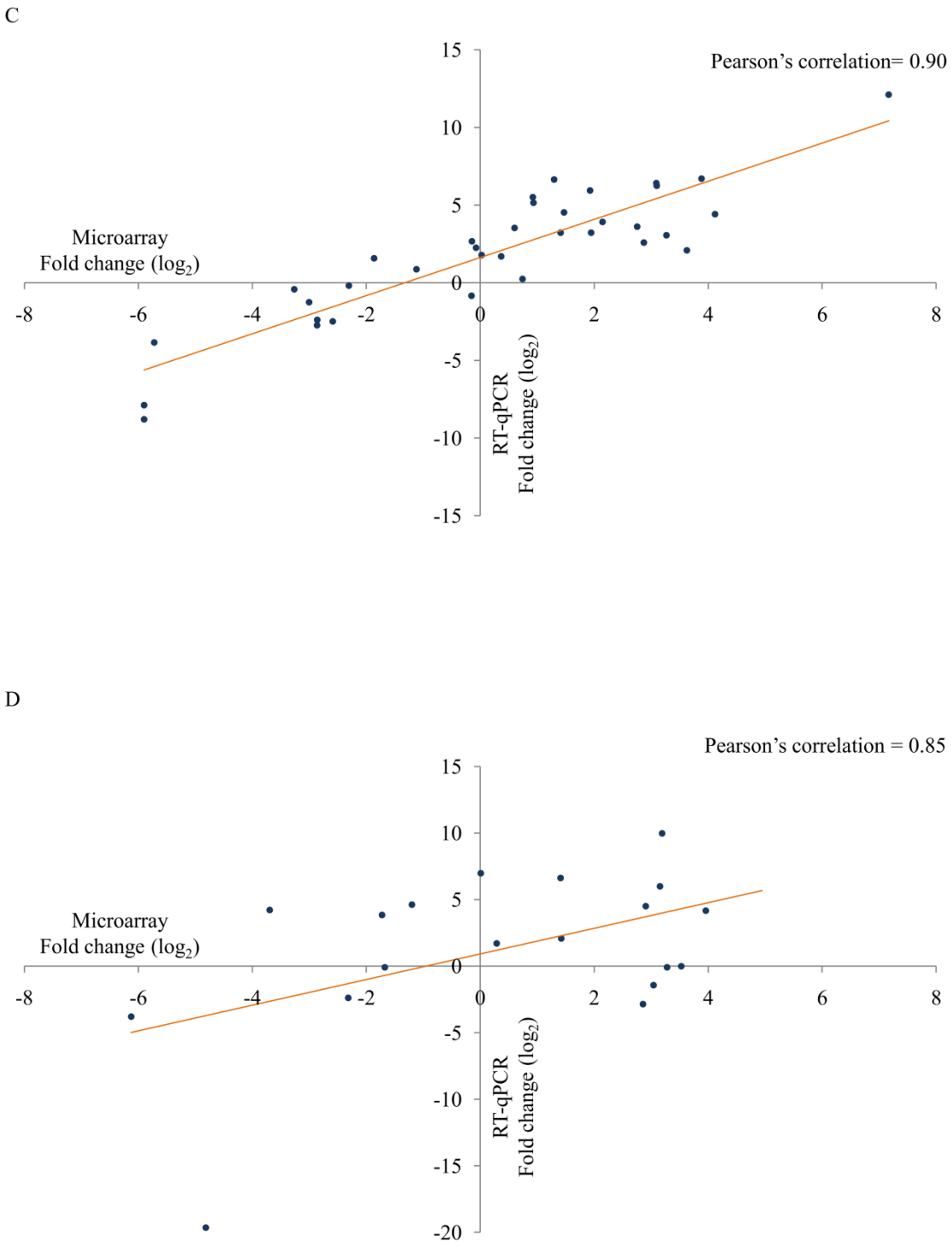

Fig. 4.18. Correlation analysis between microarray and RT-qPCR data. A) Day 1 *vs* germination at 37ºC. B) Day 2 *vs* germination at 37ºC. C) Day 3 *vs* germination at 37ºC. D) Day 4 *vs* germination at 37ºC. The X-axis values represent the fold change (log_2) of microarray data and the Y-axis values the fold change (log_2) of RT-qPCR results. Each point corresponds to the mean value of three independent samples.

Table 4.10. Fold change (log_2) values obtained after microarray hybridization and RT-qPCR assays for each gene selected for the validation.

Gene product description[a]	Locus ID[b]	Fold change (log_2)[c]							
		Day 1 *vs* 37°C		Day 2 *vs* 37°C		Day 3 *vs* 37°C		Day 4 *vs* 37°C	
		RT-qPCR	microarray	RT-qPCR	microarray	RT-qPCR	microarray	RT-qPCR	microarray
Gliotoxin biosynthesis[d]									
C6 finger domain protein GliZ	AFUA_6G09630	-2.18	0.20	-2.28	0.18	-0.84	-0.15	0.40	0.01
Nonribosomal peptide synthase GliP	AFUA_6G09660	5.69	1.82	2.21	0.37	5.52	0.92	6.98	3.19
MFS gliotoxin efflux transporter GliA	AFUA_6G09710	8.22	3.62	5.46	4.00	5.94	1.93	9.97	2.39
Iron metabolism[d]									
Nonribosomal peptide synthase SidD	AFUA_3G03420	-4.10	-1.69	-2.04	-2.60	-2.39	-2.86	-4.56	-1.72
Siderophore transcription factor SreA	AFUA_5G11260	-7.50	3.12	2.54	2.79	3.91	2.15	3.85	2.85
bZIP transcription factor HapX	AFUA_5G03920	-11.66	-2.63	-1.78	-2.68	-2.74	-2.86	-2.85	-3.70
Mycelial catalase Cat1	AFUA_3G02270	-5.48	1.05	2.45	0.59	2.59	2.87	4.21	2.01
Nitrogen metabolism[d]									
Nitrate reductase NiaD	AFUA_1G12830	-9.79	-2.12	0.90	-0.77	2.67	-0.14	1.78	-1.20
Nitrite reductase NiiA	AFUA_1G12840	1.77	-0.88	3.12	0.38	5.15	0.93	4.63	0.29
Nitrate transporter CrnA	AFUA_1G12850	3.34	-0.04	-0.69	-0.27	2.25	-0.07	1.71	-0.13
MAP kinases[d]									
MAP kinase kinase (Mkk2)	AFUA_1G05800	-0.92	-1.41	0.85	-1.38	1.56	-1.86	1.15	-2.32
MAP kinase MpkA	AFUA_4G13720	-9.55	-2.97	-2.35	-1.28	-2.49	-2.59	-2.35	-2.76
MAP kinase SakA	AFUA_1G12940	-6.70	-6.30	-1.13	-3.07	-0.43	-3.26	-0.33	-4.56
Allergens[d]									
Major allergen and cytotoxin Asp F 1	AFUA_5G02330	1.40	0.66	4.20	2.10	4.53	1.47	5.10	3.53
Major allergen Asp F 2	AFUA_4G09580	-7.61	-3.42	-1.54	-2.80	-0.19	-2.30	-0.00	-2.88
Mn superoxide dismutase MnSOD (Asp F 6)	AFUA_1G14550	-14.02	-5.72	2.01	-1.49	0.87	-1.12	0.21	-3.62
Aldehyde dehydrogenases[d]									
Aldehyde dehydrogenase (AldH12)	AFUA_2G17460	3.65	3.54	-4.74	2.29	3.05	3.27	2.76	3.15
Alpha-amylase	AFUA_4G10130	6.06	3.07	4.52	4.11	6.25	3.09	5.99	3.04
Conidial hydrophobin Hyp1/RodA	AFUA_5G09580	2.57	1.67	-3.40	-5.07	0.25	0.74	-1.43	1.15

Table 4.10. (*continued*)

Gene product description[a]	Locus ID[b]	Fold change (log_2)[c]							
		Day 1 *vs* 37°C		Day 2 *vs* 37°C		Day 3 *vs* 37°C		Day 4 *vs* 37°C	
		RT-qPCR	microarray	RT-qPCR	microarray	RT-qPCR	microarray	RT-qPCR	microarray
Conidial biosynthesis[d]									
Conidial pigment polyketide synthase PksP/Alb1	AFUA_2G17600	-1.09	-1.65	-3.33	-2.93	-1.25	-3.00	-1.58	-1.68
Conidial pigment biosynthesis 1,3,6,8-tetrahydroxynaphthalene reductase Arp2	AFUA_2G17560	3.05	2.79	-1.36	-4.15	3.23	1.41	-0.09	1.42
Conidial pigment biosynthesis scytalone dehydratase Arp1	AFUA_2G17580	5.87	0.73	0.12	0.61	1.79	0.02	2.08	2.91
Conidial pigment biosynthesis oxidase Abr1/brown 1	AFUA_2G17540	7.06	4.51	4.52	3.83	6.71	3.88	4.51	3.27
Conidial pigment biosynthesis oxidase Arb2	AFUA_2G17530	3.05	2.79	-1.36	1.20	3.22	1.95	-0.09	0.03
Phospholipases[d]									
Phosphatidylglycerol specific phospholipase C	AFUA_7G04910	9.01	2.99	4.40	2.23	-0.22	2.79	7.29	3.95
Lysophospholipase Plb2	AFUA_5G01340	-3.11	2.58	0.59	0.86	3.54	0.60	4.16	0.16
Extracelullar proteins[d]									
Extracellular alpha-1,3-glucanase/mutanase	AFUA_7G08510	7.16	4.49	0.46	2.33	3.61	2.76	4.31	2.69
Extracellular glycosyl hydrolase/cellulase	AFUA_2G00920	3.19	3.48	-4.63	4.20	2.08	3.63	-3.18	3.40
Extracellular exo-polygalacturonase	AFUA_8G06890	8.37	4.66	2.59	3.41	6.41	3.09	6.71	4.83
Extracelular cellulose binding protein (Cip2)	AFUA_6G14390	5.86	2.65	0.21	1.85	1.71	0.37	-9.60	1.82
Proteases[d]									
Aspartic-type endopeptidase	AFUA_3G01220	-0.64	1.85	-0.40	2.16	7.22	1.29	4.26	1.41
Serine protease	AFUA_7G06220	9.67	2.26	4.46	0.90	6.65	1.30	6.64	2.28
Most up-regulated during the infection[d]									
Polyphenol monooxygenase	AFUA_4G13780	11.37	3.40	6.59	2.52	14.20	2.45	13.14	1.82
GABA permease	AFUA_3G11490	7.25	4.64	1.06	4.41	4.42	4.12	-9.44	2.47
Ctr copper transporter family protein	AFUA_3G13660	-2.22	3.87	11.84	6.00	12.11	7.17	12.00	4.94
Most down-regulated during the infection[d]									
Cytochrome b5 reductase	AFUA_5G10060	-5.05	-5.36	-9.75	-5.57	-8.79	-5.90	-20.04	-6.13
Ribonuclease H1	AFUA_1G10020	-13.53	-6.13	-4.63	-4.55	-3.85	-5.72	-3.78	-4.82
Cytochrome P450 monooxygenase	AFUA_5G10050	-4.34	-5.63	-8.54	-5.57	-7.89	-5.90	-19.63	-6.78

[a]Gene product description of the genes selected to validate microarray data.
[b]GenBank accession number.
[c]Fold change in log_2 obtained for each gene. This value represents the log_2 of each day of infection minus the log_2 at 37ºC. Positive fold changes mean an up-regulation throughout the infection and negative fold changes an up-regulation during the germination at 37ºC.
[d]Group or metabolism in which each gene is involved.

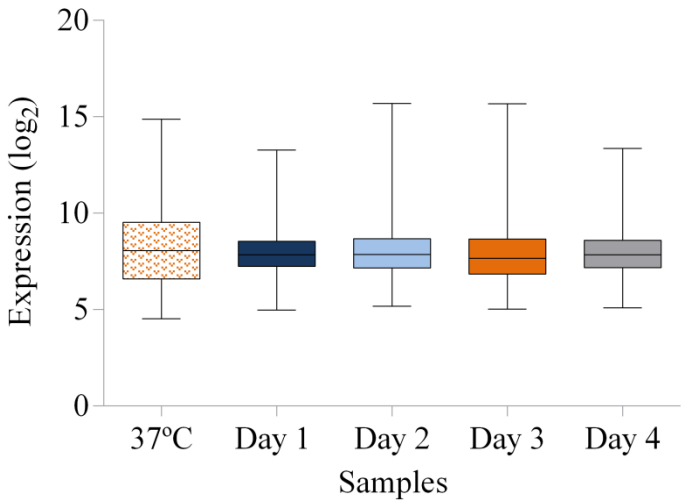

Fig. 4.19. Box plot representing the distribution of gene expression. Each sample corresponds to the mean expression of three independent samples obtained from the growth *in vitro* at 37ºC and during a disseminated infection. 37ºC: Germination at 37ºC. Day 1: day 1 post-infection. Day 2: day 2 post-infection. Day 3: day 3 post-infection. Day 4: day 4 post-infection. The Y-axis values represent the normalized gene expression (log_2).

As in the study of *A. fumigatus* germination, differentially expressed genes were classified according to the FunCat categorization except those encoding hypothetical and unclassified proteins, which were classified in two non-functional groups. In all comparisons, metabolism, hypothetical proteins and transport were the predominant groups (Table 4.11). Focusing on the up-regulated genes on each day of infection and during the germination, it was shown that the number of genes during the germination was larger than throughout the infection in all the categories. Nevertheless, the number of up-regulated genes coding for unclassified proteins was nearly the same as during the germination, and the number of those that encoded hypothetical proteins exceeded the number found during the germination on days 1, 2 and 4 post-infection (Fig. 4.21). These proteins represented roughly 15 and 40% of the differentially expressed genes on each day. Moreover, studying the 20 most up-regulated genes on each day post-infection over 50% of them encoded unclassified and hypothetical proteins (Annex I).

Tabla 4.11. Classification of differentially expressed genes among each day of infection and the germination at 37ºC.

Main category[a]	Number of differentially expressed genes[b]			
	Day 1 *vs* 37°C	**Day 2 *vs* 37°C**	**Day 3 *vs* 37°C**	**Day 4 *vs* 37°C**
Metabolism	1515	156	1318	628
Energy	318	21	242	118
Cell cycle and DNA processing	377	20	408	189
Transcription	417	26	447	195
Protein synthesis	263	5	186	117
Protein fate	586	28	567	270
Transport	748	67	688	326
Cellular comunication	250	22	252	110
Cell rescue, defense and virulence	543	58	456	251
Interaction with the environment	295	33	257	121
Cell fate	208	6	210	97
Development	32	18	36	13
Biogenesis of cellular components	471	18	471	219
Cell type differentation	205	63	191	88
Regulation of metabolism and protein function	223	13	210	95
Unclassified proteins	496	53	433	179
Hypothetical proteins	1010	116	847	350

Note: One gene can be involved in more than one biological function, which explains why the total number of genes is larger than the differentially expressed genes.

[a]Functional category according to the Munich Information Center for Protein Sequence Functional Catalogue (FunCat; http://pedant.helmholtz-muenchen.de). Genes that encode hypothetical or unclassified proteins were classified in two non-functional groups.

[b]Number of genes that showed significant differences in each comparison.

In order to determine in a more accurate way which functions were significantly represented on each day post-infection, an enrichment analysis was carried out. According to it, the largest number of significant enriched groups was found on day 1 of infection in which several groups included within metabolism (12), transport (8), cell rescue, defense and virulence (6) and transport (1) appeared. On day 2, only secondary metabolism was significantly enriched, whereas on days 3, 5 categories related to metabolism, 4 to transport and 2 to cell rescue and defense appeared significantly up-regulated. Finally, on day 4, 6 categories involved in metabolism and 2 in cell rescue, defense and virulence were significantly over-represented (Table 4.12).

A

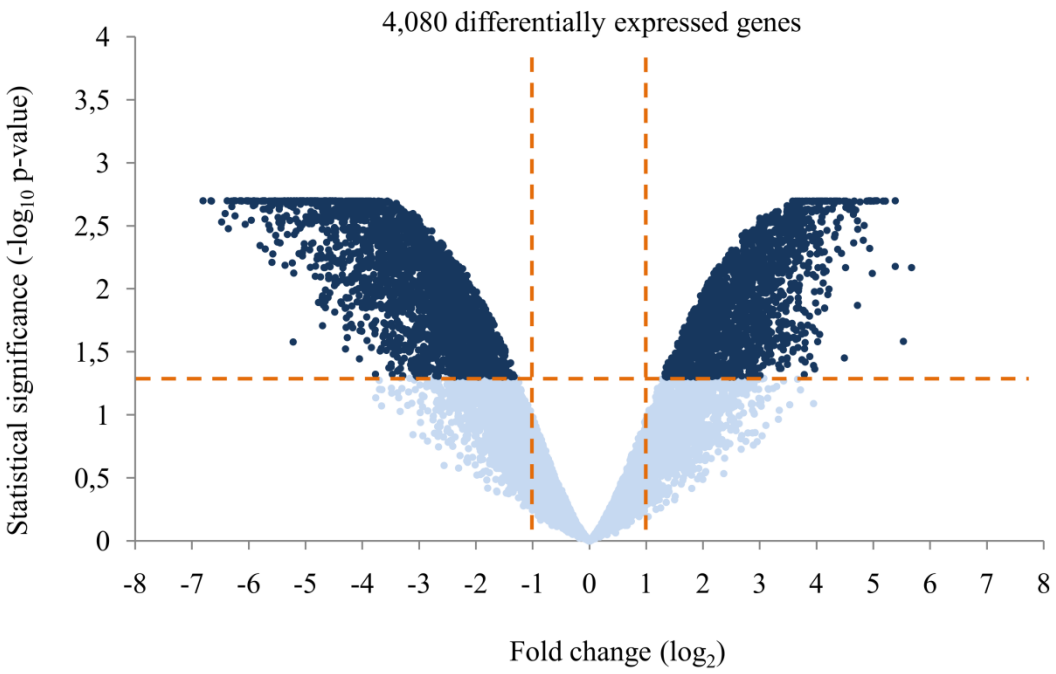
4,080 differentially expressed genes
Statistical significance (-log10 p-value)
Fold change (log2)
4
3,5
3
2,5
2
1,5
1
0,5
0
-8 -7 -6 -5 -4 -3 -2 -1 0 1 2 3 4 5 6 7 8

B

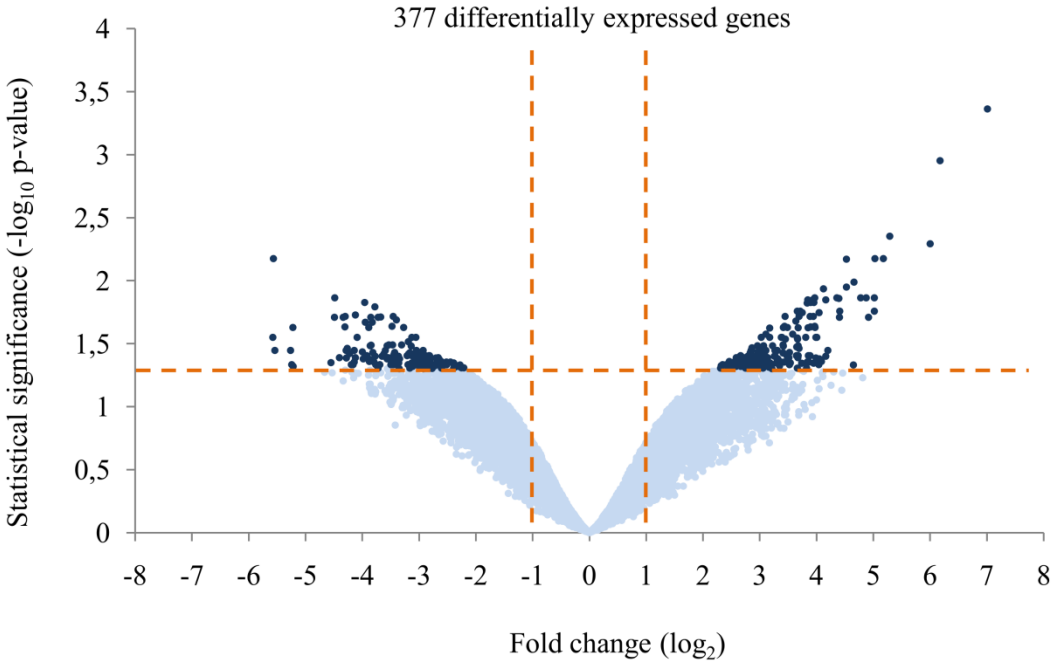
377 differentially expressed genes
Statistical significance (-log10 p-value)
Fold change (log2)
4
3,5
3
2,5
2
1,5
1
0,5
0
-8 -7 -6 -5 -4 -3 -2 -1 0 1 2 3 4 5 6 7 8

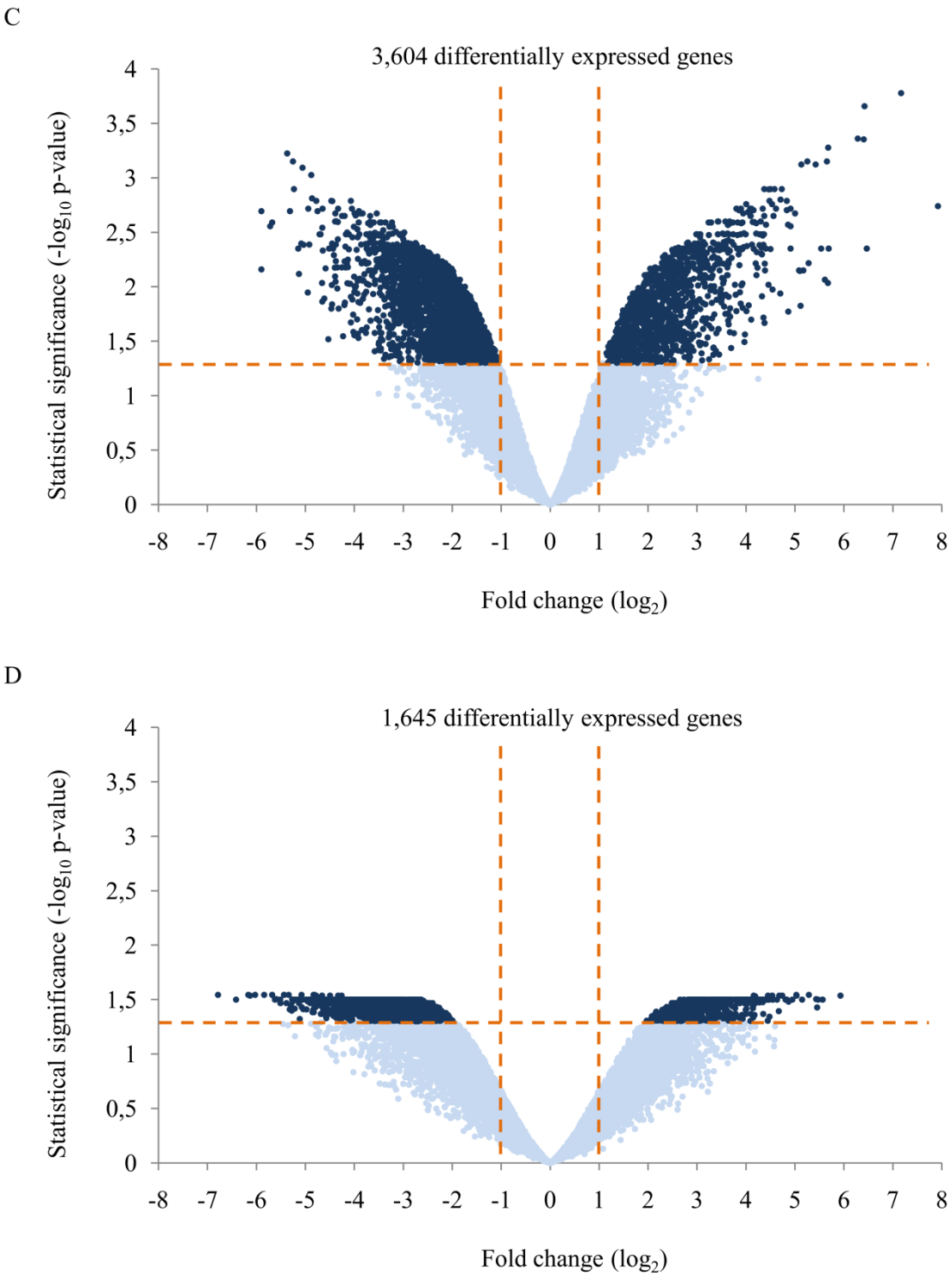

Fig. 4.20. Volcano plot of each day of infection relative to the germination at 37ºC. A) Day 1 *vs* germination at 37ºC: 4,080 differentially expressed genes. B) Day 2 *vs* germination at 37ºC: 377 differentially expressed genes. C) Day 3 *vs* germination at 37ºC: 3,604 differentially expressed genes. D) Day 4 *vs* germination at 37ºC: 1,645 differentially expressed genes. Genes differentially expressed are shown in dark blue and non-differentially expressed in light blue. The X-axis values represent the fold change (log_2) of microarray data and the Y-axis values the statistical significance ($-log_{10}$ p-value). Spots with negative fold change values indicate up-regulation at 37ºC and with positive values up-regulation on each day of infection. Each point corresponds to the mean value of three independent samples.

A

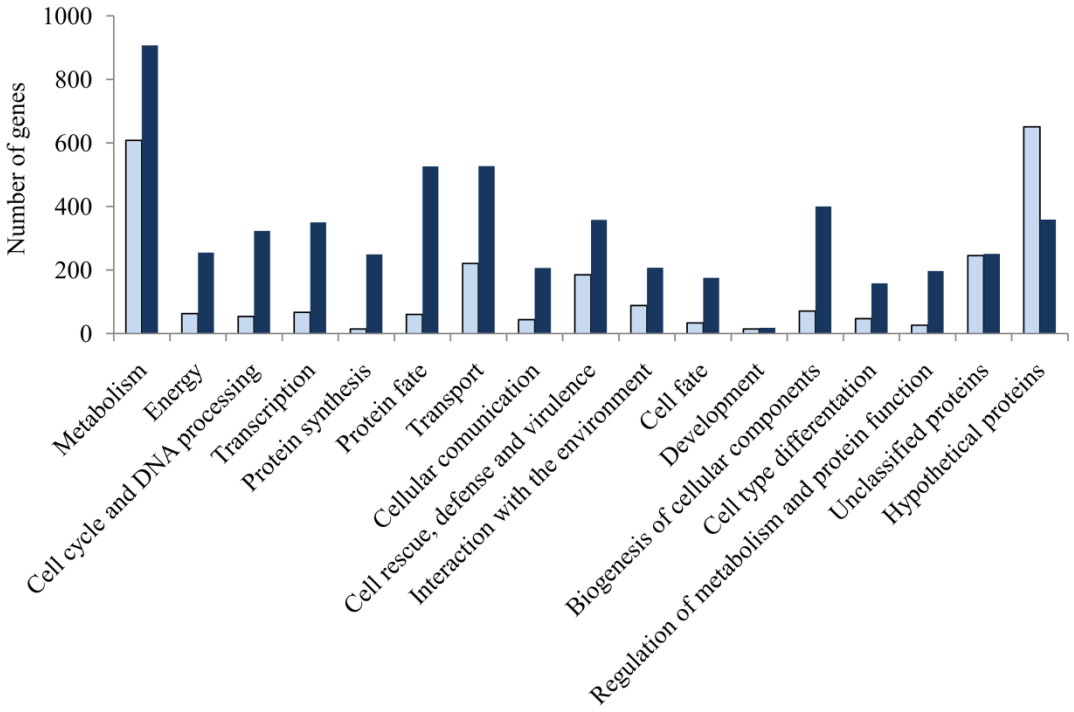
Number of genes
1000
800
600
400
200
0
Metabolism
Energy
Cell cycle and DNA processing
Transcription
Protein synthesis
Protein fate
Transport
Cellular comunication
Cell rescue, defense and virulence
Interaction with the environment
Cell fate
Development
Biogenesis of cellular components
Cell type differentiation
Regulation of metabolism and protein function
Unclassified proteins
Hypothetical proteins

B

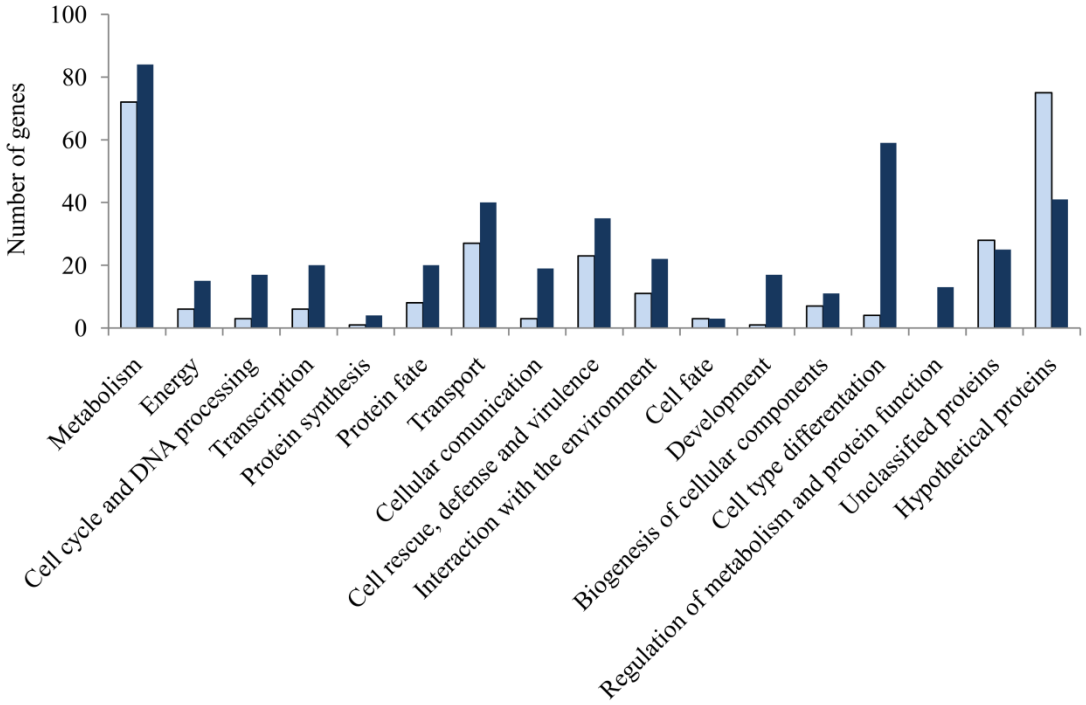
Number of genes
100
80
60
40
20
0
Metabolism
Energy
Cell cycle and DNA processing
Transcription
Protein synthesis
Protein fate
Transport
Cellular comunication
Cell rescue, defense and virulence
Interaction with the environment
Cell fate
Development
Biogenesis of cellular components
Cell type differentiation
Regulation of metabolism and protein function
Unclassified proteins
Hypothetical proteins

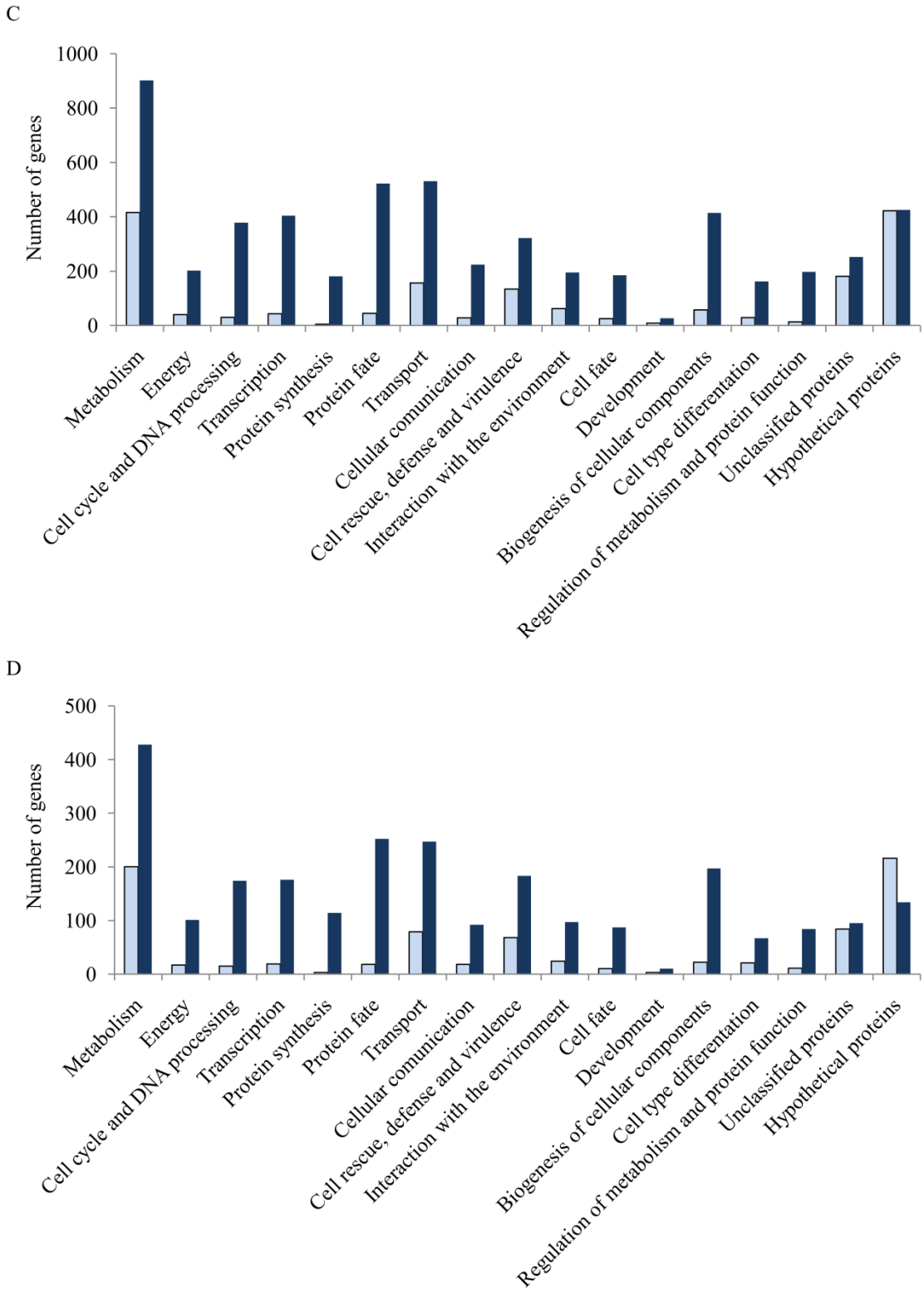

Fig. 4.21. Classification of differentially expressed genes on each day of infection and during the germination at 37ºC. Genes were classified according to FunCat categorization (http://pedant.helmholtz-muenchen.de), except those that code for unclassified and hypothetical proteins. Comparisons were as follows: A) Day 1 *vs* germination at 37ºC. B) Day 2 *vs* germination at 37ºC. C) Day 3 *vs* germination at 37ºC. D) Day 4 *vs* germination at 37ºC. Light blue and dark blue bars indicate the number of up-regulated genes on each day of infection and during the germination at 37º, respectively. One protein can be involved in more than one biological function which explains why the number of genes is larger than the total number of differentially expressed genes found in each comparison.

Table 4.12. Enriched FunCat categories up-regulated throughout the infection.

FunCat ID[a]	FunCat description[b]	Adjusted p-value[c]			
		Day 1	Day 2	Day 3	Day 4
Metabolism[d]					
01.05	C-compound and carbohydrate metabolism	1.08^{-9}		2.51^{-8}	
01.05.02.07	Sugar, glucoside, polyol and carboxylate catabolism	4.08^{-4}			
01.05.03	Polysaccharide metabolism	3.67^{-11}		1.53^{-7}	1.44^{-2}
01.05.03.03	Chitin metabolism	2.28^{-4}			
01.05.03.03.07	Chitin catabolism	2.28^{-4}			
01.20	Secondary metabolism	1.60^{-56}	5.56^{-4}	8.33^{-31}	3.33^{-18}
01.20.05.11	Metabolism of polyketides	2.24^{-4}			
01.20.15	Metabolism of derivatives of dehydroquinic acid, shikimic acid and chorismic acid	1.07^{-2}			
01.20.17.03	Metabolism of amines	7.12^{-6}			
01.20.33	Metabolism of secondary products derived from L-tryptophan	3.61^{-2}		1.05^{-2}	4.17^{-4}
01.20.36	Non-ribosomal peptide synthesis	1.02^{-4}		2.93^{-3}	
01.20.38	Metabolism of toxins/drugs				1.69^{-2}
01.25.01	Extracellular polysaccharide degradation	7.84^{-5}			
Transport[d]					
20.01.03	C-compound and carbohydrate transport	1.69^{-4}		4.59^{-4}	
20.01.11	Amine / polyamine transport	1.79^{-3}			
20.01.23	Allantoin and allantoate transport	2.66^{-3}			
20.01.25	Vitamine/cofactor transport	5.80^{-3}			
20.01.27	Drug/toxin transport	1.12^{-6}			1.15^{-3}
20.03	Transport facilities	1.12^{-6}		2.50^{-2}	1.44^{-2}
20.09.18	Cellular import	5.49^{-7}		2.50^{-2}	
20.09.18.07	Non-vesicular cellular import	8.35^{-6}		5.27^{-5}	4.73^{-4}
Cell rescue, defense and virulence[d]					
32.05.01	Resistance proteins	1.23^{-3}			
32.05.05	Virulence, disease factors	8.35^{-6}		1.58^{-3}	1.44^{-2}
32.05.05.01	Toxins	1.19^{-3}			8.21^{-4}
32.07	Detoxification	3.63^{-4}			
32.07.05	Detoxification by export	8.99^{-7}			
32.10.07	Degradation / modification of foreign (exogenous) polysaccharides	1.19^{-3}		9.16^{-5}	
Cell fate[d]					
40.01.03.03	Guidance of longitudinal cell extension	1.03^{-2}			

Note: FunCat (Munich Information Center for Protein Sequence Functional Catalogue; http://pedant.helmholtz-muenchen.de)
[a]FunCat ID of each FunCat description.
[b]Functional classification according to the FunCat Cataloque
[c]Adjusted p-value of the different functional groups obtained on each day of infection. The analysis was carried out using Fisher's test and Benjamini-Hochberg correction. Only the significant values ($p < 0.05$) are shown.
[d]FunCat main category of each significant biological function.

Regarding those groups significantly enriched during the germination at 37ºC and, in turn, down-regulated during the infection, the largest number of functional categories was observed on day 1 *versus* the germination at 37ºC, with 9 categories involved in metabolism, 8 in energy, 7 in protein synthesis, 7 in protein with binding function or cofactor requirement, 7 in transport, 5 in protein fate, 2 in biogenesis of cellular components, 3 in cell rescue, defense and virulence, 2 in regulation of metabolism and protein function, 1 in transcription, and 1 in interaction with the environment. When day 2 was compared to the germination, 2 categories related to cell rescue, defense and

virulence and 1 to metabolism were significantly enriched. In the comparisons with day 3 and 4, groups included within metabolism, transport, protein with binding function or cofactor requirement, protein fate, biogenesis of cellular components, and cell rescue, defense and virulence were significantly represented during the germination at 37ºC (Table 4.13).

Table 4.13. Enriched FunCat categories down-regulated during the *A. fumigatus* infection.

FunCat ID[a]	FunCat description[b]	Adjusted p-value[c]			
		Day 1	Day 2	Day 3	Day 4
Metabolism[d]					
01.01	Amino acid metabolism	5.57^{-03}			1.97^{-02}
01.01.03.02.01	Biosynthesis of glutamate				4.45^{-02}
01.01.09.07.01	Biosynthesis of histidine	2.54^{-02}			
01.01.11	Metabolism of the pyruvate family (alanine, isoleucine, leucine, valine) and D-alanine			2.64^{-02}	
01.03.01	Purin nucleotide/nucleoside/nucleobase metabolism	1.54^{-05}		2.02^{-03}	
01.03.01.03	Purine nucleotide/nucleoside/nucleobase anabolism	8.12^{-09}		1.49^{-05}	2.24^{-03}
01.03.04	Pyrimidine nucleotide/nucleoside/nucleobase metabolism	1.15^{-03}		1.62^{-02}	1.81^{-02}
01.03.04.03	Pyrimidine nucleotide/nucleoside/nucleobase anabolism	1.97^{-02}			
01.04	Phosphate metabolism	5.89^{-03}		8.01^{-05}	
01.05.02.04	Sugar, glucoside, polyol and carboxylate anabolism	2.16^{-02}			
01.06.05	Fatty acid metabolism		2.15^{-02}		
01.07.01	Biosynthesis of vitamins, cofactors, and prosthetic groups	2.41^{-03}			2.57^{-02}
Energy[d]					
02.01.03	Regulation of glycolysis and gluconeogenesis	1.83^{-02}			
02.10	Tricarboxylic-acid pathway (citrate cycle, Krebs cycle, TCA cycle)	4.47^{-03}			
02.11	Electron transport and membrane-associated energy conservation	7.68^{-09}			
02.11.05	Accessory proteins of electron transport and membrane-associated energy conservation	7.89^{-05}			
02.13	Respiration	7.89^{-05}			
02.13.03	Aerobic respiration	4.48^{-09}			2.57^{-02}
02.25	Oxidation of fatty acids	2.22^{-02}			
02.45.15	Energy generation (e.g. ATP synthase)	5.57^{-03}			
Cell cycle and DNA processing[d]					
10.03.01	Mitotic cell cycle and cell cycle control				2.84^{-02}
Transcription[d]					
11.02.03	mRNA synthesis			1.19^{-03}	1.02^{-02}
11.04.01	rRNA processing			5.27^{-03}	
11.04.03	mRNA processing (splicing, 5'-, 3'-end processing)	9.81^{-03}		2.03^{-02}	
Protein synthesis[d]					
12.01	Ribosome biogenesis	3.80^{-10}			
12.01.01	Ribosomal proteins	2.35^{-25}		1.21^{-02}	1.58^{-02}
12.04	Translation	1.76^{-19}			1.18^{-02}
12.04.01	Translation initiation	2.17^{-04}		9.65^{-04}	4.28^{-04}
12.04.02	Translation elongation	2.54^{-03}			
12.07	Translational control	2.24^{-03}			
12.10	Aminoacyl-tRNA-synthetases	1.35^{-05}		1.62^{-02}	1.02^{-02}
Protein fate[d]					
14.01	Protein folding and stabilization	5.94^{-07}		1.81^{-03}	1.23^{-03}
14.04	Protein targeting, sorting and translocation	2.16^{-07}		1.29^{-08}	1.92^{-02}

Table 4.13. *(continued)*

FunCat ID[a]	FunCat description[b]	Adjusted p-value[c]			
		Day 1	Day 2	Day 3	Day 4
14.07.07	Modification by ubiquitin-related proteins				2.76^{-02}
14.07.11	Protein processing (proteolytic)	1.24^{-06}			
14.10	Assembly of protein complexes	6.72^{-04}		1.36^{-03}	1.24^{-02}
14.13.01.01	Proteasomal degradation (ubiquitin/proteasomal pathway)	2.25^{-06}		3.77^{-03}	1.99^{-03}
Protein with binding function or cofactor requirement [d]					
16.01	Protein binding	1.27^{-22}		4.78^{-14}	1.79^{-07}
16.03.03	RNA binding	1.40^{-05}		5.36^{-04}	3.46^{-03}
16.07	Structural protein binding	1.08^{-02}			2.11^{-02}
16.19	Nucleotide/nucleoside/nucleobase binding	4.04^{-03}		2.38^{-04}	6.06^{-03}
16.19.03	ATP binding	1.86^{-02}		3.45^{-04}	1.23^{-03}
16.19.05	GTP binding	3.74^{-05}		3.45^{-04}	
16.21.08	Fe/S binding	1.15^{-03}			
Regulation of metabolism and protein function[d]					
18.01.07	Regulation by binding / dissociation	3.37^{-03}			
18.02.01.01	Enzyme activator	1.08^{-02}			
Cellular transport, transport facilitation and transport routes[d]					
20.01.10	Protein transport	2.49^{-09}		3.06^{-08}	1.31^{-02}
20.01.21	RNA transport	1.05^{-03}		5.44^{-06}	5.15^{-04}
20.09.01	Nuclear transport	2.98^{-02}		1.36^{-03}	1.02^{-02}
20.09.03	Peroxisomal transport	1.27^{-03}		7.12^{-03}	
20.09.04	Mitochondrial transport	3.82^{-06}			1.24^{-02}
20.09.07	Vesicular transport (Golgi network, etc.)			1.92^{-04}	
20.09.07.03	ER to Golgi transport			3.45^{-04}	
20.09.07.25	Vesicle formation			5.03^{-04}	
20.09.13	Vacuolar/lysosomal transport			1.36^{-03}	
20.09.18.09.01	Endocytosis			3.67^{-03}	
30.01	Cellular signalling			4.64^{-02}	
30.01.05.05	G-protein mediated signal transduction	3.47^{-02}		1.36^{-03}	
30.01.05.05.01	Small GTPase mediated signal transduction	1.70^{-02}		1.09^{-04}	
30.01.09.07	cAMP/cGMP mediated signal transduction			4.64^{-02}	
Cell rescue, defense and virulence[d]					
32.01	Stress response	7.84^{-11}			4.28^{-04}
32.01.05	Heat shock response	3.87^{-04}		2.64^{-02}	1.64^{-02}
32.01.07	Unfolded protein response (e.g. ER quality control)	9.48^{-06}		1.38^{-03}	6.78^{-04}
32.05.01.03	Chemical agent resistance		3.81^{-04}		
32.07	Detoxification		5.39^{-03}		
Interaction with the environment[d]					
34.11.09	Temperature perception and response	1.10^{-02}		3.51^{-03}	1.02^{-02}
Cell fate[d]					
40.01	Cell growth / morphogenesis			4.76^{-02}	
Biogenesis of cellular components[d]					
42.04	Cytoskeleton/structural proteins				2.84^{-02}
42.04.03	Actin cytoskeleton	2.98^{-02}		1.30^{-02}	
42.09	Intracellular transport vesicles			1.36^{-03}	
42.16	Mitochondrion	1.63^{-07}		2.94^{-05}	2.41^{-04}
42.19	Peroxisome			2.17^{-02}	
42.29	Bud / growth tip			2.73^{-02}	

Note: FunCat (Munich Information Center for Protein Sequence Functional Catalogue; http://pedant.helmholtz-muenchen.de)
[a]FunCat ID of each FunCat description.
[b]Functional classification according to the FunCat Catagorization.
[c]Adjusted p-value of the different functional groups obtained on each day of infection. The analysis was carried out using Fisher´s test and Benjamini-Hochberg correction. Only the significant values ($p < 0.05$) are shown.
[d]FunCat main category of each significant biological function.

The chromosomal location of the differentially expressed genes showed that the up-regulated genes during the infection were mainly located in sub-telomeric regions. Furthermore, the number of up-regulated genes during the germination was larger than those up-regulated throughout the infection; with ratios lower than 1 in the majority of the cases. Nevertheless, chromosome VII stood out with a ratio higher than 1 in all the comparisons, meaning that in this chromosome the number of up-regulated genes was larger along the infectious process (Fig.4.22). Analyzing the up-regulated genes of this chromosome and focusing on those whose up-regulation remained during 3 and 4 days of infection, the 37.50% of them encoded hypothetical proteins, although 4 transcription factors (AFUA_8G05460, AFUA_8G00750, AFUA_8G06460, AFUA_8G07000) stood out.

With the aim of identifying those genes whose up-regulation remains throughout the infection a hierarchical clustering analysis was performed with those genes that showed significant differences when the germination at 37ºC was established as the control condition. The clustering showed one region with 1,001 genes in which the expression along the infectious process was higher than during the germination (Fig. 4.23). Genes included within this region are shown in Annex II.

Analyzing the genes clustered in that region, the enrichment analysis showed that 5 groups included in metabolism, 4 in transport and 2 in cell rescue, defense and virulence were significantly represented (Table 4.14). Amongst these genes, several hidrolases, MFS transporters and transcription factors could be mentioned. However, 373 and 155 genes of the cluster coded for hypothetical and unclassified proteins, respectively (Annex II).

A

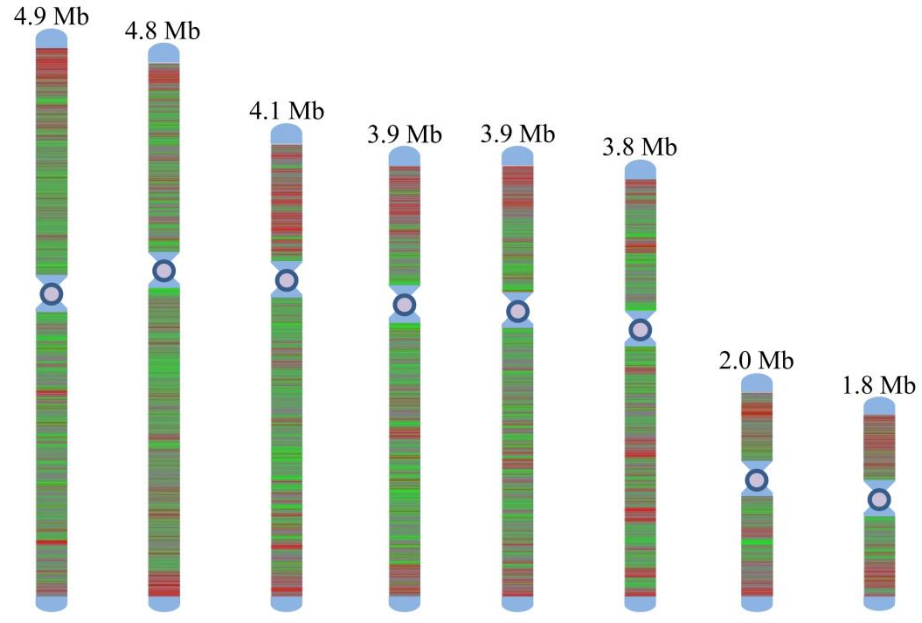

	I	II	III	IV	V	VI	VII	VIII
Day 1	242	227	260	203	230	219	129	165
37ºC	454	424	323	334	340	316	113	101
Ratio	**0.53**	**0.54**	**0.80**	**0.61**	**0.68**	**0.69**	**1.14**	**1.63**

B

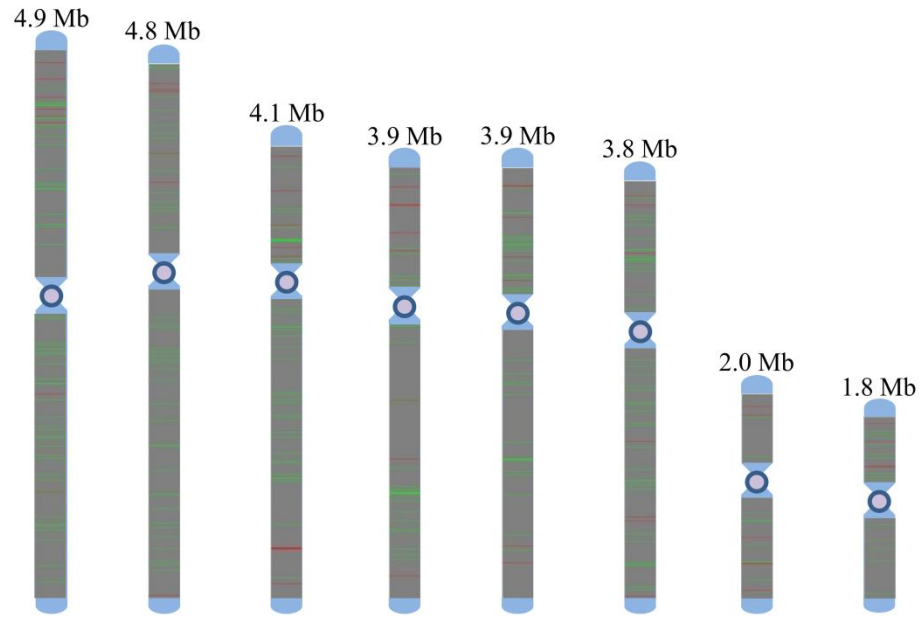

	I	II	III	IV	V	VI	VII	VIII
Day 2	25	26	28	31	20	20	14	25
37ºC	36	37	24	20	30	23	8	10
Ratio	**0.69**	**0.70**	**1.17**	**1.55**	**0.67**	**0.87**	**1.75**	**2.50**

C

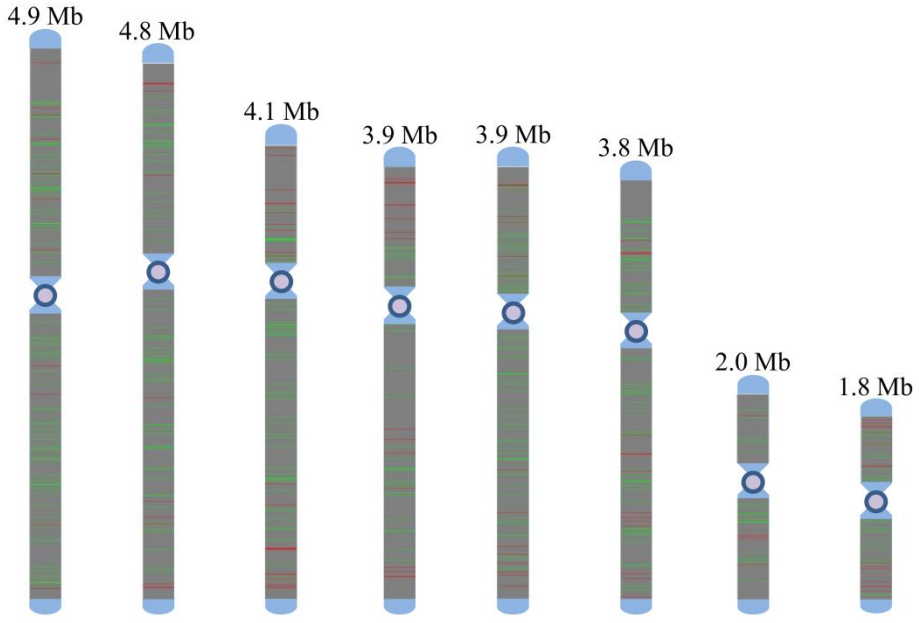

	I	II	III	IV	V	VI	VII	VIII
Day 3	148	172	180	133	148	153	97	108
37ºC	490	455	293	322	359	317	127	102
Ratio	**0.30**	**0.38**	**0.61**	**0.41**	**0.41**	**0.48**	**0.76**	**1.06**

D

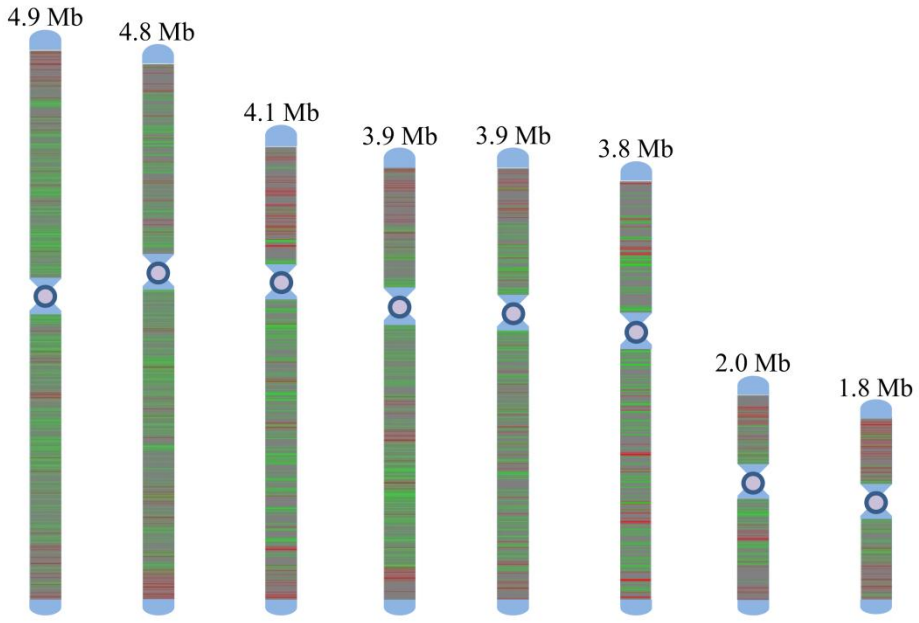

	I	II	III	IV	V	VI	VII	VIII
Day 4	72	71	91	72	70	77	42	68
37ºC	224	201	136	137	154	140	52	38
Ratio	**0.32**	**0.35**	**0.67**	**0.53**	**0.45**	**0.55**	**0.81**	**1.79**

Fig. 4.22. Chromosomal location of differentially expressed genes found in the comparison of each day of infection and the germination at 37ºC. A) Day 1. B) Day 2. C) Day 3. D) Day 4. Genes up-regulated on each day of infection are represented in red color and those up-regulated during the germination at 37ºC in green color. Blue ends correspond to telomeres and purple cycles to centromeres. The number of each chromosome and its size are indicated below and above each chromosome, respectively. The number of the up-regulated genes found on each day or during the germination, as well as the ratio, is shown at the botton of each chromosome.

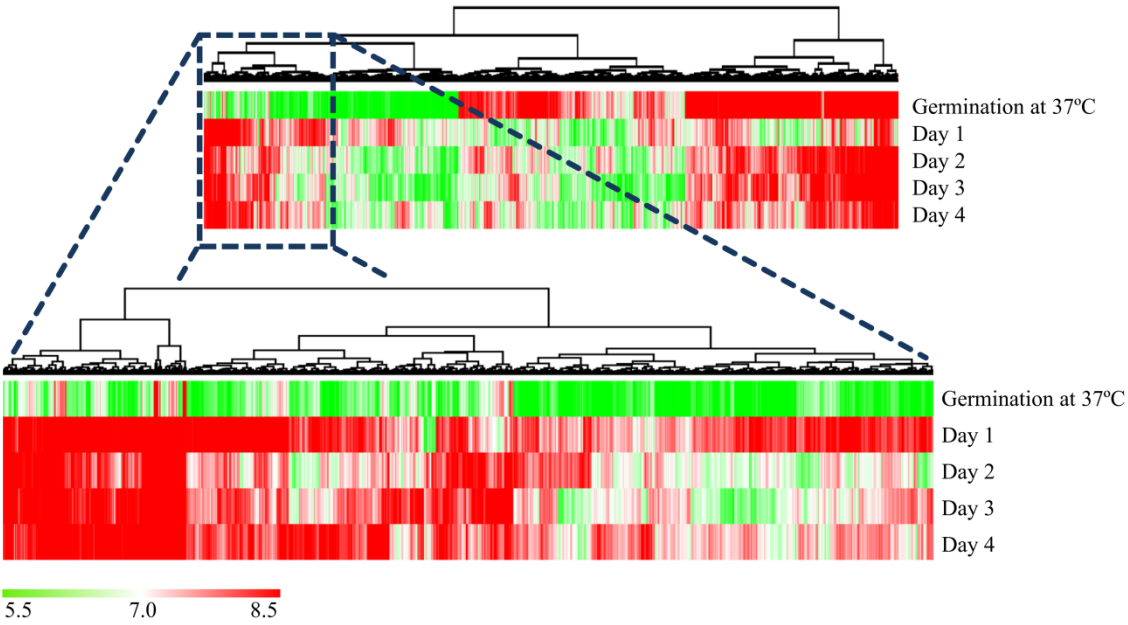

Fig. 4.23. Hierarchical clustering of those genes that were differentially expressed when the germination at 37ºC was established as the control condition. The region in which the expression along the infection was higher than during the germination *in vitro* is enlarged at the bottom. The color bar indicates the range of $\log_2$ expression values.

Tabla 4.14. Enriched FunCat categories of the cluster whose expression were up-regulated during the disseminated infection.

FunCat ID[a]	FunCat description[b]	p-value[c]
Metabolism[d]		
01.05	C-compound and carbohydrate metabolism	1.62^{-04}
01.05.03	Polysaccharide metabolism	3.37^{-06}
01.20	Secondary metabolism	1.75^{-24}
01.20.17.03	Metabolism of amines	2.30^{-02}
01.20.36	Non-ribosomal peptide synthesis	2.05^{-03}
Cellular transport, transport facilitation and transport routes[d]		
20.01.03	C-compound and carbohydrate transport	4.96^{-03}
20.03	Transport facilities	8.94^{-03}
20.09.18	Cellular import	4.61^{-04}
20.09.18.07	Non-vesicular cellular import	3.37^{-06}
Cell rescue, defense and virulence[d]		
32.05.05	Virulence, disease factors	3.28^{-02}
32.10.07	Degradation / modification of foreign (exogenous) polysaccharides	4.20^{-02}

Note: FunCat (Munich Information Center for Protein Sequence Functional Catalogue; http://pedant.helmholtz-muenchen.de)
[a]FunCat ID of each FunCat description.
[b]Functional classification according to the FunCat Catagorization.
[c]Adjusted p-value of the different functional groups obtained on each day of infection. The analysis was carried out using Fisher´s test and Benjamini-Hochberg correction. Only the significant values ($p < 0.05$) are shown.
[d]FunCat main category of each significant biological function.

4.8.1. Genes involved in *A. fumigatus* virulence and nutrient uptake using the germination at 37ºC as the control condition

Virulence related genes involved in gliotoxin biosynthesis showed up-regulation during the infection, highlighting *gliA* and *gliK* with high expression along 3 days post-infection (Table 4.15). Genes involved in nutrition acquisition systems also appeared differentially expressed when each day of infection was compared to the germination at 37ºC. Amongst these, 2 phospholipases and 22 proteases were up-regulated along the infectious process, including aspergillopepsin (AFUA_3G02970); penicillolysin/deuterolysin metalloprotease (AFUA_4G13750); alkaline serine protease (PR1)/allergen F 18-like (AFUA_7G04930); methionine aminopeptidase, type II (AFUA_8G00410); lysophospholipase Plb2 (AFUA_5G01340); and phosphatidylglycerol specific phospholipase C (AFUA_7G04910) (Table 4.16).

Table 4.15. Differentially expressed genes related to gliotoxin biosynthesis.

Gene product description[a]	Locus ID[b]	Fold change[c]			
		Day 1	Day 2	Day 3	Day 4
Aminotransferase GliI	AFUA_6G09640			**2.20**	
Nonribosomal peptide synthase GliP	AFUA_6G09660	**1.82**			
Cytochrome P450 oxidoreductase GliC	AFUA_6G09670			**1.88**	
Gliotoxin biosynthesis protein GliK	AFUA_6G09700	**3.31**		**2.86**	**2.75**
MFS gliotoxin efflux transporter GliA	AFUA_6G09710	**3.62**	**4.00**	**1.93**	
Methyltransferase GliN	AFUA_6G09720	**1.98**			**2.76**
Cytochrome P450 oxidoreductase GliF	AFUA_6G09730			**4.40**	**3.62**
Thioredoxin reductase GliT	AFUA_6G09740			**4.58**	

[a]Genes product description of the genes found on the microarray.
[b]GenBank accession number.
[c]Fold change in $\log_2$ obtained for each gene. This value represents the $\log_2$ of each day of infection minus the $\log_2$ at 37ºC. Positive fold changes (in bold) mean an up-regulation throughout the infection and negative fold changes an up-regulation during the germination at 37ºC.

Table 4.16. Differentially expressed genes that code proteases and phospholipases.

Gene product description[a]	Locus ID[b]	Fold change[c]			
		Day 1	Day 2	Day 3	Day 4
ATP-dependent Clp protease	AFUA_1G02170			-1.64	
Calpain-like protease PalBory	AFUA_1G03450			-1.99	
Glutamate carboxypeptidase	AFUA_1G03740			-2.08	-2.74
Metacaspase CasA	AFUA_1G06700	-2.78		-2.72	-3.60
26S proteasome regulatory particle subunit Rpn8, putative	AFUA_1G07540	-2.50		-2.12	-2.81
Ubiquitin-specific protease	AFUA_1G07555	**2.69**			
Mitochondrial processing peptidase alpha subunit, putative	AFUA_1G11870	-3.68		-2.68	-2.69
Mitochondrial processing peptidase beta subunit, putative	AFUA_1G14200	-4.35		-2.19	
Peptidase D	AFUA_1G14920			-1.25	
Peptidase S41 family protein	AFUA_1G17400	**1.70**		**3.42**	
Serine peptidase	AFUA_2G01250	**2.41**			
Methionine aminopeptidase, type II	AFUA_2G01750	-3.73			
Mitochondrial inner membrane AAA protease Yta12, putative	AFUA_2G02680	-2.95			
Alkaline serine protease	AFUA_2G03380	-3.52		-1.80	
Ubiquitin C-terminal hydrolase	AFUA_2G04720			-1.88	

Table. 4.16. *(continued)*

Gene product description[a]	Locus ID[b]	Fold change[c]			
		Day 1	Day 2	Day 3	Day 4
Proline iminopeptidase	AFUA_2G05000			-1.76	
Prolidase pepP	AFUA_2G07500	-2.82		-2.39	
Zinc carboxypeptidase	AFUA_2G08790	-2.20			
Proteasome component Pup2	AFUA_2G11440	-4.32		-2.28	-4.42
Mitochondrial serine protease Pim1	AFUA_2G11740	-2.36		-1.92	-2.67
Ubiquitin C-terminal hydrolase	AFUA_2G14130			-2.49	
Rhomboid family membrane protein	AFUA_2G16490	-3.22		-2.13	-3.88
Aminopeptidase Y	AFUA_3G00650			**2.04**	
Aspergillopepsin	AFUA_3G02970	**2.56**		**2.19**	
Autophagy cysteine endopeptidase Atg4	AFUA_3G05340			**3.46**	
Glutamate carboxypeptidase	AFUA_3G05450	-4.97		-2.88	-4.06
OTU-like cysteine protease	AFUA_3G05550			-3.06	-2.63
Pheromone maturation dipeptidyl aminopeptidase DapB	AFUA_3G07850			-2.05	
Aspartyl aminopeptidase	AFUA_3G08290	-3.68			
Glutamate carboxypeptidase Tre2	AFUA_3G10650	-2.58		-2.72	-2.56
Zinc metalloproteinase	AFUA_3G11160		-3.05	-1.34	
Proteasome component Prs2	AFUA_3G11300	-3.08		-2.32	-2.83
Aspartic endopeptidase Pep2	AFUA_3G11400	-4.48			
Signal peptidase I	AFUA_3G12840	-2.47		-1.78	-3.71
Mitochondrial inner membrane protease subunit Imp2, putative	AFUA_3G13840	-1.48			
Serine peptidase, family S28	AFUA_4G03790	**2.47**		**1.55**	
Aminopeptidase	AFUA_4G04210			-1.66	
Dipeptidyl peptidase	AFUA_4G06140	-3.45		-2.33	
Methionine aminopeptidase, type II	AFUA_4G06930			-2.72	-3.25
Proteasome component Pup3	AFUA_4G07420	-3.78			
CaaX prenyl protease Ste24	AFUA_4G07590	-3.57		-2.58	-4.99
Zinc metalloprotease	AFUA_4G07610				-2.84
Pitrilysin family metalloprotease Cym1	AFUA_4G07910	-2.07			
Aminopeptidase	AFUA_4G09030	-4.23		-2.79	-4.19
Aspartic-type endopeptidase	AFUA_4G09400	**3.88**			
Mitochondrial inner membrane metallopeptidase Oma1, putative	AFUA_4G09730	-2.40		-1.82	
ADAM family of metalloprotease ADM-B	AFUA_4G11150	-3.72		-3.28	
Intermembrane space AAA protease IAP-1	AFUA_4G11530	-4.59			
Alkaline serine protease Alp1	AFUA_4G11800			**1.25**	
Pheromone processing endoprotease KexB	AFUA_4G12970	-2.40		-2.80	
OTU-like cysteine protease	AFUA_4G13560			-2.48	
Penicillolysin/deuterolysin metalloprotease	AFUA_4G13750	**3.56**		**2.90**	**3.34**
Tripeptidyl peptidase A	AFUA_4G14000	**2.03**			
ThiJ/PfpI family protein	AFUA_5G01430	-2.45		-3.45	
A-pheromone processing metallopeptidase Ste23	AFUA_5G02010			-2.42	
Proteasome component Pre6	AFUA_5G02150	-3.80		-2.39	-3.18
Microsomal signal peptidase subunit Gp23	AFUA_5G03220	-2.25		-2.91	
Vacuolar aspartyl aminopeptidase Lap4	AFUA_5G03990	-3.26		-1.73	
Ubiquinol-cytochrome C reductase complex core protein 2	AFUA_5G04210	-6.01			
Aminopeptidase	AFUA_5G04330	-3.02		-2.27	-2.40
Dipeptidyl peptidase III	AFUA_5G06940			**2.35**	
Carboxypeptidase S1	AFUA_5G07330	-2.29		-2.60	
Aminopeptidase P	AFUA_5G08050	-4.09		-2.07	-2.61
Autophagic serine protease Alp2	AFUA_5G09210	-3.18		-1.82	
Peptidase	AFUA_5G09920			-1.91	
LON domain serine protease	AFUA_5G11750	-2.98		-1.72	
Mitochondrial inner membrane protease subunit 1, putative	AFUA_5G12820	-2.04	-2.90		-2.40
Aspartic endopeptidase Pep1/aspergillopepsin F	AFUA_5G13300		-3.05	-2.28	
Beta-lactamase	AFUA_5G14510			**1.78**	

Table. 4.16. *(continued)*

Gene product description[a]	Locus ID[b]	Fold change[c]			
		Day 1	Day 2	Day 3	Day 4
Signal peptide peptidase	AFUA_6G02150	-1.98		-2.34	
Amidophosphoribosyltransferase	AFUA_6G03750	-2.45		-2.82	-3.56
O-sialoglycoprotein endopeptidase	AFUA_6G04510	-1.64			
ER-associated proteolytic system protein Der1	AFUA_6G04670	-2.78		-2.32	
Proteasome component Pre5	AFUA_6G04790	-3.45			
Aspartic-type endopeptidase OpsB	AFUA_6G05350	-3.10			
Proteasome subunit alpha type 3	AFUA_6G06350	-5.19			
Proteasome component Prs3	AFUA_6G06440	-4.67			-3.05
Proteasome component Pre4	AFUA_6G06450	-4.08			
Peptidase	AFUA_6G06800	-2.81		**1.71**	
Methionine aminopeptidase, type I	AFUA_6G07330	-3.33		-2.56	-2.38
Calpain-like protein	AFUA_6G07970	**2.06**			
Metallopeptidase Mip1	AFUA_6G08640	-3.05			
Proteasome component Pre9	AFUA_6G08960	-4.02			-2.84
Metallopeptidase family M24	AFUA_6G09190	-1.82			
Dipeptidase	AFUA_6G11500	**2.77**		**1.62**	
SprT family metallopeptidase	AFUA_6G12420			-1.24	
Carboxypeptidase CpyA/Prc1	AFUA_6G13540	-3.69			
Nuclear serine protease HtrA2/Nma111	AFUA_6G13650	-2.67			
ADAM family of metalloprotease ADM-A	AFUA_6G14420			**2.14**	**2.73**
Proteasome component Pre3	AFUA_7G04650	-3.80			
Gamma-glutamyltranspeptidase	AFUA_7G04760	-3.66			-3.30
Alkaline serine protease (PR1)/allergen F18-like	AFUA_7G04930	**2.06**	**3.13**		
Probable o-sialoglycoprotein endopeptidase	AFUA_7G05240			-3.01	
Proteasome component Pre8	AFUA_7G05870	-3.73			
Metallopeptidase MepB	AFUA_7G05930	-3.72		-1.80	-2.63
Subtilisin-like alkaline protease	AFUA_7G08340			**2.00**	
NlpC/P60-like cell-wall peptidase	AFUA_8G00360	**1.91**			
Methionine aminopeptidase, type II	AFUA_8G00410	**1.96**	**3.48**	**3.47**	**3.31**
Methionine aminopeptidase, type I	AFUA_8G00460	-3.54			
Beta-lactamase	AFUA_8G01270	**2.97**			**2.88**
Oligopeptidase family protein	AFUA_8G04730	-2.35			
Signal peptidase complex component	AFUA_8G05340	-2.88			
Patatin family phospholipase	AFUA_4G08440			-1.39	
Phosphatidylinositol phospholipase C	AFUA_4G12000	-3.49		-2.70	-2.96
Lysophospholipase Plb2	AFUA_5G01340	**2.58**			
Lysophospholipase	AFUA_5G02930	-2.33			
Phospholipase/Carboxylesterase superfamily	AFUA_5G09340			-1.39	
Phospholipase	AFUA_6G02780	-3.46		-3.11	
Phosphatidylglycerol specific phospholipase C	AFUA_7G04910			**2.79**	**3.95**

[a]Genes product description of the genes found on the microarray.
[b]GenBank accession number.
[c]Fold change in $\log_2$ obtained for each gene. This value represents the $\log_2$ of each day of infection minus the $\log_2$ at 37ºC. Positive fold changes (in bold) mean an up-regulation throughout the infection and negative fold changes an up-regulation during the germination at 37ºC.

Turning to iron acquisition, the transcription factor *sreA* was up-regulated on day 1 and 2 post-infection whereas transcription factors related to sidorophore production, such as *hapX*, *srbA*, *acuM*, *hacA* and *mpkA*, showed up-regulation during the germination at 37ºC. This up-regulation was also observed in other siderophore production genes (*sidA*, *sidC*, *sidD*) and siderophore-iron related genes. However, several metaloreductases and ferric-chelate reductases were up-regulated during the infection. Something similar was observed in zinc acquisition routes, in which zinc exporters and

importers (*zrgA*, *optA*, *zrcC*, *zrfC*, *zrfH*, *zrfF* or *zrfE*), and even the transcription factor *zafA*, reduced their expression during the infection. Only the transporters PcrA and PcaA showed up-regulation *in vivo* (Table 4.17).

Table 4.17. Differentially expressed genes related to iron and zinc acquisition.

Gene product description[a]	Locus ID[b]	Fold change[c]			
		Day 1	Day 2	Day 3	Day 4
Iron acquisition[d]					
Siderophore biosynthesis					
Long-chain-fatty-acid-CoA ligase, putative (SidI)	AFUA_1G17190	-4.89		-4.02	-4.50
Nonribosomal siderophore peptide synthase SidC	AFUA_1G17200	-3.75	-3.41	-3.07	-3.83
L-ornithine N5-oxygenase SidA	AFUA_2G07680	-6.38		-2.62	-5.26
Nonribosomal peptide synthase SidE	AFUA_3G03350	**3.60**		**3.35**	**3.80**
Siderophore biosynthesis acetylase AceI (SidF)	AFUA_3G03400	-5.78		-4.38	-4.73
Enoyl-CoA hydratase/isomerase family protein SidH	AFUA_3G03410	-4.62		-3.27	-5.68
Nonribosomal peptide synthase SidD	AFUA_3G03420			-2.86	
Mitochondrial ornithine carrier protein AmcA/Ort1, putative	AFUA_8G02760	-3.00		-5.10	
siderophore-iron transporter genes					
Metalloreductase	AFUA_1G00350	2.05			
MAP kinase kinase kinase SskB	AFUA_1G10940	**1.64**			
Metalloreductase	AFUA_1G14340	**2.19**	**2.958**	**2.67**	**2.53**
Ferric-chelate reductase	AFUA_1G16040	**2.82**		**3.00**	**2.86**
FRE family ferric-chelate reductase	AFUA_1G17270	-4.01		-2.53	-2.52
Ferric-chelate reductase	AFUA_2G01270			-2.07	
Siderochrome-iron transporter MirC	AFUA_2G05730			-1.71	-2.66
4'-phosphopantetheinyl transferase NpgA/CfwA	AFUA_2G08590			-1.40	
Siderochrome-iron transporter	AFUA_3G01360	**2.49**		**2.19**	
MFS siderophore iron transporter	AFUA_3G03440	-4.64		-5.08	-5.59
Vacuolar iron transporter Ccc1	AFUA_3G09970	**2.61**		**1.97**	
Siderochrome-iron transporter	AFUA_3G13670		**4.91**	**4.91**	
Metalloreductase transmembrane component	AFUA_6G02170	**1.59**			
Ferric-chelate reductase	AFUA_6G13750			**3.37**	
Metalloreductase	AFUA_7G04970	**1.99**			
Siderochrome-iron transporter Sit1	AFUA_7G06060	-6.26		-2.76	-4.78
Metalloreductase	AFUA_7G07120	**1.94**			
Ferric-chelate reductase Fre2	AFUA_8G01310	**3.58**		**3.92**	
Transcription factors					
HLH transcription factor	AFUA_2G01260	-3.55		-1.50	
Zn cluster transcription factor Rds2	AFUA_2G12330	-2.27		-1.50	
bZIP transcription factor HacA	AFUA_3G04070	-6,15		-4.66	-4.90
MAP kinase MpkA	AFUA_4G13720	-2.97		-2.59	-2.75
bZIP transcription factor HapX	AFUA_5G03920	-2.63	-2.68	-2.86	-3.70
Siderophore transcription factor SreA	AFUA_5G11260	**3.12**	**2.79**		
Reductive iron assimilation					
FRE family ferric-chelate reductase	AFUA_1G17270	-4.01		-2.53	-2.52
Ferrooxidoreductase Fet3	AFUA_5G03790	-3.70	-4.16	-4.39	-4.84
High-affinity iron transporter FtrA	AFUA_5G03800	-4.79		-1.61	
Zinc acquisition[d]					
Zinc exporters					
DUF614 domain protein PcrA	AFUA_1G00170	**2.82**			
MFS transporter ZifD	AFUA_1G03730			-1.28	
Cation efflux family protein family ZrgA	AFUA_1G12090	-2.92		-2.92	-2.74
Oligopeptide transporter, OPT family OptA	AFUA_1G13620	-2.91		-2.55	
Copper-transporting ATPase PcaA	AFUA_1G16130	**2.89**			**3.47**

Table 4.17. *(continued)*

Gene product description[a]	Locus ID[b]	Fold change[c]			
		Day 1	Day 2	Day 3	Day 4
Zinc/cadmium resistance protein ZrcC	AFUA_2G14570	-3.56			
Copper resistance-associated P-type ATPase CccC	AFUA_3G12740			-2.50	-2.72
MFS multidrug transporter ZifE	AFUA_4G08740			-1.63	
ABC metal ion transporter YcfA	AFUA_5G07970	-3.91		-2.25	
Cation efflux family protein MmtA	AFUA_5G09830	-3.25		-1.47	
MFS transporter ZifC	AFUA_6G03860			-1.35	
Zinc importers					
ZIP metal ion transporter ZrfF	AFUA_2G08740	-3.04	-3.09	-3.99	
ZIP metal ion transporter ZrfH	AFUA_2G12050			-1.58	-2.23
ZIP Zinc transporter ZrfC	AFUA_4G09560	-4.00			
ZIP family zinc transporter ZrfE	AFUA_8G04010			-2.34	
Transcription factors					
C_2H_2 transcription factor ZafA	AFUA_1G10080	-2.85		-3.20	
Other related					
Major allergen Asp F 2	AFUA_4G09580	-3.42			

[a]Genes product description of the genes found on the microarray.
[b]GenBank accession number.
[c]Fold change in $\log_2$ obtained for each gene. This value represents the $\log_2$ of each day of infection minus the $\log_2$ at 37ºC. Positive fold changes (in bold) mean an up-regulation throughout the infection and negative fold changes an up-regulation during the germination at 37ºC.
[d]Pathway in which each gene is involved.

When it comes to nitrogen, genes involved in its utilization showed up-regulation during the infection. Amongst them, the periplasmic nitrate reductase (AFUA_3G15190), 3 ammonium and 2 urea transporters, 15 permeases and 9 amino acid transporters might be mentioned (Table 4.18).

Table 4.18. Differentially expressed genes related to nitrogen utilization.

Gene product description[a]	Locus ID[b]	Fold change[c]			
		Day 1	Day 2	Day 3	Day 4
Nitrate, nitriles and ammoniun[d]					
Ammonium transporter Mep2	AFUA_1G10930	**2.75**			
Nitrate reductase NiaD	AFUA_1G12830	-2.12			
Ammonium transporter MeaA	AFUA_2G05880	**1.86**			
Cyanide hydratase/nitrilase	AFUA_2G17500	**3.52**		**2.13**	**3.61**
Nitroreductase family protein	AFUA_3G03530	**2.37**		**2.54**	
Periplasmic nitrate reductase	AFUA_3G15190	**2.89**		**3.26**	**4.35**
Ammonium transporter MepA	AFUA_5G11020	**2.09**			
Nitrilase family protein	AFUA_6G12100	**3.19**		**2.37**	
Nitrilase family protein Nit3	AFUA_6G13230			-2.70	
Amino acids[d]					
Amino acid permease	AFUA_1G09120	**1.93**			
GABA permease	AFUA_1G12310			-1.70	
Neutral amino acid permease	AFUA_2G00180	-4.61			
GABA permease	AFUA_2G01370	**2.04**			
Amino acid permease Dip5	AFUA_2G08800	**2.63**		**2.47**	
GABA permease	AFUA_3G11490	**4.64**	**3.83**	**4.12**	
GABA permease Uga4	AFUA_4G03370	-2.08			
Amino acid permease	AFUA_5G00370	**3.74**			
GABA permease	AFUA_5G00710	**2.79**	**4.41**	**4.32**	
Amino acid permease	AFUA_5G00930	**2.57**			
Amino acid permease	AFUA_5G01510	**2.08**			

Table 4.18. *(continued)*

Gene product description[a]	Locus ID[b]	Fold change[c]			
		Day 1	Day 2	Day 3	Day 4
Amino acid permease	AFUA_5G09440			**1.74**	
Amino acid permease	AFUA_6G11100			-2.20	
GABA permease	AFUA_7G00440	**2.58**			**2.86**
Amino acid permease	AFUA_8G00840	-2.78	-3.19	-2.39	-2.48
GABA permease	AFUA_8G01450	**1.51**			
GABA permease	AFUA_8G02180	**2.24**			
Aromatic amino acid and leucine permease	AFUA_8G05860	**2.10**			
Amino acid permease	AFUA_8G06090	**2.79**			
Amino acid permease	AFUA_8G06580	**1.83**			
MFS peptide transporter, putaitve	AFUA_1G12240	**4.12**		**3.59**	
Amino acid transporter	AFUA_2G00310		-2.85		
Amino acid transporter	AFUA_2G17480			**2.71**	
Amino acid transporter Mtr	AFUA_3G00120	**2.64**			
Small oligopeptide transporter, OPT family	AFUA_3G12200	**2.25**			
Amine transporter	AFUA_3G15300			**1.80**	**2.97**
MFS peptide transporter	AFUA_4G00830	**1.69**			**3.35**
Amino acid transporter	AFUA_4G01570	**2.95**			
Amino acid transporter	AFUA_5G09300			-1.40	
Small oligopeptide transporter, OPT family	AFUA_5G13850	**1.92**			
OPT peptide transporter Mtd1	AFUA_7G00910	**2.86**			**3.06**
Amino acid transporter	AFUA_8G00720	-4.33	-3.08	-2.77	-3.52
Amino acid transporter	AFUA_8G00800	**4.10**		**1.64**	**3.40**
Amino acid transporter	AFUA_8G07200	-2.40		-2.69	
Amine oxidase	AFUA_1G13440	**1.66**		**1.56**	
Amine oxidase, flavin-containing superfamily	AFUA_5G01210	**2.05**			
Amine oxidase	AFUA_7G04180	**1.90**		**1.56**	
General amidase	AFUA_4G00370	**2.70**			
General amidase GmdB	AFUA_5G00470	**2.87**		**3.43**	**4.27**
General amidase	AFUA_5G01240	**4.14**		**1.63**	
Branched-chain amino acid aminotransferase	AFUA_1G01680	-2.63			
Aspartate aminotransferase	AFUA_1G04160			-2.23	
Aminotransferase, class V	AFUA_1G09470	-3.12		-2.42	
Aminotransferase	AFUA_1G14490			-2.24	
Aminotransferase, class III	AFUA_1G16810	-2.12			
Branched-chain amino acid aminotransferase, cytosolic	AFUA_2G10420	-4.65		-2.26	-3.66
Aminotransferase family protein LolT	AFUA_2G13295	-2.91			
Aminotransferase	AFUA_3G14690	**2.00**			
Branched-chain amino acid aminotransferase, cytosolic	AFUA_4G06160	-3.60		-2.72	-3.15
Aspartate aminotransferase	AFUA_4G10410	-4.43			
Aminotransferase, classes I and II	AFUA_4G11460	-3.42		-3.76	-3.80
Aminotransferase, classes I and II family	AFUA_5G00400	**2.36**			
Aminotransferase	AFUA_6G00370	**2.42**			
Aminotransferase	AFUA_6G03640	-3.65	-3.40	-3.34	-4.92
Aminotransferase	AFUA_7G00690	**3.46**		**2.28**	**3.74**
Aminotransferase, classes I and II family	AFUA_8G01580	**3.42**		**2.90**	**3.87**
Glutamyl-tRNA(Gln) amidotransferase subunit A	AFUA_4G04160	**2.47**		**2.61**	**2.53**
Homocitrate synthase HcsA	AFUA_4G10460	-2.76		-3.02	-3.73
Urea, uracile and uridine[d]					
Urea transporter Dur3	AFUA_1G04870	**1.54**			
Urea active transporter	AFUA_1G17570			**2.42**	
Urease accessory protein UreG	AFUA_2G12900	-3.02			
Urease accessory protein UreD	AFUA_2G16070			-2.03	-2.45
Uracil DNA N-glycosylase Ung1	AFUA_2G06140	-3.43			-2.37
Uridine kinase	AFUA_2G05430	-2.25		-2.85	

Table 4.18. *(continued)*

Gene product description[a]	Locus ID[b]	Fold change[c]			
		Day 1	Day 2	Day 3	Day 4
Pseudouridine synthase TruD/Pus7	AFUA_1G16730	-2.10		-2.40	-4.01
Pseudouridine synthase	AFUA_5G12310	-2.74		-3.21	
Pseudouridylate synthase family protein	AFUA_5G05710	-4.27		-3.45	-4.14
Pseudouridylate synthase 3	AFUA_3G13350			-1.19	
Orotidine 5'-phosphate decarboxylase PyrG	AFUA_2G08360	-3.46		-2.04	-4.59
Regulators of nitrogen metabolism[d]					
Nitrogen metabolite repression regulator NmrA	AFUA_5G02920			**2.13**	
Nitrogen permease regulator Npr2	AFUA_1G04580			-2.18	
Others related[d]					
Rheb small monomeric GTPase RhbA	AFUA_5G05480	-4.62		-2.53	-4.29

[a]Genes product description of the genes found on the microarray.
[b]GenBank accession number.
[c]Fold change in $\log_2$ obtained for each gene. This value represents the $\log_2$ of each day of infection minus the $\log_2$ at 37ºC. Positive fold changes (in bold) mean an up-regulation throughout the infection and negative fold changes an up-regulation during the germination at 37ºC.
[d]Gene product description involved in the utilization of each nitrogen sources, regulators and other genes related to nitrogen metabolism.

Finally, 17 genes that encoded allergens also showed significant differences. Amongst them, only two genes showed up-regulation along the infectious process, the cell wall protein PhiA and the elastinolytic metalloproteinase Mep (Table 4.19). Genes involved in melanin biosynthesis also showed significant differences. Whereas the conidial pigment polyketide synthase *pksP/alb1* appeared down-regulated throughout the infection, 3 genes showed up-regulation, standing out *abr1/brown1* whose up-regulation remained along 3 days post-infection (Table 4.20).

Table 4.19. Differentially expressed genes that encode for allergens.

Gene product description[a]	Locus ID[b]	Fold change[c]			
		Day 1	Day 2	Day 3	Day 4
Mn superoxide dismutase MnSOD (Asp F 6)	AFUA_1G14550	-5.72			-3.62
Extracellular cell wall glucanase Crf1/allergen Asp F 9	AFUA_1G16190	-5.65			
Allergen Asp F 4	AFUA_2G03830	-3.38			
60S acidic ribosomal protein P2/allergen Asp F 8	AFUA_2G10100	-5.80			
60S ribosomal protein L3 (Asp F 23)	AFUA_2G11850	-4.92			
Cell wall protein PhiA (Asp F 34)	AFUA_3G03060			**2.62**	
Peptidyl-prolyl cis-trans isomerase/cyclophilin (Asp F 27)	AFUA_3G07430	-4.90			
Allergen Asp F 7	AFUA_4G06670	-4.53			
Major allergen Asp F 2	AFUA_4G09580	-3.42		-2.30	
Molecular chaperone and allergen Mod-E/Hsp90/Hsp1 (Asp F 12)	AFUA_5G04170	-3.29			
Autophagic serine protease Alp2 (Asp F 18)	AFUA_5G09210	-3.18		-1.82	
Thioredoxin TrxA (Asp F 29)	AFUA_5G11320	-5.88			
Aspartic endopeptidase Pep1/aspergillopepsin F (Asp F 10)	AFUA_5G13300		-3.05	-2.28	
Allergen Asp F 3	AFUA_6G02280	-2.28			
Enolase/allergen Asp F 22	AFUA_6G06770	-3.00		-2.07	
Thioredoxin (Asp F 28)	AFUA_6G10300				-2.89
Elastinolytic metalloproteinase Mep (Asp F 5)	AFUA_8G07080			**1.40**	

[a]Genes product description of the genes found on the microarray.
[b]GenBank accession number.
[c]Fold change in $\log_2$ obtained for each gene. This value represents the $\log_2$ of each day of infection minus the $\log_2$ at 37ºC. Positive fold changes (in bold) mean an up-regulation throughout the infection and negative fold changes an up-regulation during the germination at 37ºC.

Table 4.20. Differentially expressed genes related to melanin biosynthesis.

Gene product description[a]	Locus ID[b]	Fold change[c]			
		Day 1	Day 2	Day 3	Day 4
Conidial pigment polyketide synthase PksP/Alb1	AFUA_2G17600	-1.65		-3.00	
Conidial pigment biosynthesis 1,3,6,8-tetrahydroxynaphthalene reductase Arp2	AFUA_2G17560	**2.79**			
Conidial pigment biosynthesis oxidase Abr1/brown 1	AFUA_2G17540	**4.51**	**3.83**	**3.88**	
Conidial pigment biosynthesis oxidase Arb2	AFUA_2G17530	**3.72**			**2.90**

[a]Genes product description of the genes found on the microarray.
[b]GenBank accession number.
[c]Fold change in $\log_2$ obtained for each gene. This value represents the $\log_2$ of each day of infection minus the $\log_2$ at 37ºC. Positive fold changes (in bold) mean an up-regulation throughout the infection and negative fold changes an up-regulation during the germination at 37ºC.

4.9. Generation of mutant strains

4.9.1. Generation of *A. fumigatus* Δ*abr1/brown1* knockout strain

The *abr1/brown1* gene was chosen as a deletion target as it showed up-regulation along 3 days post-infection (Table 4.20 and Fig. 4.24) and because it also appeared within the cluster highly expressed during the infectious process (Annex II). Moreover, this gene is involved in melanin biosynthesis and, according to FunCat, in the utilization of vitamins, cofactors and prostetic groups; metabolism of porphyrins; heavy metal ion transport; siderophore-iron transport, inorganic chemical agent resistance; cellular import; and homeostasis of metal ions.

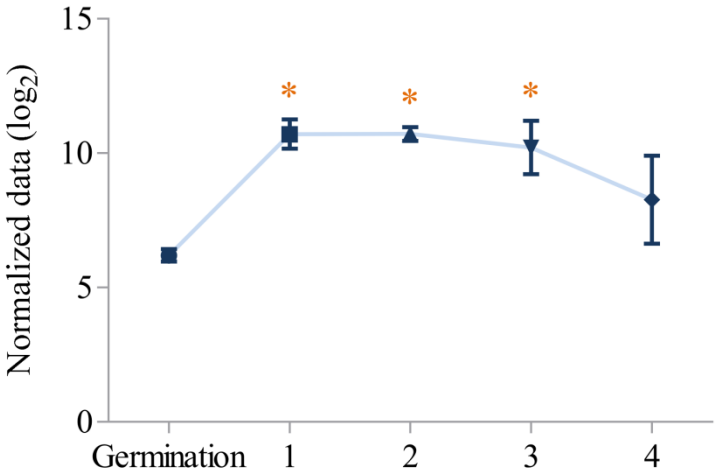

Fig. 4.24. Expression pattern of the gene *abr1/brown1*. The Y-axis values represent the gene expression ($\log_2$) obtained in each condition: Germination at 37ºC (Germination) and day 1 (1), day 2 (2), day 3 (3) and day 4 (4) post-infection. Each point corresponds to the mean value ± standard deviation of three independent samples of each time. The asterisk indicates those samples that show statistical differences ($p<0.05$) relative to the germination at 37ºC.

The amplification of the hygromycin gene and the 5' and 3' flanking regions of the gene *abr1/brown1* showed a band of the expected size in all cases. Once each fragment was purified, they were fused by a fusion PCR and then, the deletion cassette was inserted

into the pCR 2.1™ vector. Its incorporation was confirmed by PCR and the correct assembly of PCR products was confirmed by sequencing (Fig 4.25).

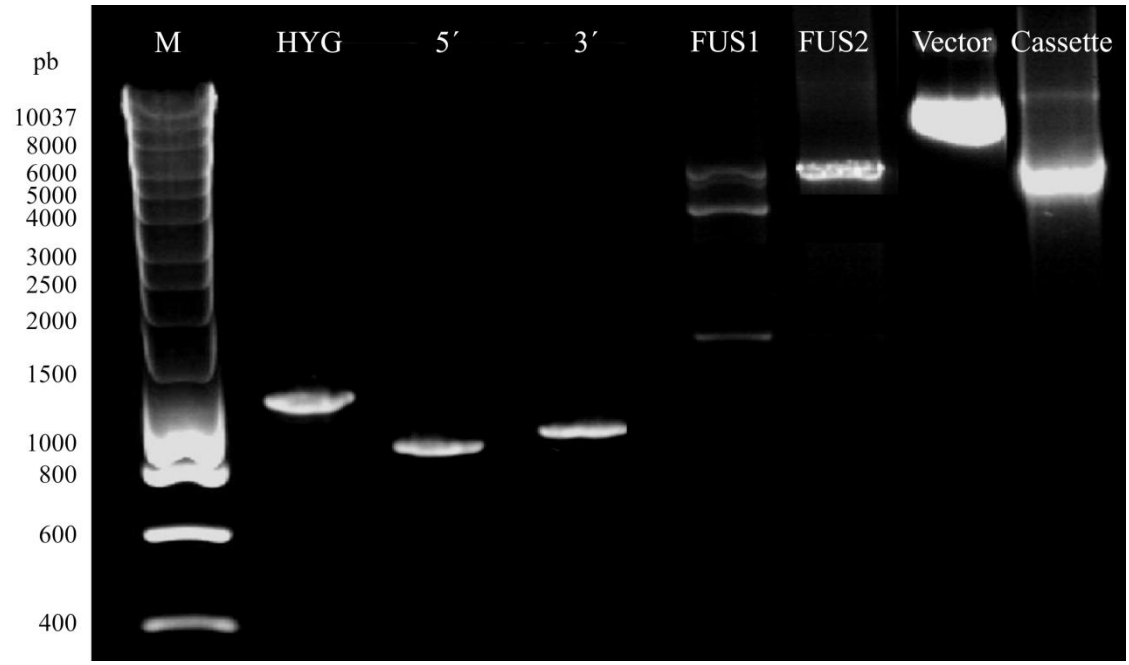

Fig. 4.25. Agarose gel electrophoresis of the PCR products obtained for the generation of *A. fumigatus* Δ*abr1/brown1*. HYG: Hygromicin gene. 5´: 5´ flancking region of the gene *abr1/brown1*. 3´: 3´ flancking region of the gene *abr1/brown1*. FUS1: PCR product obtained after the first round of the fusion PCR. FUS2: PCR product after the second round of the fusion PCR. Vector: Vector with the deletion fragment inserted. Cassette: Deletion cassette amplified using the pCR™ 2.1 vector as DNA template. M: Molecular weight marker. Hyperladder 1kb, 200-10,037 bp.

To generate *A. fumigatus* Δ*akuB*^{ku80} protoplasts, germinated conidia with germ tube 2-5 times the diameter of the spores were needed. This length was achieved after the incubation in AMML at 28ºC for 12 hours. With fewer hours germ tubes were too short and in longer times too long (Fig. 4.26). To obtain the largest number of protoplast the enzymatic digestion was carried out for 5 hours. In figure 4.26D the aspect of germinated conidia after the enzymatic digestion is shown. The transformation was carried out according to the section 3.15.

After the transformation, 5 colonies grew on SMM plates with hygromycin. Amongst them, only in 3 colonies (colonies 3, 4 and 5 of figure 4.27) the gene *abr1/brown1* was not amplified. Moreover, in these 3 colonies a band was obtained with hygromycin primers. This resistance gene was not amplified when the DNA from the other colonies and from *A. fumigatus* Δ*akuB*^{ku80} were used. PCR products obtained with hygromycin primers were sequenced, confirming that their sequences were the same as the resistance gene. Finally, colony 5 was chosen for the Southern Blot, which confirmed

that there was a single copy of the deletion cassette in the genome of this isolate (Fig. 4.28.). This isolate was used in the following experiments.

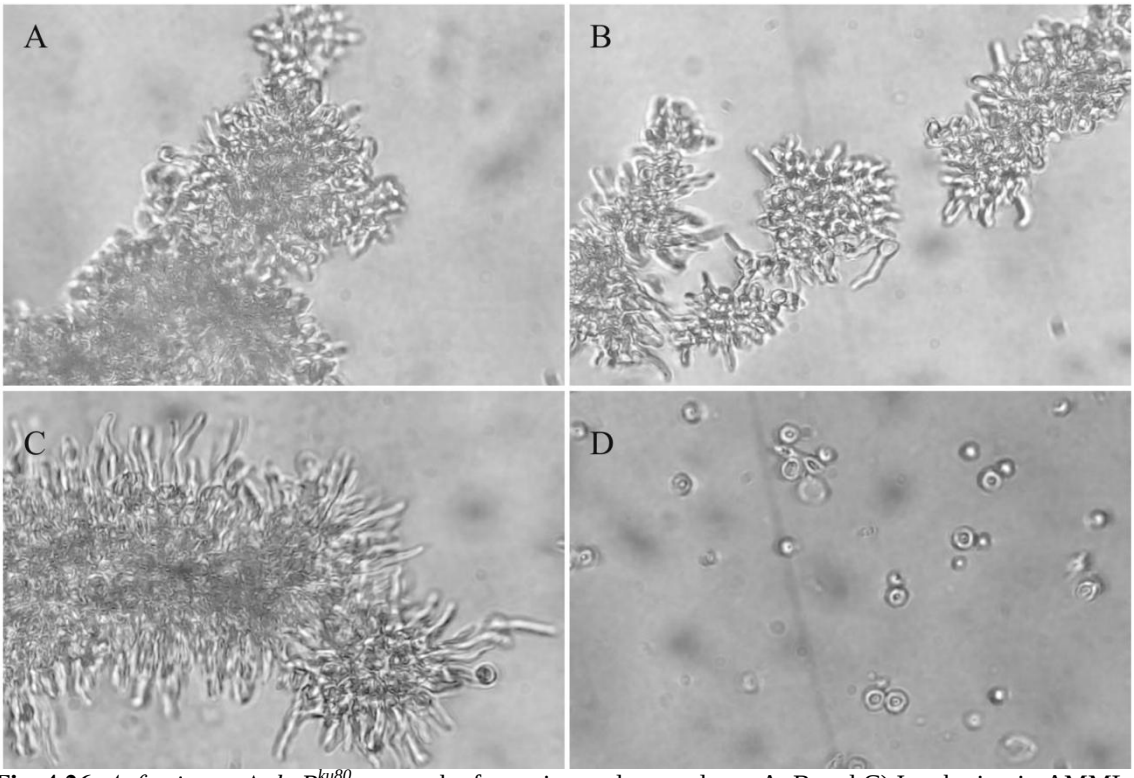

Fig. 4.26. *A. fumigatus* Δ*akuB*^{ku80} germ tube formation and protoplasts. A, B and C) Incubation in AMML for 11, 12 and 13 hours, respectively. The incubation was performed at 28ºC and with shaking at 250 rpm. D) *A. fumigatus* Δ*akuB*^{ku80} protoplasts. Germinated conidia with germ tubes 2-5 times the diameter of spores were subjected to enzymatic digestion at 28ºC for 5 hours with shaking at 100 rpm.

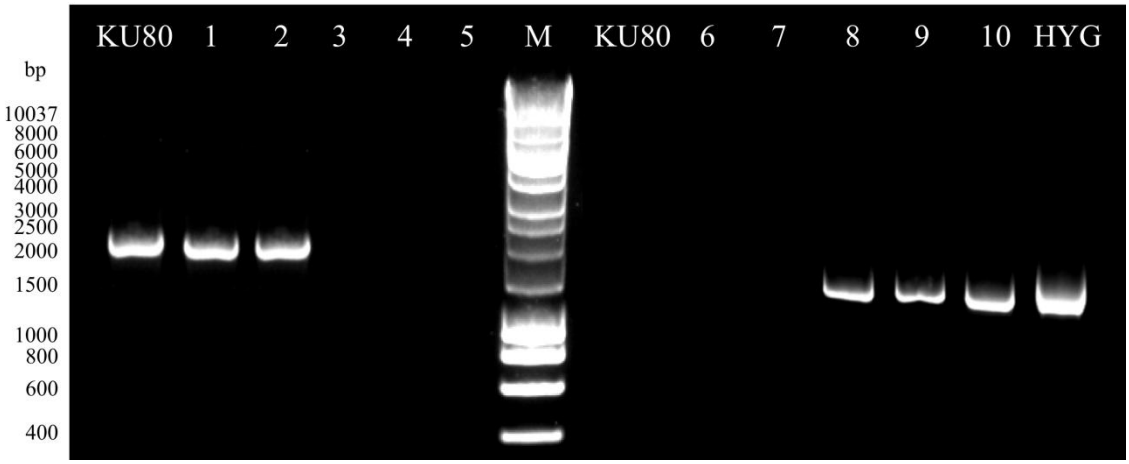

Fig. 4.27. Agarose gel electrophoresis of the PCR products obtained with the colonies grown after *A. fumigatus* Δ*akuB*^{ku80} transformation. 1-5) Amplicons obtained with the primers for the gene *abr1/brown1*. 6-10) Amplicons obtained with the primers for the hygromycin resistance gene. Lines 1 and 6: Colony 1. Lines 2 and 7: Colony 2. Lines 3 and 8: Colony 3. Lines 4 and 9: Colony 4. Lines 5 and 10: Colony 5. KU80: Amplification using *A. fumigatus* Δ*akuB*^{ku80} DNA as template. HYG: Product amplified using the plasmid pA-Hyg-OSCAR as template. M: Molecular weight marker. Hyperladder 1kb, 200-10,037 bp.

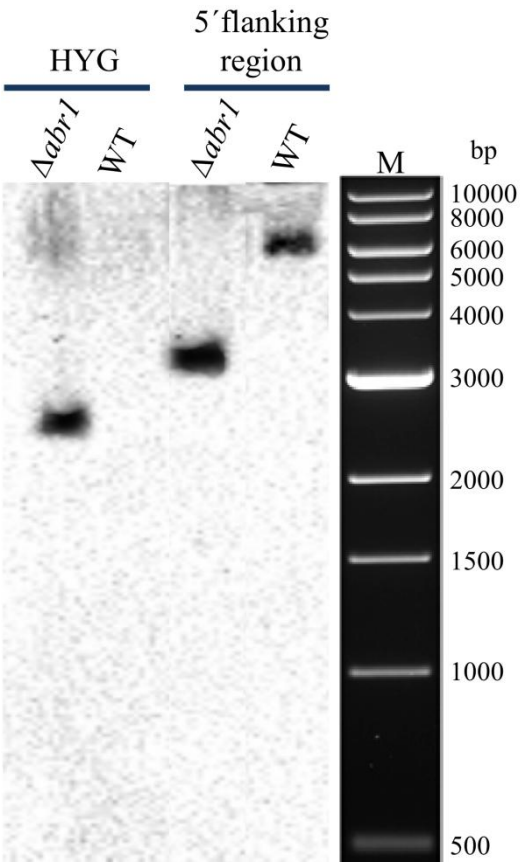

Fig. 4.28. Southern Blot analysis of *A. fumigatus* Δ*abr1/brown1*. Chromosomal DNA of *A. fumigatus* Δ*abr1/brown1* (Δ*abr1*) and *A. fumigatus* Δ*akuB*^{ku80} (WT) was cut by the restriction enzymes StuI and ScaI. ScaI cut within the hygromycin gene and within the 5´flanking region of the deletion cassette, whereas StuI cut withing the 3' flanking region of the cassette. Two probes were designed to confirm the insertion of a single copy. One probe hybridized within the 5' flanking region (5' flanking region) whereas the other one hybridized within the hygromycin gene (HYG). M: Molecular weight marker: 1K DNA ladder, 500-10,000 bp.

4.9.2. Generation of *A. fumigatus* Δ*abr1/brown1::abr1/brown1*$^{+}$ reconstituted strain

The amplification of the fragment was carried out with the primer pair CassAbr1 (Table 3.4), used for the amplification of the deletion cassette constructed to transform *A. fumigatus* Δ*akuB*^{ku80}. This way, the homologous recombination would take place in the same region as it did in the first place. Gel electrophoresis showed a band with the expected size (4,454 bp) (Fig. 4.29) and the sequencing confirmed its correct amplification.

After transformation, 12 colonies seemed to have lost the hygromycin gene whereas a band of the expected size appeared when the primers abr1 (Table 3.4) were used (Fig. 4.30). By PCR and sequencing the insertion of the gene *abr1/brown1* and the absence of the hygromycin gene were confirmed. Finally, colony 4 was chosen for the Southern Blot, which confirmed that there was a single copy of the cassette in the genome of this isolate (Fig. 4.31). This isolate was used in the following experiments.

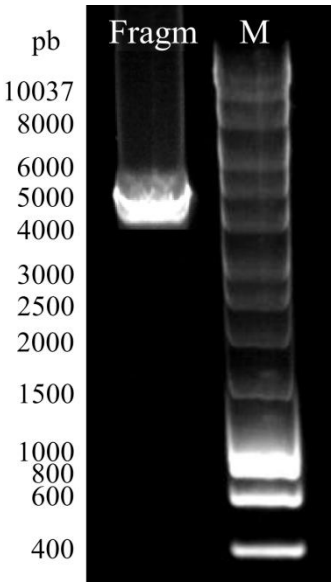

Fig. 4.29. Agarose gel electrophoresis of the fragment obtained for the generation of *A. fumigatus* Δ*abr1/brown1::abr1/brown1*$^{+}$. The amplification was carried out with the same primers used for the amplification of the deletion cassette. Fragm: Fragment amplified using *A. fumigatus* Δ*akuB*^{ku80} DNA as template. M: Molecular weight marker. Hyperladder 1kb, 200-10,037 bp.

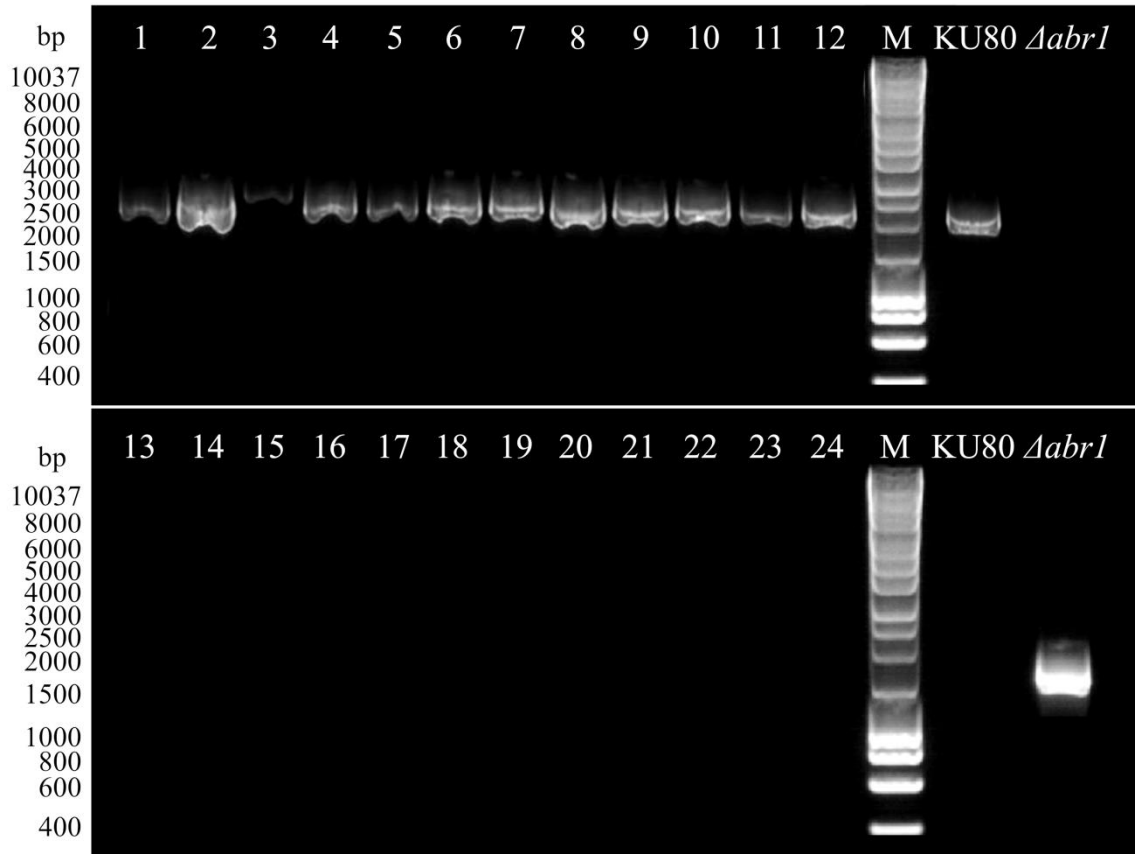

Fig. 4.30. Agarose gel electrophoresis of the PCR products obtained with the colonies grown after *A. fumigatus* Δ*abr1/brown1* transformation. 1-12) Amplicons obtained with the primers for the gene *abr1/brown1*. 13-24) Amplicons obtained with the primers for the hygromycin resistance gene. Lines 1 and 13: Colony 1. Lines 2 and 14: Colony 2. Lines 3 and 15: Colony 3. Lines 4 and 16: Colony 4. Lines 5 and 17: Colony 5. Lines 6 and 18: Colony 6. Lines 7 and 19: Colony 7. Lines 8 and 20: Colonia 8. Lines 9 and 21: Colony 9. Lines 10 and 22: Colony 10. Lines 11 and 23: Colony 11. Lines 12 and 24: Colony 12. KU80: Amplification using *A. fumigatus* Δ*akuB*^{ku80} DNA as template. *Δabr1*: Product amplified using the *A. fumigatus Δabr1/brown1* as template. M: Molecular weight marker. Hyperladder 1kb, 200-10,037 bp.

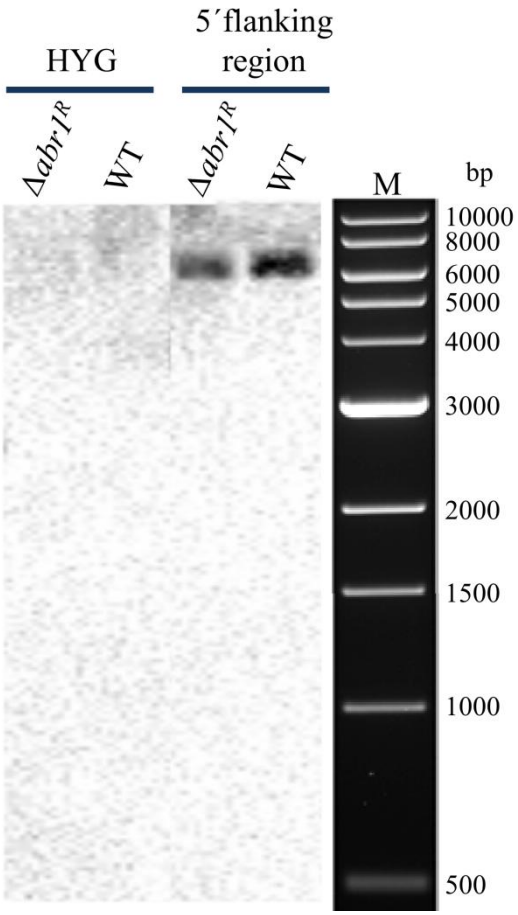

Fig. 4.31. Southern Blot analysis of *A. fumigatus* Δ*abr1/brown1::abr1/brown1*$^{+}$. Chromosomal DNA of *A. fumigatus* Δ*abr1/brown1::abr1/brown1*$^{+}$ (Δ*abr1*^{R}) and *A. fumigatus* Δ*akuB*^{ku80} (WT) was cut by the restriction enzymes StuI and ScaI. ScaI cut within the hygromycin gene and within the 5´flanking region of the deletion cassette, whereas StuI cut withing the 3' flanking region of the cassette. Two probes were designed to confirm the insertion of a single copy. One probe hybridized within the 5' flanking region (5' flanking region) whereas the other one hybridized within the hygromycin gene (HYG). M: Molecular weight marker: 1K DNA ladder, 500-10,000 bp.

4.9.3. Generation of *A. fumigatus* Δ*Trancription factor* AFUA_1G02860 (Δ*tf*) knockout strain

The transcription factor AFUA_1G02860 was chosen as a deletion target as it showed up-regulation on 4 days post-infection (Fig. 4.32) and it was also included within the cluster highly expressed during the infection. Moreover, according to FunCat, this gene seems to be involved in secondary metabolism, highly enriched during the infection process.

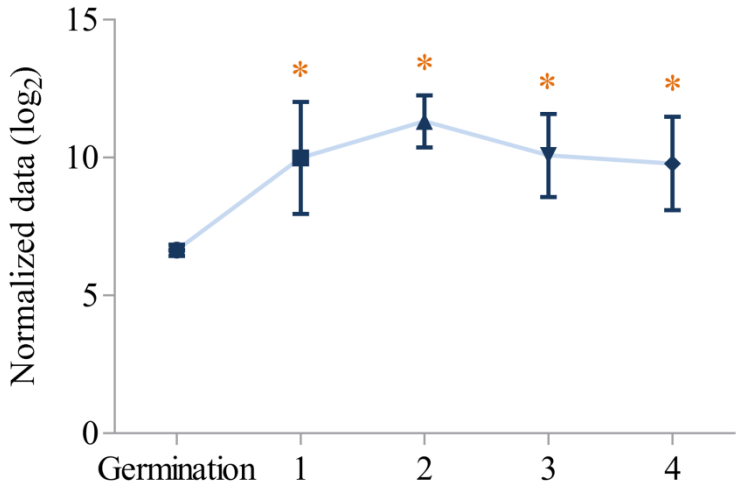

Fig. 4.32. Expression pattern of the transcription factor AFUA_1G02860. The Y-axis values represent the gene expression (log_2) obtained in each condition: Germination at 37ºC (Germination) and day 1 (1), day 2 (2), day 3 (3) and day 4 (4) post-infection. Each point corresponds to the mean value ± standard deviation of three independent samples of each time. The asterisk indicates those samples that show statistical differences ($p < 0.05$) relative to the germination at 37ºC.

The amplification of hygromycin gene and the 5' and 3' flanking regions of the transcription factor showed a band of the expected size in all cases. Once each fragment was purified, they were fused by a fusion PCR and then, the deletion cassette was inserted into pCR 2.1^{TM} vector. Its incorporation was confirmed by PCR (Fig 4.33) and the correct assembly of PCR products was confirmed by sequencing.

As in the previous experiement, protoplasts were generated after 12 hours at 28ºC with shaking at 250 rpm and the transformation was performed according to the section 3.15. After the transformation, 3 colonies grew on SMM plates with hygromycin. As shown in figure 4.34, the transcription factor was not amplified in any of them. Moreover, using hygromycin primers, a band of the expected size was obtained, which was not observed when the DNA from *A. fumigatus* Δ*akuB*^{ku80} was used as template. The PCR products amplified with hygromycin primers in the 3 colonies were sequenced, confirming that the amplicon coincided with the sequence of this resistance gene. Colony 2 was chosen for the Southern Blot, which confirmed that there was a single copy of the cassette in the genome of this isolate (Fig. 4.35). This isolate was used in the following experiments.

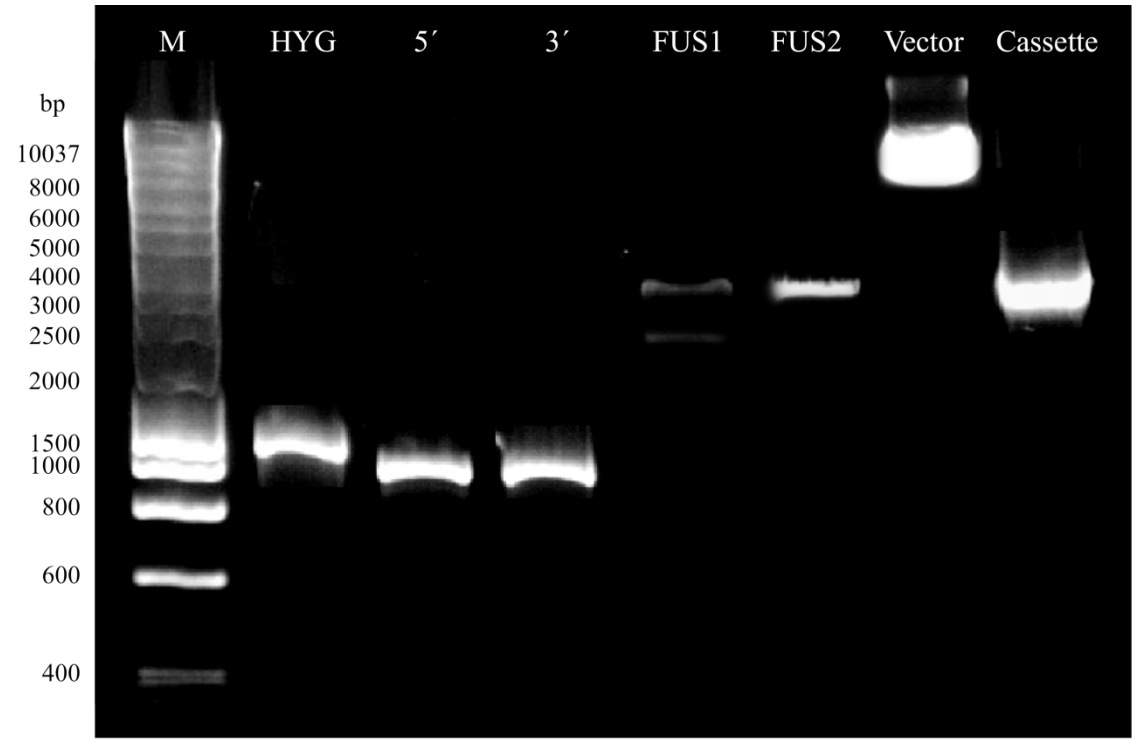

Fig. 4.33. Agarose gel electrophoresis of the PCR products obtained for the generation of *A. fumigatus* Δ*tf*. HYG: Hygromycin gene. 5': 5' flancking region of the transcription factor. 3': 3' flancking region of the transcription factor. FUS1: PCR product obtained after the first round of the fusion PCR. FUS2: PCR product after the second round of the fusion PCR. Vector: Vector with the deletion fragment inserted. Cassette: Deletion fragment amplified using the pCR™ 2.1 vector as DNA template. M: Molecular weight marker. Hyperladder 1kb, 200-10,037 bp.

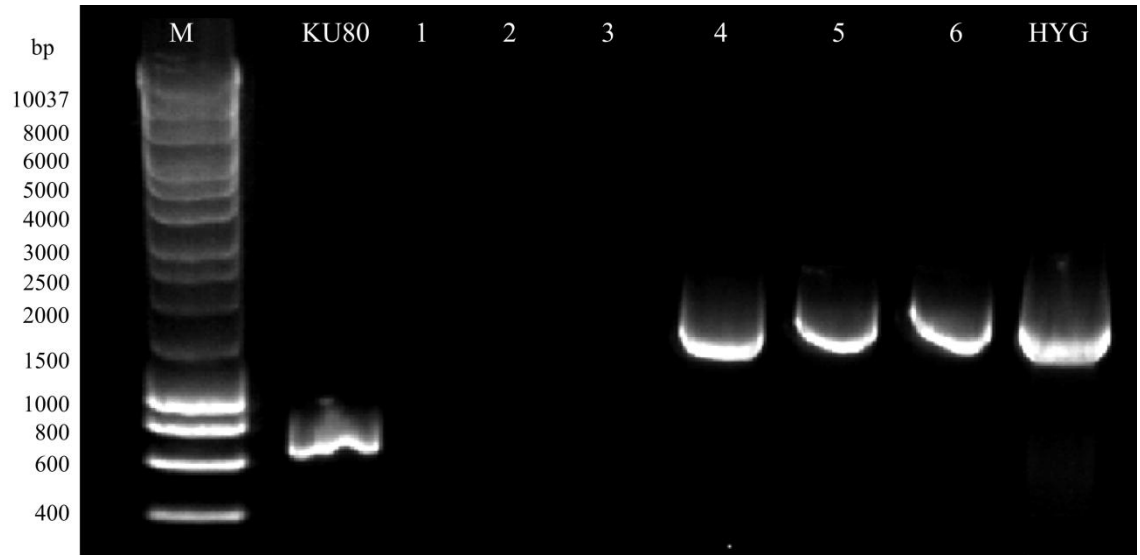

Fig. 4.34. Agarose gel electrophoresis of the PCR products obtained with the colonies grown after *A. fumigatus* Δ*akuB*^{ku80} transformation. 1-3) Amplicons obtained with the primers for the transcription factor AFUA_1G02860. 4-6) Amplicons obtained with the primers for the hygromycin resistance gene. Lines 1 and 4: Colony 1. Lines 2 and 5: Colony 2. Lines 3 and 6: Colony 3. KU80: Amplification of the transcription factor using *A. fumigatus* Δ*akuB*^{ku80} DNA as template. HYG: Product amplified with the primers for hygromycin gene using the plasmid pA-Hyg-OSCAR as template. M: Molecular weight marker. Hyperladder 1kb, 200-10,037 bp.

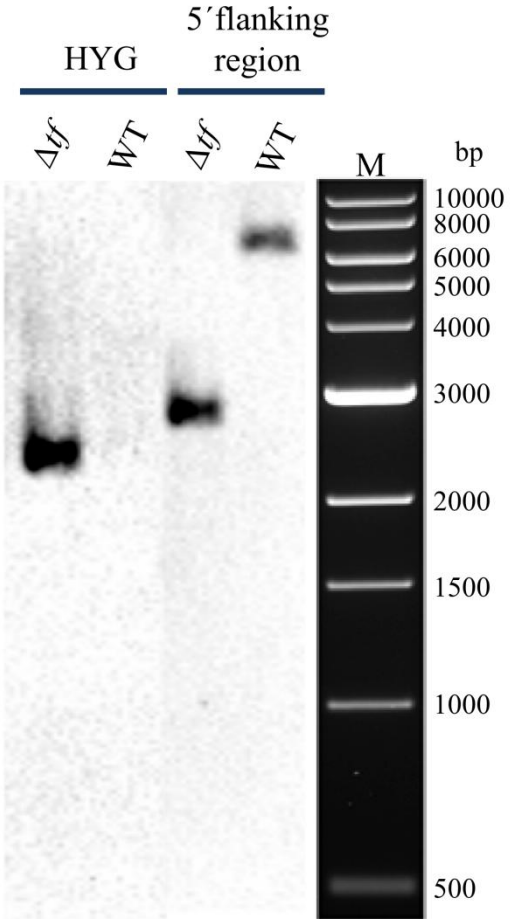

Fig. 4.35. Southern Blot analysis of *A. fumigatus* Δ*tf.* Chromosomal DNA of *A. fumigatus* Δ*tf* (Δ*tf*) and *A. fumigatus* Δ*akuB*^{ku80} (WT) was cut by the restriction enzymes MscI and ScaI. ScaI cut within the hygromycin gene, whereas MscI cut withing the 5' and 3' flanking regions of the deletion cassette. Two probes were designed to confirm the insertion of a single copy. One probe hybridized within the 5' flanking region (5' flanking region) and the other one within the hygromycin gene (HYG). M: Molecular weight marker: 1K DNA ladder, 500-10,000 bp.

4.9.4. Generation of *A. fumigatus* Δ*tf::tf*$^{+}$ reconstituted strain

The amplification of the fragment was carried out with the primer pair named CassTF, (Table 3.4) used for the amplification of the deletion cassette. Gel electrophoresis showed a band with the expected size (4,059 bp) (Fig. 4.36) and the sequencing confirmed its correct amplification.

After transformation, 7 colonies seemed to have lost the hygromycin gene. However, even though in all colonies the transcription factor was amplified, in some isolates a slight band for higromycin resistance gene was also observed (Fig. 4.37). Those isolates with no band for the resistance gene were sequenced to confirm the insertion of the transcription factor and colony 7 was chosen for the following experiments.

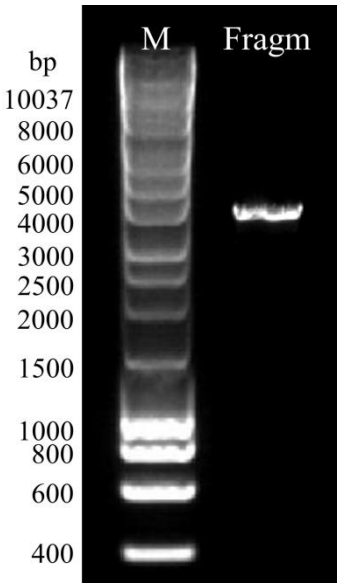

Fig. 4.36. Agarose gel electrophoresis of the PCR products obtained for the generation of *A. fumigatus* Δ*tf::tf*$^{+}$. The amplification was carried out with the same primers used for the amplification of the deletion cassette. Fragm: Fragment amplified using *A. fumigatus* Δ*akuB*^{ku80} DNA as template. M: Molecular weight marker. Hyperladder 1kb, 200-10,037 bp.

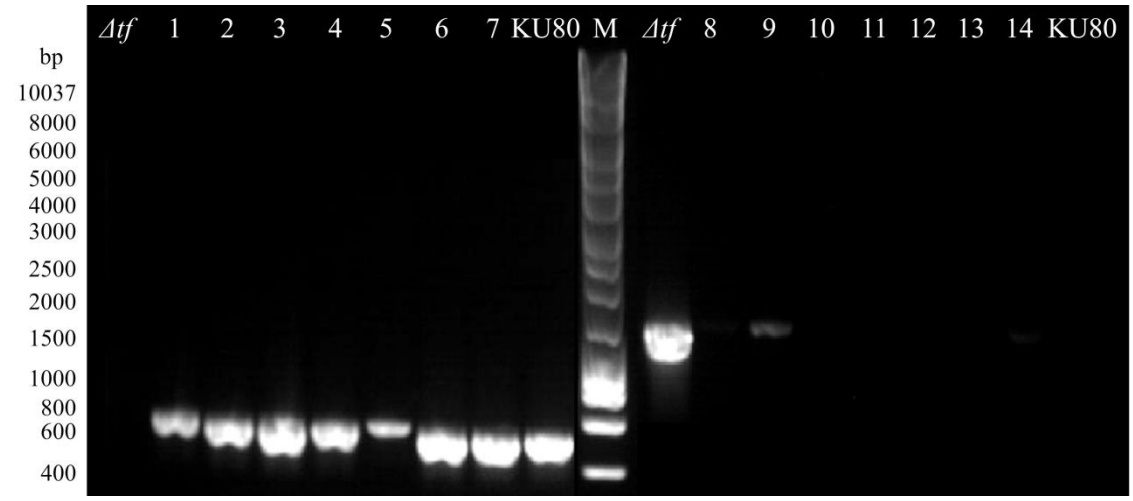

Fig. 4.37. Agarose gel electrophoresis of the PCR products obtained with the colonies grown after *A. fumigatus* Δ*tf* transformation. 1-7) Amplicons obtained with the primers for the transcription factor AFUA_1G02860. 8-14) Amplicons obtained with the primers for the hygromycin resistance gene. Lines 1 and 8: Colony 1. Lines 2 and 9: Colony 2. Lines 3 and 10: Colony 3. Lines 4 and 11: Colony 4. Lines 5 and 12: Colony 5. Lines 6 and 13: Colony 6. Lines 7 and 14: Colony 7. KU80: Amplification using the DNA from *A. fumigatus* Δ*akuB*^{ku80} as template. *Δtf*: Product amplified using the *A. fumigatus Δtf* as template. M: Molecular weight marker. Hyperladder 1kb, 200-10,037 bp.

4.10. Phenotypic studies

4.10.1. Phenotypic studies of *A. fumigatus* Δ*abr1/brown1*, its reconstituted strain and the wild type

The deletion of the gene *abr1/brown1* generated a strain with brown colonies, whose growth on SGA, PDA and AMM showed no statistical differences relative to the wild type (Fig. 4.38). When the osmotic and oxidative stress and even the stress of the cell wall were studied, the growth on every media demonstrated that this gene might not be involved in these kinds of streses. It was not involved in the utilization of carbon sources either (Fig. 4.39-4.42). Neverthelees, when the isolates were grown on porcine kidney agar, a lack of sporulation was observed with the knockout strain (Fig. 4.43).

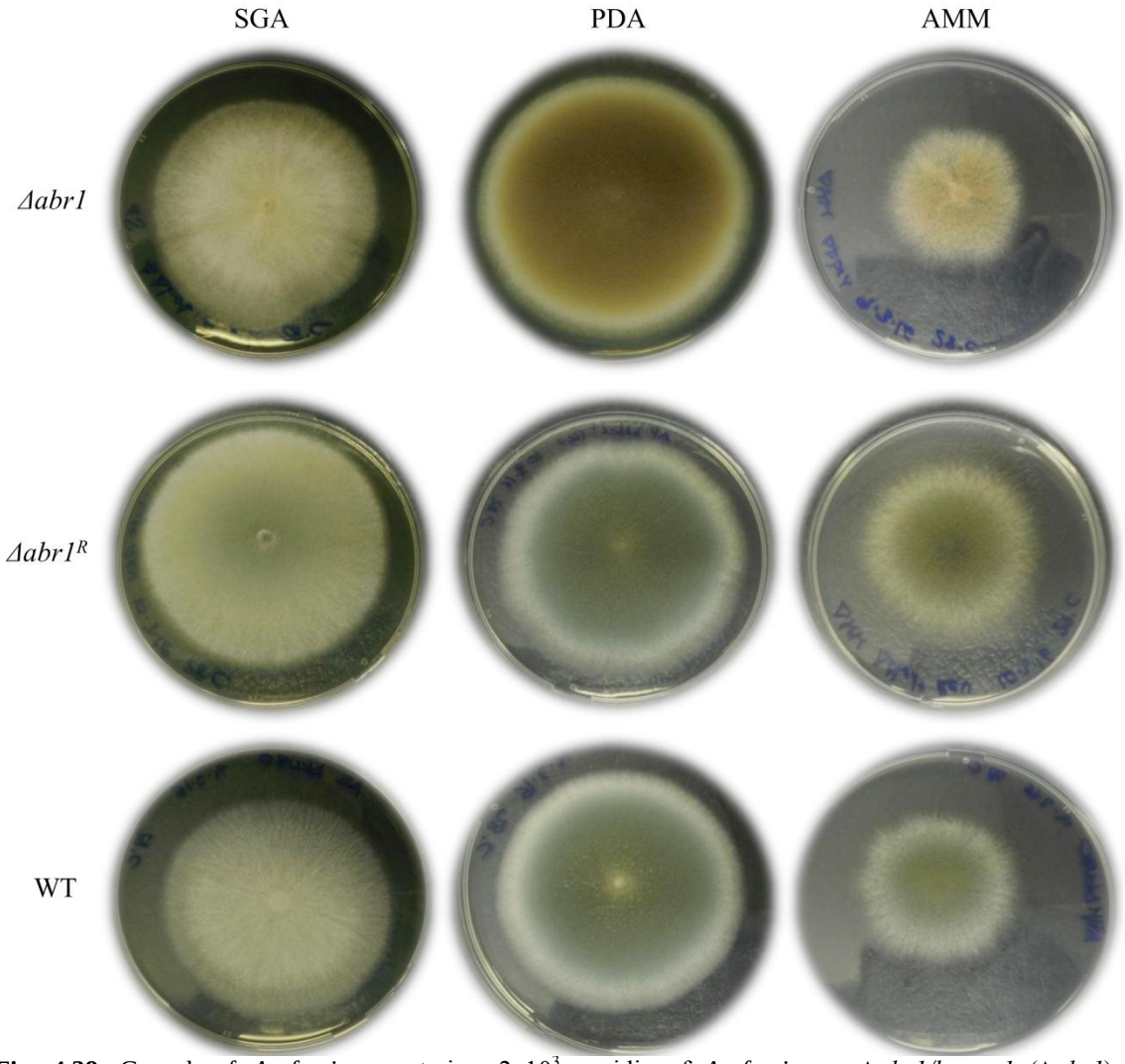

Fig. 4.38. Growth of *A. fumigatus* strains. $2x10^3$ conidia of *A. fumigatus* Δ*abr1/brown1* (Δ*abr1*), Δ*abr1/brown1*:: Δ*abr1/brown1*$^+$ (Δ*abr1*^{R}) and *A. fumigatus* Δ*akuB*^{ku80} (WT) in a total volume of 2 µl were dotted on Sabouraud Glucose Agar (SGA), Potato Dextrose Agar (PDA) and Aspergillus Minimal Medium Agar (AMM) and incubated at 28°C for 7 days.

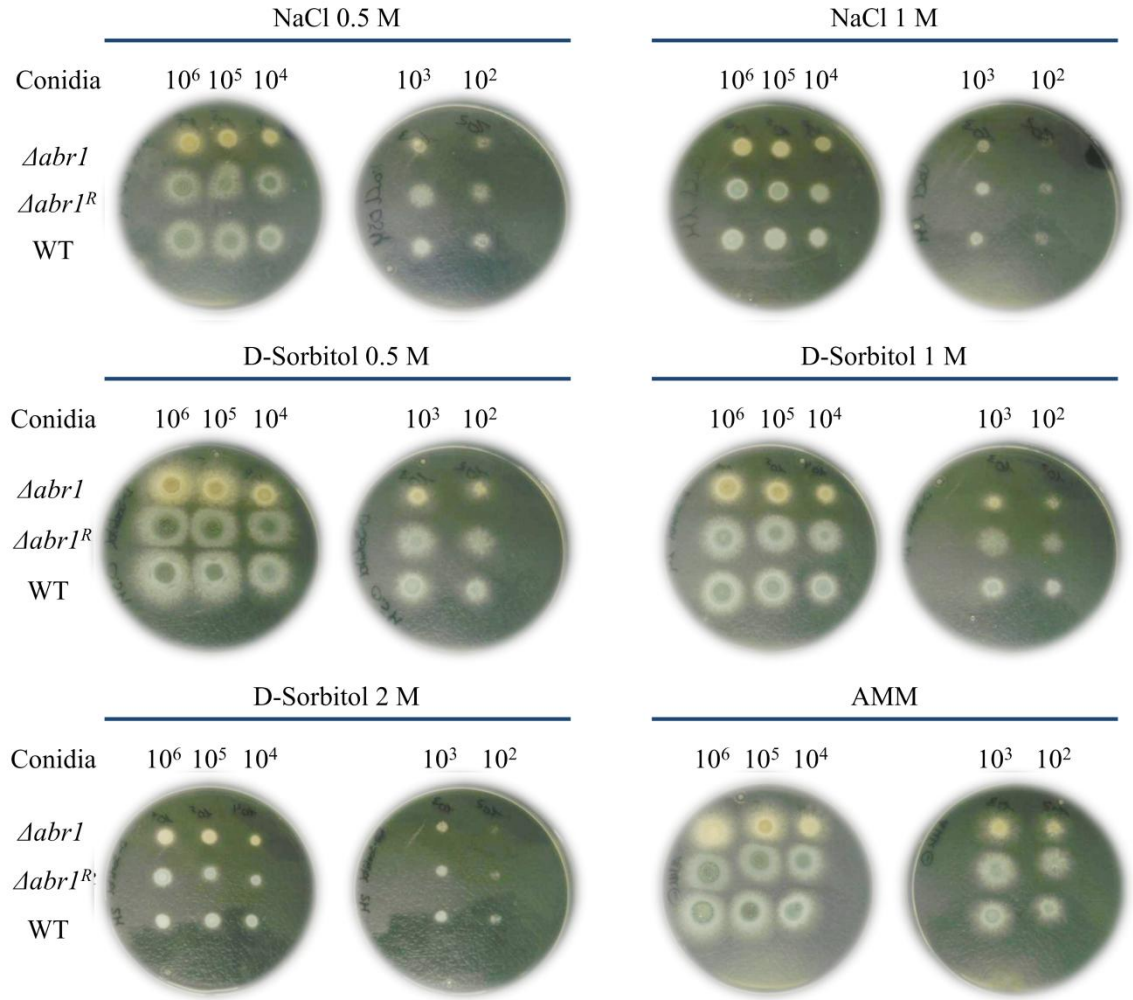

Fig. 4.39. Osmotic stress. Concentrations of conidia from 10^6 to 10^2 of *A. fumigatus* Δ*abr1/brown1* (Δ*abr1*), *A. fumigatus* Δ*abr1/brown1::* Δ*abr1/brown1*$^+$ (Δ*abr1*^{R}) and *A. fumigatus* Δ*akuB*^{ku80} (WT) in a total volume of 5 µl were dotted on AMM with NaCl (0.5 and 1 M) or D-Sorbitol (0.5, 1 and 2 M). The sample AMM corresponds to the growth on AMM without the osmotic stress. The growth was compared after the incubation at 37°C for 2 days.

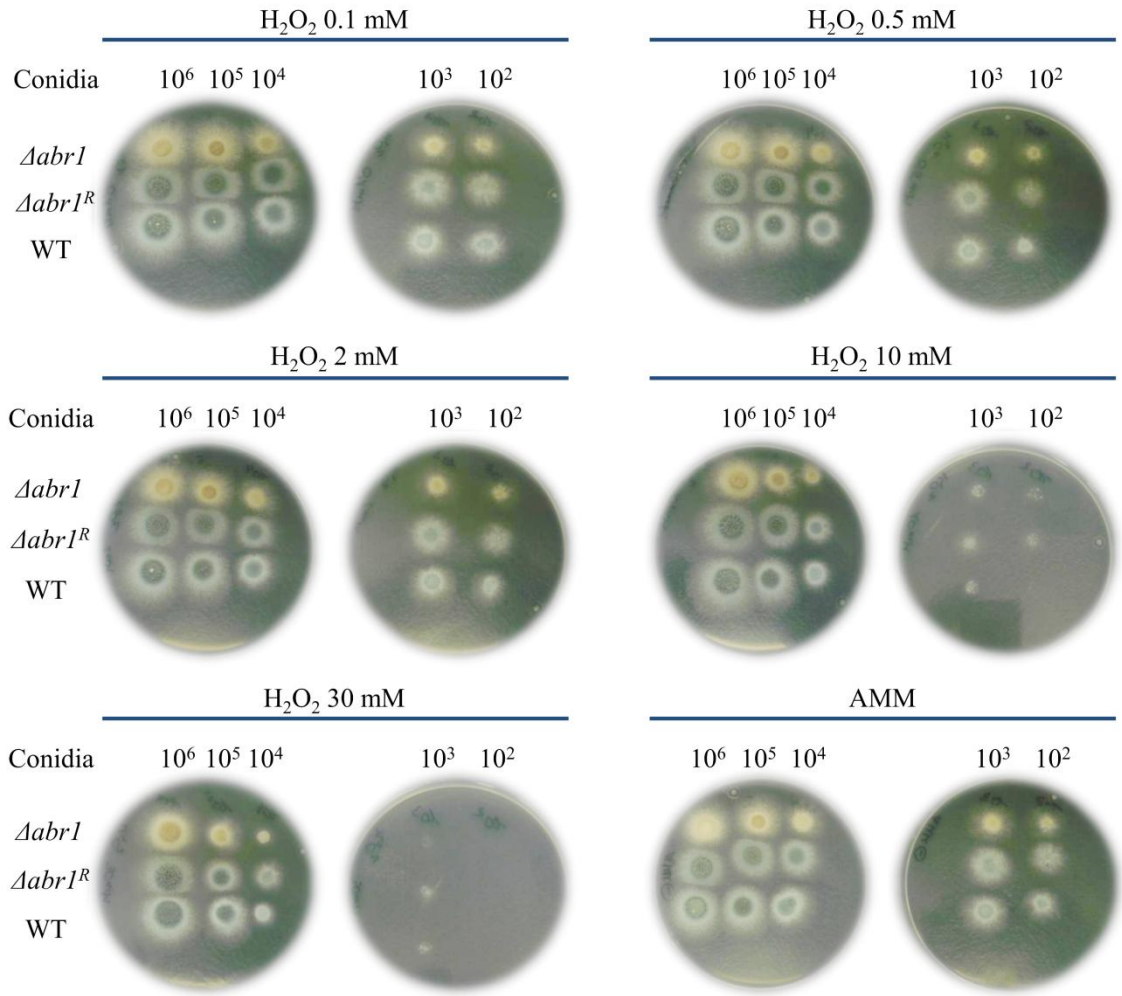

Fig. 4.40. Oxidative stress. Concentrations of conidia from 10^6 to 10^2 of *A. fumigatus* Δ*abr1/brown1* (Δ*abr1*), *A. fumigatus* Δ*abr1/brown1::* Δ*abr1/brown1*$^+$ (Δ*abr1*^{R}) and *A. fumigatus* Δ*akuB*^{ku80} (WT) in a total volume of 5 µl were dotted on AMM with H_2O_2 (0.1, 0.5, 2, 10 and 30 mM). The sample AMM corresponds to the growth on AMM without the oxidative stress. The growth was compared after the incubation at 37°C for 2 days.

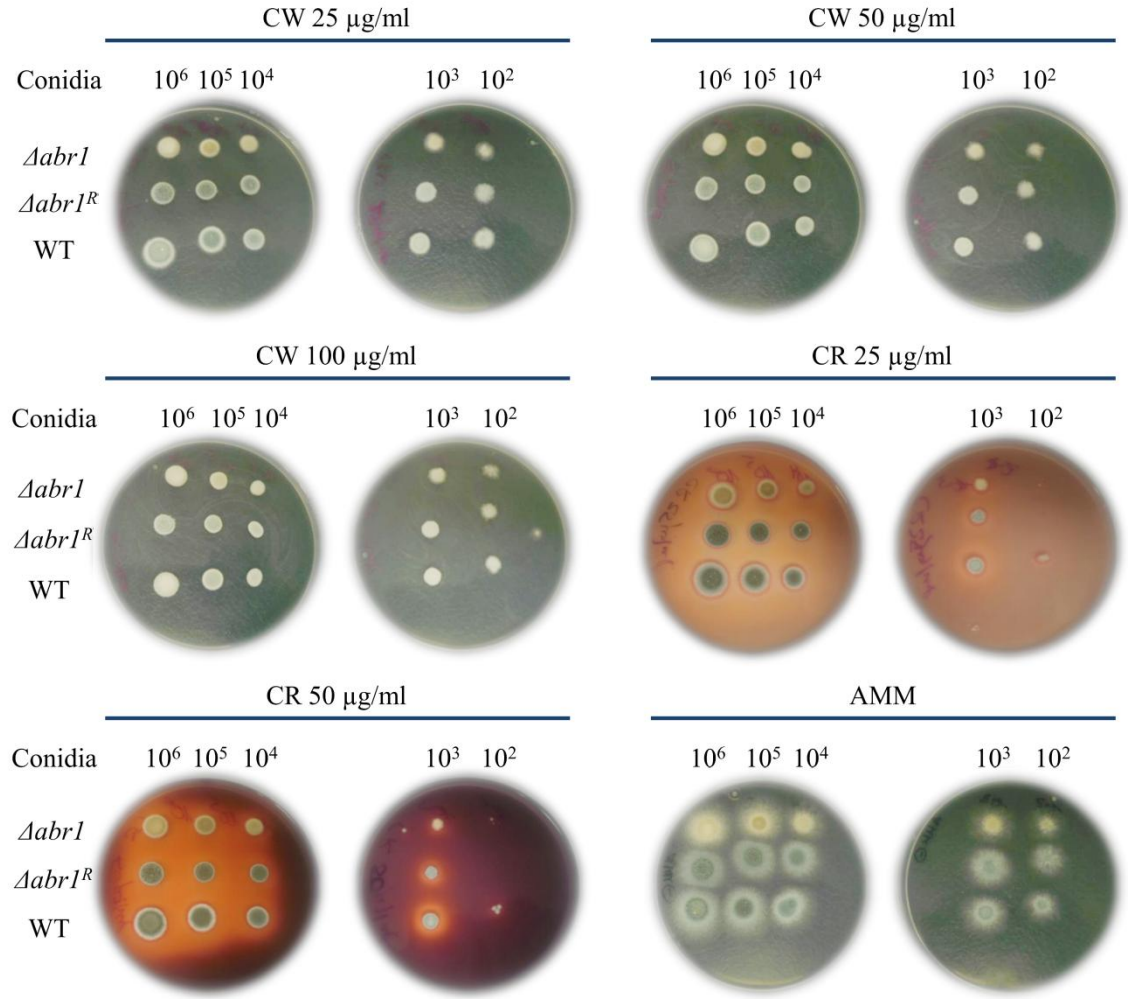

Fig. 4.41. Cell wall stress. Concentrations of conidia from 10^6 to 10^2 of *A. fumigatus* Δ*abr1/brown1* (Δ*abr1*), *A. fumigatus* Δ*abr1/brown1*:: Δ*abr1/brown1*$^+$ (Δ*abr1*^{R}) and *A. fumigatus* Δ*akuB*^{ku80} (WT) in a total volume of 5 µl were dotted on AMM with Calcofluor Wite (CW) (25, 50 and 100 µg/ml) or Congo Red (CR) (25 and 50 µg/ml). The sample AMM corresponds to the growth on AMM without the stress. The growth was compared after the incubation at 37°C for 2 days.

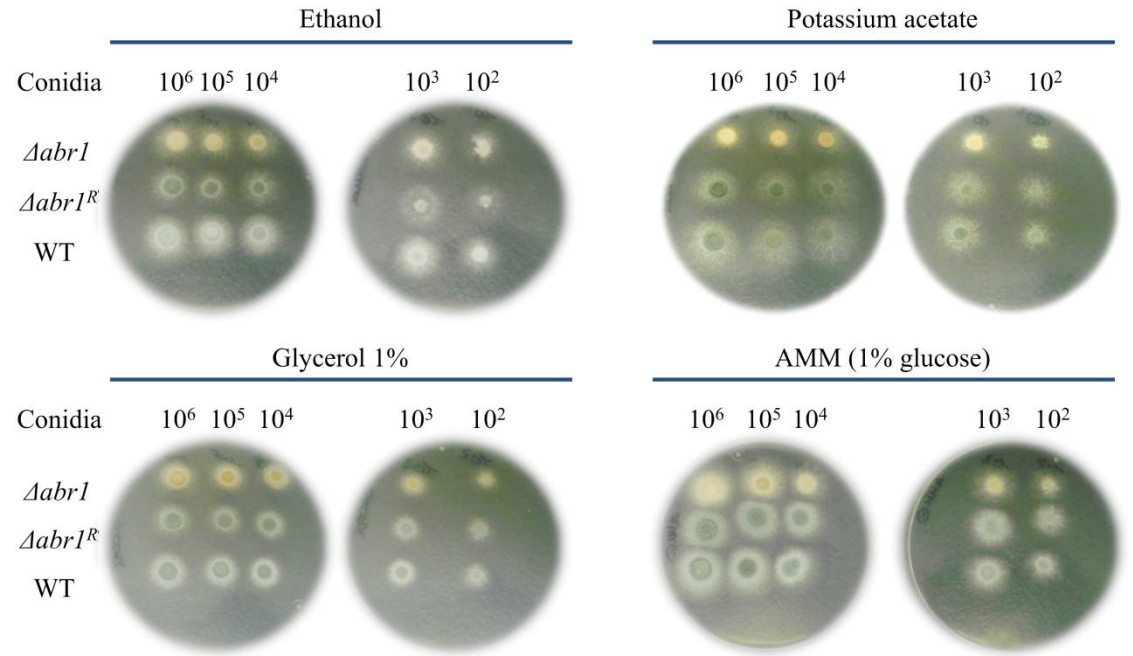

Fig. 4.42. Utilization of different carbon sources. Concentrations of conidia from 10^6 to 10^2 of *A. fumigatus* Δ*abr1/brown1* (Δ*abr1*), *A. fumigatus* Δ*abr1/brown1*:: Δ*abr1/brown1*$^+$ (Δ*abr1*^{R}) and *A. fumigatus* Δ*akuB*^{ku80} (WT) in a total volume of 5 µl were dotted on AMM with different carbon source (Ethanol, potassium acetate or glycerol). The sample AMM corresponds to the growth on AMM, whose carbon source is 1% glucose. The growth was compared after the incubation at 37°C for 2 days.

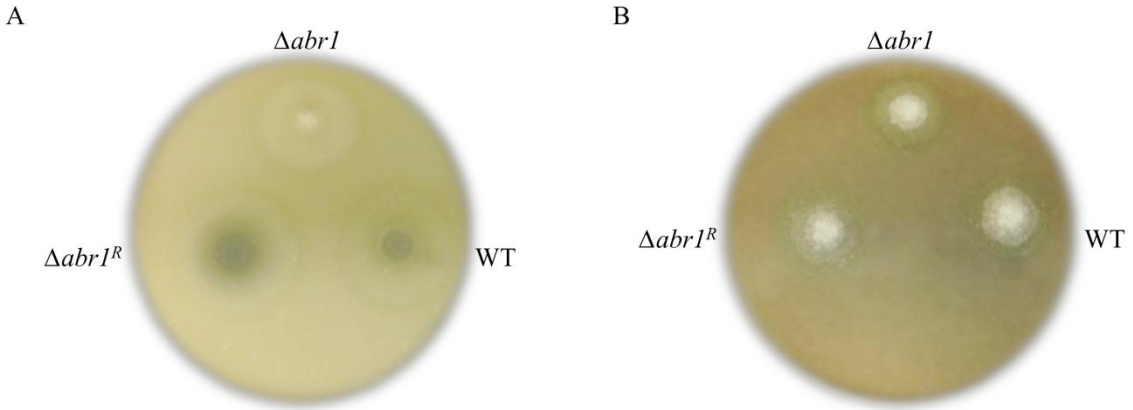

Fig. 4.43. Growth on porcine tissues. 2x10^3 conidia of *A. fumigatus* Δ*abr1/brown1* (Δ*abr1*), Δ*abr1/brown1*:: Δ*abr1/brown1*$^+$ (Δ*abr1*^{R}) and *A. fumigatus* Δ*akuB*^{ku80} (WT) in a total volume of 2 µl were dotted on porcine kidney agar (A) and porcine lung agar (B).

No differences were observed among the germination of the knockout, reconstituted and wild type strains at 37°C (Fig. 4.44). However, the study of conidial production showed that the gene *abr1/brown1* was involved in *A. fumigatus* sporulation. *A. fumigatus* Δ*abr1/brown1* produced fewer conidia relative to the wild type, with a strong decrease since the fifth week. This loss was easily observed as the brown color of its colonies wore off along the study. No sporulation was detected in the ninth week (Fig. 4.45).

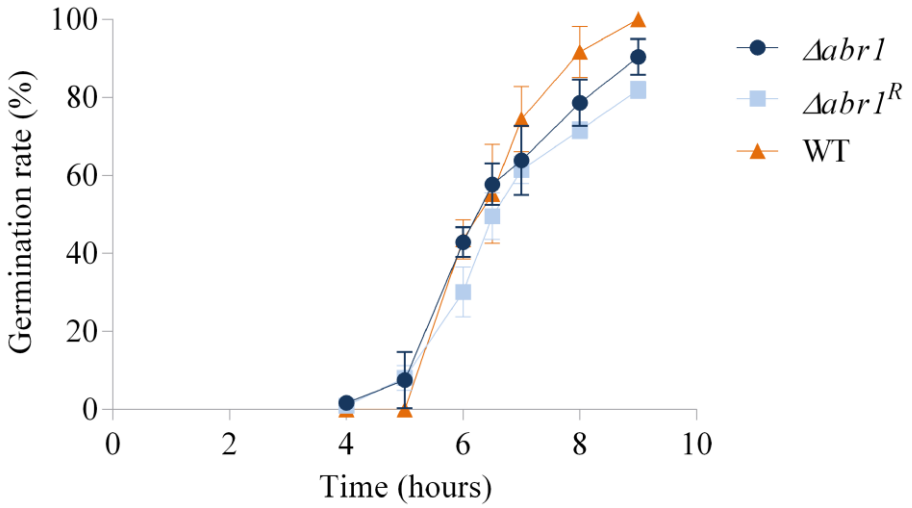

Fig. 4.44. Germination of *A. fumigatus* Δ*abr1/brown1*. Curves of germination rates of *A. fumigatus* Δ*abr1/brown1* (Δ*abr1*), *A. fumigatus* Δ*abr1/brown1*:: Δ*abr1/brown1*$^{+}$ (Δ*abr1*^{R}) and *A. fumigatus* Δ*akuB*^{ku80} (WT). Each point represents the mean value ± standard deviation of three independent samples of each time.

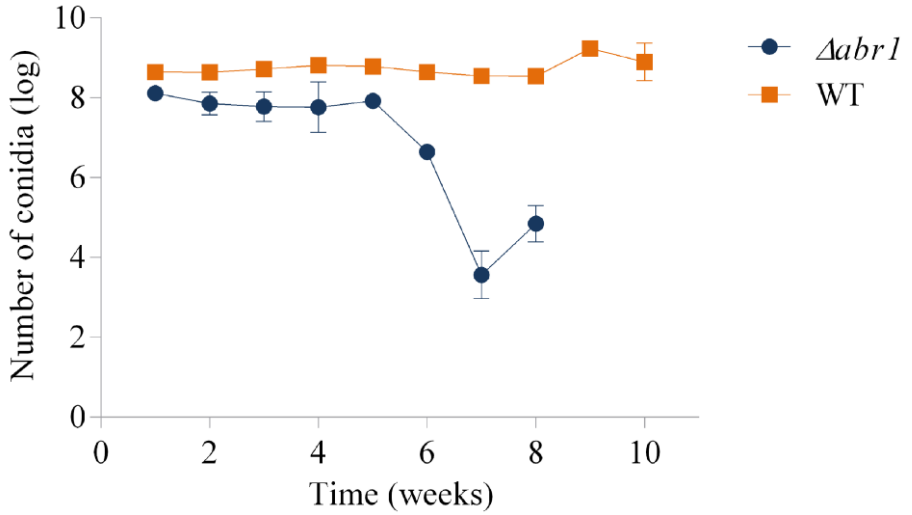

Fig. 4.45. Production of conidia. Concentration of conidia of *A. fumigatus* Δ*abr1/brown1* (Δ*abr1*) and *A. fumigatus* Δ*akuB*^{ku80} (WT). in log along 10 weeks. Each point represents the mean value ± standard deviation of three independent samples of each time.

4.10.2. Phenotypic studies of *A. fumigatus* Δ*tf*, its reconstituted strain and the wild type

The growth of *A. fumigatus* Δ*tf* and *A. fumigatus* Δ*tf::tf*$^{+}$ in different media was studied and compared with the wild type. No differences were observed in the color of the colony or their growth on SGA, PDA and AMM (Fig. 4.46). The osmotic, oxidative and cell wall stress assay demonstrated that this transcription factor might not be involved in these kinds of stresses. This gene was not involved in the utilization of carbon sources either (Fig. 4.47-4.50). However, different growth was observed when the strains were grown on porcine tissue agar as no sporulation was observed on porcine kidney agar and a slight decrease on radial growth was detected on porcine lung agar (Fig. 4.51).

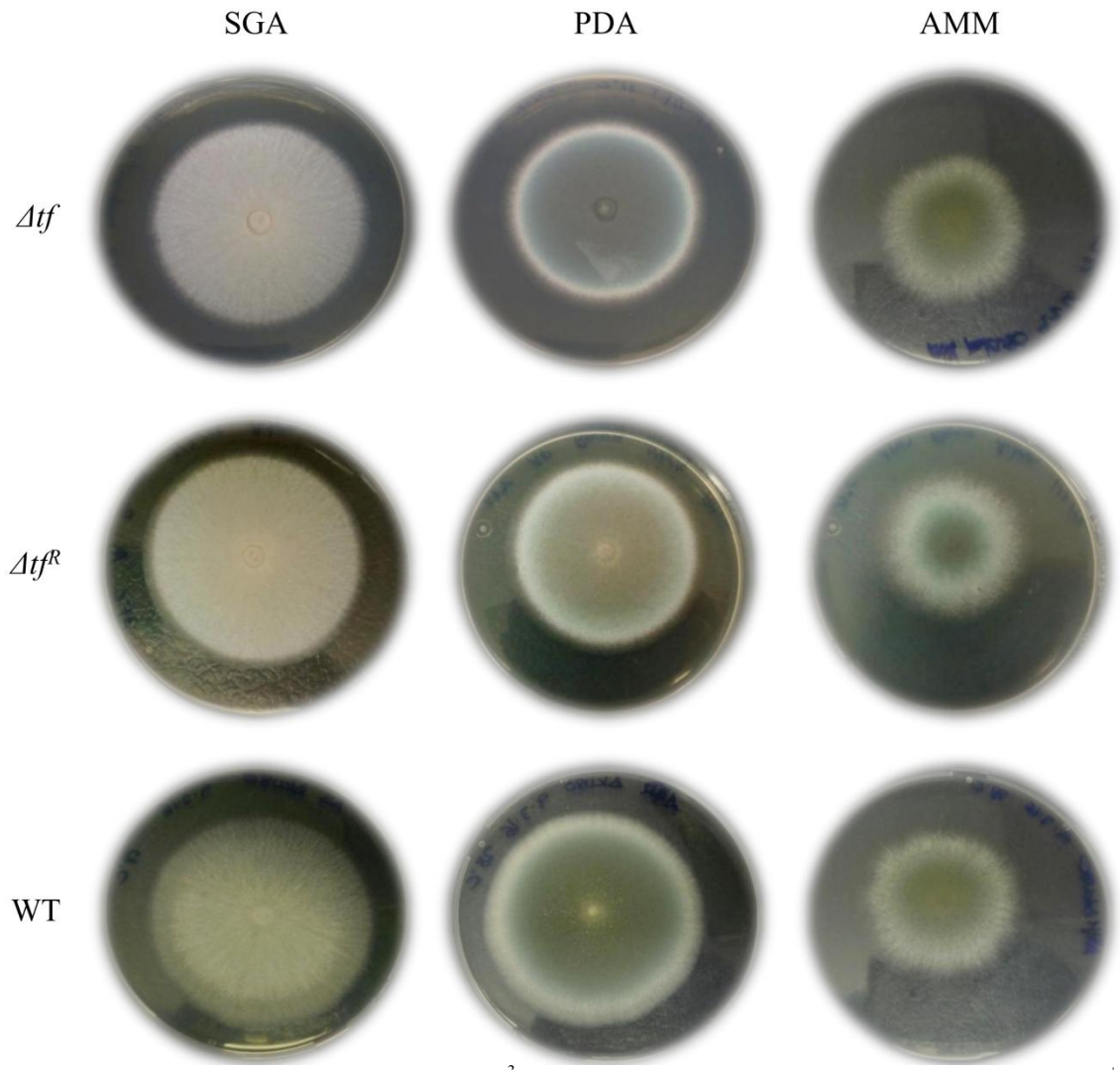

Fig. 4.46. Growth of *A. fumigatus* strains. 2x10^3 Conidia of *A. fumigatus* Δ*tf* (Δ*tf*), *A. fumigatus* Δ*tf:: tf*$^+$ (Δ*tf*^{R}) and *A. fumigatus* Δ*akuB*^{ku80} (WT) in a total volume of 2 µl were dotted on Sabouraud Glucose Agar (SGA), Potato Dextrose Agar (PDA) and Aspergillus Minimal Medium Agar (AMM) and incubated at 28°C for 7 days.

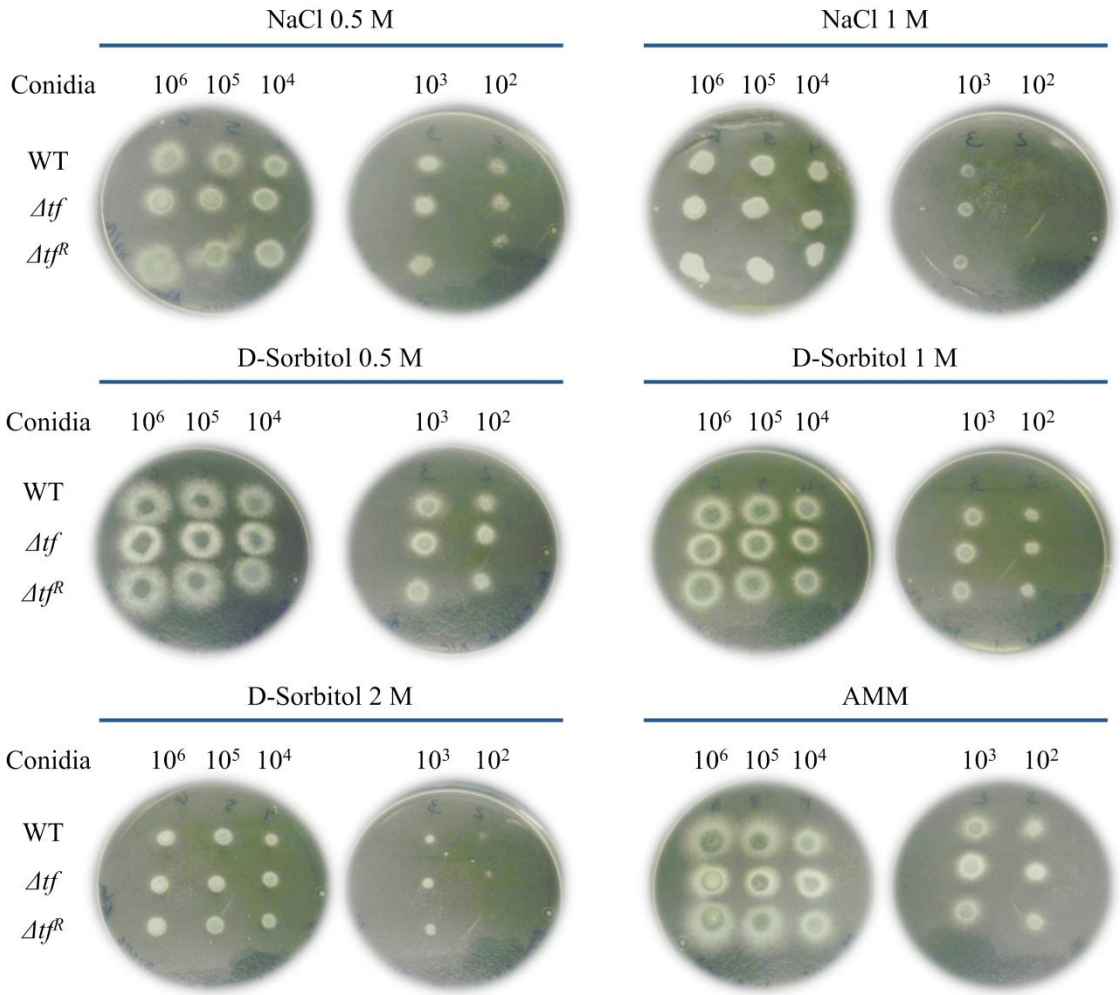

Fig. 4.47. Osmotic stress. Concentrations of conidia from 10^6 to 10^2 of *A. fumigatus* Δ*akuB*^{ku80} (WT), *A. fumigatus* Δ*tf* (Δ*tf*) and *A. fumigatus* Δ*tf*:: Δ*tf*$^{+}$ (Δ*tf*^{R}) in a total volume of 5 µl were dotted on AMM with NaCl (0.5 and 1 M) or D-Sorbitol (0.5, 1 and 2 M). The sample AMM corresponds to the growth on AMM without the osmotic stress. The growth was compared after the incubation at 37°C for 2 days.

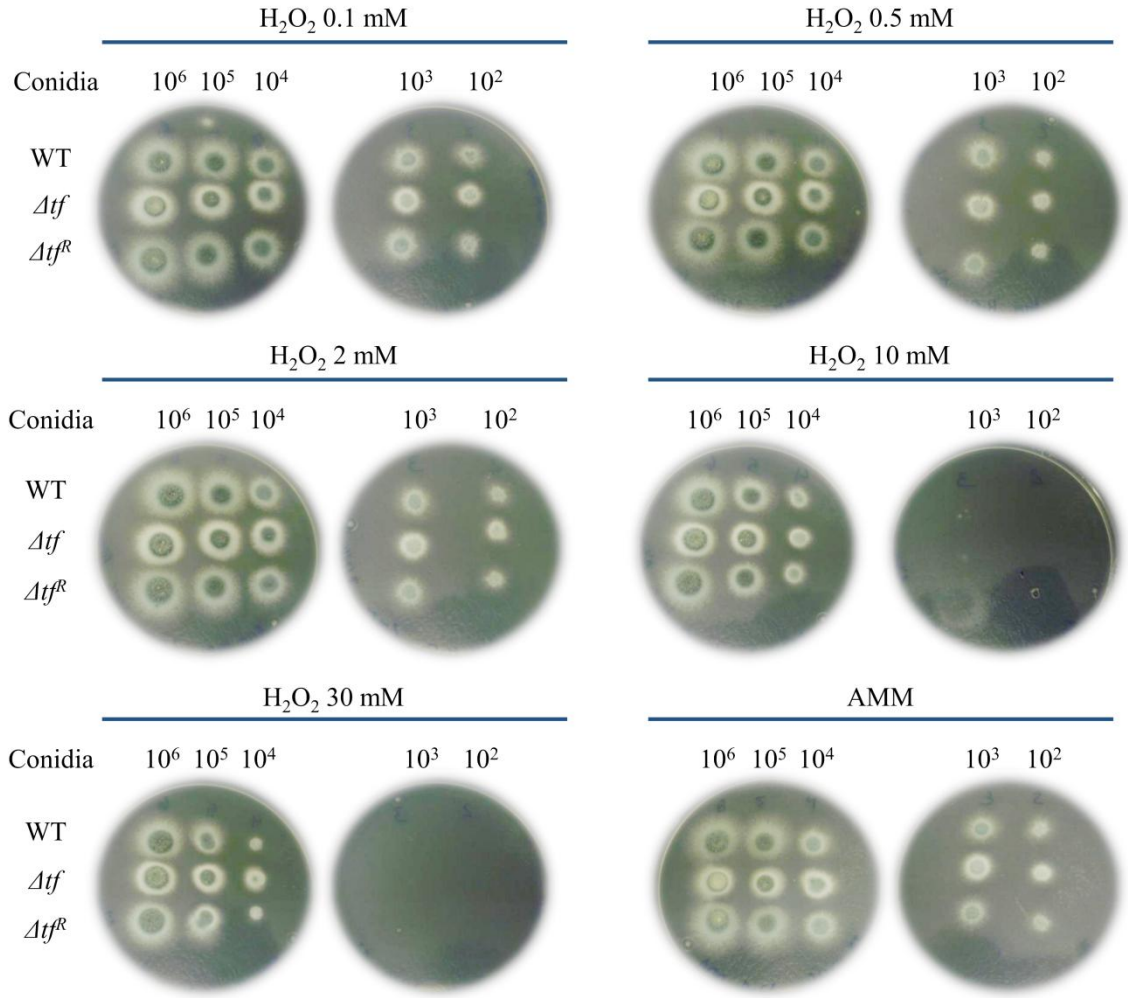

Fig. 4.48. Oxidative stress. Concentrations of conidia from 10^6 to 10^2 of *A. fumigatus* Δ*akuB*^{ku80} (WT), *A. fumigatus* Δ*tf* (Δ*tf*) and *A. fumigatus* Δ*tf*:: Δ*tf*$^{+}$ (Δ*tf*^{R}) in a total volume of 5 µl were dotted on AMM with H_2O_2 (0.1, 0.5, 2, 10 and 30 mM). The sample AMM corresponds to the growth on AMM without the oxidative stress. The growth was compared after the incubation at 37°C for 2 days.

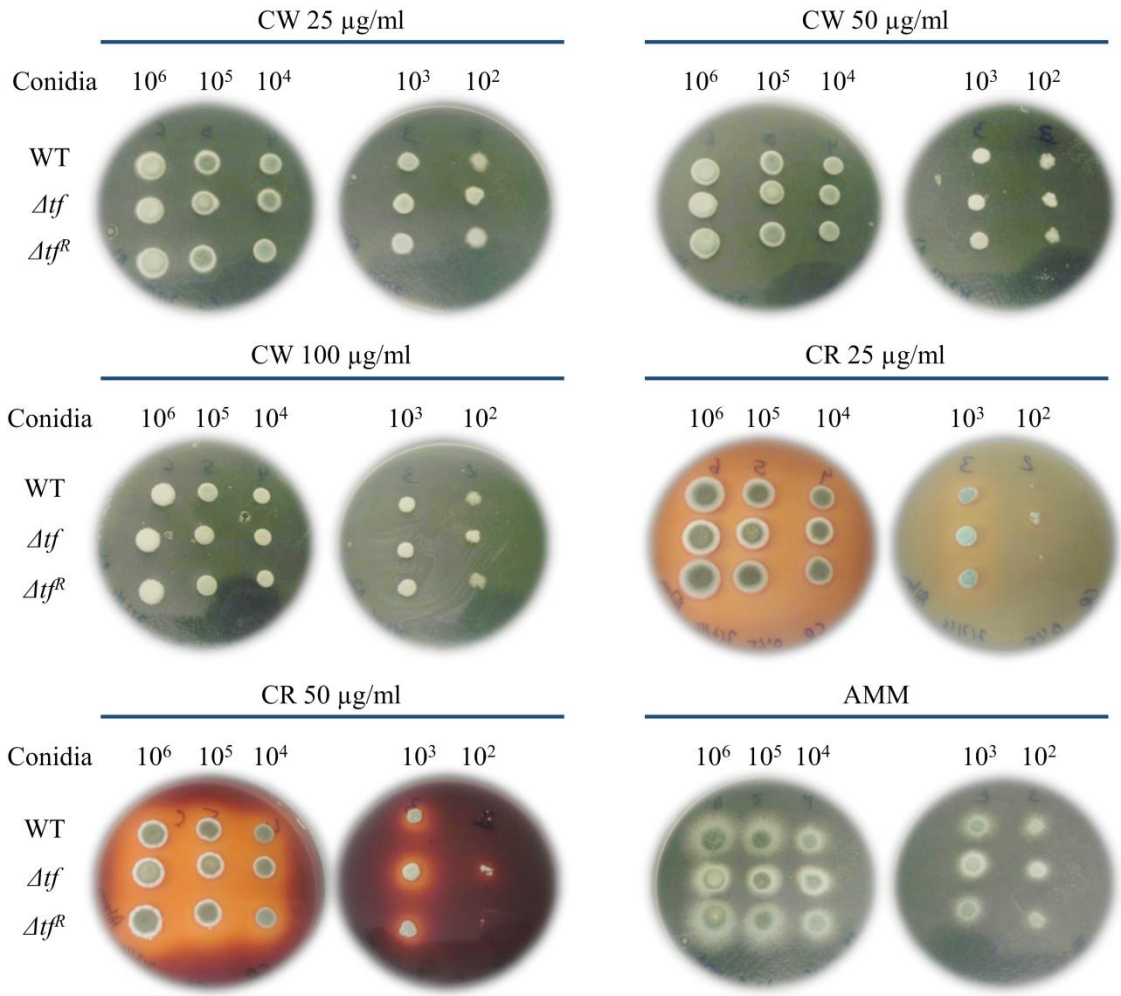

Fig. 4.49. Cell wall stress. Concentrations of conidia from 10^6 to 10^2 of *A. fumigatus* Δ*akuB*^{ku80} (WT), *A. fumigatus* Δ*tf* (Δ*tf*) and *A. fumigatus* Δ*tf*:: Δ*tf*$^{+}$ (Δ*tf*^{R}) in a total volume of 5 µl were dotted on AMM with Calcofluor Wite (CW) (25, 50 and 100 µg/ml) or Congo Red (CR) (25 and 50 µg/ml). The sample AMM corresponds to the growth on AMM without the stress. The growth was compared after the incubation at 37°C for 2 days.

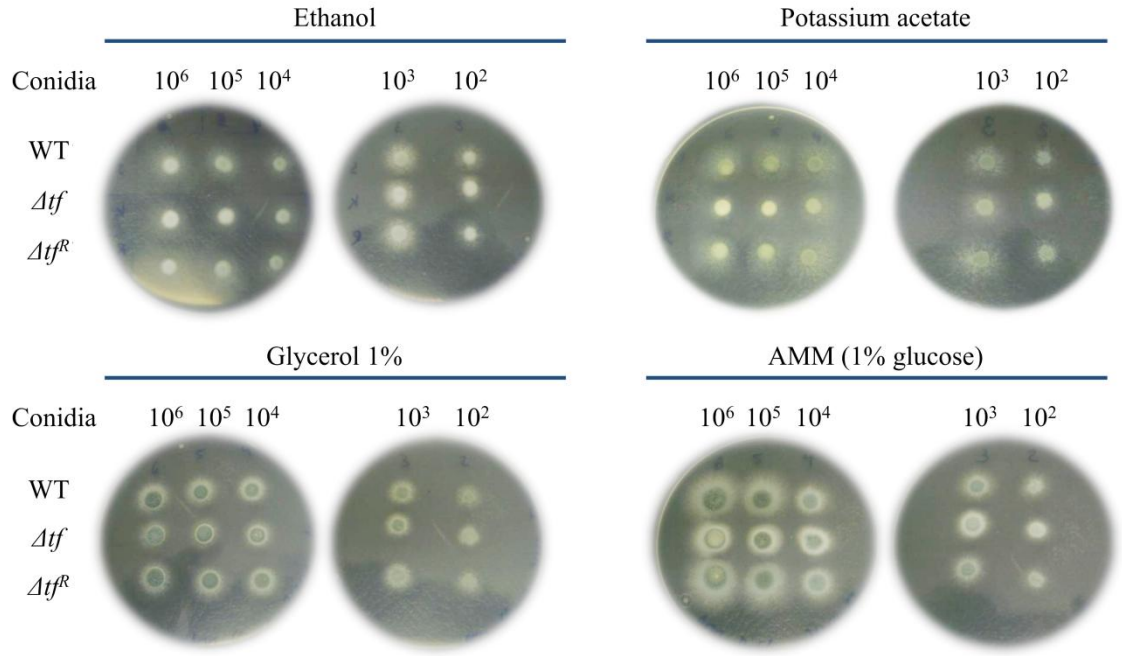

Fig. 4.50. Utilization of different carbon sources. Concentrations of conidia from 10^6 to 10^2 of *A. fumigatus* Δ*akuB*^{ku80} (WT), *A. fumigatus* Δ*tf (*Δ*tf)* and *A. fumigatus* Δ*tf::* Δ*tf*$^{+}$ (Δ*tf*^{R}*)* in a total volume of 5 µl were dotted on AMM with different carbon source (Ethanol, potassium acetate or glycerol). The sample AMM corresponds to the growth on AMM, whose carbon source is 1% glucose. The growth was compared after the incubation at 37°C for 2 days.

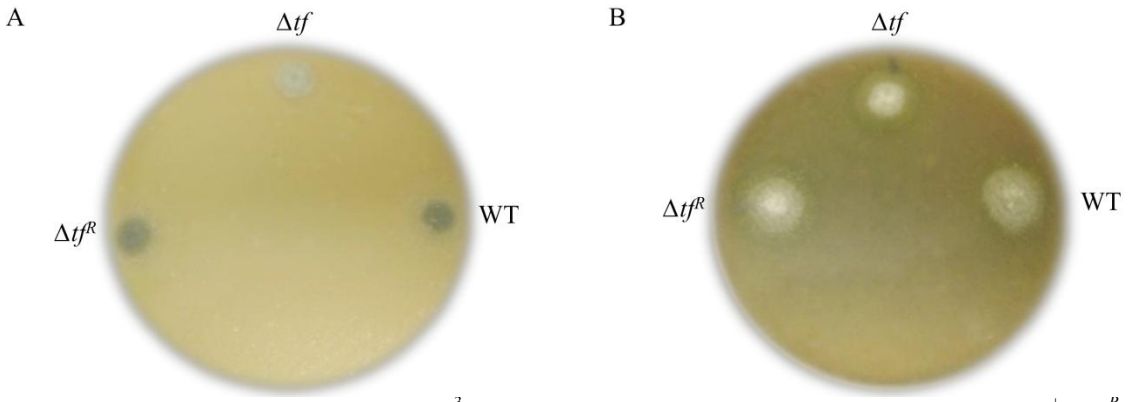

Fig. 4.51. Growth on porcine tissues. 2x10^3 Conidia of *A. fumigatus* Δ*tf* (Δ*tf*), *A. fumigatus* Δ*tf:: tf*$^{+}$ (Δ*tf*^{R}) and *A. fumigatus* Δ*akuB*^{ku80} (WT) in a total volume of 2 µl were dotted on porcine kidney agar (A) and porcine lung agar (B).

No differences were observed among the germination of the knockout and wild type strains at 37°C, even though the reconstituted strains seemed to start germinating earlier (Fig. 4.52). On the other hand, the study of conidial production showed that the deletion of the transcription factor did not influence on sporulation (Fig. 4.53).

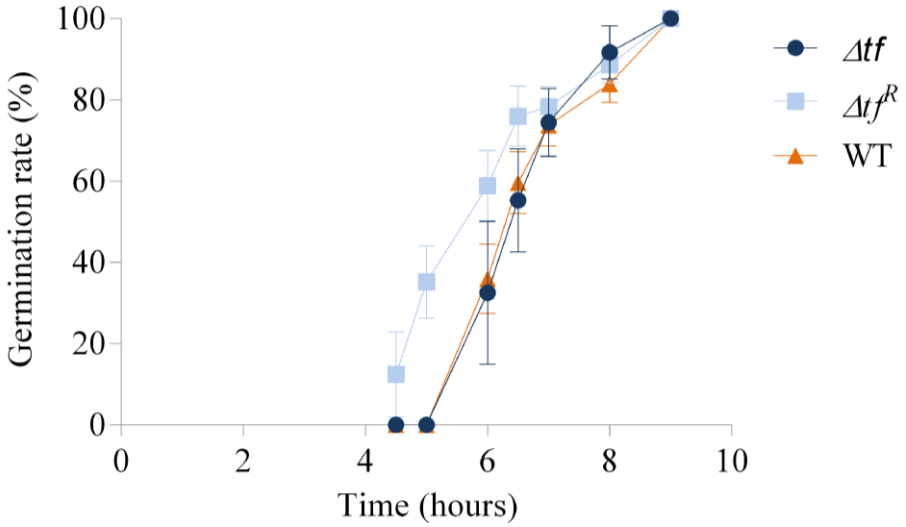

Fig. 4.52. Germination of *A. fumigatus* Δ*tf*. Curves of germination rates of *A. fumigatus* Δ*tf* (Δ*tf*), *A. fumigatus* Δ*tf::* Δ*tf*$^{+}$(Δ*tf*^{R}) and *A. fumigatus* Δ*akuB*^{ku80} (WT). Each point represents the mean value ± standard deviation of three independent samples of each time.

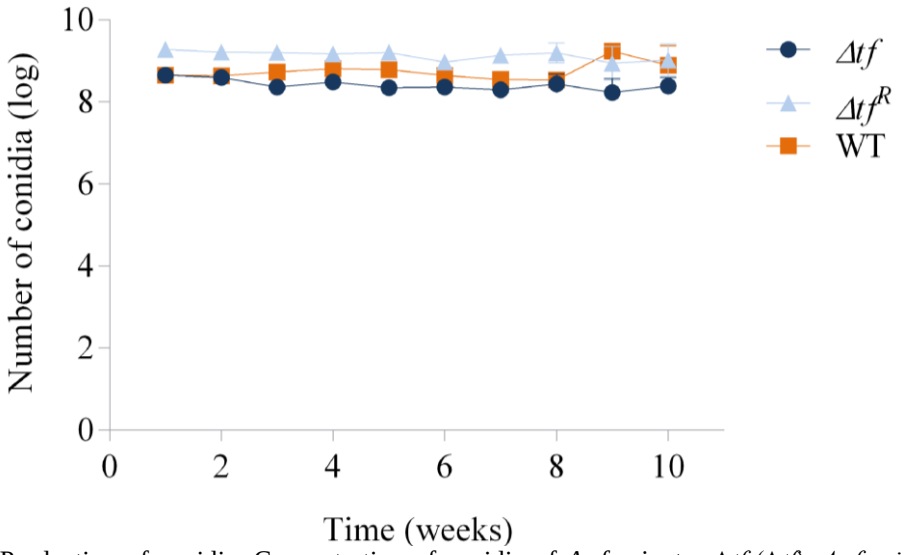

Fig. 4.53. Production of conidia. Concentration of conidia of *A. fumigatus* Δ*tf* (Δ*tf*), *A. fumigatus* Δ*tf::* Δ*tf*$^{+}$(Δ*tf*^{R}) and *A. fumigatus* Δ*akuB*^{ku80} (WT) in log along 10 weeks. Each point represents the mean value ± standard deviation of three independent samples of each time.

4.11. Cell line infections

4.11.1. Cell line infections with *A. fumigatus* Δ*abr1:brown1*

The study of the monolayer integrity of Calu-3 cells showed no statistical differences amongst the *A. fumigatus* Δ*abr1/brown1*, the reconstituted strain and the wild type when cells were infected with conidia. However, when Calu-3 cells were infected with culture filtrates statistical differences appeared in *A. fumigatus* Δ*abr1/brown1* ($p < 0.05$) (Fig. 4.54). These statistical differences were also observed in the detachment assay when A549 cells were infected with the culture filtrates of *A. fumigatus* Δ*abr1/brown1* ($p < 0.05$) (Fig. 4.55).

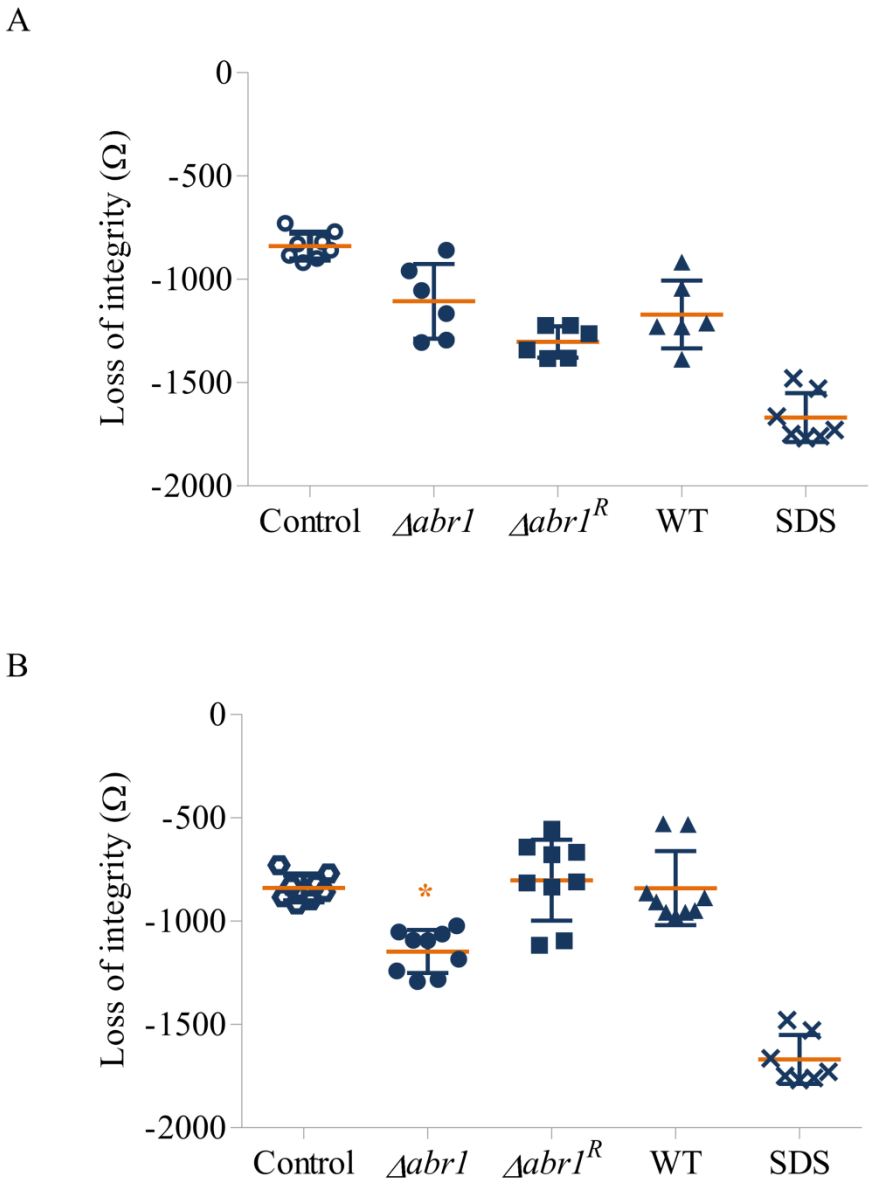

Fig. 4.54. Cell monolayer integrity of Calu-3 cells. Infections were carried out with *A. fumigatus* Δ*abr1/brown1* (Δ*abr1*), *A. fumigatus* Δ*abr1/brown1*:: Δ*abr1/brown1*$^{+}$ (Δ*abr1*^{R}) and *A. fumigatus* Δ*akuB*^{ku80} (WT). A) Infection with conidia. B) Infection with culture filtrates. The Y-axis values represent the loss of epithelial integrity (Ω) of Calu-3 cells relative to the resistance detected before the infection. Control: Samples that were not infected. SDS: Samples with a total loss of integrity due to the addition of 1% (w/v) SDS. The orange line represents the mean value and blue lines the standard deviation of three independent samples and three technical replicates. The asterisk indicates statistical differences ($p < 0.05$) relative to the wild type and the control condition.

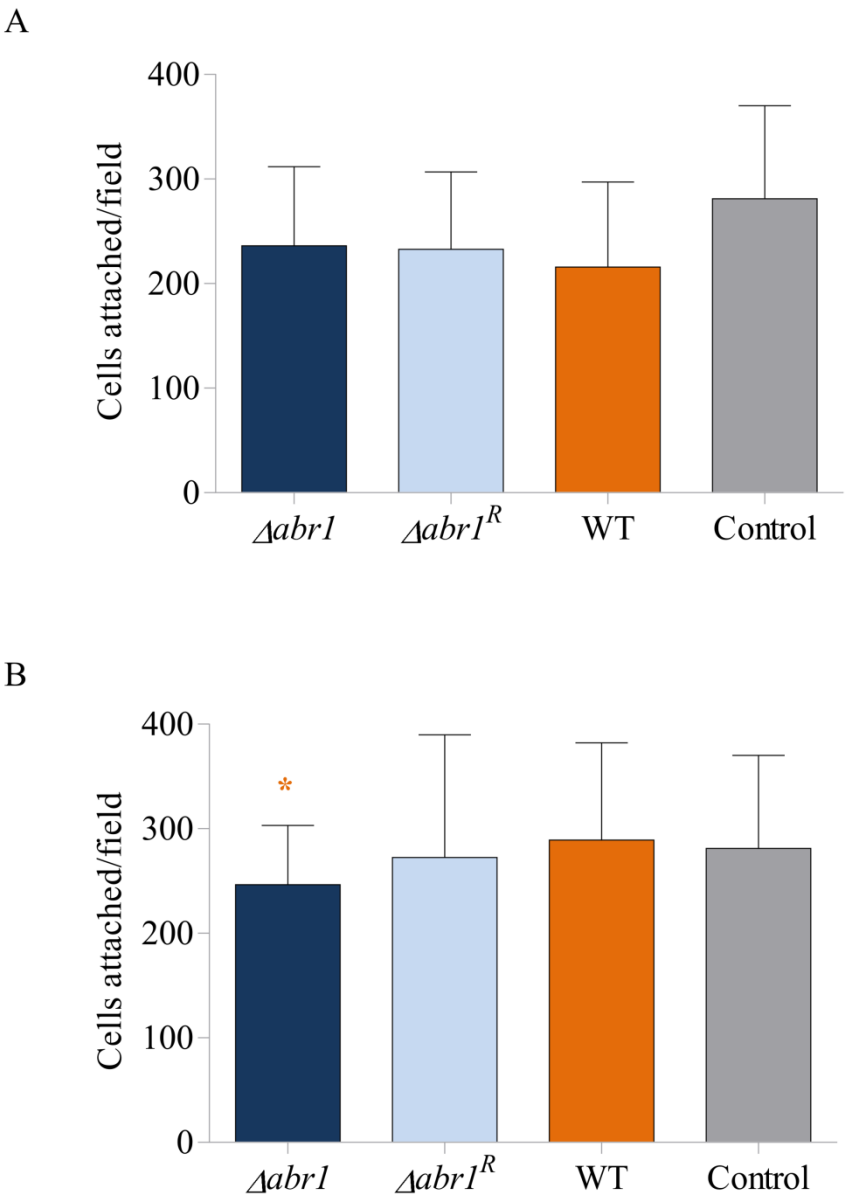

Fig. 4.55. Detachment assay of A549 cells. Infections were carried out with *A. fumigatus* Δ*abr1/brown1* (Δ*abr1*), *A. fumigatus* Δ*abr1/brown1*:: Δ*abr1/brown1*$^{+}$ (Δ*abr1*^{R}) and *A. fumigatus* Δ*akuB*^{ku80} (WT). A) Infection with conidia. B) Infection with culture filtrates. The Y-axis values represent the number of cells attached per field (x20) after the infection. Control: Number of cells attached when cells were not infected. The assay was carried out with three independ samples and three technical replicates. The asterisk indicates statistical differences ($p < 0.05$) relative to the wild type.

4.11.2. Cell line infections with *A. fumigatus* Δ*tf*

The study of the monolayer integrity of Calu-3 showed no statistical differences when conidia or culture filtrates were used (Fig. 4.56). However, when A549 cells were infected with conidia statistical differences appeared between *A. fumigatus* Δ*tf* and the wild type ($p < 0.05$) (Fig. 4.57).

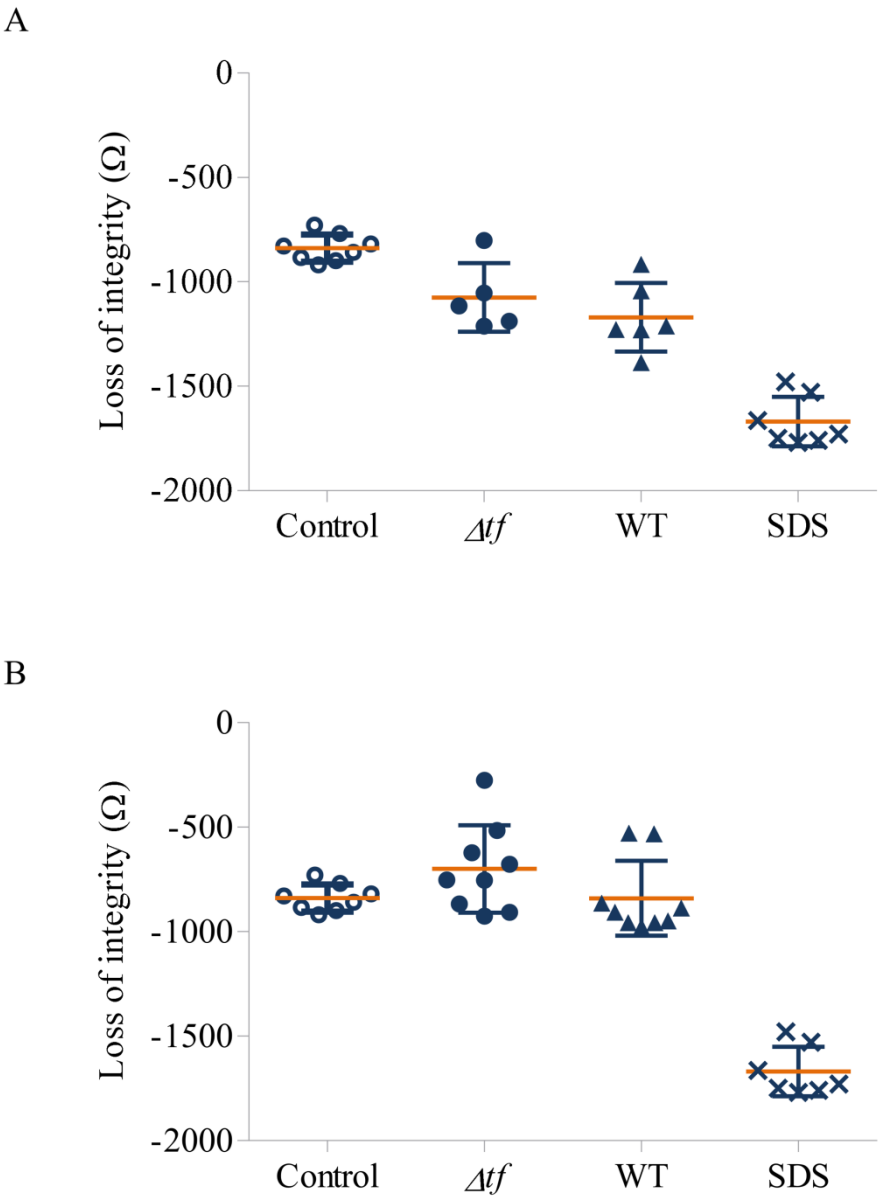

Fig. 4.56. Cell monolayer integrity of Calu-3 cells. Infections were carried out with *A. fumigatus* Δ*tf* (Δ*tf*) and *A. fumigatus* Δ*akuB*^{ku80} (WT). A) Infection with conidia. B) Infection with culture filtrates. The Y-axis values represent the loss of epithelial integrity (Ω) of Calu-3 cells relative to the resistance detected before the infection. Media: Samples that were not infected. SDS: Samples with a total loss of integrity due to the addition of 1% (w/v) SDS. The orange line represents the mean value and blue lines the standard deviation of three independ samples and three technical replicates.

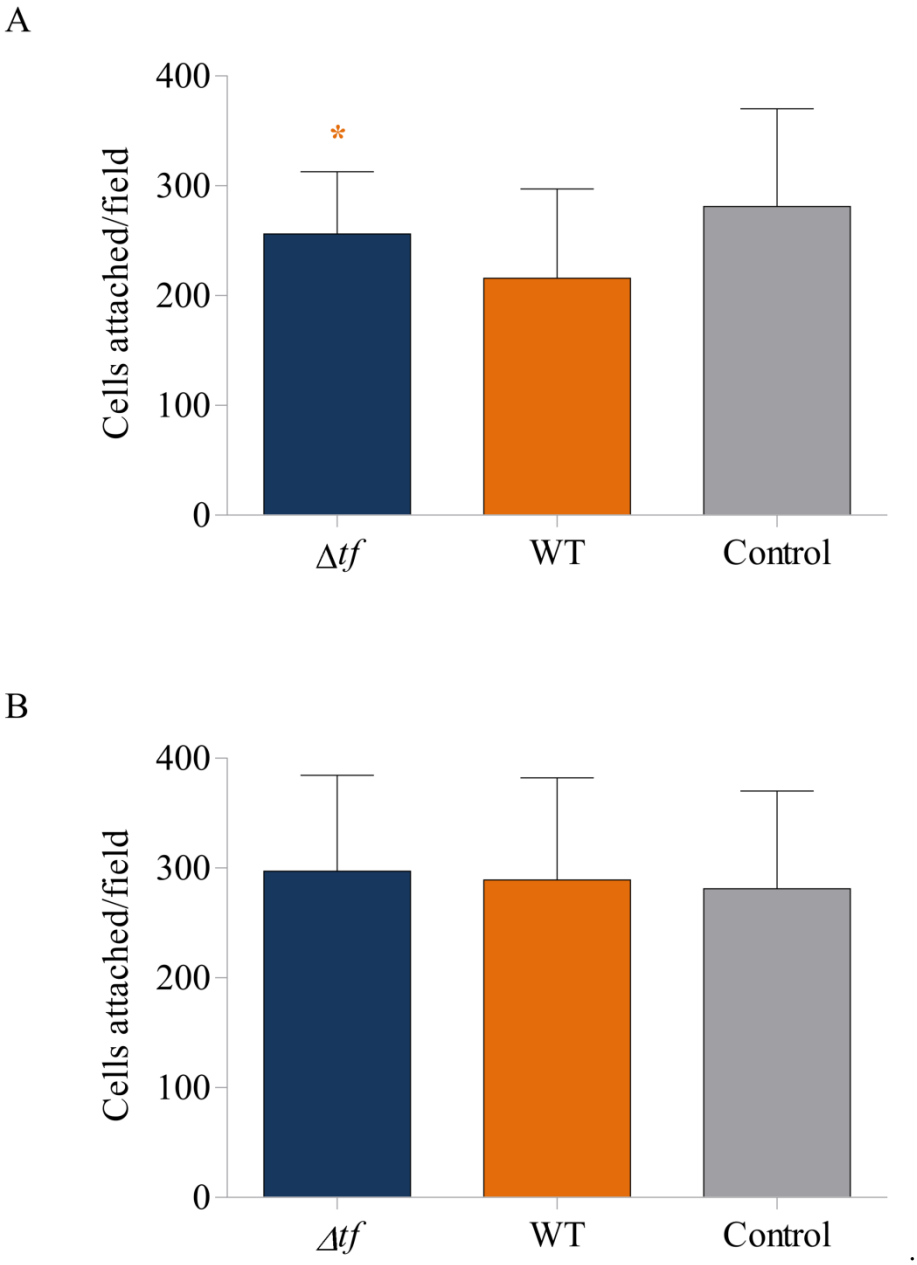

Fig. 4.57. Detachment assay of A549 cells. Infections were carried out with *A. fumigatus* Δ*tf* (Δ*tf*) and *A. fumigatus* Δ*akuB*^{ku80} (WT). A) Infection with conidia. B) Infection with culture filtrates. The Y-axis values represent the number of cells attached per field (x20) after the infection. Control: Number of cells attached when cells were not infected. The assay was carried out with three independ samples and three technical replicates. The asterisk indicates statistical differences ($p < 0.05$) relative to the wild type.

5. DISCUSSION

Aspergillus fumigatus is a saprophytic filamentous fungus that can act as an opportunistic pathogen causing a wide range of diseases. Moreover, it is considered as the most prevalent airbone pathogenic fungus. The small size of its conidia (2-3 µm), its hydrophobicity, thermotolerance and melanin content allow them to withstand a wide range of temperatures and to remain airborne for long periods (O´Gorman, 2011).

Conidial concentration indoors and outdoors is estimated to be 1-100 conidia/m^3 and people might inhale more than 100 conidia daily (Kwon-Chung & Sugui, 2013). This inhalation rarely has any adverse effect in immunocompetent individuals, even though in hypersensitive immunocompetent people the inhalation can cause allergic responses such as allergic bronchopulmonary aspergillosis (ABPA), asthma or allergic sinusitis (Moss, 2005; Denning, 2006). However, in immunocompromised patients *A. fumigatus* might develop more severe forms, standing out the invasive aspergillosis (IA). This disease is caused by *Aspergillus* spp., *A. fumigatus* being the most common etiologic agent, isolated in 56.11% of aspergillosis cases in Spain (Alastruey-Izquierdo *et al*., 2013). Furthermore, the number of patients suffering this kind of disease is on the rise (Brown *et al*., 2013; Sales-Campos *et al*., 2013) and, given that it is associated with the immune state of patients, the virulence of the fungus and the late diagnosis, it has mortality rates between 50 and 95% (del Palacio *et al*., 2003).

Aspergillus fumigatus infection starts with the inhalation of its conidia, which in immunocompromised patients may end up in their establishment in the lung, their germination and the following invasion of surrounding tissues (Dagenais & Keller, 2009). Once inhaled, the respiratory immune system initiates a series of events in order to carry out fungal clearance. Macrophages, neutrophils as well as other inflammatory cell populations, such as monocytes, natural killer and dendritric cells are the immune system barriers this pathogen is exposed to (Cramer *et al*., 2011). However, to succeed in the development of the infection, not only does *A. fumigatus* have to evade and confront the immune system of the host to prevent being swallowed and killed, but it also has to cope with numerous microenvironments. This requires resilience against changes in pH and oxygen levels, and resistance to nutrient limitation and host derived proteins (Shepardson & Cramer, 2013). Therefore, in order to carry out the germination and hyphal development, several mechanisms need to be activated, such as nutrient uptake systems or biosynthetic pathways (Dagenais & Keller, 2009), whereas

thermotolerance, toxin production, signaling and response to stress conditions must be adjusted (Abad *et al*., 2010).

Several studies have demonstrated that the pathogenesis of this fungal species is multifactorial due to a combination of its biological characteristics and the immune status of the patient (Beauvais & Latgé, 2001; Tekaia & Latgé, 2005; Osherov, 2007; Abad *et al.*, 2010). Furthermore, the idea that adaptive capabilities of the fungus growing as a saprophyte in the nature can contribute to its development as human pathogen seems to be gaining in importance (Hartmann *et al.*, 2011). Thus, understanding *A. fumigatus* pathogenesis has become a challenge, as the generation of knockout strains have not been able to prove that the loss of one or 2 genes affect the pathogenicity of the strain. The sequencing of the whole genome of *A. fumigatus* in 2005 has enabled the design of microarrays to analyze the transcriptome of the fungus under different growth conditions, which are considered as one of the best alternatives to identify virulence related genes. So far, several articles about the transcriptome of this pathogen have been published. Amongst them, its exposure to high temperatures (Nierman *et al*., 2005) or antifungals (da Silva Ferreira *et al*., 2006); the comparison between the germination and hyphal development (Sugui *et al*., 2008); and even during the infection of human cells (Oosthuizen *et al*., 2011; Morton *et al*., 2011; Perkhofer *et al*., 2015) might be mentioned. All these studies have allowed shedding light on the function and behavior of some genes and understanding how the fungus behaves in the presence of antifungals or in the host environment. However, its mechanisms of pathogenicity remain unclear.

With the aim of improving our understanding of the mechanisms that enable this fungus to cause infection, we have designed a new specific expression microarray (AWAFUGE, Agilent Whole *A. fumigatus* Genome Expression 44K v.1) using all the mRNA sequences available from the NCBI database and the eArray system developed by Agilent Technology. The strain selected for the design of the microarray was *A. fumigatus* Af-293 due to the fact that this strain was isolated from a lung biopsy from a neutropenic patient with IA (Anderson & Denning, 2001), it was the first strain of *A. fumigatus* whose genome was sequenced (Nierman *et al.*, 2005) and because it has been used in both *in vitro* and *in vivo* experiments (Power *et al.*, 2006, Gravelat *et al.*, 2008, Lamarre *et al.*, 2008, McDonagh *et al.*, 2008, Fraczek *et al*., 2010, Morton *et al.*, 2011, Farnell *et al.*, 2012). The microarray designed was used to study the transcriptome of

this pathogen during the germination and along a disseminated infection. These results provided us with enough information to detect interesting genes and generate mutant strains to study their implication in virulence.

One of the most cited physiological characteristics of this pathogen has been its ability to survive to high temperatures, as it tolerates temperatures higher than 50°C, and its optimal temperature is around 37°C (Krijgsheld *et al.*, 2013). Hence, it is plausible that the mechanisms of thermotolerance involve the expression of stress resistance genes that, at the same time, confer unique virulence properties to the fungus (Bhabhra & Askew, 2005). Consistent with this, Araujo & Rodrigues (2004) demonstrated that temperature plays a crucial role in the correlation between the germination rate and pathogenicity, concluding that *A. fumigatus* is the most able to adapt to extreme changes in environmental conditions.

A crucial event in the infectious process is conidial germination, given that at this stage conidia have to adapt to the host environment and to overcome the immune system as well as to germinate. It is known that the first step in the germination of *Aspergillus* consists of breaking the spore dormancy followed by isotropic swelling, establishment of cell polarity, formation of the germ tube and maintenance of polar growth (Barhoom & Sharon, 2004; Harris & Momany, 2004). However, despite the knowledge about the different stages of germination, little is known about all molecular aspects of the processes taking place during this period.

To date, different studies have been developed focusing on the germination of *Aspergillus* genus (Araujo & Rodrigues, 2004; Lamarre *et al*., 2008; Leeuwen *et al*., 2013). However, comparison of the findings between studies is very difficult owing to the use of different fungal species or time intervals. With regard to *A. fumigatus*, several studies have analyzed the transcriptomic changes among samples incubated at different temperatures for the same incubation times (Nierman *et al.*, 2005; Low *et al.*, 2011; Krishnan *et al.*, 2014). Nevertheless, *A. fumigatus* germination rate differs at each temperature. The higher the temperature is, the faster conidia germinate. Thus, these studies not only compared samples with different temperatures, but also with different growth rates, which could affect expression differences. Taking this into consideration, and using the AWAFUGE microarray (v.1) designed by our research group, we decided to investigate the adaptive changes of *A. fumigatus* to host temperature, studying the

transcriptome obtained at 24ºC, representing the environmental temperature, and at 37°C, reflecting the host temperature, in samples with the same growth rate. Furthermore, given that germination is the first step in the infectious process, we focused on this stage to identify functional and gene expression changes potentially linked to virulence in order to shed light on the mechanisms of adaptation and virulence of this fungus during this early stage of infection. Following the study of the germination rate at different times, samples with 15-30% germination rates were chosen to carry out transcriptomic analyses as all germinated conidia were of a similar size and because with larger incubation times hyphae were too long (Fig. 4.2A). Moreover, using samples with the same germination rate could allow minimizing the expression changes that are due to the growth rate. Specifically, cultures were incubated at 37ºC for 6.5 hours and at 24ºC for 18 hours (Fig. 4.2B). It should be emphasized that no changes were detected in pH, indicating that this factor had no effect on gene expression changes.

Transcriptome profiling results showed that 1,249 genes were differently expressed (Fig. 4.4). To validate these results, RT-qPCR assays were carried out with the genes found to be most differentially up-regulated and those related to virulence which showed significant differences. The RT-qPCR results confirmed the differential expression of the 28 selected genes with the same direction of expression changes in both methods, although the magnitude of them differs considerably. According to the literature, RNA quality, different efficiencies of reverse transcriptases and priming methods, the effect of dye biases, and the variable efficiency of RT-qPCR at later cycles are some of the factors which can affect the correlation between microarray and RT-PCR results (Morey *et al*., 2006). Moreover, a different normalization procedure was applied in each method, which could also explain the different magnitudes of the tested genes. On the other hand, the correlation between the two methods yielded a high significant Pearson´s correlation value of 0.89, taking into account that a correlation of 1 would mean a perfect positive correlation between the two methods (Fig. 4.10). Overall, the agreement between the microarray data and the RT-qPCR results together with the high Pearson´s correlation underline the effectiveness and the reliability of the AWAFUGE microarray (v.1). These properties make this microarray suitable for use in further studies analyzing the virulence mechanisms or the response of *A. fumigatus* to environmental changes or during murine or human cell infections.

Thanks to the functional classification of *A. fumigatus* genome available in the Munich Information Center for Protein Sequence Functional Catalogue (FunCat; http://pedant.helmholtz-muenchen.de), the biological functions of the differentially expressed genes at 24 and 37ºC were explored. As shown in Table 4.1, metabolism, hypothetical proteins and unclassified proteins were the groups mostly represented. Regarding the enrichment analysis, C-compound and carbohydrate metabolism, secondary metabolism and lipid, fatty acid and isoprenoid metabolism were some of the groups significantly up-regulated at 37°C. In a previous study, comparing the transcriptome of *A. fumigatus* at 25 and 37°C, up-regulated genes involved in metabolism also appeared at 37°C (Krishnan *et al.*, 2014), which was explained based on the faster growth of the fungus at 37°C. However, in our study, both cultures at 24 and 37°C had the same germination rate, so the results showed that the metabolic adjustments not only depend on the faster growth of this fungus but also on the temperature in which the germination takes place. Moreover, the significant groups at 24°C, related to rRNA processing and synthesis, tRNA processing and modification, and RNA degradation, showed that RNA pathways are down-regulated at 37°C. On the other hand, it should be pointed out the high percentage of differentially expressed genes coded for hypothetical (26.10%) or unclassified proteins (30.82%). It is true that these genes mean a limitation of the conclusions of our study, although at the same time, they stress the importance that these unknown genes might have during the germination of this fungus and point to avenues for future research.

To study the effect that the different incubation times (6.5 and 18 hours) could have on the medium, a germination study with the addition of fresh medium was performed. With this study, we could conclude that the temperature was the main factor that determined the expression changes of the 50% of the genes (14/28 genes) analyzed in samples with 15-30% germination rates, with a high Pearson´s correlation (0.86). Focusing on the 20 most expressed genes detected by microarray data, those genes that showed different expression patterns in this analysis encoded unclassified proteins, and those with no statistical differences coded for proteins mainly related to secondary metabolism and C-compound and carbohydrate metabolism (Table 4.8 & Annex III). As secondary metabolism is affected by several nutritional conditions, such as amino acid, nitrogen and iron sources (Bayram & Braus, 2012), it is understandable that the addition of fresh medium could replenish the consumed nutrients, decreasing the need to

stimulate different metabolisms. The same would happen with the carbon source of the medium, whose availability could be increased by the addition of fresh medium. These results highlighted the importance that the isotropic swelling and the formation of a germ tube had since the beginning of the germination, altering the medium conditions even when the majority of the conidia had not yet germinated.

One of the metabolic pathways that appeared up-regulated at 37ºC was gliotoxin biosynthesis, previously related to *A. fumigatus* virulence (Bok *et al*., 2006; Sugui *et al*., 2007b; Spikes *et al*., 2008; Gallagher *et al*., 2012; Scharf *et al*., 2012). Gliotoxin is a non-ribosomal peptide toxin that contributes to the virulence of *A. fumigatus* with its cytotoxic, genotoxic and apoptotic properties (Grovel *et al*., 2002; Nieminen *et al*., 2002; Kweon *et al*., 2003). The gliotoxin gene cluster comprises 13 genes (Gardiner & Howlett, 2005) and their expression depends on various factors such as pH, temperature, hypoxia, and unknown factors during infection (Sugui *et al*., 2008; McDonagh *et al*., 2008). Moreover, this toxin has been detected in lung and serum of mice suffering from aspergilosis and even in patients with IA (Richard *et al*., 1996; Lewis *et al*., 2005). Our results showed that some genes involved in gliotoxin biosynthesis were up-regulated at 37°C (Table 4.3), such as *gliZ*, a transcription factor which regulates gliotoxin biosynthesis (Bok *et al*., 2006), and *gliP*, a non-ribosomal peptide synthetase which catalyses the first step of gliotoxin biosynthesis (Balibar & Walsh, 2006). The analysis following the addition of fresh medium showed a clear up-regulation at 37ºC of the gene that encodes GliZ, demonstrating that the expression of this gene is directly influenced by the heat shock. However, the expression pattern of the gene that encodes GliP indicated that the heat shock did not directly stimulate the up-regulation of this gene (Fig. 4.11B). According to the literature, *gliZ* is a positive regulator of *gliP* and its up-regulation enhances the production of gliotoxin (Bok, *et al.*, 2006). Nevertheless, Dhingra *et al.* (2012) showed different expression patterns among *gliZ* and *gliP* when *veA*, a major fungal regulatory gene, was deleted, which was explained based on a possible influence of *veA* on *gliP* by unknown mechanisms. Therefore, the expression of *gliP* could be controlled by other regulators, apart from *gliZ*, which might have been affected by the addition of fresh medium.

Nutrient uptake also showed significant differences at 24 and 37ºC. In fact, amongst proteases and phospholipases, lysophospholipase Plb3, aspartic endopeptidase Pep1/aspergillopepsin F and elastinolytic metalloproteinase Mep, previously described

as virulence factors, were up-regulated at 37ºC. This last protein is also known as allergen Asp F 5, has extracellular activity and is able to degrade collagen and elastin (Markaryan *et al.*, 1994; Sirakova *et al.*, 1994). The aspartic endopeptidase Pep1/aspergillopepsin F is an extracellular enzyme also known as allergen Asp F 10 (Lee & Kolattukudy, 1995). Finally, lysophospholipase Plb3 is a cytosolic protein that belongs to the phospholipase B family and that has phospholipase, lysophospholipase and transacylase phospholipase activity (Shen *et al.*, 2004). Taking all this into account, and the other proteases up-regulated at 37ºC, the expression of theses degrading enzymes might be influenced by the heat shock and facilitate the establishment of the fungus in the host during the first steps of germination.

Genes involved in iron metabolism were also found to be differentially expressed in our study. This is interesting due to the fact that iron is a limiting nutrient *A. fumigatus* finds in the host environment and its ability to acquire this metal is related to virulence (Schrettl *et al.*, 2007; 2010; Haas, 2014). As mentioned in the introduction, despite this fungus lacking specific uptake systems for host iron sources such as ferritin, heme group-containing molecules or transferrin, *A. fumigatus* has developed two high-affinity iron uptake systems to overcome iron starvation: reductive iron assimilation (RIA) and siderophore-assisted iron uptake (Schrettl *et al.*, 2004). In order to maintain iron homeostasis, two transcriptional factors are mainly necessary, SreA and HapX, the levels of which are negatively correlated: when iron concentrations are high enough, SreA represses the expression of *hapX* gene and high-affinity iron uptake. However, during iron starvation conditions, HapX mediates the repression of the *sreA* gene expresion, activating iron uptake through siderophores. Our microarray results showed that *sreA* was up-regulated at 24°C, whereas *hapX*, and other genes (*sidD*, *sidC*, *sidG* and *sidI*) involved in the assembly of fusarine C and ferricrocin siderophores were up-regulated at 37°C. Two genes that encoded 2 siderophore-iron transporters, *mirB* and *mirC*, also showed up-regulation at 37ºC, but their roles in virulence have not yet been studied. Interestingly, after the addition of fresh medium, *sreA* were not up-regulated at 24ºC, but *sidD* showed up-regulation at 24ºC, unlike in the microarray data (Fig. 4.11C-D). Nevertheless, in samples with 40-60% germination rates, its expression difference was reduced, which might indicate a slight increase of its expression at 37ºC. Therefore, the iron uptake through siderophores appears not to be affected by the heat shock, but

rather by a possible decrease of iron availability in the culture medium during the isotropic swelling and germ tube formation at 37°C.

Zinc metabolism was another metal showing up-regulation at 37ºC. As mentioned previously in introduction, *A. fumigatus* has 2 transcription factors, ZafA and PacC, that regulate zinc homeostasis and that have been described as virulence factors (Bignell *et al.*, 2005; Moreno *et al.*, 2007). These genes did not show significant differences, but zinc importers, such as ZrfA and ZrfC, did. It should be pointed out that the expression of these transporters is influenced by the transcription factors mentioned above, increasing their expression in zinc-limiting conditions. Therefore, despite the fact that ZafA or PacC were not up-regulated in our results, the up-regulation found in zinc transporters might indicate that the uptake of this metal is enhanced to allow the proper conidial germination.

Another metabolic pathway whose genes were found to be differentially expressed in our microarray results and that has been related to virulence was nitrogen metabolism. *Aspergillus* can use a wide range of nitrogen sources and contributes significantly to global nitrogen recycling via nitrate assimilation (Dagenais & Keller, 2009). Accordingly, 3 genes involved in nitrogen metabolism were up-regulated at 37°C. Two of them encode nitrate reductases (NiaD and AFUA_5G10420), and the other, the nitrite reductase NiiA, which was the most up-regulated gene (Table 4.6). With the addition of fresh medium, the results showed that in 15-30% germination rate samples only the gene that encode the nitrite reductase NiiA appeared to be up-regulated at 24ºC, whereas in 40-60% germination samples the genes that code for the nitrite reductase NiiA and the nitrate reductase NiaD were up-regulated at 37ºC (Fig. 4.11E-F). These expression changes detected in our study could mean that the uptake of nitrogen is up-regulated in line with the growth of *A. fumigatus* at 37ºC and a possible consumption of nitrogen sources, as in the iron case. Moreover, this pathogen may be able to obtain nitrogen from other sources such as amino acids, being several genes implicated in their utilization also differentially expressed.

Finally, *A. fumigatus* may be responsible for various allergic diseases such as extrinsic allergic alveolitis, asthma, allergic sinusitis, and ABPA (Park & Mehrad, 2009). More than 20 allergenic molecules are known to be produced by this fungus, and some of them, in addition to their allergenic activities, are also related to virulence (Abad *et al.*,

2010; Chaudhary & Marr, 2011; Low *et al.*, 2011). Our results reveal that nine genes that encode allergens were highly up-regulated when *A. fumigatus* germinated at 37°C; the most up-regulated allergens being the MnSOD (Asp F 6), the major allergen Asp F 2 and the major allergen and cytotoxin Asp F 1. Only one gene that codes for a cell wall glucanase/allergen F 16-like appears to be up-regulated at 24°C (Table 4.7). Asp F 6 provides protection against ROS, autoimmunity problems in patients and antigen activities. Asp F 2 has biological activity associated with binding to laminin during lung colonization; and Asp F 1 is related to virulence due to the inhibition of protein biosynthesis and its cytotoxic and apoptotic activities (Abad *et al.*, 2010). According to the addition of fresh medium results, the expression of allergens seems to take place at the beginning of the germination. In 15-30% germination samples, Asp F 2 and Asp F 6 were also up-regulated at 37ºC, being only Asp F 6 up-regulated at 24ºC in 40-60% germination rates samples (Fig. 4.11G-I). Furthermore, the up-regulation in 15-30% germination rates not only highlighted the importance of the production of these allergens during the first steps of germination, but also the effect of a higher temperature. However, Asp F 1 showed no statistical differences in 15-30% germination rates samples, pointing out the effect of the medium in the production of this allergen, which might be stimulated by a depletion of nutritional sources.

To sum up, this is the first study that compares the transcriptomes of germinated conidia at 24 and 37°C taking into account the germination rate. According to our results, *A. fumigatus* modifies the expression of genes mainly related to metabolism and down-regulates RNA pathways in order to adapt to the new conditions at 37ºC. Moreover, the high percentages of differentially expressed genes that encode hypothetical or unclassified proteins imply that many of these unknown genes must be essential during the germination of this fungus, whose study might improve the understanding of the infection caused by this pathogen. Amongst the genes related to virulence up-regulated at 37ºC, we found genes coding for allergenic proteins and several genes involved in gliotoxin biosynthesis and nutrient uptake such as nitrogen, zinc and iron metabolism. Furthermore, the addition of fresh medium has demonstrated the importance of the isotropic swelling, which can alter the growth medium even before reaching the 15-30% germination rate. Gene expression in iron and nitrogen metabolism appears to be influenced by the availability of these nutrients in the medium, whereas in allergen production, the temperature, the germination stage and the medium conditions seem to

be involved. Therefore, the expression changes detected in our study, might demonstrate not only the rapid heat shock adaptation of *A. fumigatus*, but also its efficient ability to uptake the nutrients from the medium during the earliest steps of germination, which might be another aspect that allows it to germinate easily in the host environment.

As the AWAFUGE microarray (v.1) proved to be a highly effective and reliable tool to analyze the expression changes of *A. fumigatus* in different conditions, the next step was to study the transcriptome of this fungus during a mice infection. In recent years murine models have brought significant developments in the study of *A. fumigatus* pathogenesis and even in antifungal therapy against aspergillosis (McDonagh *et al*., 2008; Gehrke *et al*., 2010; Park *et al*., 2012; Salas *et al*., 2013; Seyedmousavi *et al*., 2013; Amarsaikhan *et al*., 2014; Jiang *et al*., 2014). The availability of genetically defined strains of mice, immunological reagents, ease of handling and cost are the factors why this infection is widely performed (Clemons & Stevens, 2005). Murine infections can be established by intranasal, intravenous or intra-abdominal routes (Schmidt, 2002). Nevertheless, intra-abdominal infections are barely carried out and the intranasal may cause some problems as delivery of fungal cells to the lungs can be variable, particularly since they often fail to reach terminal airways. In fact, fungal lesions are likely to arise from *A. fumigatus* conidia deposited in larger airways rather than in alveoli, the characteristic site of human disease (Hohl, 2014). On the other hand, intravenous infection is a method easily standardized because the fungal inoculum is directly injected into the blood stream, resulting in a good correlation between infection dose and mortality rates (Paulussen *et al*., 2014).

Several studies have been carried out with murine infections to analyze the pathogenesis of *A. fumigatus*. However, the majority of them used strains in which a gene of interest were deleted and whose virulence was compared to the wild type (Bok *et al*., 2006; Kupfahl *et al*., 2006; Gehrke *et al*., 2010; Park *et al*., 2012; Jiang *et al*., 2014). Regarding transcriptomic assays, only one experiment has been performed in bronchoalveolar lavage from intranasally infected animals (McDonagh *et al*., 2008).

Given that the lung is the main target in aspergillosis, most studies were focused on intranasal infections. Nonetheless, in profoundly immunocompromised patients hyphae fragments can break off into the bloodstream disseminating throughout the body and

infecting organs other than the lungs (Dagenais & Keller, 2009). Little is known about the behavior of the fungus when the bloodstream is achieved so, in order to understand how this mold behaves during dissemination an intravenous infection was performed. Furthermore, as neutrophils are the key effector cells in the immune response against *A. fumigatus*, and neutropenic patients have the highest risk of developing invasive aspergilosis (Mircescu *et al*., 2009), immunosuppression with cyclophosphamide was performed.

Analysing the fungal burden of each organ extracted, the spleen seemed to be the primary site of infection on day 1, which agreed with a previous study in BALB/c mice (Mirkov *et al*., 2011). However, the fungal burden in this organ decreased throughout the infection, which was also observed, although at a lower level, in lung. Only in the kidney a steady increase was detected, whose infection was confirmed by histology. These results are in agreement with Jouvion *et al.* (2012), who demonstrated how kidney was the main target in immunocompetent mice intravenously infected with *A. fumigatus*. This, together with our results, suggested that the fungus may have encountered a permissible environment in kidneys to develop the infection, making this organ suitable for transcriptomic analysis, as its results might reflect in a better way the infectious process.

Statistical comparisons of normalized transcriptome profile data showed no differences amongst the four days of infection when test ANOVA was performed using day 1 post-infection as reference. These results demonstrated the ability of this pathogen to quickly adapt to the host environment in the first 24 hours, enabling the progression of the infection, as observed in histology and in fungal burden data. To identify those genes up-regulated *in vivo*, data from each day post-infection was compared to the results obtained from the germination of *A. fumigatus* at 37ºC. These comparisons showed that between 350 and 4,100 genes were differentially expressed (Fig. 4.20) and a hierarchical clustering allowed the identification of 1,001 genes highly up-regulated along the infection.

With regard to the enrichment analysis, basic metabolisms, such as amino acid, nucleotide and phosphate metabolism, as well as functional groups related to transcription, protein synthesis and fate, transport, and biogenesis of cellular components were down-regulated during the infectious process. Amongst them, stress

response, heat shock response, and temperature perception and response should be pointed out, meaning that once the infection is established *A. fumigatus* is already adapted to host environment (Table 4.13). With regard to the course of infection, and in particular to those genes identified by the hierarchical cluster analysis, metabolisms associated with pathogenesis such as secondary metabolism, cell rescue, defense and virulence and the synthesis of non-ribosomal peptides were up-regulated during the infection. This up-regulation was also observed in import systems with a large representation of MFS transporters (45%). These genes function as uniporters, symporters or antiporters (Pao *et al*., 1998) and export a variety of substrates, including carbohydrates, drugs, metabolites, nucleosides, amino acids, organic and inorganic anions, cations and various Kreb's cycle intermediates. Moreover, some of them have been even associated with antifungal resistance and with the detoxification of components of the immune system (Osherov, 2007). The necessity of C-compounds and carbohydrates such as polysaccharides *in vivo* was also demonstrated as their metabolisms, degradation and transport routes were highly enriched on the four days post-infection. There were many hydrolases that can help in nutrient uptake among the genes involved in these pathways, such as polygalacturonase, lyases, beta-glucosidase and alpha-amylase (Annex II). These kinds of enzymes help in nutrient uptake, so their up-regulation during infection might indicate their important role in this process. According to the literature, alpha-amylases are enzymes that hydrolyze glycogen and starch (El-Fallal *et al*., 2012), the main energy reservoir of mammals, and could provide the fungus with the carbon source it needs to grow. It should be pointed out that the glycogen storage capability in kidneys is not very high (Krebs & Yoshida, 1963), so the up-regulation observed in these hydrolases might be an indication of the strategy followed by *A. fumigatus* to deal with the limiting conditions found in this organ. On the other hand, beta-glucosidase, polygalacturonases, beta-xylanases and beta-xylosidases are enzymes related to the degradation of cellulose, hemicellulose and pectin, compounds typically found in plant cell walls (Biswas *et al*., 1988; Lee *et al*., 1996; Beg *et al*., 2001; Gomathi *et al*., 2014). Therefore, despite the fact that these kinds of enzymes are usually associated with the degradation of plant cell walls, their up-regulation in a mammalian host might indicate their implication within a cluster that is activated along the infectious process and that includes other indispensable enzymes for the development of the infection.

The secondary metabolism has been strongly associated with fungal pathogenicity and with an increase in fungal pathogen virulence (Scharf *et al*., 2014, McDonagh *et al*., 2008). In our study, secondary metabolism was significantly highlighted on each day of infection, which is also observed in the chromosomal distribution of differentially expressed genes, as genes involved in this metabolism are usually located in sub-telomere regions (Palmer & Keller, 2010). Gliotoxin biosynthesis is a clear example of this kind of metabolism. In the previous study of *A. fumigatus* germination at 24 and 37ºC, some genes involved in this pathway showed up-regulation at 37ºC, and when the infection was compared to this germination, most of its genes were up-regulated on at least one day post-infection. In fact, *gliA*, *gliF*, *gliI*, *gliK*, and *gliP* were also present in the cluster highly expressed during the infectious process (Table 4.15 & Annex II). Several studies have demonstrated that gliotoxin production is not involved in virulence when cyclophosphamide was used in mice infections (Kwon-Chung & Sugui, 2009). However, the up-regulation found in our results, especially in the transporter used to secrete gliotoxin (*gliA*), may prove the importance of this toxin in *A. fumigatus* invasiveness. Indeed, Lewis *et al*. (2005) detected its presence in lung and serum of mice suffering from aspergilosis that had been previously immunocompromised by cyclophosphamide treatment. Therefore, even though this toxin does not seem to be involved in the virulence of this pathogen in neutropenic mice, its detection makes this pathway gain in importance as a target for diagnostic strategies.

During an infection, several nutrients may not be easily available in the host environment. Referring to metals, such as iron, zinc and manganese, a struggle for their acquisition is established between host and pathogen when an infection is developed (Ding *et al*., 2014). The iron in plasma is sequestered in phagosomal compartments or bound to proteins in the blood stream (Ganz, 2009) whereas zinc and manganese are chelated by immune cells (Corbin *et al*., 2008; Hood & Skaar, 2012). Therefore, it is quite reasonable to assume that in such limited nutrient conditions, metal uptake genes should be more highly expressed as an infection progresses. However, studying the infectious process using the germination as a control condition, the results were not as expected.

Among these, siderophore production, which is another important example of secondary metabolism and essential for the development of an infection, should be mentioned as it did not show up-regulation during the infectious process when the germination at 37ºC

was established as the control condition. The most remarkable expression data were found on the transcriptional factors *sreA* and *hapX*, which are necessary for maintaining iron homeostasis. As mentioned above, when iron concentrations are high enough, SreA represses the expression of the gene *hapX* and high-affinity iron uptake (Schrettl *et al*., 2008). However, during iron starvation conditions, HapX mediates the repression of *sreA*, activating iron uptake through siderophores (Schrettl *et al*., 2010). Moreover, studies carried out using Δ*sreA*, Δ*hapX*, Δ*sidA*, Δ*sidC* and Δ*sidD* mutants in murine models demonstrated the importance of siderophores during infection. While Δ*sreA* did not present attenuated virulence (Schrettl *et al*., 2008), Δ*hapX*, Δ*sidC* and Δ*sidD* did (Schrettl *et al*., 2007; 2010), the virulence being completely attenuated with Δ*sidA* (Hissen, 2005). In our results, *sreA* appeared up-regulated on two days post-infection whereas *hapX* showed down-regulation on all days analyzed. Other transcription factors related to siderophore production, such as SrbA, AcuM, HacA and MpkA, were also down-regulated during the infection, which explains the down-regulation detected for siderophores (Table 4.17). Therefore, it seems that siderophore biosynthesis is enhanced during the germination at 37ºC, decreasing its production once the infection has been established in kidneys. Indeed, siderophores seemed to be relevant during the first few hours of an intranasal infection (McDonagh *et al*., 2008), which may be due to a lower iron concentration in lungs, compared to kidneys, or to a higher need for siderophores during the germination at 37 ºC. It should be mentioned that down-regulations were not constant over the 4 days analyzed; suggesting that the siderophore pathway may be adapted according to the iron availability. On the other hand, the up-regulation found in the nonribosomal peptide synthase SidE might agree with Power *et al.* (2006), who proposed that this gene was not involved in siderophore production.

Zinc availability in living tissues is also quite low, as most of it is bound to intracellular and extracellular zinc-binding proteins (Iyengar & Woittiez, 1988; Foote & Delves, 1984) and, during an infection, it is chelated by neutrophils (Corbin *et al*., 2008; Hayden *et al*., 2013). As mentioned, *A. fumigatus* has two transcription factors and various transporters which are up-regulated in zinc-limiting conditions. Nevertheless, in our results, the transcription factor zafA, as well as zinc transporters, showed down-regulation during the infection, highlighting their intense activity during conidial germination. The absence of up-regulation during the infectious process may mean that there are no extreme zinc-limiting conditions in kidneys, even though the loss of

significant differences observed in some genes may indicate an adaptation of *A. fumigatus* to its availability, as in the case of iron.

Taking into account the nutrient-limited condition in host environment and the down-regulation detected in essential pathways related to metal adquisition, it is plausible that this fungus could obtain these compounds through other routes, for instance, hydrolase and phospholipase activity. Amongst hydrolases, proteases have been previously described as related to nutrient uptake in invasive growth as they are able to degrade collagen, elastin, fibrinogen and casein and their activity has been proved to be involved in the invasiveness of *A. fumigatus* strains (Reichard *et al*., 1990; Kolattukudy *et al*., 1993; Blanco *et al*., 2002). In our results, 22 proteases out of 102 differentially expressed were up-regulated during the infection (Table 4.16), among these, a dipeptidase (AFUA_6G11500) that also showed up-regulation during an intranasal infection (McDonagh *et al*., 2008). These enzymes hydrolyze polypeptides into smaller peptides and amino acids, facilitating their absorption by the cell (Rao *et al*., 1998) and increasing the availability of nutrients. An example of this could be found in iron. In mammals iron is stored in different proteins such as ferritin, transferrin, ferroxidase or lactoferrin (Pérez Surribas, 2005), some of which can be found in extracellular fluid or blood plasma (Gomme *et al*., 2005; Adlerova *et al*., 2008; Linder, 2013). Therefore, it is possible that following the breakdown of these proteins the iron concentration increases, raising the level of availability and reducing siderophore production. In the previous study in which fresh medium was added during the germination at 37ºC, a down-regulation of siderophore-related genes was observed, indicating that their regulation is highly related to iron availability. In the case of zinc, it should be highlighted that murine animals were immunocompromised by cyclophosphamide, decreasing their neutrophils levels. These cells are responsible for chelating this metal during an infection thanks to the calprotectin, a specific regulator of extracellular *A. fumigatus* hyphal growth (Clark *et al*., 2016) Therefore, this decrease in neutrophils might also affect zinc chelation and in turn, increase its availability.

Previous studies have suggested siderophores and zinc transporters as diagnostic or antifungal therapeutic targets owing to the fact that pathogen growth is altered in knockout strains (Schrettl *et al*., 2004; 2007; Moreno *et al*., 2007; Moore, 2013; Amich *et al*., 2014; Bertuzzi *et al*., 2014; Haas 2014; Vicentefranqueira *et al*., 2015). Nevertheless, according to our results these targets may only be useful during the

earliest stages of infection. It seems that once the infection is established in the kidney, a reduction in these nutrient uptake systems takes place and/or this pathogen obtains the nutrients required through other mechanisms, such as those mentioned above.

On the other hand, phospholipases break ester bonds of phosphoglycerides, destabilising host cell membranes and causing cell lysis (Rementeria *et al*., 2005). These proteins have been considered as virulence factors for other species such as *C. albicans* and *C. neoformans* (Ibrahim *et al*., 1995; Cox *et al*., 2001). In *A. fumigatus* their role in virulence is currently being discovered. Birch *et al*., (2004) raised doubts about their involvement in virulence, as the production of B phospholipases by *A. fumigatus* clinical isolates was lower than by environmental isolates, with only phospholipase C more highly expressed in clinical isolates. However, Winkelströter *et al.* (2015) have demonstrated the implication of PtcB phosphatase in *A. fumigatus* virulence, as an avirulent strain results from a Δ*ptcB* mutation, stressing its importance as virulence factor. In our results, 5 phospholipases appeared up-regulated during the germination at 37ºC. Nevertheless, phospholipase C (AFUA_7G04910) and lysophospholipase Plb2 were up-regulated along the infection. Therefore, it seems plausible to reconsider the role of these proteins during the infection of *A. fumigatus*.

Another nutrient that affects *A. fumigatus* growth is nitrogen. According to our results, several genes involved in its acquisition and utilization were significantly expressed, giving an insight into the nitrogen sources this pathogen found in kidneys. As mentioned previously, the main pathway to uptake this nutrient is the reduction of nitrate to ammonium and its final incorporation in the amino acids glutamate and glutamine (Pateman *et al*., 1967; Johnstone *et al*., 1990). According to our results, only the periplasmic nitrate reductase (AFUA_3G15190) showed up-regulation on every day of infection. However, different nitrogen sources also seemed to be available in these organs, such as ammonium and nitriles, whose transporters and genes involved in their hydrolysis were up-regulated *in vivo*. Amino acid may constitute another nitrogen source during *A. fumigatus* invasive growth as several transporters, and genes related to them showed up-regulation during the infection. Indeed, seven permeases were also up-regulated in bronchoalveolar lavages from infected mice (McDonagh *et al*. 2008), highlighting the role of this source of nitrogen during the infection. The differentially expression found in urea transporters and pseudouridine synthases should also be pointed out. Kidneys produce urine, which mainly contains urea as well as uridine and

pseudouridine (Koshida *et al.*, 1985; Yang & Bankir, 2005) so; these compounds might constitute another nitrogen source in these organs. On the other hand, the down-regulation of RhbA during the infection may support the hypothesis that the availability of nitrogen was not as limiting as thought. This gene seems to be implicated in *A. fumigatus* virulence and in nutrient sensing, up-regulating in nitrogen-limiting conditions (Panepinto *et al*. 2002). Therefore, according to our results, *A. fumigatus* might be provided with enough mechanisms to deal with nitrogen availability in kidneys without reaching nitrogen-limiting conditions.

Finally, it should be highlighted the large number of allergen that showed significant expression changes when the infection was compared to the germination at 37ºC. As shown in table 4.19, the main differences appeared in the comparison of day 1 with 14 allergens down-regulated on that day post-infection. In the previous study of the germination at 24 and 37ºC, allergen expression was up-regulated due to the temperature and nutrients of the medium. Therefore, the results obtained during the infection might reflect the importance of allergens during the germination of this pathogen.

The high percentage of differentially expressed genes coding for hypothetical or unclassified proteins that were up-regulated on each day post-infection should be emphasised. Analyzing the comparison of each day post-infection relative to the germination at 37ºC, around 50% of the 20 most up-regulated genes on each day corresponded to these kinds of proteins. The percentage was also remarkable in the cluster highly expressed *in vivo*. In this case, 37.2% and 15.5% of the genes corresponded to hypothetical and unclassified proteins. All these results highlight the importance these unknown genes may have during *A. fumigatus* infection and the intensive research that must be carried out as they may become targets for the diagnosis or treatment of IA.

To sum up, this is the first *A. fumigatus* transcriptomic study that analyzes its gene expression profiles over 4 days of a disseminated infection, comparing them to its germination at 37ºC. According to the results, expression patterns changed considerably between the growth *in vitro* and the established infection. It seems that it is during the earliest stages of germination that *A. fumigatus* has to deal with the host environment but once established, genes involved in polysaccharide and secondary metabolism,

transport systems and degradation/modification of foreign polysaccharides are enhanced to further develop the infection. On the other hand, essential elements such as nitrogen, iron and zinc seem to be available enough during the infectious process in the kidneys. Whereas amino acids, nitriles, ammonium or urea might provide the fungus with the nitrogen needed, siderophore and metal transport routes appeared down-regulated during the infection. This suggests that *A. fumigatus* might obtain these metals through other pathways, such as protease and phospholipase activities, with the possibility that these nutrients are released after protein degradation and cell lysis. Therefore, even though microarray data always produce preliminary results and further research needs to be carried out; the results cast doubt on the choice of metal acquisition routes for developing therapeutic and diagnostic methods. These targets may be useful only during the germination of this pathogen, or in preventive treatments, but not once the infection is established. Nevertheless, genes involved in polysaccharide and secondary metabolisms, and even those that encode unclassified and hypothetical proteins, stand out as indispensable pathways for extending the infection, underlining the need to gain further knowledge of these genes, as some of them could serve as diagnostic targets.

Considering microarray data, the next step was to choose a gene that seemed to have implication in the development of the infection and study the effect of its deletion. The strain chosen for knockout development was *A. fumigatus* Δ*akuB*^{KU80} as the homologous integration is higher than with other *A. fumigatus* strains (da Silva Ferreira *et al*., 2006). Following an intensive study, one route that showed up-regulation during the infection was melanin biosynthesis, which was described as an important virulence determinant in fungi, protecting against UV irradiation, host immune system and ROS (Langfelder *et al*., 2003). According to microarray data, three genes involved in its biosynthesis appeared up-regulated along the infectious process. This is interesting given that melanin is typically found in *A. fumigatus* conidia and biofilm (Beauvais *et al*., 2007), and the expression of its genes *in vivo* has been related to lung and nasal infections, but not to a disseminated infection (Youngchim *et al*., 2004). Amongst the three genes up-regulated on microarray results, *abr1/brown1* stood out as it showed the highest expression *in vivo* (Table 4.20). The FunCat categorization classifies this gene within the metabolism of vitamins, cofactors, and prosthetic groups; secondary metabolism; transport; disease, virulence and defense; and homeostasis. Taking all this into

consideration, *abr1/brown1* was chosen to develop an *A. fumigatus* knockout strain with the aim of determining whether this gene is involved in virulence or in other processes.

The deletion of the gene *abr1/brown1* generated a strain that produced brown colonies (Fig. 4.38). Phenotypic analysis showed that this gene might not be involved in osmotic, oxidative or cell wall stress. However, its implication in conidia production was confirmed as the number of conidia was significantly reduced relative to the wild type, with a complete loss of sporulation in the ninth week. Moreover, studying its growth on porcine tissues, a lack of sporulation was observed on kidney agar. These results could demonstrate that this gene is necessary for the proper growth in this organ, and in turn, during a disseminated infection. Cell line infections carried out with *A. fumigatus* Δ*abr1/brown1* conidia showed no statistical differences relative to the wild type. Nevertheless, when cells were infected with the culture filtrates, an increasing damage was observed, suggesting that this knockout might produce and secrete a toxic intermediate. Jackson *et al*., (2009) tested the deletion of the genes involved in melanin biosynthesis in *Galleria mellonella* and the virulence was enhanced in all cases with the exception of the mutant lacking the gene *abr1/brown1*. The toxicity found in the culture filtrates casts doubt on the results observed by these authors, which could be confirmed with a different animal model infection. So far, and according to our preliminary data, melanin biosynthesis does not seem to be an adequate target to prevent the infection given that highly pathogenic strains are developed with the deletion of its genes. However, an intensive research should be carried out to shed light on the pathogenicity of these knockout strains and the role of the melanin during the infection.

On the other hand, as transcription factors seem to be a promising strategy to study *A. fumigatus* virulence, a knockout strain of one of these genes was developed. Transcription factors are essential in the signal transduction pathways, being the last link between signal flow and target genes expression (Shelest, 2008). Therefore, this strategy gives the opportunity to identify virulence genes as one transcription factor frequently controls the expression of multiple genes. The choice was based on those up-regulated along the infectious process, being the transcription factor AFUA_1G02860 finally chosen. This gene was up-regulated on the 4 days post-infection.

The deletion of the transcription factor AFUA_1G02860 originates a knockout strain with dark green or dull green colonies and its growth under different stress conditions

showed no differences relative to the wild type. Thus, this transcription factor might not play an important role in osmotic or oxidative stress response. Moreover, as C-compound and carbohydrates metabolism was highly up-regulated along the infection, the growth with different carbon sources was studied, but no differences were found. Studying its growth on porcine tissues, there was an important loss of sporulation on kidney agar and even a slight decrease in radial growth on lung agar. Thus, this gene seems to be involved in the proper growth not only in kidney but also in lung, primary focus of invasive aspergillosis. Regarding cell line infections, a reduction in cell damage was only observed when A549 cells were infected with conidia of *A. fumigatus* Δ*tf*. According to the FunCat this transcription factor might be involved in secondary metabolism, but infections carried out with culture filtrates did not showed significant differences relative to the wild type, indicating that extracellular components did not differ with the deletion. All these results suggested that this transcription factor may regulate genes involved in cell damage that are activated during the germination, even though, more studies need to be done to shed light on the specific role of this gene.

The implication in pathogenesis of the genes deleted indicated that microarrays are a good strategy to select genes virtually related to the development of an infection. Furthermore, transcriptomic analysis of knockouts strains might give even more accurate information of their role. This way, the next step will be to perform mice infections and transcriptomic studies of the mutant strains developed. These results will allow us to assess whether any of them show attenuation in virulence and to shed light on the biological functions in which they are involved, which could lead to identify potentially targets to develop diagnostic and treatment methods.

6. CONCLUSIONS

1. The expression microarray designed demonstrated a high effectiveness and reliability on studying *Aspergillus fumigatus* transcriptome in different conditions, which allowed us to select genes highly up-regulated *in vivo* that might be involved in *A. fumigatus* pathogenesis.

2. *Aspergillus fumigatus* is able to change its metabolism and quickly adapt to the environment and host conditions, as observed after a heat shock before reaching 15-30% germination rates or in the first 24 hours after dissemination in mice.

3. Essential nutrients seem to be available enough for the fungus in kidneys which could be due to the activity of its degrading enzymes, down-regulating the uptake systems needed under starvation conditions.

4. The down-regulation observed in siderophore production and metal transport routes during a disseminated infection raises doubts about their potential as therapeutic or diagnostic methods.

5. The large number of differentially expressed genes that encode hypothetical or unclassified proteins not only during the germination but also along a disseminated infection stresses the importance that these unknown genes might have during *A. fumigatus* infection and points to avenues for future research.

6. The deletion of the conidial pigment biosynthesis oxidase Abr1/brown1 generates an isolate with an increase in host cell damage, which might suggest that melanin biosynthesis may not be a good target to develop therapies against IA.

7. The C_2H_2 transcription factor AFUA_1G02860 seems to be involved in host cell damage during the germination of *A. fumigatus* and in the proper growth in kidney and lung, gaining in importance as virulence factor.

7. REFERENCES

Abad A., Fernández-Molina J. V., Bikandi J., Ramírez A., Margareto J., Sendino J., Hernando F. L., Pontón J., Garaizar J., Rementeria A. 2010. What makes *Aspergillus fumigatu*s a sucessful pathogen? Genes and molecules involved in invasive aspergillosis. *Rev Iberoam Micol*. 27: 155-182.

Abarca L.M. 2000. Taxonomía e identificación de especies implicadas en la aspergilosis nosocomial. *Rev Iberoam Micol*. 17: S79-S84.

Adlerova L., Bartoskova A., Faldyna M. 2008. Lactoferrin: a review. *Veterinarni Medicina*. 53:457-468.

Alastruey-Izquierdo A., Mellado E., Cuenca-Estrella M. 2012. Current section and species complex concepts in *Aspergillus*: recommendations for routine daily practice. *Ann N Y Acad Sci.* 1273:18-24.

Alastruey-Izquierdo A., Mellado E., Peláez T., Pemán J., Zapico S., Alvarez M., Rodríguez-Tudela J.L., Cuenca-Estrella M. 2013. Population-based survey of filamentous fungi and antifungal resistance in Spain (FILPOP Study). *Antimicrob Agents Chemother*. 57:3380-3387.

Alker A.P., Mwapasa V., Meshnick S.R. 2004. Rapid real-time PCR genotyping of mutations associated with sulfadoxine-pyrimethamine resistance in *Plasmodium falciparum*. *Antimicrob Agents Chemother*. 48:2924-2929.

Amarsaikhan N., O'Dea E.M., Tsoggerel A., Owegi H., Gillenwater J., Templeton S.P. 2014. Isolate-dependent growth, virulence, and cell wall composition in the human pathogen *Aspergillus fumigatus*. *PLoS One*. 9:e100430.

Amich J., Bignell E. 2016. Amino acid biosynthetic routes as drug targets for pulmonary fungal pathogens: what is known and why do we need to know more? *Curr Opin Microbiol*. 32:151-158.

Amich J., Calera J.A. 2014. Zinc acquisition: a key aspect in *Aspergillus fumigatus* virulence. *Mycopathologia*. 178:379-385.

Amich J., Dümig M., O'Keeffe G., Binder J., Doyle S., Beilhack A., Krappmann S. 2016. Exploration of sulfur assimilation of *Aspergillus fumigatus* reveals biosynthesis of sulfur-containing amino acids as a virulence determinant. *Infect Immun*. 84:917-929.

Amich J., Schafferer L., Haas H., Krappmann S. 2013. Regulation of sulphur assimilation is essential for virulence and affects iron homeostasis of the human-pathogenic mould *Aspergillus fumigatus*. PLoS Pathog. 9:e1003573.

Amich J., Vicentefranqueira R., Leal F., Calera J.A. 2010. *Aspergillus fumigatus* survival in alkaline and extreme zinc-limiting environments relies on the induction of a zinc homeostasis system encoded by the *zrfC* and *aspf2* genes. *Eukaryot Cell*. 9:424-437.

Amich J., Vicentefranqueira R., Mellado E., Ruiz-Carmuega A., Leal F., Calera J.A. 2014. The ZrfC alkaline zinc transporter is required for *Aspergillus fumigatus* virulence and its growth in the presence of the Zn/Mn-chelating protein calprotectin. *Cell Microbiol*. 16:548-564.

Amitani R., Taylor G., Elezis E.N., Llewellyn-Jones C., Mitchell J. Kuze F., Cole P.J., Wilson R. 1995. Purification and characterization of factors produced by *Aspergillus fumigatus* which affect human ciliated respiratory epithelium. *Infect Immun*. 63:3266-3271.

Anderson, M., Denning, D. W. 2001. *Aspergillus fumigatus* isolate AF293 (NCPF 7367). http://www.aspergillus.org.uk/content/aspergillus-fumigatus-isolate-af293-ncpf-7367.

Araujo R., Rodrigues A.G. 2004. Variability of germinative potential among pathogenic species of *Aspergillus*. *J Clin Microbiol.* 42:4335-4337.

Arruda L.K., Platts-Mills T.A., Fox J.W., Chapman M.D. 1990. *Aspergillus fumigatus* allergen I, a major IgE-binding protein, is a member of the mitogillin family of cytotoxins. *J Exp Med*. 172:1529-1532.

Askew D.S. 2008. *Aspergillus fumigatus*: virulence genes in a street-smart mold. *Curr Opin Microbiol*. 11:331-337.

Balibar C.J., Walsh C.T. 2006. GliP, a multimodular nonribosomal peptide synthetase in *Aspergillus fumigatus*, makes the diketopiperazine scaffold of gliotoxin. *Biochemistry*. 45:15029-15038.

Banerjee B., Kurup V.P. 2003. Molecular biology of *Aspergillus* allergens. *Front Biosci*. 8:S128-S139.

Barhoom S., Sharon A. 2004. cAMP regulation of "pathogenic" and "saprophytic" fungal spore germination. *Fungal Genet Biol*. 41:317-326.

Bayram O., Braus G.H. 2012. Coordination of secondary metabolism and development in fungi: the velvet family of regulatory proteins. *FEMS Microbiol Rev*. 36:1-24.

Beauvais A., Bozza S., Kniemeyer O., Formosa C., Balloy V., Henry C., Roberson R.W., Dague E., Chignard M., Brakhage A.A., Romani L., Latgé J.P. 2013. Deletion of the α-(1,3)-glucan synthase genes induces a restructuring of the conidial cell wall responsible for the avirulence of *Aspergillus fumigatus*. *PLoS Pathog*. 9:e1003716.

Beauvais A., Latge J.P. 2001. Membrane and cell wall targets in *Aspergillus fumigatus*. *Drug Resist Updat*. 4:38-49.

Beauvais A., Schmidt C., Guadagnini S., Roux P., Perret E., Henry C., Paris S., Mallet A., Prévost M.C., Latgé J.P. 2007. An extracellular matrix glues together the aerial-grown hyphae of *Aspergillus fumigatus*. *Cell Microbiol*. 9:1588-1600.

Beffa T., Staib F., Lott Fischer J., Lyon P.F., Gumowski P., Marfenina O.E., Dunoyer-Geindre S., Georgen F., Roch-Susuki R., Gallaz L., Latgé J.P. 1998. Mycological control and surveillance of biological waste and compost. *Med Mycol*. 36 Suppl 1:137-145.

Beg Q.K., Kapoor M., Mahajan L., Hoondal G.S. 2001. Microbial xylanases and their industrial applications: a review. *Appl Microbiol Biotechnol*. 56:326-338.

Bertout S., Badoc C., Mallié M., Giaimis J., Bastide J.M. 2002. Spore diffusate isolated from some strains of *Aspergillus fumigatus* inhibits phagocytosis by murine alveolar macrophages. FEMS Immunol *Med Microbiol*. 33:101-106.

Bertout, S., Badoc C., Mallié M., Giaimis J., Bastide J.M. 2002. Spore diffusate isolated from some strains of *Aspergillus fumigatus* inhibits phagocytosis by murine alveolar macrophages. *FEMS Immunol Med Microbiol*. 33:101-106.

Bertuzzi M., Schrettl M., Alcazar-Fuoli L., Cairns T.C., Muñoz A., Walker L.A., Herbst S., Safari M., Cheverton A.M., Chen D., Liu H., Saijo S., Fedorova N.D., Armstrong-James D., Munro C.A., Read N.D., Filler S.G., Espeso E.A., Nierman W.C., Haas H., Bignell E.M. 2014. The pH-responsive PacC transcription factor of *Aspergillus fumigatus* governs epithelial entry and tissue invasion during pulmonary aspergillosis. *PLoS Pathog*. 10:e1004413.

Bhabhra R., Askew, D.S. 2005. Thermotolerance and virulence of *Aspergillus fumigatus*: role of the fungal nucleolus. *Med Mycol.* 43 Suppl 1:S87-S93.

Bièche I., Olivi M., Champème M.H., Vidaud D., Lidereau R., Vidaud M. 1998. Novel approach to quantitative polymerase chain reaction using real-time detection: application to the detection of gene amplification in breast cancer. *Int J Cancer*. 78:661-666.

Bignell E., Negrete-Urtasun S., Calcagno A.M., Haynes K., Arst H.N. Jr., Rogers T. 2005. The *Aspergillus* pH-responsive transcription factor PacC regulates virulence. *Mol Microbiol*. 55:1072-1084.

Birch M., Denning D.W., Robson G.D. 2004. Comparison of extracellular phospholipase activities in clinical and environmental *Aspergillus fumigatus* isolates. *Med Mycol*. 42:81-86.

Biswas S.R., Mishra A.K., Nand, G. 1988. Xylanase and beta-xylosidase production by *Aspergillus ochraceus* during growth on lignocelluloses. *Biotechnol Bioeng*. 31:613-616.

Blanco J.L., Hontecillas R., Bouza E., Blanco I., Pelaez T., Muñoz P., Perez Molina J., Garcia M.E. 2002. Correlation between the elastase activity index and invasiveness of clinical isolates of *Aspergillus fumigatus*. *J Clin Microbiol*. 40:1811-1813.

Blatzer M., Schrettl M., Sarg B., Lindner H.H., Pfaller K., Haas H. 2011. SidL, an *Aspergillus fumigatus* transacetylase involved in biosynthesis of the siderophores ferricrocin and hydroxyferricrocin. *Appl Environ Microbiol*. 77:4959-4966.

Bok J.W., Chung D., Balajee S.A., Marr K.A., Andes D., Nielsen K.F., Frisvad J.C., Kirby K.A., Keller N.P. 2006. GliZ, a transcriptional regulator of gliotoxin biosynthesis, contributes to *Aspergillus fumigatus* virulence. *Infect Immun*. 74:6761-6768.

Brakhage A.A., Langfelder K. 2002. Menacing mold: the molecular biology of *Aspergillus fumigatus*. *Annu Rev Microbiol*. 56:433-455.

Brakhage A.A., Liebmann B. 2005. *Aspergillus fum*igatus conidial pigment and cAMP signal transduction: significance for virulence. *Med Mycol*. 43 Suppl 1:S75-S82.

Brazma A., Vilo J. 2000. Gene expression data analysis. *FEBS Lett*. 480:17-24.

Breakspear A., Momany M. 2007. The first fifty microarray studies in filamentous fungi. *Microbiology*. 153:7-15.

Brown G.D., Denning D.W., Gow N.A., Levitz S.M., Netea M.G., White T.C. 2013. Hidden killers: human fungal infections. *Sci Transl* Med. 4:165rv13.

Bryant P.A., Venter D., Robins-Browne R., Curtis N. 2004. Chips with everything: DNA microarrays in infectious diseases. *Lancet Infect Dis*. 4:100-111.

Bullen J.J. 1981. The significance of iron in infection. *Rev Infect Dis*. 3:1127-1138.

Bünger J., Westphal G., Mönnich A., Hinnendahl B., Hallier E., Müller M. 2004. Cytotoxicity of occupationally and environmentally relevant mycotoxins. *Toxicology*. 202:199-211.

Burger G., Strauss J., Scazzocchio C., Lang B.F. 1991. *nirA*, the pathway-specific regulatory gene of nitrate assimilation in *Aspergillus nidulans*, encodes a putative GAL4-type zinc finger protein and contains four introns in highly conserved regions. *Mol Cell Biol*. 11:5746-5755.

Calera J.A., Paris S., Monod M., Hamilton A.J., Debeaupuis J.P., Diaquin M., López-Medrano R., Leal F., Latgé J.P. 1997. Cloning and disruption of the antigenic catalase gene of *Aspergillus fumigatus*. *Infect Immun*. 65:4718-4724.

Carlile M.J., Watkinson S.C., Gooday G. 2001. Fungal cells and vegetative growth. In: The Fungi. 2ª ed. Academic Press. USA. p. 85-184.

Chaudhary N., Marr K.A. 2011. Impact of *Aspergillus fumigatus* in allergic airway diseases. *Clin Transl Allergy*. 1:4.

Cheng J., Zhang Y., Li Q. 2004. Real-time PCR genotyping using displacing probes. *Nucleic Acids Res*. 32:e61.

Clark H.L., Jhingran A., Sun Y., Vareechon C., de Jesus Carrion S., Skaar E.P., Chazin W.J., Calera J.A., Hohl T.M., Pearlman E. 2016. Zinc and Manganese chelation by neutrophil S100A8/A9 (Calprotectin) limits extracellular *Aspergillus fumigatus* hyphal growth and corneal infection. *J Immunol*. 196:336-344.

Clemons K.V., Stevens D.A. 2005. The contribution of animal models of aspergillosis to understanding pathogenesis, therapy and virulence. *Med Mycol*. 43 Suppl 1:S101-S110.

Corbin B.D., Seeley E.H., Raab A., Feldmann J., Miller M.R., Torres V.J., Anderson K.L., Dattilo B.M., Dunman P.M., Gerads R., Caprioli R.M., Nacken W., Chazin W.J., Skaar E.P. 2008. Metal chelation and inhibition of bacterial growth in tissue abscesses. *Science*. 319:962-965.

Cox G.M., McDade H.C., Chen S.C., Tucker S.C., Gottfredsson M., Wright L.C., Sorrell T.C., Leidich S.D., Casadevall A., Ghannoum M.A., Perfect J.R. 2001. Extracellular phospholipase activity is a virulence factor for *Cryptococcus neoformans*. *Mol Microbiol*. 39:166-175.

Coyle C.M., Kenaley S.C., Rittenour W.R., Panaccione D.G. 2007. Association of ergot alkaloids with conidiation in *Aspergillus fumigatus*. *Mycologia*. 99:804-811.

Cramer R.A. Jr., Gamcsik M.P., Brooking R.M., Najvar L.K., Kirkpatrick W.R., Patterson T.F., Balibar C.J., Graybill J.R., Perfect J.R., Abraham S.N., Steinbach W.J. 2006. Disruption of a nonribosomal peptide synthetase in *Aspergillus fumigatus* eliminates gliotoxin production. *Eukaryot Cell*. 5:972-980.

Cramer R.A., Rivera A., Hohl T.M. 2011. Immune responses against *Aspergillus fumigatus*: what have we learned?. *Curr Opin Infect Dis*. 24:315-322.

Crameri R. 1998. Recombinant *Aspergillus fumigatus* allergens: from the nucleotide sequences to clinical applications. *Int Arch Allergy Immunol*. 115:99-114.

Crameri R. 1999. Epidemiology and molecular basis of the involvement of *Aspergillus fumigatus* in allergic diseases. *Contrib Microbiol*. 2:44-56.

Crameri R., Glaser A.G., Vilhelmsson M., Zeller S., Rhyner C. 2010. Overview of *Aspergillus allergens*. In: Aspergillosis: from diagnosis to prevention. Pasqualotto AC (ed). Springer. UK. p.655-69.

da Silva Ferreira M.E., Kress M.R., Savoldi M., Goldman M.H., Härtl A., Heinekamp T., Brakhage A.A., Goldman G.H. 2006. The *akuB*^{KU80} mutant deficient for nonhomologous end joining is a powerful tool for analyzing pathogenicity in *Aspergillus fumigatus*. *Eukaryot Cell*. 5:207-211.

da Silva Ferreira M.E., Malavazi I., Savoldi M., Brakhage A.A., Goldman M.H., Kim H.S., Nierman W.C., Goldman G.H. 2006. Transcriptome analysis of *Aspergillus fumigatus* exposed to voriconazole. *Curr Genet*. 50:32-44.

Dagenais T.R.T., Keller N.P. 2009. Pathogenesis of *Aspergillus fumigatus* in invasive aspergillosis. *Clin Microbiol Rev*. 22: 447-465.

de Vries R.P., Visser J. 2001. *Aspergillus* enzymes involved in degradation of plant cell wall polysaccharides. *Microbiol Mol Biol Rev*. 65:497-522.

del Palacio A., Cuétara M. S., Pontón J. 2003. El diagnóstico de laboratorio de la aspergilosis invasora. *Rev Iberoam Micol*. 20:90-98.

del Palacio A., Cuétara M.S., Pontón J. 2003. Invasive aspergillosis. *Rev Iberoam Micol*. 20:77-78.

d'Enfert C. 1997. Fungal spore germination: insights from the molecular genetics of *Aspergillus nidulans* and *Neurospora crassa*. *Fungal Genet. Biol*. 21:163-172.

Denning D.W. 2006. *Aspergillosis*. Schering-Plough Corporation. UK. p. 1-76.

Denning, D.W. 1998. Invasive aspergillosis. Clin Infect Dis. 26:781-805.

Dhingra S., Andes D., Calvo A.M. 2012. VeA regulates conidiation, gliotoxin production, and protease activity in the opportunistic human pathogen *Aspergillus fumigatus*. *Eukaryot Cell*. 11:1531-1543.

Ding C., Festa R.A., Sun T.S., Wang Z.Y. 2014. Iron and copper as virulence modulators in human fungal pathogens. *Mol Microbiol*. 93:10-23.

Dolan S.K., O'Keeffe G., Jones G.W., Doyle S. 2015. Resistance is not futile: gliotoxin biosynthesis, functionality and utility. *Trends Microbiol*. 23:419-428.

Drakos P.E., Nagler A., Or R., Naparstek E., Kapelushnik J., Engelhard D., Rahav G., Ne'emean D., Slavin S. 1993. Invasive fungal sinusitis in patients undergoing bone marrow transplantation. *Bone Marrow Transplant*. 12:203-208.

Eichner R.D., Al Salami M., Wood P.R., Müllbacher A. 1986. The effect of gliotoxin upon macrophage function. *Int J Immunopharmacol*. 8:789-797.

Eisendle M., Schrettl M., Kragl C., Müller D., Illmer P., Haas H. 2006. The intracellular siderophore ferricrocin is involved in iron storage, oxidative-stress resistance, germination, and sexual development in *Aspergillus nidulans*. *Eukaryot Cell*. 5:1596-1603.

Ejzykowicz D.E., Cunha M.M., Rozental S., Solis N.V., Gravelat F.N., Sheppard D.C., Filler S.G. 2009. The *Aspergillus fumigatus* transcription factor Ace2 governs pigment production, conidiation and virulence. *Mol Microbiol*. 72:155-169.

El-Fallal A., Abou Dobara M., El-Sayed A., Omar N. 2012. Starch and Microbial α-Amylases: From Concepts to Biotechnological Applications. In: Carbohydrates - Comprehensive Studies on Glycobiology and Glycotechnology. Chuan-Fa Chang, editor. Egypt: InTech. p. 459-488.

Farnell E., Rousseau K., Thornton D.J., Bowyer P., Herrick S.E. 2012. Expression and secretion of *Aspergillus fumigatus* proteases are regulated in response to different protein substrates. *Fungal Biol*. 116:1003-1012.

Flückiger S., Mittl P.R., Scapozza L., Fijten H., Folkers G., Grütter M.G., Blaser K., Crameri R. 2002. Comparison of the crystal structures of the human manganese superoxide dismutase and the homologous *Aspergillus fumigatus* allergen at 2-A resolution. *J Immunol*. 168:1267-1272.

Foote J.W., Delves H.T. 1984. Albumin bound and alpha 2-macroglobulin bound zinc concentrations in the sera of healthy adults. *J Clin Pathol*. 37:1050-1054.

Fortún J., Meije Y., Fresco G., Moreno S. 2012. Aspergilosis. Formas clínicas y tratamiento. *Enferm Infecc Microbiol Clin*. 30:201-208.

Fraczek M.G., Rashid R., Denson M., Denning D.W., Bowyer P. 2010. *Aspergillus fumigatus* allergen expression is coordinately regulated in response to hydrogen peroxide and cyclic AMP. *Clin Mol Allergy*. 8:15.

Fraga D., Meulia T., Fenster S. 2008. Real Time PCR. In: Current Protocols Essential Laboratory Techniques. Gallagher S.R., Wiley E.A. (eds). John Wiley & Sons. USA. p. 10.3.1-103.33.

Gaither L.A., Eide D.J. 2001. Eukaryotic zinc transporters and their regulation. *Biometals*. 14:251-270.

Gallagher L., Owens R.A., Dolan S.K., O'Keeffe G., Schrettl M., Kavanagh K., Jones G.W., Doyle S. 2012. The *Aspergillus fumigatus* protein GliK protects against oxidative stress and is essential for gliotoxin biosynthesis. *Eukaryot Cell*. 11:1226-1238.

Gams W., Christensen M., Onions A.H., Pitt J.I., Samson R.A. 1985. Infrageneric taxa of *Aspergillus*. In: Advances in *Penicillium* and *Aspergillus* Systematics. Samson R.A., Pitt J.I. (eds). Plenum Press. USA. p.55-62.

Ganz T. 2009. Iron in innate immunity: starve the invaders. *Curr Opin Immunol*. 21:63-67.

García M.E., Caballero J., Blanco I., Cruzado M., Costas E., Blanco J.L. 2006. Changes in the elastase activity and colonization ability of *Aspergillus fumigatus* after successive inoculations in mice. *Rev Iberoam Micol*. 23:221-223.

Gardiner D.M., Howlett B.J. 2005. Bioinformatic and expression analysis of the putative gliotoxin biosynthetic gene cluster of *Aspergillus fumigatus*. *FEMS Microbiol Lett*. 248:241-248.

Gastebois A., Clavaud C., Aimanianda V., Latge J.P. 2009. *Aspergillus fumigatus*: cell wall polysaccharides, their biosynthesis and organization. *Future Microbiol*. 4:583-595.

Gehrke A., Heinekamp T., Jacobsen I.D., Brakhage A.A. 2010. Heptahelical receptors GprC and GprD of *Aspergillus fumigatus* are essential regulators of colony growth, hyphal morphogenesis, and virulence. *Appl Environ Microbiol*. 76:3989-3998.

Gerson S.L., Talbot G.H., Hurwitz S., Strom B.L., Lusk E.J., Cassileth P.A. 1984. Prolonged granulocytopenia: the major risk factor for invasive pulmonary aspergillosis in patients with acute leukemia. *Ann Intern Med*. 100:345-51.

Gibson N.J. 2006. The use of real-time PCR methods in DNA sequence variation analysis. *Clin Chim Acta*. 363:32-47.

Glass N.L., Rasmussen C., Roca M.G., Read N.D. 2004. Hyphal homing, fusion and mycelial interconnectedness. *Trends Microbiol*. 12:135-141.

Gomathi V., Gayathri S., Anupama B., Teixeira da Silva J.A., Gnanamanickam S.S. 2014. Molecular Aspects of Polygalacturonase- Inhibiting Proteins (PGIPs) in Plant Defense. In: Floriculture, Ornamental and Plant Biotechnology. Advances and Topical Issues. Teixeira da Silva, JA, editor. Global Science Books. Japan. p. 373-379.

Gomme P.T., McCann K.B., Bertolini J. 2005. Transferrin: structure, function and potential therapeutic actions. *Drug Discov Today*. 10:267-273.

Gravelat F.N., Doedt T., Chiang L.Y., Liu H., Filler S.G., Patterson T.F., Sheppard D.C. 2008. In vivo analysis of *Aspergillus fumigatus* developmental gene expression determined by real-time reverse transcription-PCR. *Infect Immun*. 76:3632-3639.

Greene R. 2005. The radiological spectrum of pulmonary aspergillosis. *Med Mycol*. 43 Suppl 1:S147-S154.

Grovel O., Pouchus Y., Robiou du Pont T., Montagu M., Amzil Z., Verbist J. 2002. Ion trap MS(n) for identification of gliotoxin as the cytotoxic factor of a marine strain of *Aspergillus fumigatus* Fresenius. *J Microbiol Methods*. 48:171-179.

Gsaller F., Hortschansky P., Beattie S.R., Klammer V., Tuppatsch K., Lechner B.E., Rietzschel N., Werner E.R., Vogan A.A., Chung D., Mühlenhoff U., Kato M., Cramer R.A., Brakhage A.A., Haas H. 2014. The Janus transcription factor HapX controls fungal adaptation to both iron starvation and iron excess. *EMBO J*. 33:2261-2276.

Guarro J. 2003. Etiología de la aspergilosis invasora. In: Guía de bolsillo de la aspergilosis invasora. Pontón J. (ed.). Revista Iberoamericana de Micología. Spain. p. 9-12.

Guarro J., Orzechowski X., Severo L.C. 2010. Differences and similarities amongst Pathogenic *Aspergillus* species. In: Aspergillosis: from diagnosis to prevention. Pasqualotto A.C. (ed). Springer. Netherlands. p. 7-32.

Haas C.E., Rodionov D.A., Kropat J., Malasarn D., Merchant S.S., de Crécy-Lagard V. 2009. A subset of the diverse COG0523 family of putative metal chaperones is linked to zinc homeostasis in all kingdoms of life. *BMC Genomics*. 10:470.

Haas H. 2014. Fungal siderophore metabolism with a focus on *Aspergillus fumigatus*. *Nat Prod Rep*. 31:1266-1276.

Haas H., Eisendle M., Turgeon B.G. 2008. Siderophores in fungal physiology and virulence. *Annu Rev Phytopathol*. 46:149-187.

Halliwell B., Gutteridge J.M. 1984. Role of iron in oxygen radical reactions. *Methods Enzymol*. 105:47-56.

Harris S.D. 2006. Cell polarity in filamentous fungi: shaping the mold. *Int Rev Cytol*. 251:41-77.

Harris S.D., Momany M. 2004. Polarity in filamentous fungi: moving beyond the yeast paradigm. *Fungal Genet Biol*. 41:391-400.

Hartmann T., Sasse C., Schedler A., Hasenberg M., Gunzer M., Krappmann S. 2011. Shaping the fungal adaptome--stress responses of *Aspergillus fumigatus*. *Int J Med Microbiol*. 301:408-416.

Hau J. 2008. Animal Models for Human Diseases: An Overview. In: Sourcebook of models for biomedical research. Conn P.M. (ed). Humana Press. USA. p. 3-24.

Hawksworth D.L., Crous P.W., Redhead S.A., Reynolds D.R., Samson R.A., Seifert K.A., Taylor J.W., Wingfield M.J., Abaci O., Aime C., Asan A., Bai F.Y., de Beer Z.W., Begerow D., Berikten D., Boekhout T., Buchanan P.K., Burgess T., Buzina W., Cai L., Cannon P.F., Crane J.L., Damm U., Daniel H.M., van Diepeningen A.D., Druzhinina I., Dyer P.S., Eberhardt U., Fell J.W., Frisvad J.C., Geiser D.M., Geml J., Glienke C., Gräfenhan T., Groenewald J.Z., Groenewald M., de Gruyter J., Guého-Kellermann E., Guo L.D., Hibbett D.S., Hong S.B., de Hoog G.S., Houbraken J., Huhndorf S.M., Hyde K.D., Ismail A., Johnston P.R., Kadaifciler D.G., Kirk P.M., Kõljalg U., Kurtzman C.P., Lagneau P.E., Lévesque C.A., Liu X., Lombard L., Meyer W., Miller A., Minter D.W., Najafzadeh M.J., Norvell L., Ozerskaya S.M., Oziç R., Pennycook S.R., Peterson S.W., Pettersson O.V., Quaedvlieg W., Robert V.A., Ruibal C., Schnürer J., Schroers H.J., Shivas R., Slippers B., Spierenburg H., Takashima M., Taşkın E., Thines M., Thrane U., Uztan A.H., van Raak M., Varga J., Vasco A., Verkley G., Videira S.I., de Vries R.P., Weir B.S., Yilmaz N., Yurkov A., Zhang N. 2011. The amsterdam declaration on fungal nomenclature. *IMA Fungus*. 2:105-112.

Hayden J.A., Brophy M.B., Cunden L.S., Nolan E.M. 2013. High-affinity manganese coordination by human calprotectin is calcium-dependent and requires the histidine-rich site formed at the dimer interface. *J Am Chem Soc*. 135:775-787.

Heinekamp T., Thywißen A., Macheleidt J., Keller S., Valiante V., Brakhage A.A. 2013. *Aspergillus fumigatus* melanins: interference with the host endocytosis pathway and impact on virulence. *Front Microbiol*. 3:440.

Hensel M., Arst H.N. Jr, Aufauvre-Brown A., Holden D.W. 1998. The role of the *Aspergillus fumigatus* areA gene in invasive pulmonary aspergillosis. *Mol Gen Genet*. 258:553-557.

Higuchi R., Dollinger G., Walsh P.S., Griffith R. 1992. Simultaneous amplification and detection of specific DNA sequences. *Biotechnology* (NY). 10:413-417.

Higuchi R., Fockler C., Dollinger G., Watson R. 1993. Kinetic PCR analysis: real-time monitoring of DNA amplification reactions. *Biotechnology* (NY). 11:1026-1030.

Hissen A.H., Wan A.N., Warwas M.L., Pinto L.J., Moore M.M. 2005. The *Aspergillus fumigatus* siderophore biosynthetic gene *sidA*, encoding L-ornithine N5-oxygenase, is required for virulence. *Infect Immun*. 73:5493-5503.

Hohl T.M. 2014. Overview of vertebrate animal models of fungal infection. *J Immunol Methods*. 410:100-112.

Hohl T.M., Feldmesser M. 2007. *Aspergillus fumigatus*: principles of pathogenesis and host defense. *Eukaryot Cell*. 6:1953-1963.

Holdom M.D., Lechenne B., Hay R.J., Hamilton A.J., Monod M. 2000. Production and characterization of recombinant *Aspergillus fumigatus* Cu, Zn superoxide dismutase and its recognition by immune human sera. *J Clin Microbiol*. 38:558-562.

Hood M.I., Skaar E.P. 2012. Nutritional immunity: transition metals at the pathogen-host interface. *Nat Rev Microbiol*. 10:525-537.

Hope W.W., Walsh T.J., Denning D.W. 2005a. Laboratory diagnosis of invasive aspergillosis. *Lancet Infect Dis.* 5:609-622.

Hope W.W., Walsh T.J., Denning D.W. 2005b. The invasive and saprophytic syndromes due to *Aspergillus* spp. Med Mycol.43 Suppl 1:S207-S238.

Houbraken J., de Vries R.P., Samson R.A. 2014. Modern taxonomy of biotechnologically important *Aspergillus* and *Penicillium* species. *Adv Appl Microbiol*. 86:199-249.

Hubka V., Nováková A., Kolarík A., Jurjević Ž., Peterson S.W. 2014. Revision of *Aspergillus* section Flavipedes: seven new species and proposal of section Jani sect. nov. *Mycologia.* 107:169-208.

Hwang C.S., Baek Y.U., Yim H.S., Kang S.O. 2003. Protective roles of mitochondrial manganese-containing superoxide dismutase against various stresses in *Candida albicans*. *Yeast.* 20:929-941.

Ibrahim A.S., Mirbod F., Filler S.G., Banno Y., Cole G.T., Kitajima Y., Edwards J.E. Jr., Nozawa Y., Ghannoum M.A. 1995. Evidence implicating phospholipase as a virulence factor of *Candida albicans*. *Infect Immun*. 63:1993-1998.

Ibrahim-Granet O., Dubourdeau M., Latgé J.P., Ave P., Huerre M., Brakhage A.A., Brock M. 2008. Methylcitrate synthase from *Aspergillus fumigatus* is essential for manifestation of invasive aspergillosis. *Cell Microbiol*. 10:134-148.

Ibrahim-Granet O., Philippe B., Boleti H., Boisvieux-Ulrich E., Grenet D., Stern M., Latgé J.P. 2003. Phagocytosis and intracellular fate of *Aspergillus fumigatus* conidia in alveolar macrophages. *Infect Immun*. 71:891-903.

Iyengar V., Woittiez J. 1988. Trace elements in human clinical specimens: evaluation of literature data to identify reference values. *Clin Chem*. 34:474-481.

Jackson J.C., Higgins L.A., Lin X. 2009. Conidiation color mutants of *Aspergillus fumigatus* are highly pathogenic to the heterologous insect host Galleria mellonella. *PLoS One*. 4:e4224.

Jadoun J., Shadkchan Y., Osherov N. 2004. Disruption of the *Aspergillus fumigatus argB* gene using a novel in vitro transposon-based mutagenesis approach. *Curr Genet*. 45:235-241.

Jahn B., Langfelder K., Schneider U., Schindel C., Brakhage A.A. 2002. PKSP-dependent reduction of phagolysosome fusion and intracellular kill of *Aspergillus fumigatus* conidia by human monocyte-derived macrophages. *Cell Microbiol*. 4:793-803.

Jain R., Valiante V., Remme N., Docimo T., Heinekamp T., Hertweck C., Gershenzon J., Haas H., Brakhage A.A. 2011. The MAP kinase MpkA controls cell wall integrity, oxidative stress response, gliotoxin production and iron adaptation in *Aspergillus fumigatus*. *Mol Microbiol*. 82:39-53.

Jiang H., Shen Y., Liu W., Lu L. 2014. Deletion of the putative stretch-activated ion channel Mid1 is hypervirulent in *Aspergillus fumigatus*. *Fungal Genet Biol*. 62:62-70.

Johnstone I.L., McCabe P.C., Greaves P., Gurr S.J., Cole G.E., Brow M.A., Unkles S.E., Clutterbuck A.J., Kinghorn J.R., Innis M.A. 1990. Isolation and characterisation of the *crnA-niiA-niaD* gene cluster for nitrate assimilation in *Aspergillus nidulans*. *Gene*. 90:181-192.

Jouvion G., Brock M., Droin-Bergère S., Ibrahim-Granet O. 2012. Duality of liver and kidney lesions after systemic infection of immunosuppressed and immunocompetent mice with *Aspergillus fumigatus*. *Virulence*. 3:43-50.

Kao R., Davies J. 1995. Fungal ribotoxins: a family of naturally engineered targeted toxins? *Biochem Cell Biol*. 73:1151-1159.

Kao R., Davies J. 1999. Molecular dissection of mitogillin reveals that the fungal ribotoxins are a family of natural genetically engineered ribonucleases. *J Biol Chem*. 274:12576-12582.

Kauffman H.F., Tomee J.F., van de Riet M.A., Timmerman A.J., Borger P. 2000. Protease-dependent activation of epithelial cells by fungal allergens leads to morphologic changes and cytokine production. *J Allergy Clin Immunol*. 105:1185-1193.

Kaur S., Singh S. 2014. Biofilm formation by *Aspergillus fumigatus*. *Med Mycol*. 52:2-9.

Kindich R., Florl A.R., Jung V., Engers R., Müller M., Schulz W.A., Wullich B. 2005. Application of a modified real-time PCR technique for relative gene copy number quantification to the determination of the relationship between NKX3.1 loss and MYC gain in prostate cancer. *Clin Chem*. 51:649-652.

Knutsen A.P., Hutcheson P.S., Slavin R.G., Kurup V.P. 2004. IgE antibody to *Aspergillus fumigatus* recombinant allergens in cystic fibrosis patients with allergic bronchopulmonary aspergillosis. *Allergy*. 59:198-203.

Köhli M., Galati V., Boudier K., Roberson R.W., Philippsen P. 2008. Growth-speed-correlated localization of exocyst and polarisome components in growth zones of *Ashbya gossypii* hyphal tips. *J Cell Sci*. 121:3878-389.

Kolattukudy P.E., Lee J.D., Rogers L.M., Zimmerman P., Ceselski S., Fox B., Stein B., Copelan E.A. 1993. Evidence for possible involvement of an elastolytic serine protease in aspergillosis. *Infect Immun*. 61:2357-2368.

Königshoff M., Wilhelm J., Bohle R.M., Pingoud A., Hahn M. 2003. HER-2/neu gene copy number quantified by real-time PCR: comparison of gene amplification, heterozygosity, and immunohistochemical status in breast cancer tissue. *Clin Chem*. 49:219-229.

Koshida K., Harmenberg J., Borgström E., Wahren B., Andersson L. 1985. Pseudouridine and uridine in normal kidney and kidney cancer tissues. *Urol Res*. 13:219-221.

Kousha M., Tadi R., Soubani A.O. 2011. Pulmonary aspergillosis: a clinical review. *Eur Respir Rev*. 20:156-74.

Krappmann S. 2008. Pathogenicity determinants and allergens. In: The aspergilli. Goldman GH, Osmani SA (eds).CRC Press. USA. p. 377-400.

Krappmann S., Bignell E.M., Reichard U., Rogers T., Haynes K., Braus G.H. 2004. The *Aspergillus fumigatus* transcriptional activator CpcA contributes significantly to the virulence of this fungal pathogen. *Mol Microbiol*. 52:785-799.

Krappmann S., Braus G.H. 2005. Nitrogen metabolism of *Aspergillus* and its role in pathogenicity. *Med Mycol*. 43 Suppl 1:S31-40.

Krebs H.A., Yoshida T. 1963. Renal gluconeogenesis. 2. The gluconeogenic capacity of the kidney cortex of various species. *Biochem J*. 89:398-400.

Krijgsheld P., Bleichrodt R., van Veluw G.J., Wang F., Müller W.H., Dijksterhuis J., Wösten H.A. 2013. Development in *Aspergillus*. *Stud Mycol*. 74:1-29.

Krishnan K., Ren Z., Losada L., Nierman W.C., Lu L.J., Askew, D.S. 2014. Polysome profiling reveals broad translatome remodeling during endoplasmic reticulum (ER) stress in the pathogenic fungus *Aspergillus fumigatus*. *BMC Genomics* 15:159.

Kudla B., Caddick M.X., Langdon T., Martinez-Rossi N.M., Bennett C.F., Sibley S., Davies R.W., Arst H.N. Jr. 1990. The regulatory gene *areA* mediating nitrogen metabolite repression in *Aspergillus nidulans*. Mutations affecting specificity of gene activation alter a loop residue of a putative zinc finger. *EMBO J*. 9:1355-1364.

Kumagai T., Nagata T., Kudo Y., Fukuchi Y., Ebina K., Yokota K. 1999. Cytotoxic activity and cytokine gene induction of Asp-hemolysin to murine macrophages. *Nippon Ishinkin Gakkai Zasshi*. 40:217-222.

Kumar A., Reddy L.V., Sochanik A., Kurup V.P. 1993. Isolation and characterization of a recombinant heat shock protein of *Aspergillus fumigatus*. *J Allergy Clin Immunol*. 91:1024-30.

Kupfahl C., Heinekamp T., Geginat G., Ruppert T., Härtl A., Hof H., Brakhage A.A. 2006. Deletion of the *gliP* gene of *Aspergillus fumigatus* results in loss of gliotoxin production but has no effect on virulence of the fungus in a low-dose mouse infection model. *Mol Microbiol*. 62:292-302.

Kupfahl C., Michalka A., Lass-Flörl C., Fischer G., Haase G., Ruppert T., Geginat G., Hof H. 2008. Gliotoxin production by clinical and environmental *Aspergillus fumigatus* strains. *Int J Med Microbiol*. 298:319-327.

Kweon Y.O., Paik Y.H., Schnabl B., Qian T., Lemasters J.J., Brenner D.A. 2003. Gliotoxin-mediated apoptosis of activated human hepatic stellate cells. *J Hepatol*. 39:38-46.

Kwon-Chung K.J., Sugui J.A. 2009. What do we know about the role of gliotoxin in the pathobiology of *Aspergillus fumigatus*?. *Med Mycol*. 47 Suppl 1:S97-S103.

Kwon-Chung, K.J., Sugui, J.A. 2013. *Aspergillus fumigatus*-What makes the species a ubiquitous human fungal pathogen?. *PLoS Pathog*. 9: e1003743.

Lamarre C., LeMay J.D., Deslauriers N., Bourbonnais Y. 2001. *Candida albicans* expresses an unusual cytoplasmic manganese-containing superoxide dismutase (SOD3 gene product) upon the entry and during the stationary phase. *J Biol Chem*. 276:43784-43791.

Lamarre C., Sokol S., Debeaupuis J.P., Henry C., Lacroix C., Glaser P., Coppée J.Y., François J.M., Latgé J.P. 2008. Transcriptomic analysis of the exit from dormancy of *Aspergillus fumigatus* conidia. *BMC Genomics*. 9:417.

Lambou K., Lamarre C., Beau R., Dufour N., Latge J.P. 2010. Functional analysis of the superoxide dismutase family in *Aspergillus fumigatus*. *Mol Microbiol*. 75:910-923.

Langfelder K., Streibel M., Jahn B., Haase G., Brakhage A.A. 2003. Biosynthesis of fungal melanins and their importance for human pathogenic fungi. *Fungal Genet Biol*. 38:143-158.

Latchman D.S. 1993. Transcription factors: an overview. *Int J Exp Pathol*. 74:417-422.

Latgé J.P. *Aspergillus fumigatus* and aspergillosis. 1999. *Clin Microbiol Rev*. 12:310-350.

Lee J, Kwon KS, Hah YC. 1996. Regulation of beta-glucosidase biosynthesis in *Aspergillus nidulans*. *FEMS Microbiol Lett*. 135:79-84.

Lee J.D., Kolattukudy P.E. 1995. Molecular cloning of the cDNA and gene for an elastinolytic aspartic proteinase from *Aspergillus fumigatus* and evidence of its secretion by the fungus during invasion of the host lung. *Infect Immun*. 63:3796-3803.

Lee M.J., Sheppard D.C. 2016. Recent advances in the understanding of the *Aspergillus fumigatus* cell wall. *J Microbiol*. 54:232-242.

Leeuwen M.R., Krijgsheld P., Menke H., Stam H., Stark J., Wösten, H.A., Dijksterhuis, J. 2013. Germination of conidia of *Aspergillus niger* is accompanied by major changes in RNA profiles. *Stud Mycol*. 74:59-70.

Lessing F., Kniemeyer O., Wozniok I., Loeffler J., Kurzai O., Haertl A., Brakhage A.A. 2007. The *Aspergillus fumigatus* transcriptional regulator AfYap1 represents the major regulator for defense against reactive oxygen intermediates but is dispensable for pathogenicity in an intranasal mouse infection model. *Eukaryot Cell*. 6:2290-2302.

Lewis R.E., Wiederhold N.P., Chi J., Han X.Y., Komanduri K.V., Kontoyiannis D.P., Prince RA. 2005. Detection of gliotoxin in experimental and human aspergillosis. *Infect Immun*. 73:635-637.

Liebmann B., Müller M., Braun A., Brakhage A.A. 2004. The cyclic AMP-dependent protein kinase a network regulates development and virulence in *Aspergillus fumigatus*. *Infect Immun*. 72:5193-5203.

Lin C.J., Sasse C., Gerke J., Valerius O., Irmer H., Frauendorf H., Heinekamp T., Straßburger M., Tran V.T., Herzog B., Braus-Stromeyer S.A., Braus G.H. 2015. Transcription Factor SomA Is Required for Adhesion, Development and Virulence of the Human Pathogen *Aspergillus fumigatus*. *PLoS Pathog*. 11:e1005205.

Linder M.B., Szilvay G.R., Nakari-Setälä T., Penttilä M.E. 2005. Hydrophobins: the protein-amphiphiles of filamentous fungi. *FEMS Microbiol Rev*. 29:877-896.

Linder M.C. 2013. Mobilization of stored iron in mammals: a review. *Nutrients*. 5:4022-4050.

Liu D., Coloe S., Baird R., Pederson J. 2000. Rapid mini-preparation of fungal DNA for PCR. *J Clin Microbiol*. 38:471.

Liu J., Yang Z.J., Meng Z.H. 1996. The isolation, purification and identification of fumitremorgin B produced by *Aspergillus fumigatus*. *Biomed Environ Sci*. 9:1-11.

López-Ribot J.L., Casanova M., Murgui A., Martínez J.P. 2004. Antibody response to *Candida albicans* cell wall antigens. *FEMS Immunol Med Microbiol*. 41:187-196.

Loussert C., Schmitt C., Prevost M.C., Balloy V., Fadel E., Philippe B., Kauffmann-Lacroix C., Latgé J.P., Beauvais A. 2010. *In vivo* biofilm composition of *Aspergillus fumigatus*. *Cell Microbiol*. 12:405-410.

Low S.Y., Dannemiller K., Yao M., Yamamoto N., Peccia J. 2011. The allergenicity of *Aspergillus fumigatus* conidia is influenced by growth temperature. Fungal Biol. 115:625-632.

Lumbreras C., Gavaldà J. 2003. Aspergilosis invasora: manifestaciones clínicas y tratamiento. *Rev Iberoam Micol*. 20:79-89.

Mabey Gilsenan J., Cooley J., Bowyer P. 2012. CADRE: the Central *Aspergillus* Data REpository 2012. *Nucleic Acids Res*. 40:D660-D666.

Markaryan A., Morozova I., Yu H., Kolattukudy P.E. 1994. Purification and characterization of an elastinolytic metalloprotease from *Aspergillus fumigatus* and immunoelectron microscopic evidence of secretion of this enzyme by the fungus invading the murine lung. *Infect Immun*. 62:2149-2157.

Marzluf G.A. 1993. Regulation of sulfur and nitrogen metabolism in filamentous fungi. *Annu Rev Microbiol*. 47:31-55.

Maschmeyer G., Haas A., Cornely O.A. 2007. Invasive aspergillosis: epidemiology, diagnosis and management in immunocompromised patients. *Drugs*. 67:1567-1601.

McDonagh A., Fedorova N. D., Crabtree J., Yu, Y., Kim S., Chen D., Loss O., Cairns T., Goldman G., Armstrong-James D., Haynes K., Haas H., Schrettl M., May G., Nierman W.C., Bignell E. 2008.

Subtelomere directed gene expression during initiation of invasive aspergillosis. *PLoS Pathog*. 4:e1000154.

Medina I., Carbonell J., Pulido L., Madeira S.C., Goetz S., Conesa A., Tárraga J., Pascual-Montano A., Nogales-Cadenas R., Santoyo J., García F., Marbà M., Montaner D., Dopazo J. 2010. Babelomics: an integrative platform for the analysis of transcriptomics, proteomics and genomic data with advanced functional profiling. *Nucleic Acids Res*. 38:W210-W213.

Mircescu M.M., Lipuma L., van Rooijen N., Pamer E.G., Hohl T.M. 2009. Essential role for neutrophils but not alveolar macrophages at early time points following *Aspergillus fumigatus* infection. *J Infect Dis*. 200:647-656.

Mirkes P.E. 1974. Polysomes, ribonucleic acid, and protein synthesis during germination of *Neurospora crassa* conidia. *J Bacteriol*. 117:196-202.

Mirkov I., Stojanovic I., Glamoclija J., Stosic-Grujicic S., Zolotarevski L., Kataranovski D., Kataranovski M. 2011. Differential mechanisms of resistance to sublethal systemic *Aspergillus fumigatus* infection in immunocompetent BALB/c and C57BL/6 mice. *Immunobiology*. 216:234-242.

Mitchell C.G., Slight J., Donaldson K. 1997. Diffusible component from the spore surface of the fungus *Aspergillus fumigatus* which inhibits the macrophage oxidative burst is distinct from gliotoxin and other hyphal toxins. *Thorax*. 52:796-801.

Momany M. 2002. Polarity in filamentous fungi: establishment, maintenance and new axes. *Curr Opin Microbiol*. 5:580-585.

Monod M., Capoccia S., Léchenne B., Zaugg C., Holdom M., Jousson O. 2002. Secreted proteases from pathogenic fungi. *Int J Med Microbiol*. 292:405-419.

Moore M.M. 2013. The crucial role of iron uptake in *Aspergillus fumigatus* virulence. *Curr Opin Microbiol*. 16:692-699.

Moreno M.A., Ibrahim-Granet O., Vicentefranqueira R., Amich J., Ave P., Leal F., Latgé J.P., Calera J.A. 2007. The regulation of zinc homeostasis by the ZafA transcriptional activator is essential for *Aspergillus fumigatus* virulence. *Mol Microbiol*. 64:1182-1197.

Morey J.S., Ryan J.C., Van Dolah F.M. 2006. Microarray validation: factors influencing correlation between oligonucleotide microarrays and real-time PCR. *Biol Proced Online*. 8:175-193.

Morton C.O., Varga J.J., Hornbach A., Mezger M., Sennefelder H., Kneitz S., Kurzai O., Krappmann S., Einsele H., Nierman W.C., Rogers T.R., Loeffler J. 2011. The temporal dynamics of differential gene expression in *Aspergillus fumigatus* interacting with human immature dendritic cells in vitro. *PLoS One*. 6:e16016.

Moss R.B. 2005. Pathophysiology and immunology of allergic bronchopulmonary aspergillosis. *Med Mycol*. 43 Suppl 1:S203-S206.

Müllbacher A., Eichner R.D. 1984. Immunosuppression in vitro by a metabolite of a human pathogenic fungus. *Proc Natl Acad Sci USA*. 81:3835-3837.

Müller F.M., Seidler M., Beauvais A. 2011. *Aspergillus fumigatus* biofilms in the clinical setting. *Med Mycol*. 49 Suppl 1:S96-S100.

Muszkieta L., Carrion Sde J., Robinet P., Beau R., Elbim C., Pearlman E., Latgé J.P. 2014. The protein phosphatase PhzA of *A. fumigatus* is involved in oxidative stress tolerance and fungal virulence. *Fungal Genet Biol*. 66:79-85.

Nicolle M.C., Benet T., Vanhems P. 2011. Aspergillosis: nosocomial or community-acquired? *Med Mycol*. 49 Suppl 1:S24-S29.

Nieminen S.M., Mäki-Paakkanen J., Hirvonen M.R., Roponen M., von Wright A. 2002. Genotoxicity of gliotoxin, a secondary metabolite of *Aspergillus fumigatus*, in a battery of short-term test systems. *Mutat Res*. 520:161-170.

Nierman W.C., Pain A., Anderson M.J., Wortman J.R., Kim H.S., Arroyo J., Berriman M., Abe K., Archer D.B., Bermejo C., Bennett J., Bowyer P., Chen D., Collins M., Coulsen R., Davies R., Dyer P.S., Farman M., Fedorova N., Fedorova N., Feldblyum T.V., Fischer R., Fosker N., Fraser A., García J.L., García M.J., Goble A., Goldman G.H., Gomi K., Griffith-Jones S., Gwilliam R., Haas B., Haas H., Harris D., Horiuchi H., Huang J., Humphray S., Jiménez J., Keller N., Khouri H., Kitamoto K., Kobayashi T., Konzack S., Kulkarni R., Kumagai T., Lafon A., Latgé J.P., Li W., Lord A., Lu C., Majoros W.H., May G.S., Miller B.L., Mohamoud Y., Molina M., Monod M., Mouyna I., Mulligan S., Murphy L., O'Neil S., Paulsen I., Peñalva M.A., Pertea M., Price C., Pritchard B.L., Quail M.A., Rabbinowitsch E., Rawlins N., Rajandream M.A., Reichard U., Renauld H., Robson G.D., Rodriguez de Córdoba S., Rodríguez-Peña J.M., Ronning C.M., Rutter S., Salzberg S.L., Sanchez M., Sánchez-Ferrero J.C., Saunders D., Seeger K., Squares R., Squares S., Takeuchi M., Tekaia F., Turner G., Vazquez de Aldana C.R., Weidman J., White O., Woodward J., Yu J.H., Fraser C., Galagan J.E., Asai K., Machida M., Hall N., Barrell B., Denning D.W. 2005. Genomic sequence of the pathogenic and allergenic filamentous fungus *Aspergillus fumigatus*. *Nature*. 438:1151-1156.

O´Gorman C.M. 2011. Airborne *Aspergillus fumigatus* conidia: a risk of factor for aspergillosis. *Fung Biol Rev.* 25:151-157.

O'Gorman C.M., Fuller H.T., Dyer P.S. 2009. Discovery of a sexual cycle in the opportunistic fungal pathogen *Aspergillus fumigatus*. *Nature*. 457:471-474.

Oide S., Krasnoff S.B., Gibson D.M., Turgeon B.G. 2007. Intracellular siderophores are essential for ascomycete sexual development in heterothallic Cochliobolus heterostrophus and homothallic Gibberella zeae. *Eukaryot Cell*. 1339-1353.

Oliver J.D., Kaye S.J., Tuckwell D., Johns A.E., Macdonald D.A., Livermore J., Warn P.A., Birch M., Bromley M.J. 2012. The *Aspergillus fumigatus* dihydroxyacid dehydratase Ilv3A/IlvC is required for full virulence. *PLoS One*. 7:e43559.

Oosthuizen J.L., Gomez P., Ruan J., Hackett T.L., Moore M.M., Knight D.A., Tebbutt S.J. 2011. Dual organism transcriptomics of airway epithelial cells interacting with conidia of *Aspergillus fumigatus*. *PLoS One*. 6:e20527.

Orciuolo E., Stanzani M., Canestraro M., Galimberti S., Carulli G., Lewis R., Petrini M., Komanduri K.V. 2007. Effects of *Aspergillus fumigatus* gliotoxin and methylprednisolone on human neutrophils: implications for the pathogenesis of invasive aspergillosis. *J Leukoc Biol*. 82:839-848.

Osherov N. 2007. The virulence of *Aspergillus fumigatus*. In New insights in medical mycology. Kavanagh K. (ed.). Springer. Netherlands. p.185-212.

Osherov N., May G.S. 2001. The molecular mechanisms of conidial germination. *FEMS Microbiol Lett*. 99:153-160.

Palmer J.M., Keller N.P. 2010. Secondary metabolism in fungi: does chromosomal location matter? *Curr Opin Microbiol*. 13:431-436.

Panepinto J.C., Oliver B.G., Amlung T.W., Askew D.S., Rhodes JC. 2002. Expression of the *Aspergillus fumigatus* rheb homologue, *rhbA*, is induced by nitrogen starvation. *Fungal Genet Biol*. 36:207-214.

Panepinto J.C., Oliver B.G., Fortwendel J.R., Smith D.L., Askew D.S., Rhodes J.C. 2003. Deletion of the *Aspergillus fumigatus* gene encoding the Ras-related protein RhbA reduces virulence in a model of Invasive pulmonary aspergillosis. *Infect Immun*. 71:2819-2826.

Pao S.S, Paulsen I/T., Saier MH. 1998. Major Facilitator Superfamily. *Microbiol Mol Biol Rev*. 62: 1-34.

Paris S., Debeaupuis J.P., Crameri R., Carey M., Charlès F., Prévost M.C., Schmitt C., Philippe B., Latgé J.P. 2003a. Conidial hydrophobins of *Aspergillus fumigatus*. *Appl Environ Microbiol*. 69:1581-1588.

Paris S., Wysong D., Debeaupuis J.P., Shibuya K., Philippe B., Diamond R.D., Latgé JP. 2003b. Catalases of *Aspergillus fumigatus*. *Infect Immun*. 71:3551-3562.

Park H.S., Bayram O., Braus G.H., Kim S.C., Yu J.H. 2012. Characterization of the velvet regulators in *Aspergillus fumigatus*. *Mol Microbiol*. 86:937-953.

Park S.J., Mehrad B. 2009. Innate immunity to *Aspergillus* species. *Clin Microbiol Rev*. 22:535-551.

Pateman J.A., Cove D.J. 1967. Regulation of nitrate reduction in *Aspergillus nidulans*. *Nature*. 215:1234-1237.

Pateman J.A., Rever B.M., Cove D.J. 1967. Genetic and biochemical studies of nitrate reduction in *Aspergillus nidulans*. *Biochem J*. 104:103-111.

Paulussen C., Boulet G.A., Cos P., Delputte P., Maes L.J. 2014. Animal models of invasive aspergillosis for drug discovery. *Drug Discov Today*. 19:1380-1386.

Paz Z., García-Pedrajas M.D., Andrews D.L., Klosterman S.J., Baeza-Montañez L., Gold S.E. 2011. One step construction of *Agrobacterium*-Recombination-ready-plasmids (OSCAR), an efficient and robust tool for ATMT based gene deletion construction in fungi. *Fungal Genet Biol*. 48:677-684.

Peñalva M.A., Tilburn J., Bignell E., Arst H.N. Jr. 2008. Ambient pH gene regulation in fungi: making connections. *Trends Microbiol*. 16:291-300.

Pepeljnjak S., Slobodnjak Z., Segvić M., Peraica M., Pavlović M. 2004. The ability of fungal isolates from human lung aspergilloma to produce mycotoxins. *Hum Exp Toxicol*. 23:15-19.

Pérez Surribas D. 2005. Proteínas relacionadas con el metabolismo del hierro. *Química Clínica*. 24:5-40.

Perkhofer S., Zenzmaier C., Frealle E., Blatzer M., Hackl H., Sartori B., Lass-Flörl C. 2015. Differential gene expression in *Aspergillus fumigatus* induced by human platelets in vitro. *Int J Med Microbiol*. 305:327-338.

Peterson S.W., Varga J., Frisvad J.C., Samson R.A. 2008. Phylogeny and subgeneric taxonomy of *Aspergillus*. In: *Aspergillus* in the genomic era. Varga J., Samson R.A. (eds). Wegeningen Academic Publishers. Netherlands. p.33-56.

Philpott C.C., Leidgens S., Frey A.G. 2012. Metabolic remodeling in iron-deficient fungi. *Biochim Biophys Acta*. 1823:1509-1520.

Pihet M., Vandeputte P., Tronchin G., Renier G., Saulnier P., Georgeault S., Mallet R., Chabasse D., Symoens F., Bouchara J.P. 2009. Melanin is an essential component for the integrity of the cell wall of *Aspergillus fumigatus* conidia. *BMC Microbiol*. 9:177.

Porcheron G., Garénaux A., Proulx J., Sabri M., Dozois C.M. 2013. Iron, copper, zinc, and manganese transport and regulation in pathogenic Enterobacteria: correlations between strains, site of infection and the relative importance of the different metal transport systems for virulence. *Front Cell Infect Microbiol*. 3:90.

Power T., Ortoneda M., Morrissey J.P., Dobson A.D. 2006. Differential expression of genes involved in iron metabolism in *Aspergillus fumigatus*. *Int Microbiol*. 9:281-287.

Priebe S., Kreisel C., Horn F., Guthke R., Linde J. 2014. FungiFun2: a comprehensive online resource for systematic analysis of gene lists from fungal species. *Bioinformatics*. 31:445-6.

Priebe S., Linde J., Albrecht D., Guthke R., Brakhage A.A. 2011. FungiFun: a web-based application for functional categorization of fungal genes and proteins. *Fungal Genet Biol*. 48:353-358.

Priyadarsiny P., Swain P.K., Sarma P.U. 2003. Expression and characterization of Asp f1, an immunodominant allergen/antigen of *A. fumigatus* in insect cell. *Mol Cell Biochem*. 252:157-163.

Rao M.B., Tanksale A.M., Ghatge M.S., Deshpande V.V. 1998. Molecular and biotechnological aspects of microbial proteases. *Microbiol Mol Biol Rev*. 62:597-635.

Raper K.B., Fennel D.I. 1965. The genus *Aspergillus*. Williams and Wilkins. USA. p. 1-686.

Reeves E.P., Murphy T., Daly P., Kavanagh K. 2004. Amphotericin B enhances the synthesis and release of the immunosuppressive agent gliotoxin from the pulmonary pathogen *Aspergillus fumigatus*. *J Med Microbiol*. 53:719-725.

Reichard U., Büttner S., Eiffert H., Staib F., Rüchel R. 1990. Purification and characterisation of an extracellular serine proteinase from *Aspergillus fumigatus* and its detection in tissue. *J Med Microbiol*. 33:243-251.

Rementeria A., López-Molina N., Ludwig A., Vivanco A. B., Bikandi J., Pontón J. Garaizar J. 2005. Genes and molecules involved in *Aspergillus fumigatus* virulence. *Rev Iberoam Micol*. 22:1-23.

Rhodes J.C., Brakhage A.A. 2006. Molecular Determinants of Virulence in *Aspergillus fumigatus*. In: Molecular Principles of Fungal Pathogenesis. Heitman J., Filler S.G., Edwards J.E. Jr., Mitchell A.P. (eds). ASM Press. USA. p. 333-345.

Richard J.L., Dvorak T.J., Ross P.F. 1996. Natural occurrence of gliotoxin in turkeys infected with *Aspergillus fumigatus*, Fresenius. *Mycopathologia*. 134:167-170.

Robson G.D., Huang J., Wortman J., Archer D.B. 2005. A preliminary analysis of the process of protein secretion and the diversity of putative secreted hydrolases encoded in *Aspergillus fumigatus*: insights from the genome. *Med Mycol*. 2005 Suppl 1:S41-S47.

Ryckeboer J., Mergaert J., Coosemans J., Deprins K., Swings J. 2003. Microbiological aspects of biowaste during composting in a monitored compost bin. *J Appl Microbiol*. 94:127-37.

Saeed A.I., Sharov V., White J., Li J., Liang W., Bhagabati N., Braisted J., Klapa M., Currier T., Thiagarajan M., Sturn A., Snuffin M., Rezantsev A., Popov D., Ryltsov A., Kostukovich E., Borisovsky I., Liu Z., Vinsavich A., Trush V., Quackenbush J. 2003. TM4: a free, open-source system for microarray data management and analysis. *Biotechniques*. 34:374-378.

Salas V., Pastor F.J., Calvo E., Sutton D.A., Fothergill A.W., Guarro J. 2013. Evaluation of the *in vitro* activity of voriconazole as predictive of *in vivo* outcome in a murine *Aspergillus fumigatus* infection model. *Antimicrob Agents Chemother*. 57:1404-1408.

Sales-Campos H., Tonani L., Cardoso C.R., Kress M.R. 2013. The immune interplay between the host and the pathogen in *Aspergillus fumigatus* lung infection. *Biomed Res Int*. 2013:693023.

Samson R., Varga J. 2012. Molecular Systematics of *Aspergillus* and its Teleomorphs. In: *Aspergillus*: Molecular Biology and Genomics. Machida M. & Gomi K (eds). Caister Academic Press. UK. p. 19-40.

Samson R.A., Hong S., Peterson S.W., Frisvad J.C., Varga J. 2007. Polyphasic taxonomy of *Aspergillus* section *Fumigati* and its teleomorph *Neosartorya*. *Stud Mycol.* 59:147-203.

Samson R.A., Visagie C.M., Houbraken J., Hong S.B., Hubka V., Klaassen C.H., Perrone G., Seifert K.A., Susca A., Tanney J.B., Varga J., Kocsubé S., Szigeti G., Yaguchi T., Frisvad J.C. 2014. Phylogeny, identification and nomenclature of the genus *Aspergillus*. *Stud Mycol.* 78:141-713**.**

Samson R.A.,Varga, J. 2009. What is a species in *Aspergillus*?. *Med Mycol.* 47: S13-S20.

Scharf D.H., Heinekamp T., Brakhage A.A. 2014. Human and plant fungal pathogens: the role of secondary metabolites. *PLoS Pathog*. 10:e1003859.

Scharf D.H., Heinekamp T., Remme N., Horstchansky P., Brakhage A.A., Hertweck, C. 2012. Biosynthesis and function of gliotoxin in *Aspergillus fumigatus*. *Appl Microbiol Biotechnol*. 93:467-472.

Scharf D.H., Remme N., Heinekamp T., Hortschansky P., Brakhage A.A., Hertweck C. 2010. Transannular disulfide formation in gliotoxin biosynthesis and its role in self-resistance of the human pathogen *Aspergillus fumigatus*. *J Am Chem Soc*. 132:10136-10141.

Schmidt A. 2002. Animal models of aspergillosis - also useful for vaccination strategies? *Mycoses*. 45:38-40.

Schoberle T.J., Nguyen-Coleman C.K., Herold J., Yang A., Weirauch M., Hughes T.R., McMurray J.S., May G.S. 2014. A novel C_2H_2 transcription factor that regulates *gliA* expression interdependently with GliZ in *Aspergillus fumigatus*. *PLoS Genet*. 10:e1004336.

Schrettl M., Beckmann N., Varga J., Heinekamp T., Jacobsen I.D., Jöchl C., Moussa T.A., Wang S., Gsaller F., Blatzer M., Werner E.R., Niermann W.C., Brakhage A.A., Haas H. 2010. HapX-mediated adaption to iron starvation is crucial for virulence of *Aspergillus fumigatus*. *PLoS Pathog*. 6:e1001124.

Schrettl M., Bignell E., Kragl C., Joechl C., Rogers T., Arst H.N. Jr, Haynes K., Haas H. 2004. Siderophore biosynthesis but not reductive iron assimilation is essential for *Aspergillus fumigatus* virulence. *J Exp Med*. 200:1213-1219.

Schrettl M., Bignell E., Kragl C., Sabiha Y., Loss O., Eisendle M., Wallner A., Arst H.N. Jr, Haynes K., Haas H. 2007. Distinct roles for intra- and extracellular siderophores during *Aspergillus fumigatus* infection. *PLoS Pathog*. 3:1195-1207.

Schrettl M., Carberry S., Kavanagh K., Haas H., Jones G.W., O'Brien J., Nolan A., Stephens J., Fenelon O., Doyle S. 2010. Self-protection against gliotoxin-a component of the gliotoxin biosynthetic cluster, GliT, completely protects *Aspergillus fumigatus* against exogenous gliotoxin. *PLoS Pathog*. 6:e1000952.

Schrettl M., Kim H.S., Eisendle M., Kragl C., Nierman W.C., Heinekamp T., Werner E.R., Jacobsen I., Illmer P., Yi H., Brakhage A.A., Haas H. 2008. SreA-mediated iron regulation in *Aspergillus fumigatus*. *Mol Microbiol*. 70:27-43.

Segal B.H., Walsh T.J. 2006. Current approaches to diagnosis and treatment of invasive aspergillosis. *Am J Respir Crit Care Med*. 173:707-717

Seyedmousavi S., Mouton J.W., Verweij P.E., Brüggemann R.J. 2013. Therapeutic drug monitoring of voriconazole and posaconazole for invasive aspergillosis. *Expert Rev Anti Infect. Ther*. 11:931-941.

Shafeeq S., Kuipers O.P., Kloosterman T.G. 2013. The role of zinc in the interplay between pathogenic streptococci and their hosts. *Mol Microbiol*. 88:1047-1057.

Sharon H., Hagag S., Osherov N. 2009. Transcription factor PrtT controls expression of multiple secreted proteases in the human pathogenic mold *Aspergillus fumigatus*. *Infect Immun*. 77: 4051-4060.

Shelest E. 2008. Transcription factors in fungi. *FEMS Microbiol Lett*. 286:145-151.

Shen D.K., Noodeh A.D., Kazemi A., Grillot R., Robson G., Brugère J.F. 2004. Characterisation and expression of phospholipases B from the opportunistic fungus *Aspergillus fumigatus*. *JF*. *FEMS Microbiol Lett*. 239:87-93.

Shepardson K.M., Cramer R.A. 2013. Fungal cell wall dynamics and infection site microenvironments: signal integration and infection outcome. *Curr Opin Microbiol*. 16:385-390.

Shibuya K., Takaoka M., Uchida K., Wakayama M., Yamaguchi H., Takahashi K., Paris S., Latge J.P., Naoe S. 1999. Histopathology of experimental invasive pulmonary aspergillosis in rats: pathological

comparison of pulmonary lesions induced by specific virulent factor deficient mutants. *Microb Pathog*. 27:123-31.

Shinohara C., Hasumi K., Endo A. 1993. Inhibition of oxidized low-density lipoprotein metabolism in macrophage J774 by helvolic acid. *Biochim Biophys Acta*. 1167:303-306.

Sinclair S.A., Krämer U. 2012. The zinc homeostasis network of land plants. *Biochim Biophys Acta*. 1823:1553-1567.

Sirakova T.D., Markaryan A., Kolattukudy P.E. 1994. Molecular cloning and sequencing of the cDNA and gene for a novel elastinolytic metalloproteinase from *Aspergillus fumigatus* and its expression in Escherichia coli. *Infect Immun*. 62:4208-4218.

Smith J.M., Davies J.E., Holden D.W. 1993. Construction and pathogenicity of *Aspergillus fumigatus* mutants that do not produce the ribotoxin restrictocin. *Mol Microbiol*. 9:1071-1077.

Smith T.D., Calvo A.M. 2014. The *mtfA* transcription factor gene controls morphogenesis, gliotoxin production, and virulence in the opportunistic human pathogen *Aspergillus fumigatus*. *Eukaryot Cell*. 13:766-775.

Soubani A.O., Chandrasekar P.H. 2002. The clinical spectrum of pulmonary aspergillosis. *Chest*. 121:1988-1999.

Spikes S., Xu R., Nguyen C.K., Chamilos G., Kontoyiannis D.P., Jacobson R.H., Ejzykowicz D.E., Chiang L.Y., Filler S.G., May G.S. 2008. Gliotoxin production in *Aspergillus fumigatus* contributes to host-specific differences in virulence. *J Infect Dis*. 197:479-486.

Stanzani M., Orciuolo E., Lewis R., Kontoyiannis D.P., Martins S.L., St John L.S., Komanduri KV. 2005. *Aspergillus fumigatus* suppresses the human cellular immune response via gliotoxin-mediated apoptosis of monocytes. *Blood*. 105:2258-65.

Subramanian Vignesh K., Landero Figueroa J.A., Porollo A., Caruso J.A., Deepe G.S. Jr. 2013. Granulocyte macrophage-colony stimulating factor induced Zn sequestration enhances macrophage superoxide and limits intracellular pathogen survival. *Immunity*. 39:697-710.

Sugui J.A., Kim H.S., Zarember K.A., Chang Y.C., Gallin J.I., Nierman W.C., Kwon-Chung K.J. 2008. Genes differentially expressed in conidia and hyphae of *Aspergillus fumigatus* upon exposure to human neutrophils. *PLoS One*. 3:e2655.

Sugui J.A., Pardo J., Chang Y.C., Müllbacher A., Zarember K.A., Galvez E.M., Brinster L., Zerfas P., Gallin J.I., Simon M.M., Kwon-Chung K.J. 2007a. Role of *laeA* in the regulation of *alb1*, *gliP*, conidial morphology, and virulence in *Aspergillus fumigatus*. *Eukaryot Cell*. 6:1552-1561.

Sugui J.A., Pardo J., Chang Y.C., Zarember K.A., Nardone G., Galvez E.M., Müllbacher A., Gallin J.I., Simon M.M., Kwon-Chung K.J. 2007b. Gliotoxin is a virulence factor of *Aspergillus fumigatus*: *gliP* deletion attenuates virulence in mice immunosuppressed with hydrocortisone. *Eukaryot Cell*. 6:1562-1569.

Taheri-Talesh N., Horio T., Araujo-Bazán L., Dou X., Espeso E.A., Peñalva M.A., Osmani S.A., Oakley BR. 2008. The tip growth apparatus of *Aspergillus nidulans*. *Mol Biol Cell*. 19:1439-1449.

Taylor J.W. 2011. One Fungus = One Name: DNA and fungal nomenclature twenty years after PCR. *IMA Fungus.* 2:113-120.

Tekaia F., Latgé J.P. 2005. *Aspergillus fumigatus*: saprophyte or pathogen? *Curr Opin Microbiol*. 8:385-392.

Thanh N.V., Rombouts F.M., Nout M.J. 2005. Effect of individual amino acids and glucose on activation and germination of *Rhizopus oligosporus* sporangiospores in tempe starter. *J Appl Microbiol*. 99:1204-1214.

Thau N., Monod M., Crestani B., Rolland C., Tronchin G., Latgé J.P., Paris S. 1994. Rodletless mutants of *Aspergillus fumigatus*. *Infect Immun*. 62:4380-4388.

Tsai H.F., Wheeler M.H., Chang Y.C., Kwon-Chung K.J. 1999. A developmentally regulated gene cluster involved in conidial pigment biosynthesis in *Aspergillus fumigatus*. *J Bacteriol*. 181:6469-7647.

Tsunawaki S., Yoshida L.S., Nishida S., Kobayashi T., Shimoyama T. 2004. Fungal metabolite gliotoxin inhibits assembly of the human respiratory burst NADPH oxidase. Infect Immun.72:3373-3382.

van Hal N.L., Vorst O., van Houwelingen A.M., Kok E.J., Peijnenburg A., Aharoni A., van Tunen A.J., Keijer J. 2000. The application of DNA microarrays in gene expression analysis. *J Biotechnol*. 78:271-280.

Van Leeuwen M.R., Smant W., de Boer W., Dijksterhuis J. 2008. Filipin is a reliable in situ marker of ergosterol in the plasma membrane of germinating conidia (spores) of *Penicillium discolor* and stains intensively at the site of germ tube formation. *J Microbiol Methods*. 74:64-73.

Van Leeuwen M.R., Van Doorn T.M., Golovina E.A., Stark J., Dijksterhuis J. 2010. Water- and air-distributed conidia differ in sterol content and cytoplasmic microviscosity. *Appl Environ Microbiol*. 76:366-369.

Vicentefranqueira R., Amich J., Laskaris P., Ibrahim-Granet O., Latgé J.P., Toledo H., Leal F., Calera J.A. 2015. Targeting zinc homeostasis to combat *Aspergillus fumigatus* infections. *Front Microbiol*. 6:160.

Vicentefranqueira R., Moreno M.A., Leal F., Calera J.A. 2005. The *zrfA* and *zrfB* genes of *Aspergillus fumigatus* encode the zinc transporter proteins of a zinc uptake system induced in an acid, zinc-depleted environment. *Eukaryot Cell*. 4:837-848.

Wallner A., Blatzer M., Schrettl M., Sarg B., Lindner H., Haas H. 2009. Ferricrocin, a siderophore involved in intra- and transcellular iron distribution in *Aspergillus fumigatus*. *Appl Environ Microbiol*. 75:4194-4196.

Wang D.N., Toyotome T., Muraosa Y., Watanabe A., Wuren T., Bunsupa S., Aoyagi K., Yamazaki M., Takino M., Kamei K. 2014. GliA in *Aspergillus fumigatus* is required for its tolerance to gliotoxin and affects the amount of extracellular and intracellular gliotoxin. *Med Mycol*. 52:506-518.

Ward C.L., Dempsey M.H., Ring C.J., Kempson R.E., Zhang L., Gor D., Snowden B.W., Tisdale M. 2004. Design and performance testing of quantitative real time PCR assays for influenza A and B viral load measurement. *J Clin Virol*. 29:179-188.

Watanabe A., Kamei K., Sekine T., Waku M., Nishimura K., Miyaji M., Tatsumi K., Kuriyama T. 2004. Effect of aeration on gliotoxin production by *Aspergillus fumigatus* in its culture filtrate. *Mycopathologia*. 157:245-254.

Willger S.D., Puttikamonkul S., Kim K.H., Burritt J.B., Grahl N., Metzler L.J., Barbuch R., Bard M., Lawrence C.B., Cramer R.A. Jr. 2008. A sterol-regulatory element binding protein is required for cell polarity, hypoxia adaptation, azole drug resistance, and virulence in *Aspergillus fumigatus*. *PLoS Pathog*. 4:e1000200.

Winkelströter L.K., Bom V.L., de Castro P.A., Ramalho L.N., Goldman M.H., Brown N.A., Rajendran R., Ramage G., Bovier E., Dos Reis T.F., Savoldi M., Hagiwara D., Goldman G.H. 2015. High osmolarity glycerol response PtcB phosphatase is important for *Aspergillus fumigatus* virulence. *Mol Microbiol*. 96:42-54.

Yamada A., Kataoka T., Nagai K. 2000. The fungal metabolite gliotoxin: immunosuppressive activity on CTL-mediated cytotoxicity. *Immunol Lett*. 71:27-32.

Yamazaki M., Fujimoto H., Kawasaki T. 1980. Chemistry of tremorogenic metabolites. I. Fumitremorgin A from *Aspergillus fumigatus*. *Chem Pharm Bull* (Tokyo). 28:245-254.

Yang B., Bankir L. 2005. Urea and urine concentrating ability: new insights from studies in mice. *Am J Physiol Renal Physiol*. 288:F881-F896.

Yasmin S., Alcazar-Fuoli L., Gründlinger M., Puempel T., Cairns T., Blatzer M., Lopez J.F., Grimalt J.O., Bignell E., Haas H. 2012. Mevalonate governs interdependency of ergosterol and siderophore biosyntheses in the fungal pathogen *Aspergillus fumigatus*. *Proc Natl Acad Sci USA*. 109:E497-E504.

Yokota K., Shimada H., Kamaguchi A., Sakaguchi O. 1977. Studies on the toxin of *Aspergillus fumigatus*. VII. Purification and some properities of hemolytic toxin (asp-hemolysin) from culture filtrates and mycelia. *Microbiol Immunol*. 21:11-22.

Youngchim S., Morris-Jones R., Hay R.J., Hamilton A.J. 2004. Production of melanin by *Aspergillus fumigatus*. *J Med Microbiol*. 53:175-181.

Zhao Y., Liu J., Wang J., Wang L., Yin H., Tan R., Xu Q. 2004. Fumigaclavine C improves concanavalin A-induced liver injury in mice mainly via inhibiting TNF-alpha production and lymphocyte adhesion to extracellular matrices. *J Pharm Pharmacol*. 56:775-782.

Zmeili O.S., Soubani A.O. 2007. Pulmonary aspergillosis: a clinical update. *QJM*. 100:317-34.

Microbiology (2015), **161**, 490–502 DOI 10.1099/mic.0.000021

Aspergillus fumigatus transcriptome response to a higher temperature during the earliest steps of germination monitored using a new customized expression microarray

Mónica Sueiro-Olivares,[1] Jimena V. Fernandez-Molina,[1] Ana Abad-Diaz-de-Cerio,[1] Eva Gorospe,[2] Elisabeth Pascual,[2] Xabier Guruceaga,[1] Andoni Ramirez-Garcia,[1] Javier Garaizar,[3] Fernando L. Hernando,[1] Javier Margareto[2] and Aitor Rementeria[1]

Correspondence
Aitor Rementeria
aitor.rementeria@ehu.es

[1]Department of Immunology, Microbiology and Parasitology, Faculty of Science and Technology, University of the Basque Country (UPV/EHU), Spain

[2]Tecnalia Research & Innovation, 48160 Derio, Spain

[3]Department of Immunology, Microbiology and Parasitology, Faculty of Pharmacy, University of the Basque Country (UPV/EHU), Spain

Aspergillus fumigatus is considered to be the most prevalent airborne pathogenic fungus and can cause invasive diseases in immunocompromised patients. It is known that its virulence is multifactorial, although the mechanisms of pathogenicity remain unclear. With the aim of improving our understanding of these mechanisms, we designed a new expression microarray covering the entire genome of *A. fumigatus*. In this first study, we analysed the transcriptomes of this fungus at the first steps of germination after being grown at 24 and 37 °C. The microarray data revealed that 1249 genes were differentially expressed during growth at these two temperatures. According to our results, *A. fumigatus* modified significantly the expression of genes related to metabolism to adapt to new conditions. The high percentages of genes that encoded hypothetical or unclassified proteins differentially expressed implied that many as yet unknown genes were involved in the establishment of *A. fumigatus* infection. Furthermore, amongst the genes implicated in virulence upregulated at 37 °C on the microarray, we found those that encoded proteins mainly related to allergens (Asp F1, Asp F2 and MnSOD), gliotoxin biosynthesis (GliP and GliZ), nitrogen (NiiA and NiaD) or iron (HapX, SreA, SidD and SidC) metabolism. However, gene expression in iron and nitrogen metabolism might be influenced not only by heat shock, but also by the availability of nutrients in the medium, as shown by the addition of fresh medium.

Received 18 December 2014
Accepted 19 December 2014

INTRODUCTION

Aspergillus fumigatus is a saprophytic mould and is considered to be the most prevalent airborne pathogenic fungus. This is particularly due to the fact that it spreads widely and disperses easily thanks to its conidia, which are extremely well suited for air dispersal. Their small size (2–3 μm), hydrophobicity, thermotolerance and melanin content allow them to withstand a wide range of temperatures and to remain airborne for long periods (O'Gorman, 2011). Furthermore, their small size allows them to overcome the defence mechanisms of the nasal cavity and other structures of the upper respiratory tract to reach the lung alveoli. On average, it is estimated that a person may inhale up to 200 conidia per day (Latgé, 1999).

Despite this high exposure of humans to conidia, they are not responsible for illnesses in immunocompetent hosts, as conidia levels are controlled by immune mechanisms. However, in immunocompromised individuals conidia can overcome the immune defence mechanisms, resulting in their establishment in the lung (Latgé, 1999). Once there,

Abbreviations: AWAFUGE, Agilent Whole *A. fumigatus* Genome Expression; RT-qPCR, reverse transcription quantitative PCR; UPV/EHU, University of the Basque Country.

The AWAFUGE microarray design was submitted to ArrayExpress under accession number A-MEXP-2352. The *A. fumigatus* gene expression data obtained following hybridization with the microarray have been deposited in ArrayExpress under accession number E-MTAB-1910.

Four supplementary tables are available with the online Supplementary Material.

the conidia germinate and subsequently start to colonize or even invade the surrounding tissue (Dagenais & Keller, 2009) causing invasive aspergillosis with mortality rates of 70–90 %. These high mortality rates are mainly due to the weakened immune system of the patients, the virulence of the fungus and late diagnosis (del Palacio *et al.*, 2003).

A crucial event in the infectious process of this pathogen is conidial germination, given that at this stage conidia have to adapt to the host environment and to overcome the immune system as well as to germinate. It is known that the first step in conidial germination consists of breaking the spore dormancy followed by isotropic swelling, establishment of cell polarity, formation of a germ tube and maintenance of polar growth (Barhoom & Sharon, 2004; Harris & Momany, 2004). However, despite our knowledge about the different stages of germination, little is known about the molecular aspects of the processes taking place during this period.

To date, several studies have demonstrated that the pathogenesis of this fungal species is multifactorial due to a combination of its biological characteristics and the immune status of patients (Beauvais & Latgé, 2001; Tekaia & Latgé, 2005; Osherov, 2007; Abad *et al.* 2010). Furthermore, it is generally assumed that some physiological characteristics of *A. fumigatus* allow it to be an efficient opportunist pathogen, with thermotolerance playing an important role (Rementeria *et al.*, 2005). *A. fumigatus* has developed mechanisms that allow it to grow at 37 °C and to tolerate temperatures >50 °C, which might contribute to the virulence of this pathogen.

The availability of the whole-genome sequence of *A. fumigatus* since 2005 has enabled the design of microarrays and these have been used to analyse the transcriptome of the fungus under different growth conditions. With the aim of improving our understanding of the adaptation of *A. fumigatus* to host environments and its mechanisms of pathogenicity, we have designed and validated a new specific expression microarray, AWAFUGE (Agilent Whole *A. fumigatus* Genome Expression 44K v.1), which could provide useful information about the transcriptome of this pathogen. As germination is a crucial event in the development of the infection, in this study we focused on the effect of host temperature during the first steps of germination. Specifically, after being cultured at 24 or 37 °C, the transcriptomes of the conidia were compared to identify functional and gene expression changes potentially linked to virulence in order to shed light on the mechanisms of adaptation and virulence of this fungus during this early stage of infection. We also studied whether the expression changes detected were only due to the temperature of incubation, analysing the expression of selected genes after the addition of fresh medium when the isotropic swelling had taken place.

METHODS

***A. fumigatus* strain, media and growth conditions.** *A. fumigatus* strain Af-293 was used in this study and grown on potato dextrose agar (Cultimed) at 28 °C for 7 days. Conidia were harvested and washed twice with saline/Tween solution (0.9 % NaCl/0.02 % Tween 20). The concentration of conidia was determined using an haemocytometer and was adjusted to 10^7 conidia ml^{-1}. Furthermore, the viability was evaluated in terms of the percentage of conidia that were able to grow on Sabouraud glucose agar (Cultimed) considering c.f.u. ml^{-1} after culture at 37 °C for 24 h, assessed by recounting the conidia with the haemocytometer.

The germination rate was determined on the basis of three independent assays. *A. fumigatus* conidia at a concentration of 10^7 conidia ml^{-1} were grown in 50 ml RPMI 1640 medium (Sigma Aldrich) and samples were incubated at 24 or 37 °C, both with shaking at 120 r.p.m. in a continuous incubation. In addition, to study the effect of nutrient consumption of the medium, cultures incubated for 16 h at 24 °C were centrifuged for 5 min at 2500 r.p.m. and then fresh medium, preheated at 24 or 37 °C, was added and incubated at 24 and 37 °C, respectively. Once inoculated, aliquots of 500 µl of each sample were fixed with 50 µl fixing solution (10 % formaldehyde/10 % SDS) and stained with Calcofluor white (Becton Dickinson) at different times. Cultures with 15–30 and 40–60 % germination rates were centrifuged for 5 min at 2500 r.p.m., and then washed twice with saline/Tween solution. The final pellet of these samples was weighed, placed in 10 µl RNAlater mg^{-1} (Qiagen) and stored at −20 °C until RNA extraction. Cultures from the continuous incubation with 15–30 % germination rates were used in the transcriptomic studies. To assess whether the medium retained the same characteristics despite the different lengths of culture used for the two temperatures, the pH of the medium was measured at starting and harvesting times.

RNA isolation. Three biological replicates of germinated conidia from each condition were used for RNA extraction. Samples of 100 mg (wet weight) were ground three times using an agate mortar in the presence of liquid nitrogen. Afterwards, total RNA was extracted with an RNeasy Plant Mini kit (Qiagen). Samples were treated with DNase I (amplification grade; Sigma Aldrich), and RNA concentration and quality were measured with a NanoPhotometer (Implen). Then, RNA integrity was assessed using a 2100 Bioanalyzer (Agilent Technologies) by the Advanced Research Facilities Service (SGIker) at the University of the Basque Country (UPV/EHU). The 2100 Bioanalyzer generated an RNA integrity number that indicated the suitability of RNA samples for gene expression analysis. Finally, extracted RNA was stored at −80 °C until use.

Expression microarray design. The AWAFUGE microarray v.1 was designed using the eArray system (Custom Microarray Design; Agilent Technologies; http://earray.chem.agilent.com/earray/). The AWAFUGE microarray v.1 included 28 890 probes to monitor the expression of the 9630 *A. fumigatus* genes (three 60 bp probes per gene). In addition, 62 quality control genes were incorporated, also with three targets for each gene and each repeated five times on the microarray, to correct for the variations caused by biological and technical factors. Of these control genes, 52 were chosen from the 9630 genes of *A. fumigatus*, five from *Mus musculus* and the other five from *Homo sapiens* (Table S1, available in the online Supplementary Material). Lastly, the eArray system automatically included positive and negative controls, selected by Agilent for use in commercial microarrays, resulting in a final microarray of 45 220 probes. The format adopted was four microarrays per glass slide (4 × 44K).

Transcriptome profiling studies. The transcriptional profiling of this study was carried out by Tecnalia Research & Innovation. RNA samples obtained from the continuous cultures with 15–30 % germination rates were used in the transcriptomic studies. The profiling was based on three independent RNA samples obtained from each of the conditions, 24 and 37 °C, and on two technical replicates. Total RNA (1 µg) from each sample was amplified and

Table 1. Genes selected (list of genes of the microarray) and primers used in the RT-qPCR

Target	Primer names	Sequence (5′→3′)	T_m (°C)	GC content (%)	Size of cDNA amplicon (bp)
Most upregulated at 37 °C					
L-Amino acid oxidase LaoA	F-LaoA	TTCAAGACAGTTGCCAGTGC	60.03	50	148
	R-LaoA	ATTCACGCCAATCGAGGTAG	60.10	50	
Extracellular proline-rich protein	F-Extracel	TCCATCCACAGTCACGGTAA	59.96	50	120
	R-Extracel	CCAGTGCCAGTACCAGGATT	59.99	55	
NACHT domain protein	F-NACHT	ATAGGCGACGTGGTTGTAGG	60.02	55	127
	R-NACHT	CACTTCTGCCTGCGTTCATA	60.01	50	
Dimethylallyl tryptophan synthase SirD-like	F-SirD	ATTTGTTTCCCCATCATCCA	59.99	40	121
	R-SirD	GTGCTGTACACCCGGAGATT	60.00	55	
CobW domain protein	F-CobW	GTCATTGAGAGCACGGGAAT	60.08	50	108
	R-CobW	CTCATCCACCAGCATCTCCT	60.22	55	
Nitrite reductase NiiA	F-NiiA	TCCTCGCTACAGGCTCAGAT	60.12	55	113
	R-NiiA	AGCGAACTCGATGAGACGTT	60.02	50	
Thioredoxin	F-Thiored	TTGATGTCGATGAGCAGGAG	59.94	50	103
	R-Thiored	CCCACAGCTTCACCAATCTT	60.11	50	
RNase H1	F-H1	CTTAAAGAACGGCCAAGACG	59.88	50	129
	R-H1	GCTCGTAACTCGGCTACCTG	60.04	60	
RTA1 domain protein	F-RTA1	CAACCTGCGTCTTTGCTACA	60.05	50	111
	R-RTA1	ACACGTAACCGCAATCATCA	60.00	45	
C4-dicarboxylate transporter/malic acid transport protein, putative	F-C4	GGACTGGCTCTTCTGATTGC	59.96	55	134
	R-C4	TGCAAAACGAATCTCAGCAC	60.00	45	
Most upregulated at 24 °C					
Catalase	F-Catal	CCATCCAGATGTGTGGTGAG	59.95	55	150
	R-Catal	CGAATGGATCAAATCCCAAC	60.13	45	
Pyruvate dehydrogenase E1 component α subunit	F-E1	AATCATGAGGTGGCAGAAGC	60.23	50	117
	R-E1	CACGGTACGTCCTCGGTACT	60.05	60	
NAD-dependent epimerase/dehydratase family protein	F-NAD	CGGTTGCAAAGCCAACTACT	60.30	50	143
	R-NAD	TCTGGAAGGACTCCGTATCG	60.21	55	
FAD-binding monooxygenase	F-FADmon	ACGGAACAGCATTCATCCTC	60.08	50	123
	R-FADmon	CTGCAGCGTCTTTGACTGAG	59.92	55	
ATP/GTP-binding protein	F-ATP/GTP	GTGGACTACCCCAAGGAACA	59.82	55	128
	R-ATP/GTP	CGGAATGCGAAAGAGAAGTC	59.96	50	
NmrA-like family protein	F-NmrA	TTTGCTATGCTGTGCTCTGG	60.16	50	131
	R-NmrA	CCACCTCTCGAAATCCTTCA	60.19	50	
Glycosyltransferase	F-Glyco	CACTGCAACCGTCAAAGCTA	60.05	50	124
	R-Glyco	GTGTCGTGGCCTGATATCCT	59.96	55	
Zn^{2+}-dependent hydrolase	F-Zn2	TTTGGAGACCGATTCCTTTG	60.04	45	140
	R-Zn2	TGCCCAAGTTGAGAATAGCA	59.42	45	
Replication factor C subunit	F-FactorC	GTGCATGACGTCCAGATACG	60.14	55	139
	R-FactorC	TTTGTGCAGTGTGGTCCATT	60.01	45	
Conidiation-specific protein Con-10	F-Con10	ATCTCTCTGGCGGACCACTA	59.83	55	145
	R-Con10	AACACCCCTGGCTCTACCTC	60.51	60	
Related to virulence					
C6 finger domain protein GliZ	F-GliZ	GGGCATGTCTTTGAACCCTA	59.93	50	137
	R-GliZ	ACCAGCGTACTCCGAAACTG	60.31	55	
Non-ribosomal peptide synthase GliP	F-GliP	TCGTGACCTTGCTCATTCTG	59.98	50	115
	R-GliP	GTCAATGTCGCCCAAGAGAT	60.08	50	
Non-ribosomal peptide synthase SidD	F-SidD	ACCAGGATGCTACGAACACC	60.00	55	134
	R-SidD	TCCACCAAGAGCGAAGAAGT	59.99	50	
Siderophore transcription factor SreA	F-SreA	CCTGCCTACAACAACCGAGT	60.17	55	126
	R-SreA	ATTCTTTCCCGCATCGTTTT	60.80	40	
Nitrate reductase NiaD	F-NiaD	GACGCCCTGCTAGTGAGAAG	60.16	60	102

Table 1. cont.

Target	Primer names	Sequence (5′→3′)	T_m (°C)	GC content (%)	Size of cDNA amplicon (bp)
	R-NiaD	CACTCGGAACCAAGGATTGT	59.97	50	
Major allergen and cytotoxin Asp F1	F-AspF1	CCACAGCCGTGTCTGTTCTA	59.90	55	109
	R-AspF1	CGCTTGTCTTCCCATTTGTT	60.11	45	
Major allergen Asp F2	F-AspF2	TCTGTGATCGCAGCTACACC	60.02	55	133
	R-AspF2	ACAGCAGGCACATGGTACAG	59.78	55	
Manganese superoxide dismutase MnSOD	F-MnSOD	CCTACGTCAATGGCCTGAAT	59.96	50	138
	R-MnSOD	TCCAGAAGAGGGAATGGTTG	60.04	50	
Housekeeping genes					
Actin 1 Act1	F-Act1	TCATCATGCGCGACAGCTTA	63.95	50	179
	R-Act1	CGTGCTCGATGGGGTATCTG	63.86	60	
Glyceraldehyde 3-phosphate dehydrogenase GpdA	F-GdpA	CTCCCTCCAACAAGGACTGG	61.99	60	115
	R-GpdA	AGCTTGCCGTTGAGAGAAGG	61.98	55	

labelled with Cy3 fluorescent dye using an Amino Allyl MessageAmp II aRNA Amplification kit (Ambion), and hybridized to individual arrays (one sample per array) in accordance with the manufacturer's recommendations (Agilent Technologies). After washing, microarray slides were scanned using a GenePix 4100A scanner (Axon Instruments) and image analysis was performed using associated software (GenePix Pro 6.0; Molecular Devices).

Reverse transcription quantitative PCR (RT-qPCR). In order to validate the results obtained using the microarray, three independent RNA samples from growth under each of the two conditions, different from those used in microarray analysis, were subjected to RT-qPCR by the SGIker at the UPV/EHU. Twenty of the most upregulated genes as well as eight genes with significant differences that had been related to virulence were selected for the validation. In addition to these, two other genes, actin 1 (*act1*) and glyceraldehyde 3-phospate dehydrogenase (*gpdA*), were included as housekeeping genes. Specific primer pairs were designed using Primer 3 (v.0.4.0; http://bioinfo.ut.ee/primer3-0.4.0/) software to amplify each gene (Table 1).

The cDNA was generated from 1 μg total RNA using an AffinityScript Multiple Temperature cDNA Synthesis kit (Agilent Technologies) in a total volume of 20 μl. Afterwards, 10 μl each sample was set up using Brilliant III Ultra-Fast QPCR Master Mix (Agilent Technologies) in which 300 nM ROX dye, 10 ng cDNA and 500 nM primers were added per reaction.

RT-qPCR experiments were performed in 96-well plates in a 7900HT Fast Real-Time PCR System (Applied Biosystems). The PCR amplification conditions were 3 min at 95 °C followed by 40 cycles of 95 °C for 5 s and 60 °C for 20 s. The specificity of the primer pairs was verified by melting curve analysis following the last amplification cycle. No-template controls and minus-reverse transcriptase controls (samples in which no reverse transcriptase was added) were also included.

This analysis was also carried out using BioMark HD Nanofluidic qPCR System technology (Fluidigm) combined with a GE 48.48 Dynamic Array integrated fluidic circuit (Fluidigm) in samples in which fresh medium was added. Briefly, the cDNA was preamplified using a Qiagen Multiplex PCR kit (Qiagen) and 50 nM primers. The PCR amplification conditions were 15 min at 95 °C followed by 14 cycles of 95 °C for 15 s and 60 °C for 4 min, followed by treatment with Exonuclease I (New England Biolabs). Gene expression analysis of the preamplified amplicons was performed with a GE 48.48 Dynamic Array integrated fluidic circuit using the Master Mix SsoFast EvaGreen Supermix with Low ROX (Bio-Rad) in which 2.7 μl preamplified cDNA and 500 nM primers were added. The PCR amplification conditions consisted of 40 min at 70 °C, 30 s at 60 °C and 1 min at 95 °C, followed by 35 cycles of 5 s at 96 °C and 20 s at 60 °C. After the final amplification cycle, a melting curve analysis was carried out. No-template controls and minus-reverse transcriptase controls were also included in these assays.

Data analysis. Gene expression data obtained after microarray hybridizations were analysed using GeneSpring GX software (v.12; Agilent Technologies) and the Babelomics server (http://www.babelomics.org) (Medina *et al.*, 2010). The normalization procedure was carried out using GeneSpring GX software and specific recommendations for one-colour hybridizations. Basically, after subtracting the background intensity and $\log_2$ data transformation, a global normalization (75th percentile shift normalization) was performed followed by a baseline transformation to the median of all samples. Each gene was considered to be positively expressed if in the three independent samples all the specific probes designed for it were hybridized. Afterwards, levels of expression were compared using Student's *t*-test to identify genes differentially expressed in *A. fumigatus* conidia cultured under the two conditions studied, i.e. 24 and 37 °C. Multiple testing with Benjamini–Hochberg correction was applied in order to control for the occurrence of false positives. A gene was considered to be differentially expressed if $P<0.05$. Results were expressed as $\log_2$ fold change, representing the $\log_2$ at 24 °C minus the $\log_2$ at 37 °C. Differentially expressed genes were classified into functional groups using FungiFun (Priebe *et al.*, 2011, 2014). The enrichment P value of each FunCat category was performed establishing Fisher's test, and Benjamini–Hochberg adjustment method as the parameters to carry out the procedure. A category was considered significant if $P<0.05$.

The analysis of RT-qPCR results was carried out using the SDS v.2.4 software (Applied Biosystems) or Analysis Software v.3.1.3 (Fluidigm). In both cases, the data were normalized with results for the *act1* and *gpdA* housekeeping genes using GenEx v.5.4 (MultiD). Then, relative quantification of gene expression was performed by the $\Delta\Delta C_t$ method and the significance of differences was assessed using Student's *t*-test ($P<0.05$). Finally, fold changes were standardized by $\log_2$ transformation and compared with microarray data using Pearson's correlation. The $\log_2$ fold change thresholds were set at >1 and <-1, meaning an increase of the expression of more than twice at 24 °C and an increase of more than twice at 37 °C, respectively.

Microarray accession numbers. The AWAFUGE microarray v.1 design was submitted to the ArrayExpress database at the European

Bioinformatics Institute (http://www.ebi.ac.uk/miamexpress/) under accession number A-MEXP-2352. The *A. fumigatus* gene expression data obtained following hybridization with the microarray have also been deposited in the ArrayExpress database under accession number E-MTAB-1910.

RESULTS

Viability and germination of conidia

The viability of *A. fumigatus* Af-293 conidia was 75.82 ± 14.50 %. To study the early expression of this fungus, a germination rate of 15–30 % was selected given the size of the germinated conidia (Fig. 1a). This was faster at 37 than at 24 °C. Specifically, in cultures at 37 °C, cells reached these germination rates after 6.5 h of incubation, whereas at 24 °C these rates were achieved after 18 h of incubation (Fig. 1b). Measurements showed no differences in pH between starting (pH 7.2) and harvesting times in either of the cultures (pH 7.1 ± 0.11). Hence, for the microarray analysis and its validation by RT-qPCR, germinated cells were obtained after different lengths of incubation at 37 and 24 °C (i.e. 6.5 and 18 h, respectively). In addition, to study the effect of nutrient source depletion, this expression analysis was also performed following the addition of fresh medium. In this case, cultures after 16 h of incubation at 24 °C, which showed swelling and 1–4 % germination rates, were used. After the addition of fresh medium, samples with 15–30 and 40–60 % germination rates were harvested, which were reached after 1.5 and 3 h of incubation at 37 °C and 3 and 6 h at 24 °C (Fig. 1). The total RNA from each condition was obtained, transcribed into cDNA and used in hybridization or RT-qPCR studies, as indicated in each case.

Gene expression in response to temperature

Three samples from *A. fumigatus* grown at each temperature were hybridized with the microarray. The data obtained in these transcriptomic studies were deposited in the ArrayExpress through the MIAMExpress tool. Following hybridizations, normalized data were represented graphically (Fig. 2a), showing similar expression at the two temperatures. However, the statistical comparisons showed that 1249 genes were expressed differentially (Fig. 2b). Negative or positive $\log_2$ fold changes meant upregulation at 37 or 24 °C, respectively. Overall, 591 genes were upregulated at 37 °C and 658 genes were upregulated at 24 °C (Table S2). Amongst them, 385 were unclassified proteins and 326 hypothetical proteins. According to the functional classification and the enrichment *P* values of each functional group, eight categories were significantly enriched at 37 °C, being C-compound and carbohydrate metabolism, secondary metabolism, lipid, fatty acid and isoprenoid metabolism, non-vesicular cellular import, NAD/NADP binding, non-ribosomal peptide synthesis, fatty acid metabolism, and degradation of leucine. At 24 °C, eight categories also appeared to be enriched, although in this case the functional groups were rRNA processing, ribosome biogenesis, rRNA synthesis, RNA binding, rRNA modification, tRNA processing, tRNA modification and RNA degradation (Table 2).

We also analysed the location of the significantly expressed genes along *A. fumigatus* chromosomes, but no specific distribution was observed. The ratio of upregulated genes found at 24 versus 37 °C was ~1 in each chromosome (data not shown).

In addition, several genes involved in metabolic pathways related to virulence appeared to be upregulated at 37 °C. These genes were involved with gliotoxin biosynthesis, nitrogen and iron metabolism, and encoding allergens. Specifically, the upregulated genes related to gliotoxin biosynthesis included those that encoded GliP, GliJ, GliZ and a GliP-like proteins, whilst in relation to iron metabolism, there was upregulation of the gene which encoded bZIP transcription factor HapX, and genes related to siderophore biosynthesis and transporters (SidD, SidC, MirB and MirC). With regard to nitrogen metabolism, upregulation was found in three genes that encoded the nitrite reductase NiiA and two nitrate reductases, one of these being the nitrate reductase NiaD and the other one AFUA_5G10420. Finally, nine genes that encoded allergens were upregulated at 37 °C. Amongst them, those that coded for the manganese superoxide dismutase MnSOD, the major allergen Asp F2, and the major allergen and cytotoxin Asp F1 showed the highest upregulation. In contrast, only two genes related to iron metabolism, those which coded for the siderophore transcription factor SreA and the homoaconitase LysF, and a cell wall glucanase/allergen F16-like protein, showed upregulation at 24 °C (Table 3).

RT-qPCR validation of microarray data

Twenty genes that showed the greatest differential expression in the microarrays, 10 of them upregulated at 37 °C and the other 10 at 24 °C, as well as eight genes related to virulence, whose expression levels are shown in Table S2, were selected for RT-qPCR analysis to validate the results obtained with the microarray experiments. The specific primer pairs designed for each selected gene are listed in Table 1. In addition, *act1* and *gpdA* genes were used as housekeeping genes. RT-qPCR results were normalized.

A negative $\log_2$ fold change was interpreted as meaning genes were upregulated at 37 °C, whilst a positive $\log_2$ fold change was taken to indicate upregulation at 24 °C. RT-qPCR results were compared and correlated with the data obtained from the same genes on the microarray (Fig. 3a). Pearson's correlation coefficient between microarray and RT-qPCR data was high, with a value of 0.91 (Fig. 3b).

The expression of these genes was analysed after the addition of fresh medium and compared with the results obtained in the validation of microarray data to determine whether the temperature was the only factor affecting the expression. This analysis showed that 14 genes agreed with the microarray; Pearson's correlation between these results being 0.86. Only four genes appeared to have a different

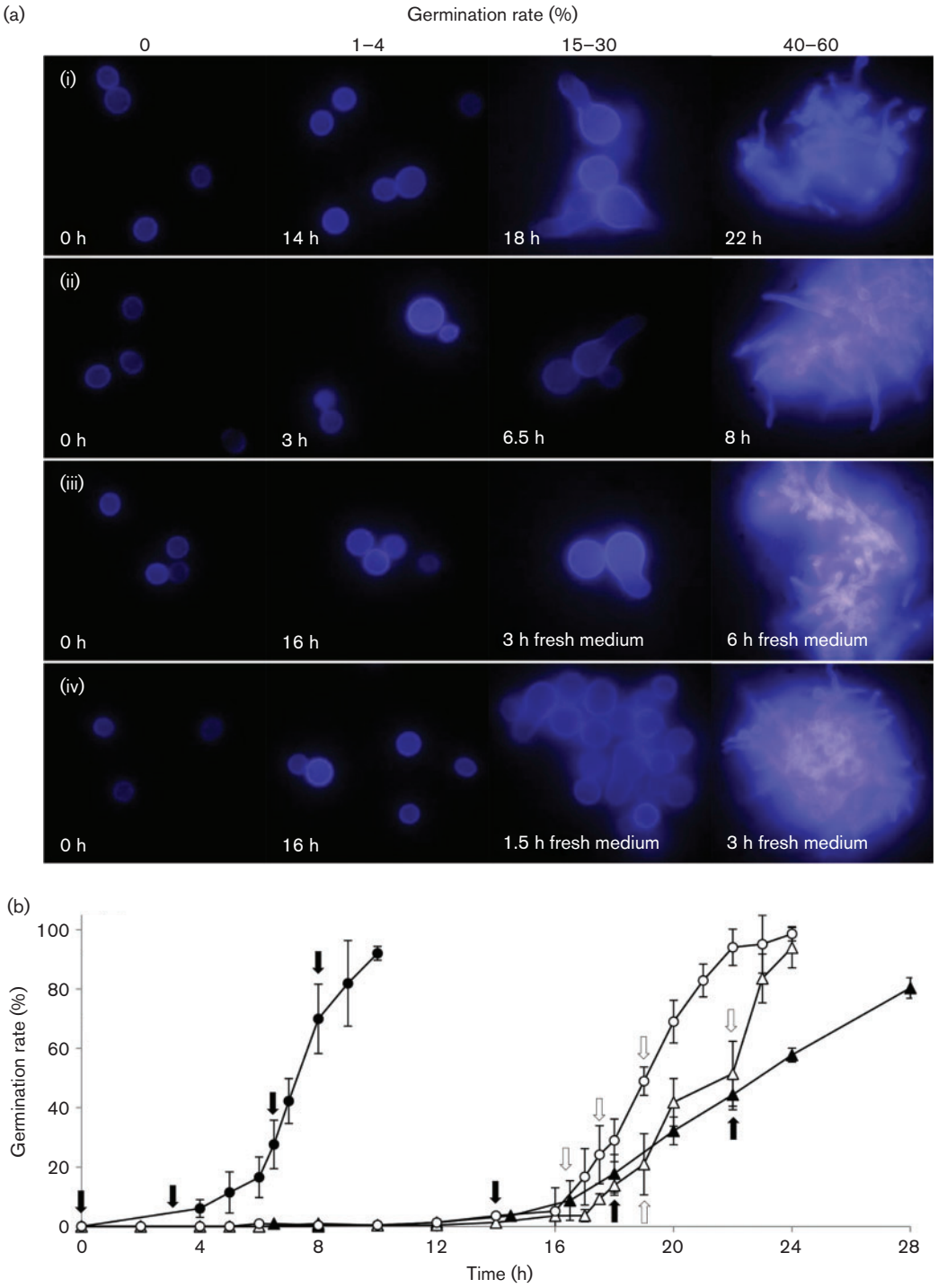

Fig. 1. Germination of *A. fumigatus*. (a) Calcofluor white staining of *A. fumigatus* Af-293. Each image shows the percentage of germination and the hours of incubation. (i) and (ii) Continuous incubation at 24 and 37 °C, respectively. (iii) and (iv) Incubation at 24 and at 37 °C, respectively, following the addition of fresh medium after 16 h of incubation at 24 °C. (b) Curves of germination rates of *A. fumigatus* Af-293. Each point represents the mean ± SD of three replicates of each time. Black and white arrows indicate the time points at which samples were obtained. Continuous incubation at 24 (▲) and 37 °C (●). Incubation at 24 (△) and at 37 °C (○) following the addition of fresh medium after 16 h of incubation at 24 °C.

expression pattern related to microarray analysis (those that encoded the NACHT domain protein, the ATP/GTP-binding protein, the nitrite reductase NiiA and the non-ribosomal peptide synthase SidD) and 10 genes had fold changes below the thresholds previously established (Table S3). In samples with 40–60 % germination rates after the addition of fresh

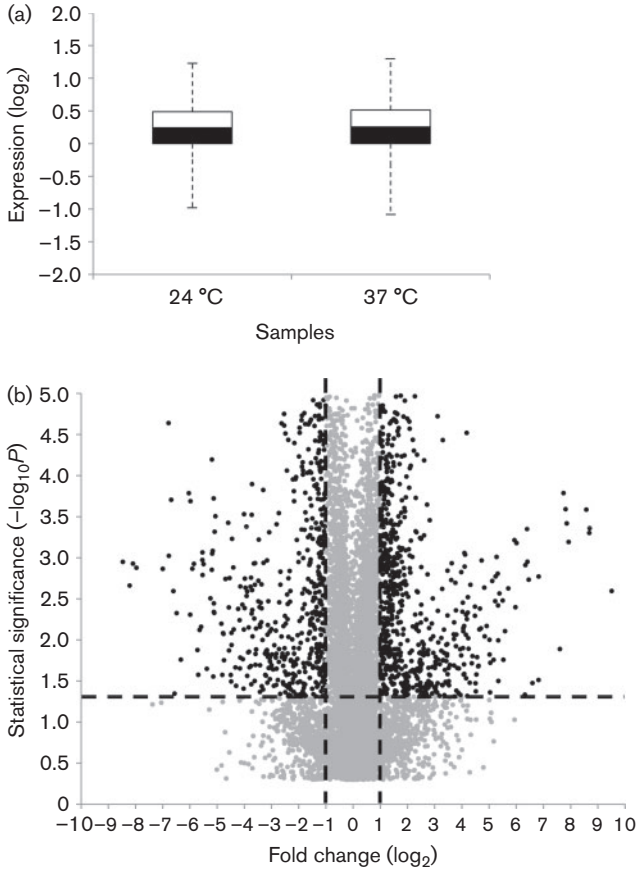

Fig. 2. Gene expression analysis. (a) Box plot representing the distribution of gene expression. Each sample corresponds to the mean expression of three independent samples obtained from growth at 24 and 37 °C, respectively. The *y*-axis values represent the gene expression (log_2). (b) Volcano plot showing differentially (black) and non-differentially (grey) expressed genes. The *x*-axis values represent the fold change (log_2) of microarray data and the *y*-axis values represent the statistical significance ($-log_{10}P$). Spots with negative fold change values indicate upregulation at 37 °C and spots with positive values indicate upregulation at 24 °C.

Table 2. Enriched FunCat categories at 24 and 37 °C

FunCat description*	*P* value†	Genes/ category‡
37 °C		
C-compound and carbohydrate metabolism	2.45×10^{-9}	97/858
Secondary metabolism	6.72×10^{-3}	77/870
Lipid, fatty acid and isoprenoid metabolism	6.72×10^{-3}	56/577
Non-vesicular cellular import	1.96×10^{-2}	24/190
NAD/NADP binding	1.99×10^{-2}	24/193
Non-ribosomal peptide synthesis	2.06×10^{-2}	8/32
Fatty acid metabolism	2.43×10^{-2}	19/142
Degradation of leucine	3.99×10^{-2}	6/21
24 °C		
rRNA processing	1.91×10^{-47}	85/188
Ribosome biogenesis	4.61×10^{-22}	58/182
rRNA synthesis	4.62×10^{-12}	27/70
RNA binding	3.36×10^{-11}	59/308
rRNA modification	4.18×10^{-5}	9/17
tRNA processing	4.66×10^{-2}	12/60
tRNA modification	4.66×10^{-2}	10/45
RNA degradation	4.66×10^{-2}	13/70

*Functional classification according to the Munich Information Center for Protein Sequence Functional Catalogue (FunCat; http://pedant.helmholtz-muenchen.de).
†Enrichment *P* value of each FunCat description obtained after Fisher's test and Benjamini–Hochberg correction.
‡Number of upregulated genes found in each functional group relative to the total number in each category.

medium, 17 genes agreed with the expression found on the microarray. Nevertheless, five genes showed different expression (those that encoded the Zn^{2+}-dependent hydrolase, the ATP/GTP-binding protein, the FAD-binding monooxygenase, the glycosyltransferase and MnSOD) (Table S3).

Focusing on the genes related to virulence, three out of nine genes agreed with the microarray data in samples with 15–30 % germination rates. Amongst the genes involved with gliotoxin biosynthesis, only *gliZ* appeared to be upregulated at 37 °C in all cases. In iron metabolism, there was upregulation of the non-ribosomal peptide synthase SidD at 24 °C in 15–30 % germination rate samples, whereas in nitrogen metabolism, upregulation at 37 °C was found only in 40–60 % germination samples. Finally, amongst the allergens analysed, only Asp F2 and MnSOD were upregulated at 37 °C in 15–30 % germination rate samples (Fig. 4).

DISCUSSION

Infection by *A. fumigatus* starts with conidia inhalation, which in immunocompromised individuals results in conidia establishment in the lung, germination and invasion of the surrounding lung tissue. Taking the host environment into account, conidial germination and growth requires the activation of nutrient sensing, nutrient uptake and acquisition, and biosynthetic pathways, knowledge of which would be essential for understanding the pathogenesis of *A. fumigatus* (Dagenais & Keller, 2009).

Due to the multifactorial virulence of *A. fumigatus*, apart from direct site mutagenesis, the best methods to identify genes related to virulence appear to be transcriptomic and proteomic analysis. In line with this, various different transcriptomic experiments, such as exposure to antifungal drugs (da Silva Ferreira *et al.*, 2006), high temperatures (Nierman *et al.*, 2005), germination and hyphae development (Sugui *et al.*, 2008), and even infection of human cells (Morton *et al.*, 2011; Oosthuizen *et al.*, 2011), have

Table 3. Genes related to virulence expressed differentially on the microarray

Gene product description*	Locus ID†	24 °C‡	37 °C‡	Fold change§
Gliotoxin biosynthesis				
Non-ribosomal peptide synthase GliP	AFUA_6G09660	−3.376	1.689	−5.065
Membrane dipeptidase GliJ	AFUA_6G09650	−4.574	−0.184	−4.390
C6 finger domain protein GliZ	AFUA_6G09630	−1.638	1.484	−3.122
Non-ribosomal peptide synthase GliP-like	AFUA_3G12920	−1.174	0.189	−1.362
Iron metabolism				
MFS siderochrome iron transporter MirB	AFUA_3G03640	−2.496	2.199	−4.695
bZIP transcription factor HapX	AFUA_5G03920	−1.100	0.855	−1.955
Non-ribosomal peptide synthase SidD	AFUA_3G03420	−1.094	0.690	−1.784
Non-ribosomal siderophore peptide synthase SidC	AFUA_1G17200	−0.647	0.667	−1.314
Siderochrome iron transporter MirC	AFUA_2G05730	−0.353	0.699	−1.052
Mitochondrial ornithine carrier protein AmcA/Ort1, putative	AFUA_8G02760	−0.529	0.483	−1.013
Siderophore transcription factor SreA	AFUA_5G11260	0.585	−0.632	1.218
Homoaconitase LysF	AFUA_5G08890	0.950	−1.130	2.080
Nitrogen metabolism				
Nitrite reductase NiiA	AFUA_1G12840	−4.979	2.684	−7.663
Nitrate reductase NiaD	AFUA_1G12830	−1.331	1.685	−3.017
Nitrate reductase	AFUA_5G10420	−0.273	0.941	−1.213
Allergens of *A. fumigatus*				
Manganese superoxide dismutase MnSOD	AFUA_1G14550	−2.165	1.599	−3.765
Major allergen Asp F2	AFUA_4G09580	−2.865	0.166	−3.032
Major allergen and cytotoxin Asp F1	AFUA_5G02330	−1.874	0.942	−2.816
Aspartic endopeptidase Pep1/aspergillopepsin F	AFUA_5G13300	−1.142	0.742	−1.884
Allergenic cerato-platanin Asp F13	AFUA_2G12630	−0.993	0.836	−1.829
Cell wall galactomannoprotein Mp2/allergen F17-like	AFUA_2G05150	−0.769	0.798	−1.567
Cell wall serine/threonine-rich galactomannoprotein Mp1	AFUA_4G03240	−0.658	0.814	−1.473
Elastinolytic metalloproteinase Mep	AFUA_8G07080	−0.722	0.447	−1.169
Extracellular cellulase CelA/allergen Asp F7-like, putative	AFUA_5G08030	−0.314	0.715	−1.029
Cell wall glucanase/allergen F16-like	AFUA_6G03230	0.561	−0.655	1.216

*Product description of the genes found on the microarray.

†GenBank accession number (http://www.ncbi.nlm.nih.gov/gene/).

‡Normalized expression data ($\log_2$) under each condition. The normalization was carried out using GeneSpring GX software. After subtracting the background intensity and $\log_2$ data transformation, a global normalization was performed followed by a baseline transformation to the median of all samples.

§Fold change ($\log_2$) obtained for each gene. This value represents the $\log_2$ at 24 °C minus the $\log_2$ at 37 °C. Negative fold changes indicate upregulation at 37 °C and positive fold changes indicate upregulation at 24 °C.

been carried out in an attempt to shed light on the pathogenesis of *A. fumigatus*. However, the mechanisms of pathogenicity of *A. fumigatus* remain unclear. To improve our understanding of the mechanisms that enable this fungus to cause infection, we designed an *A. fumigatus* microarray using the information from all of the mRNA sequences available from the National Center for Biotechnology Information database and the eArray system developed by Agilent Technology. The strain selected for the design of the microarray as well as for this study was *A. fumigatus* Af-293 due to the fact that this strain was isolated from a lung biopsy from a neutropenic patient with invasive aspergillosis (Anderson & Denning, 2001), it was the first strain of *A. fumigatus* whose genome was sequenced (Nierman *et al.*, 2005), and because it has been used in both *in vitro* and *in vivo* experiments (Power *et al.*, 2006; Gravelat *et al.*, 2008; Lamarre *et al.*, 2008; McDonagh *et al.*, 2008; Fraczek *et al.*, 2010; Morton *et al.*, 2011; Farnell *et al.*, 2012).

Although aspergillosis can be attributed to a combination of the immune status of the patient and the biological characteristics of the fungus, it is believed that some physiological characteristics of *A. fumigatus* allow it to be an efficient opportunistic pathogen (Abad *et al.*, 2010). Amongst these characteristics, its ability to survive high temperatures is one of the most cited, as it tolerates temperatures >50 °C and its optimal temperature is around 37 °C (Krijgsheld *et al.*, 2013). Hence, it is plausible that the mechanisms of thermotolerance involve the expression of stress resistance genes that, at the same time, confer unique virulence properties to the fungus (Bhabhra & Askew, 2005). Consistent with this, Araujo & Rodrigues (2004) demonstrated that temperature plays a crucial role in the correlation between

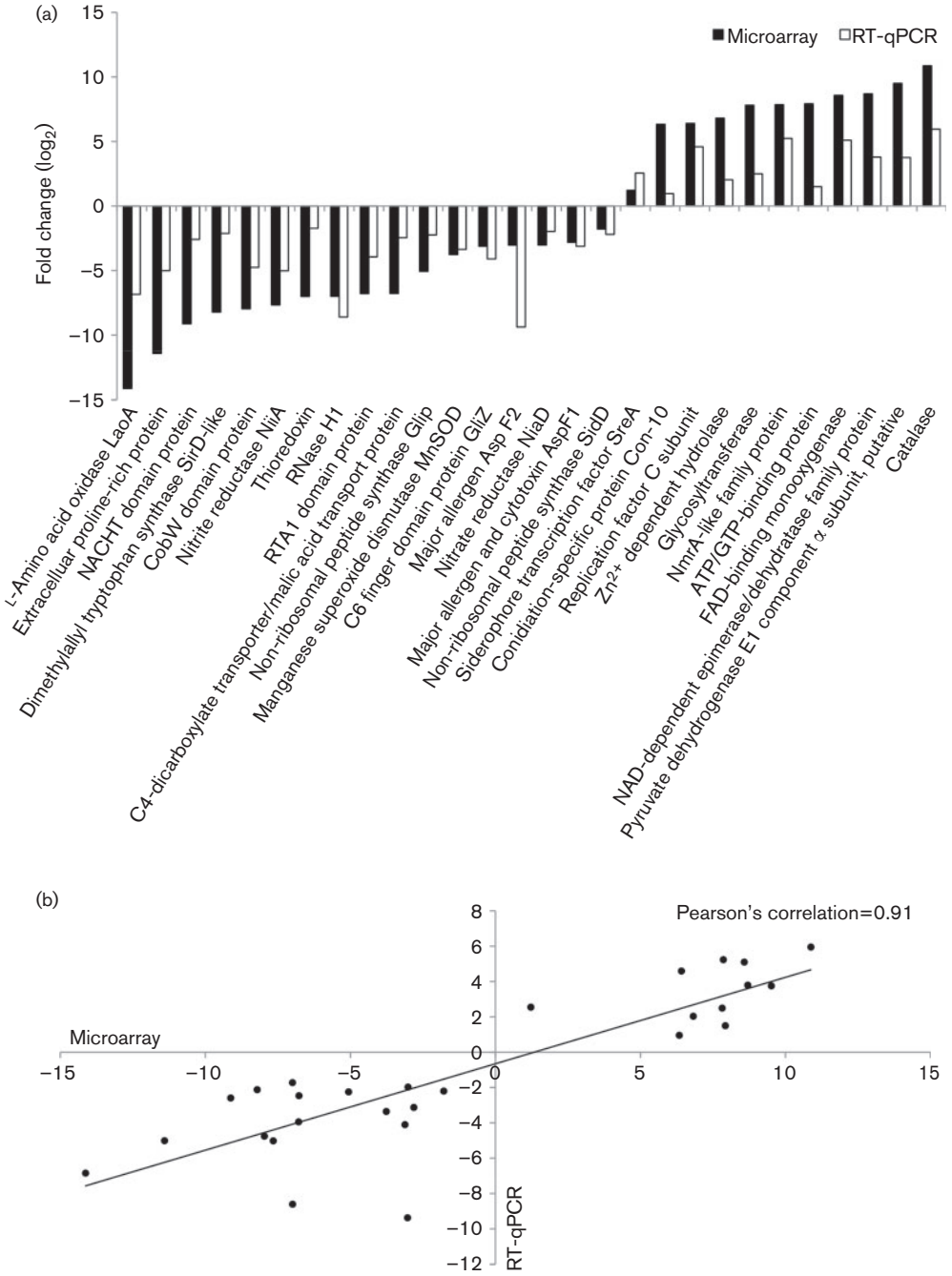

Fig. 3. Comparison of the results obtained by microarray and RT-qPCR. (a) Comparative levels of gene expression between the microarray and RT-qPCR. Negative fold changes indicate upregulation at 37 °C and positive fold changes indicate upregulation at 24 °C. (b) Correlation analysis between microarray and RT-qPCR data. The *x*-axis values represent the fold change (log_2) of microarray data and the *y*-axis values represent the fold change (log_2) of RT-qPCR results. Each point corresponds to the mean value from three independent samples.

germination rate and pathogenicity, showing how germination is a crucial step in the development of aspergillosis and concluding that *A. fumigatus* is most able to adapt to extreme changes in environmental conditions. To date, several studies have analysed the transcriptomic changes at different temperatures (Nierman *et al.*, 2005; Low *et al.*, 2011; Krishnan *et al.*, 2014), without considering the different growth rate reached at each temperature. Taking this into consideration, we decided to investigate the adaptive changes of *A. fumigatus* to host temperature, using

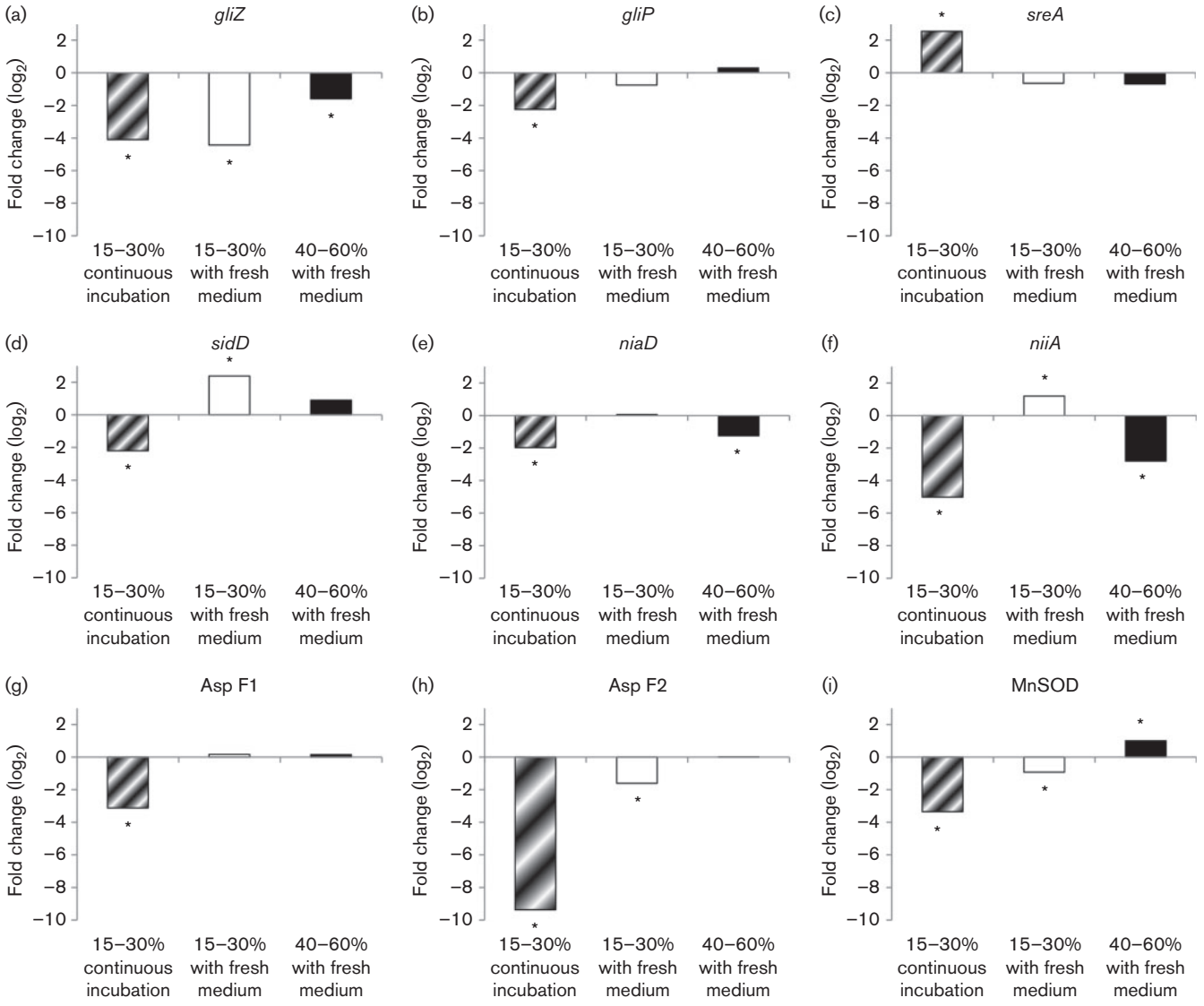

Fig. 4. Expression levels of genes related to virulence: *gliZ* (a), *gliP* (b), *sreA* (c), *sidD* (d), *niaD* (e), *niiA* (f), Asp F1 (g), Asp F2 (h) and MnSOD (i). Negative $\log_2$ fold changes indicate upregulation at 37 °C and positive fold changes indicate upregulation at 24 °C. An asterisk indicates data above or below the thresholds established (>1 and <-1).

the AWAFUGE microarray v.1 to study the transcriptome at 24 °C, representing the environmental temperature, and at 37 °C, reflecting the host temperature. We focused on the first steps of germination to identify those genes expressed differentially at both temperatures when 15–30 % of conidia had germinated at both temperatures, as all germinated conidia were of a similar size (Fig. 1a), and because using samples with the same germination rate might minimize expression changes due to the growth rate. Specifically, cultures were incubated at 37 °C for 6.5 h and at 24 °C for 18 h (Fig. 1b). It should be emphasized that no changes were detected in pH, indicating that this factor had no effect on gene expression changes.

Transcriptome profiling results showed that 1249 genes were expressed differently (Fig. 2b, Table S2). To validate these results, RT-qPCR assays were carried out with the genes found to be most differentially upregulated and those related to virulence which showed significant differences (Table 1). The RT-qPCR results confirmed the differential expression of the 28 selected genes with a highly significant Pearson's correlation value of 0.91 despite using different samples in microarray and RT-qPCR assays (Fig. 3). Overall, these results underline the effectiveness and the reliability of the AWAFUGE microarray v.1, making it suitable for use in further studies analysing the virulence mechanisms or the response of *A. fumigatus* to environmental changes, or during murine or human cell infections.

The 9630 genes, the whole genome of *A. fumigatus*, have been classified into 18 functional groups according to the FunCat categorization. Building on this, we explored the

significant functional categories of the subset of genes found to be expressed differentially. As shown in Table 2, the predominant functional groups at 37 °C were those mainly involved in metabolism. In a previous study, comparing the transcriptome of *A. fumigatus* at 25 and 37 °C, upregulated genes involved in metabolism also appeared at 37 °C (Krishnan *et al.*, 2014), which was explained based on the faster growth of the fungus at 37 °C. However, in our study, both cultures at 24 and 37 °C had the same germination rate, so the results showed that the metabolic adjustments not only depend on the faster growth of this fungus, but also on the temperature at which the germination takes place. Moreover, the significant groups at 24 °C, related to rRNA processing and synthesis, tRNA processing and modification, and RNA degradation, showed that RNA pathways are downregulated at 37 °C. However, it should be pointed out the high percentage of differentially expressed genes coded for hypothetical (26.10 %) or unclassified proteins (30.82 %). It is true that these genes mean a limitation on the conclusions of our study, although at the same time they stress the importance that these unknown genes might have during the germination of this fungus and point to avenues for future research.

With the addition of fresh medium, we concluded that temperature was the main factor that determined the expression changes of 50 % of the genes (14/28 genes) analysed in samples with 15–30 % germination rates, with a high Pearson's correlation (0.86). Focusing on the 20 most expressed genes detected by microarray data, those genes that showed different expression patterns in this analysis encoded unclassified proteins, and with no statistical differences encoded proteins mainly related to secondary metabolism and C-compound and carbohydrate metabolism (Table S4). As secondary metabolism is affected by several nutritional conditions, such as amino acid, nitrogen and iron sources (Bayram & Braus, 2012), it is understandable that the addition of fresh medium could replenish the consumed nutrients, decreasing the need to stimulate different metabolisms. These results highlighted the importance that the isotropic swelling and the formation of a germ tube had since the beginning of the germination – altering the medium conditions even when the majority of the conidia had not yet germinated.

Several studies have been carried out during the last decade studying the germination of *Aspergillus* spp. (Araujo & Rodrigues, 2004; Lamarre *et al.*, 2008; van Leeuwen *et al.*, 2013). However, comparison of the findings between studies is very difficult owing to the use of different fungal species or time intervals. However, in previous studies, some metabolic pathways were found to be related to virulence, namely those for gliotoxin (Bok *et al.*, 2006; Scharf *et al.*, 2012), iron metabolism (Schrettl *et al.*, 2007, 2010; Haas, 2012) and allergens (Chaudhary & Marr, 2011; Low *et al.*, 2011). Analysing these findings together with our results, we found significant differences in expression for some genes involved in these pathways and the results were validated by RT-qPCR assays (Fig. 3a).

Our results showed that some genes involved in gliotoxin biosynthesis were upregulated at 37 °C (Table 3), such as *gliZ*, a transcription factor which regulates gliotoxin biosynthesis, and *gliP*, a non-ribosomal peptide synthetase which catalyses the first step of gliotoxin biosynthesis. Furthermore, analysis following the addition of fresh medium showed a clear upregulation at 37 °C of the gene that encodes GliZ, demonstrating that the expression of this gene is directly influenced by heat shock. However, the expression pattern of the gene that encodes GliP indicated that heat shock did not directly stimulate the upregulation of this gene (Fig. 4a, b). According to the literature, *gliZ* is a positive regulator of *gliP* and its over-regulation enhances the production of gliotoxin (Bok *et al.*, 2006). Nevertheless, Dhingra *et al.* (2012) showed different expression patterns amongst *gliZ* and *gliP* when *veA*, a major fungal regulatory gene, was deleted, which was explained based on a possible influence of *veA* on *gliP* by unknown mechanisms. Therefore, the expression of *gliP* could be controlled by other regulators, apart from *gliZ*, which might have been affected by the addition of fresh medium.

Genes involved in iron metabolism were also found to be expressed differentially in our study. In order to maintain iron homeostasis, two transcriptional factors are necessary, *sreA* and *hapX*. *sreA* represses the expression of high-affinity iron uptake when iron concentrations are high enough (Schrettl *et al.*, 2008). *hapX* mediates adaptation to iron starvation conditions, in which iron uptake through siderophores is activated (Schrettl *et al.*, 2010), and other authors have recently demonstrated a dual role in high- and low-iron conditions (Gsaller *et al.*, 2014). Our microarray results showed that *sreA* was upregulated at 24 °C, whereas *hapX*, SidD and SidC siderophores as well as MirB and MirC siderophore transporters were upregulated at 37 °C. Interestingly, after the addition of fresh medium, *sreA* expression levels were not upregulated, but *sidD* showed upregulation at 24 °C, unlike in the microarray data (Fig. 4c). Therefore, iron uptake through siderophores appears not to be affected by heat shock, but rather by a possible decrease of iron availability in the culture medium during isotropic swelling and germ tube formation at 37 °C.

Another metabolic pathway whose genes were found to be expressed differentially in our microarray results and that has been related to virulence was nitrogen metabolism. *Aspergillus* can use a wide range of nitrogen sources and contributes significantly to global nitrogen recycling via nitrate assimilation (Dagenais & Keller, 2009). Accordingly, three genes involved in nitrogen metabolism were upregulated at 37 °C. Two of them encode nitrate reductases (NiaD and AFUA_5G10420), and the other, the nitrite reductase NiiA, which was the most upregulated gene (Table 3). With the addition of fresh medium, the results showed that in 15–30 % germination rate samples only the gene that encodes the nitrite reductase NiiA appeared to be upregulated at 24 °C, whereas in 40–60 % germination samples the genes that code for the nitrite reductase NiiA

and the nitrate reductase NiaD were upregulated at 37 °C (Fig. 4e, f). These expression changes detected in our study could mean that the uptake of nitrogen is upregulated in line with the growth of *A. fumigatus* at 37 °C and a possible consumption of nitrogen sources as in the iron case.

Finally, *A. fumigatus* may be responsible for various allergic diseases such as extrinsic allergic alveolitis, asthma, allergic sinusitis and allergic bronchopulmonary aspergillosis (Park & Mehrad, 2009). More than 20 allergenic molecules are known to be produced by this fungus and some of them, in addition to their allergenic activities, are also related to virulence (Abad *et al.*, 2010). Our results reveal that nine genes that encode allergens were highly upregulated when *A. fumigatus* germinated at 37 °C; the most upregulated allergens being MnSOD (Asp F6), the major allergen Asp F2, and the major allergen and cytotoxin Asp F1. Only one gene that codes for cell wall glucanase/allergen F16-like appears to be upregulated at 24 °C (Table 3). According to the results obtained after the addition of fresh medium, the expression of allergens seems to take place at the beginning of germination. In 15–30 % germination samples, Asp F2 and MnSOD were also upregulated at 37 °C, MnSOD being only upregulated at 24 °C in 40–60 % germination rates samples (Fig. 4g–i). Furthermore, the upregulation in 15–30 % germination rates not only highlighted the importance of the production of these allergens during the first steps of germination, but also the effect of higher temperature. However, Asp F1 showed no statistical differences in 15–30 % germination rates samples, pointing out the effect of the medium in the production of this allergen, which might be stimulated by a depletion of nutritional sources.

This is the first study to compare the transcriptomes of germinated conidia at 24 and 37 °C taking into account the germination rate. According to our results, *A. fumigatus* modifies the expression of genes mainly related to metabolism and downregulates RNA pathways in order to adapt to the new conditions at 37 °C. Moreover, the high percentages of differentially expressed genes that encode hypothetical or unclassified proteins imply that many of these unknown genes must be essential during the germination of this fungus, whose study might improve our understanding of the infection caused by the fungus. Amongst the genes related to virulence upregulated at 37 °C, we found genes coding for allergenic proteins, and several genes involved in gliotoxin biosynthesis, and nitrogen and iron metabolism. Furthermore, the addition of fresh medium demonstrated the importance of isotropic swelling, which can alter the growth medium even before reaching the 15–30 % germination rate. Gene expression in iron and nitrogen metabolism appears to be influenced by the availability of these nutrients in the medium, whereas in allergen production, the temperature, the germination stage and the medium conditions seem to be involved. Therefore, the expression changes detected in our study might demonstrate not only the rapid heat shock adaptation of *A. fumigatus*, but also its efficient ability to uptake nutrients from the medium during the earliest steps of germination, which might be another aspect that allows it to germinate easily in the host environment.

ACKNOWLEDGEMENTS

This work was partly funded by the University of Basque Country (UPV/EHU) (PES13/03, GIU12/44 and UFI11/25), the Government of the Basque Country (S-PC11UN007) and the Ministry of Economy and Competitiveness (MICINN CSD2009-00006). M. S.-O. has been supported by Pre-doctoral Research Grants of the Government of the Basque Country. J. V. F.-M. has been supported by Pre-doctoral Research Grants of the UPV/EHU. Technical and human support provided by Advanced Research Facilities (SGIker) of the UPV/EHU is gratefully acknowledged. We are grateful to Ideas Need Communicating Language Services for improving the use of English in the manuscript.

REFERENCES

Abad, A., Fernández-Molina, J. V., Bikandi, J., Ramírez, A., Margareto, J., Sendino, J., Hernando, F. L., Pontón, J., Garaizar, J. & Rementeria, A. (2010). What makes *Aspergillus fumigatus* a successful pathogen? Genes and molecules involved in invasive aspergillosis. *Rev Iberoam Micol* **27**, 155–182.

Anderson, M. & Denning, D. W. (2001). *Aspergillus fumigatus* isolate AF293 (NCPF 7367). http://www.aspergillus.org.uk/indexhome.htm?secure/sequence_info/./genomeetings/isolate.htm~main

Araujo, R. & Rodrigues, A. G. (2004). Variability of germinative potential among pathogenic species of *Aspergillus*. *J Clin Microbiol* **42**, 4335–4337.

Barhoom, S. & Sharon, A. (2004). cAMP regulation of "pathogenic" and "saprophytic" fungal spore germination. *Fungal Genet Biol* **41**, 317–326.

Bayram, O. & Braus, G. H. (2012). Coordination of secondary metabolism and development in fungi: the velvet family of regulatory proteins. *FEMS Microbiol Rev* **36**, 1–24.

Beauvais, A. & Latgé, J. P. (2001). Membrane and cell wall targets in *Aspergillus fumigatus*. *Drug Resist Updat* **4**, 38–49.

Bhabhra, R. & Askew, D. S. (2005). Thermotolerance and virulence of *Aspergillus fumigatus*: role of the fungal nucleolus. *Med Mycol* **43** (Suppl 1), 87–93.

Bok, J. W., Chung, D., Balajee, S. A., Marr, K. A., Andes, D., Nielsen, K. F., Frisvad, J. C., Kirby, K. A. & Keller, N. P. (2006). GliZ, a transcriptional regulator of gliotoxin biosynthesis, contributes to *Aspergillus fumigatus* virulence. *Infect Immun* **74**, 6761–6768.

Chaudhary, N. & Marr, K. A. (2011). Impact of *Aspergillus fumigatus* in allergic airway diseases. *Clin Transl Allergy* **1**, 4.

da Silva Ferreira, M. E., Malavazi, I., Savoldi, M., Brakhage, A. A., Goldman, M. H. S., Kim, H. S., Nierman, W. C. & Goldman, G. H. (2006). Transcriptome analysis of *Aspergillus fumigatus* exposed to voriconazole. *Curr Genet* **50**, 32–44.

Dagenais, T. R. T. & Keller, N. P. (2009). Pathogenesis of *Aspergillus fumigatus* in invasive aspergillosis. *Clin Microbiol Rev* **22**, 447–465.

del Palacio, A., Cuétara, M. S. & Pontón, J. (2003). [Laboratory diagnosis of invasive aspergillosis]. *Rev Iberoam Micol* **20**, 90–98 (in Spanish).

Dhingra, S., Andes, D. & Calvo, A. M. (2012). VeA regulates conidiation, gliotoxin production, and protease activity in the

opportunistic human pathogen *Aspergillus fumigatus*. *Eukaryot Cell* **11**, 1531–1543.

Farnell, E., Rousseau, K., Thornton, D. J., Bowyer, P. & Herrick, S. E. (2012). Expression and secretion of *Aspergillus fumigatus* proteases are regulated in response to different protein substrates. *Fungal Biol* **116**, 1003–1012.

Fraczek, M. G., Rashid, R., Denson, M., Denning, D. W. & Bowyer, P. (2010). *Aspergillus fumigatus* allergen expression is coordinately regulated in response to hydrogen peroxide and cyclic AMP. *Clin Mol Allergy* **8**, 15.

Gravelat, F. N., Doedt, T., Chiang, L. Y., Liu, H., Filler, S. G., Patterson, T. F. & Sheppard, D. C. (2008). *In vivo* analysis of *Aspergillus fumigatus* developmental gene expression determined by real-time reverse transcription-PCR. *Infect Immun* **76**, 3632–3639.

Gsaller, F., Hortschansky, P., Beattie, S. R., Klammer, V., Tuppatsch, K., Lechner, B. E., Rietzschel, N., Werner, E. R., Vogan, A. A. & other authors (2014). The Janus transcription factor HapX controls fungal adaptation to both iron starvation and iron excess. *EMBO J* **33**, 2261–2276.

Haas, H. (2012). Iron – a key nexus in the virulence of *Aspergillus fumigatus*. *Front Microbiol* **3**, 28.

Harris, S. D. & Momany, M. (2004). Polarity in filamentous fungi: moving beyond the yeast paradigm. *Fungal Genet Biol* **41**, 391–400.

Krijgsheld, P., Bleichrodt, R., van Veluw, G. J., Wang, F., Müller, W. H., Dijksterhuis, J. & Wösten, H. A. (2013). Development in *Aspergillus*. *Stud Mycol* **74**, 1–29.

Krishnan, K., Ren, Z., Losada, L., Nierman, W. C., Lu, L. J. & Askew, D. S. (2014). Polysome profiling reveals broad translatome remodeling during endoplasmic reticulum (ER) stress in the pathogenic fungus *Aspergillus fumigatus*. *BMC Genomics* **15**, 159.

Lamarre, C., Sokol, S., Debeaupuis, J. P., Henry, C., Lacroix, C., Glaser, P., Coppée, J. Y., François, J. M. & Latgé, J. P. (2008). Transcriptomic analysis of the exit from dormancy of *Aspergillus fumigatus* conidia. *BMC Genomics* **9**, 417.

Latgé, J. P. (1999). *Aspergillus fumigatus* and aspergillosis. *Clin Microbiol Rev* **12**, 310–350.

Low, S. Y., Dannemiller, K., Yao, M., Yamamoto, N. & Peccia, J. (2011). The allergenicity of *Aspergillus fumigatus* conidia is influenced by growth temperature. *Fungal Biol* **115**, 625–632.

McDonagh, A., Fedorova, N. D., Crabtree, J., Yu, Y., Kim, S., Chen, D., Loss, O., Cairns, T., Goldman, G. & other authors (2008). Subtelomere directed gene expression during initiation of invasive aspergillosis. *PLoS Pathog* **4**, e1000154.

Medina, I., Carbonell, J., Pulido, L., Madeira, S. C., Goetz, S., Conesa, A., Tárraga, J., Pascual-Montano, A., Nogales-Cadenas, R. & other authors (2010). Babelomics: an integrative platform for the analysis of transcriptomics, proteomics and genomic data with advanced functional profiling. *Nucleic Acids Res* **38** (Web Server issue), W210-W213.

Morton, C. O., Varga, J. J., Hornbach, A., Mezger, M., Sennefelder, H., Kneitz, S., Kurzai, O., Krappmann, S., Einsele, H. & other authors (2011). The temporal dynamics of differential gene expression in *Aspergillus fumigatus* interacting with human immature dendritic cells *in vitro*. *PLoS One* **6**, e16016.

Nierman, W. C., Pain, A., Anderson, M. J., Wortman, J. R., Kim, H. S., Arroyo, J., Berriman, M., Abe, K., Archer, D. B. & other authors (2005). Genomic sequence of the pathogenic and allergenic filamentous fungus *Aspergillus fumigatus*. *Nature* **438**, 1151–1156.

O'Gorman, C. M. (2011). Airborne *Aspergillus fumigatus* conidia: a risk of factor for aspergillosis. *Fungal Biol Rev* **25**, 151–157.

Oosthuizen, J. L., Gomez, P., Ruan, J., Hackett, T. L., Moore, M. M., Knight, D. A. & Tebbutt, S. J. (2011). Dual organism transcriptomics of airway epithelial cells interacting with conidia of *Aspergillus fumigatus*. *PLoS One* **6**, e20527.

Osherov, N. (2007). The virulence of *Aspergillus fumigatus*. In *New Insights in Medical Mycology*, pp. 185–212. Edited by K. Kavanagh. Dordrecht: Springer.

Park, S. J. & Mehrad, B. (2009). Innate immunity to *Aspergillus* species. *Clin Microbiol Rev* **22**, 535–551.

Power, T., Ortoneda, M., Morrissey, J. P. & Dobson, A. D. (2006). Differential expression of genes involved in iron metabolism in *Aspergillus fumigatus*. *Int Microbiol* **9**, 281–287.

Priebe, S., Linde, J., Albrecht, D., Guthke, R. & Brakhage, A. A. (2011). FungiFun: a web-based application for functional categorization of fungal genes and proteins. *Fungal Genet Biol* **48**, 353–358.

Priebe, S., Kreisel, C., Horn, F., Guthke, R. & Linde, J. (2014). FungiFun2: a comprehensive online resource for systematic analysis of gene lists from fungal species. *Bioinformatics* doi:10.1093/bioinformatics/btu627 [Epub ahead of print].

Rementeria, A., López-Molina, N., Ludwig, A., Vivanco, A. B., Bikandi, J., Pontón, J. & Garaizar, J. (2005). [Genes and molecules involved in *Aspergillus fumigatus* virulence]. *Rev Iberoam Micol* **22**, 1–23 (in Spanish).

Scharf, D. H., Heinekamp, T., Remme, N., Hortschansky, P., Brakhage, A. A. & Hertweck, C. (2012). Biosynthesis and function of gliotoxin in *Aspergillus fumigatus*. *Appl Microbiol Biotechnol* **93**, 467–472.

Schrettl, M., Bignell, E., Kragl, C., Sabiha, Y., Loss, O., Eisendle, M., Wallner, A., Arst, H. N., Jr, Haynes, K. & Haas, H. (2007). Distinct roles for intra- and extracellular siderophores during *Aspergillus fumigatus* infection. *PLoS Pathog* **3**, e128.

Schrettl, M., Kim, H. S., Eisendle, M., Kragl, C., Nierman, W. C., Heinekamp, T., Werner, E. R., Jacobsen, I., Illmer, P. & other authors (2008). SreA-mediated iron regulation in *Aspergillus fumigatus*. *Mol Microbiol* **70**, 27–43.

Schrettl, M., Beckmann, N., Varga, J., Heinekamp, T., Jacobsen, I. D., Jöchl, C., Moussa, T. A., Wang, S., Gsaller, F. & other authors (2010). HapX-mediated adaption to iron starvation is crucial for virulence of *Aspergillus fumigatus*. *PLoS Pathog* **6**, e1001124.

Sugui, J. A., Kim, H. S., Zarember, K. A., Chang, Y. C., Gallin, J. I., Nierman, W. C. & Kwon-Chung, K. J. (2008). Genes differentially expressed in conidia and hyphae of *Aspergillus fumigatus* upon exposure to human neutrophils. *PLoS One* **3**, e2655.

Tekaia, F. & Latgé, J. P. (2005). *Aspergillus fumigatus*: saprophyte or pathogen? *Curr Opin Microbiol* **8**, 385–392.

van Leeuwen, M. R., Krijgsheld, P., Bleichrodt, R., Menke, H., Stam, H., Stark, J., Wösten, H. A. & Dijksterhuis, J. (2013). Germination of conidia of *Aspergillus niger* is accompanied by major changes in RNA profiles. *Stud Mycol* **74**, 59–70.

Edited by: V. Cid